

PROCEEDINGS



Montana Mining and Mineral Symposium 2018
October 10–October 13, 2018
Montana Bureau of Mines and Geology
Special Publication 120

*Cover photo: Battle Butte—A dacite flow-dome complex in the Hog Heaven Volcanic Field of northwestern Montana.
Photo: Kaleb Scarberry.*

TABLE OF CONTENTS

Technical Papers:

Annual Update on Mining in Montana	<i>Garrett Smith</i>	1
Small Mines and Mineral Exploration in Montana: Regulatory Overview and Examples from the Field.....	<i>Bausch and Mohrmann</i>	7
Building a Hard Rock Mineral Assessment for the State of Montana.....	<i>Thale and Metesh</i>	11
Water Chemistry Changes in the Berkeley Pit, Butte, Montana... ..	<i>McGrath, Icopini, and Duaiame</i>	17
Japan Law Twins from the PC Mine, Jefferson County, Montana.....	<i>Peter Knudsen</i>	25
The Epithermal Environment in the Yellowstone Hydrothermal System.....	<i>Larson and Fairley</i>	27
History and Geology of Henderson Gulch, Montana’s First Gold Discovery	<i>Ted Antonioli</i>	31
Three Mines: The Early Career of Joseph Pardee.....	<i>Anne Millbrooke</i>	35
The Mineral Display of the 1893 World’s Fair: How Montana Became Known as the Treasure State.....	<i>Michael J. Goble</i>	47
Magmatic Processes that Produce Porphyry Copper Deposits: From Batholith Formation to Anhydrite, Apatite, and Zircon Mineralogy.....	<i>John H. Dilles</i>	53
An Overview of Mesozoic Magmatism in Montana.....	<i>Scarberry and Yakovlev</i>	57
Late Cretaceous Magmatism and Upper Crustal Shortening within the Bannack Volcanic Field, Southwest Montana	<i>Jesse G. Mosolf</i>	63
Orbicular Alteration at the Clementine Porphyry Copper Prospect of Southwest Montana: Defining the Edges of Advective Flow in the Porphyry Copper Paradigm....	<i>G.H. Brimhall</i>	71
Assessing the Potential for New and Economic Polymetallic Deposit Types within the Stillwater Complex, Montana	<i>Bow and others</i>	85
Precious Metal Mineralogy, S-Isotopes, and a New LA-ICP-MS Date for the Easton and Pacific Lode Mines, Virginia City District, Montana	<i>Gammons, Mosolf, and Poulson</i>	91
New Investigations of the Economic Geology of the Historic Elkhorn Mining District, Jefferson County, Montana	<i>Brown, Gammons, and Poulson</i>	101
Advances in Precious-Metal Mineral Exploration at Broadway Gold’s Cu–Au Madison Project in the Silver Star Mining District, Montana	<i>Mulholland and Smeenk</i>	113
Cathodoluminescent Quartz Textures Reveal Importance of Recrystallization in Veins Formed in the Butte Porphyry Cu–Mo Deposit.....	<i>Acosta, Reed, and Watkins</i>	121
An Overview of the Pogo Gold Mine (AK).....	<i>Ethan L. Coppage</i>	127
Preliminary Structural Analysis and Geologic Relationships between Precambrian Belt Rocks and Oligocene Igneous Rocks in the Kofford Ridge 7.5' Quadrangle, Northwestern Montana.....	<i>Smith and Scarberry</i>	131
Carlin-Type Gold Deposits: Exploration Targets and Techniques at the Gold Bar District, Roberts Mountain, Nevada	<i>Ian Kallio</i>	137
Mineralogy and Fluid Inclusion Study of the Crystal Mountain Fluorite Mine, Ravalli County, Montana.....	<i>Gronidin and Gammons</i>	141

**PROCEEDINGS,
MONTANA MINING AND MINERAL SYMPOSIUM 2018
TECHNICAL PAPERS AND ABSTRACTS
Special Publication 120**

Edited by Kaleb C. Scarberry and Susan Barth
Montana Bureau of Mines and Geology



Bruce Cox discusses the geology of the Cable Mine (photo: A. Roth).



The student poster session at Montana Tech (photo: A. Roth).

Annual Update on Mining in Montana

Garrett Smith

Geochemist, Montana Department of Environmental Quality, Helena, Montana

Background and Duties

The Hard Rock Mining Bureau (HRMB) is the program within the Montana Department of Environmental Quality that regulates the mechanized exploration and development of all ore, rock, or mineral substances from hard rock sources. Although that definition encompasses a wide variety of operations, the resources that are excluded from the HRMB's authority include bentonite, clay, coal, natural gas, oil, peat, sand and alluvial gravel, scoria, soil materials, and uranium. In general, the HRMB oversees the operations conducted under small miner exclusion statements (SMES, ≤ 5 acres), exploration licenses, and operating permits.

The administrative duties and the permitting procedures that apply to the HRMB originate primarily from the Metal Mine Reclamation Act and Montana Environmental Policy Act, which were both enacted in 1971 (see 82-4-301, MCA and 75-1-101, MCA). These duties include issuing timely and complete decisions for permit applications and modifications, and ensuring permitted mineral development occurs with adequate protection of other resources. This is often coordinated with other permits obtained through State or Federal agencies. The HRMB also reviews the annual reports or renewal statements submitted by the operators, and conducts annual inspections to review the mining and reclamation status at each site and to offer compliance assistance. Performance bonds (i.e., financial assurances) are held by HRMB for operating permits, exploration projects, and some SMES sites, in order to perform any potential reclamation work that is not completed by the operator. The bonds are reviewed annually and recalculated at a minimum of every 5 years or following significant permit modifications.

Operating Permit Updates

The following discussion focuses primarily on hard rock operating permits and proposed projects that are currently under review, but it does not address the many active SMES (>400) and exploration projects (>150) underway across the State. As of September 2018, there are 78 permits administered by HRMB, which include 7 sites in the process of reclamation and closure, and 10 pending permits that are under the HRMB's review or awaiting actions from the operator or cooperating agencies before work can begin. There are also several permits that include multiple mining locations under one operation and reclamation plan. This is more common with quarries and surficial rock picking operations, which typically acquire specific types of rock from relatively small locations spread over a large area. Considering these additional locations, there are currently 229 sites covered by operating permits (fig. 1) and inspected by HRMB staff.

Hard rock mining and milling permits encompass a total area of approximately 87,000 acres (<0.1% of Montana), but a smaller fraction of that land is actually disturbed by mining operations. Many of the sites contain a permitted disturbance area within a relatively larger permit area, which often corresponds to property ownership boundaries. The operations that supply rock products (e.g., rip rap, railroad ballast, decorative and dimensional stone) account for 45% of all land permitted for hard rock mining. Base metal mines (e.g., Cu, Mo, Pb, Zn) cover 23% of all permitted land, while precious metal mines (e.g., Au, Ag, Pt, Pd, Rh) cover just under 20%. The remaining land is permitted for mining, milling, and processing a wide variety of products, including cement materials, talc, limestone, garnets, and sapphires.

When reviewing the number of actively producing operations (i.e., generating material and revenue), it becomes clear that rock product sites outnumber the industrial mineral and metal mine sites. Decorative and dimensional stone operations often benefit from low market barriers, meaning the capital and equipment requirements to begin an operation are relatively low, the operation and reclamation plans are relatively simple, and permitting actions for rock product operations often receive little public attention or litigation. Markets may be more volatile for base metal and precious metal mines, but some active operations have applied to amend their

Hard Rock Operating Permits 2018

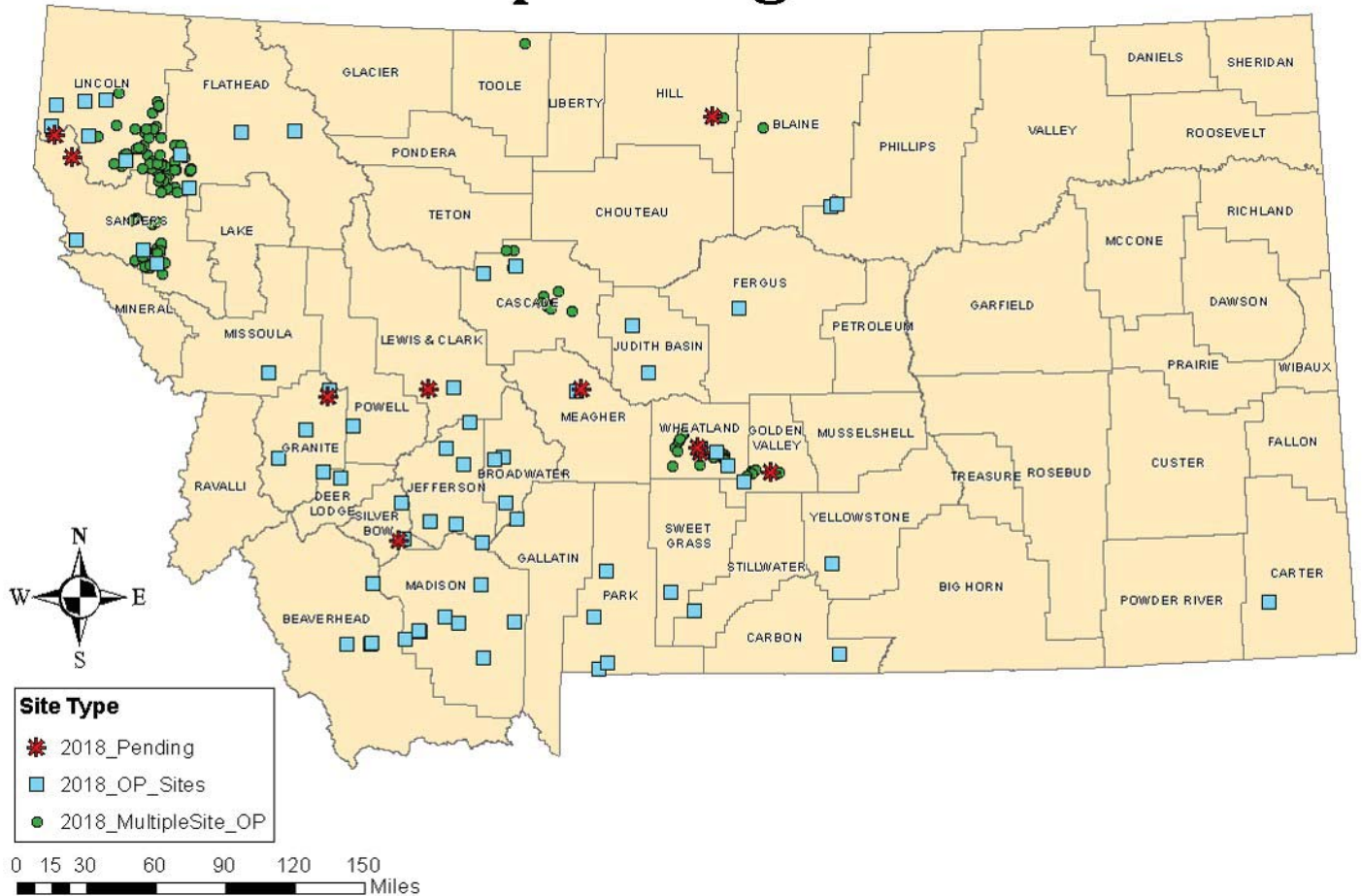


Figure 1. Map showing the location of Operating Permit (OP) sites, multiple quarry sites that are grouped under one OP, and pending OP sites that are dependent on a response from the operator or permitting action from the agency before work can begin.

permits to extend production. Most of the metal mines in Montana are currently in care and maintenance status or in the process of final reclamation and closure. In contrast, many industrial mineral mines and rock quarries have amended their permits in recent years to extend production. Surficial rock picking operations continue to expand, but they are also experiencing increased competition in many regions. Updates about some of the major developments at active operations and pending projects are included below.

Continental Mine, Montana Resources (Cu, Mo, Ag)

Montana Resources in Butte continues to produce ore from the D-North area of the Continental Pit, while stripping overburden in the D-East expansion area to expose additional ore reserves. The overburden is being used as construction material around the site, particularly for raising the tailings embankment to a higher elevation. Copper concentrates were also produced from leach pad solutions at the Horseshoe Bend precipitation plant, and the nearby water treatment plant continued to treat the effluent stream for reuse in the mill circuit.

In mid-2018, Montana Resources began receiving waste material removed from the Parrot Tailings area, near the Butte Silver Bow county shops and Civic Center. The waste removal is conducted under the direction of the Natural Resource Damage Program, with the excavated material then stockpiled and disposed within waste facilities on the mine site. Through 2017 and 2018, Montana Resources has conducted reclamation on approximately 90 acres of the East Dump Complex, which is visible to the public on the southern and eastern sides of the mine site.

In late 2017, Montana Resources submitted a permit amendment application to HRMB to raise the west embankment of the tailings facility to an elevation of 6,450 ft (fig. 2). Among other construction logistics, this



Figure 2. Northwest view across the tailings impoundment at Montana Resources in Butte. An amendment application was submitted to raise the elevation of the west embankment (distant center of photo) and increase the storage capacity of the facility.

expansion would necessitate water management on the west side of the facility, to prevent tailings pond seepage and potential degradation of groundwater beneath the nearby ridge. The baseline studies and engineering designs for the expansion have been reviewed by an Engineer of Record and Independent Review Panel, as specified in 2015 legislation. HRMB provided a draft approval of the permit amendment in August 2018, and is now working on an Environmental Impact Statement (EIS) to analyze and disclose potential impacts related to the amendment.

Golden Sunlight Mine, Barrick Gold Corp. (Au, Ag)

Since late 2015, Golden Sunlight has been producing ore from the underground workings within Mineral Hill Pit. Underground development continues at the mine, and the mill operates in batch mode. The mill also continues to receive and process material brought in by third parties, often originating from historic waste rock and tailings from across the region. This program generates revenue, as third party ore suppliers are paid for gold recovery, and it provides an environmental benefit to the waste removal sites. Some small operators have been limited by the low grades found in the waste and by current gold prices, which have fluctuated between \$1,200 and \$1,350 per ounce in the past 12 months.

Recent revisions to the permit include management of storm runoff from the Far East Dump and a runoff diversion channel near the North East Dump Complex. Reclamation work continues on portions of the North East Dump Complex and the Far East Dump. Golden Sunlight submitted an amendment application in 2017 for the development of new underground workings in the Apex area, to the north of Mineral Hill Pit. The ore mineralogy in the Apex area is similar to that in Mineral Hill Pit, but the underground mining method would target pods of ore, located within 100 to 900 ft below ground surface. An Environmental Assessment (EA) was prepared by HRMB through 2018, and the final draft of the EA is anticipated in the fourth quarter.

Stillwater Mine (Nye), Sibanye–Stillwater Ltd. (Pt, Pd, Rh, Au, Cu, Ni)

Stillwater Mining Co. was acquired by Sibanye Gold Ltd. of South Africa in mid-2017, becoming Sibanye–Stillwater Ltd. Normal operations continued through 2018 at the Stillwater Mine near Nye. The Tunnel Boring Machine located at the 5000 East Portal is being utilized for advancing the underground workings as part of the Blitz project. A new portal will be developed on the Blitz side, just north of the existing portal. Expansion of the East Side Waste Rock Dump continued, with liner placement occurring in phases before the waste rock is placed and then contoured, soiled, and seeded. Following infiltration testing and a dye tracer study, two infiltration ponds were constructed at the Hertzler impoundment. Other changes include an expansion of the biological water treatment to handle 3,000 gallons per minute, and upgrades to the east side rail system.

East Boulder Mine, Sibanye–Stillwater Ltd. (Pt, Pd, Rh, Au, Cu, Ni, Co)

Similar to the Stillwater Mine, the East Boulder Mine continued normal operations through 2018. A permit revision for a groundwater mixing zone was approved by HRMB and the Forest Service, which will address non-point release of nitrogen to groundwater. The mixing zone will allow the company to address cumulative contributions to a groundwater nitrate plume from various sources within the permit boundary. These internal sources include meteoric water infiltration through the tailings impoundment embankments built from waste rock. Other site activities include planning upgrades for the portals and raising the impoundment through Stages 4 and 5, which should provide additional tailings storage capacity to 2030. The Forest Service will develop an environmental review document for the Stage 6 expansion, which would increase storage area to the west of the current impoundment footprint. The company is also developing plans for a potential waste rock storage site and associated water management features in Lewis Gulch.

Troy Mine, Hecla Mining Co. (Cu, Ag) Closure

After acquiring the Troy Mine in 2015, Hecla Mining Co. (Hecla) continues to implement the reclamation plan, by demolishing the mill and other surface structures, maintaining the pipeline to convey mine water to the impoundment, and by covering and vegetating other portions of the impoundment. An amendment was submitted in 2017 to change the soil capping thickness on the impoundment, which was approved following HRMB's issuance of Record of Decision 1/8/2018. Reclamation work was conducted on the tailings impoundment through mid-2018.

Black Butte Copper Project, Sandfire Resources America Inc. (Cu) Pending

Sandfire Resources (formerly Tintina Resources) submitted an operating permit application to develop the upper and lower Johnny Lee copper deposits, located approximately 15 mi north of White Sulphur Springs. The underground mine would utilize "cut and fill" methods to extract ore and backfill the completed stopes with cemented paste tailings. The proposed facilities would include a lined surface impoundment that would contain cemented paste tailings and waste rock, storage ponds for process water and storm water collection, a water treatment plant, groundwater infiltration galleries for treated water discharge, a cement plant, and a mill facility with crushing and flotation capabilities.

The HRMB issued a draft approval of the mine permit application in September 2017. Further development of the project requires additional permits and plans outside the authority of HRMB, covering components like air quality, the discharge of treated water, and water rights. An EIS is currently being prepared to analyze and disclose potential impacts related to the project.

Montana Limestone Resources, LLC (Limestone, Lime)

Montana Limestone Resources is proposing to develop a limestone mine and a plant to produce lime. The new permit area would encompass 546 acres, located approximately 2.5 mi west of Drummond. The project would consist of multiple quarry areas and associated mine infrastructure, producing roughly 7,000 tons of Mission Canyon Formation limestone per week. Other facilities would include a crushing and screening plant, a preheater rotary kiln that processes limestone into lime, and facilities to store, load, and ship the final product. The HRMB issued a draft approval of the permit application in 2018, and the HRMB will now prepare an EA for the proposed project.

Yellowstone Mine, Imerys S.A. (Talc)

Construction began in 2017 to relocate the primary site access road to the south of its previous location. The construction of a new road was necessary to allow for expansion of the East Overburden Disposal Area. The road was conceptually approved by HRMB in Amendment 7 (2006), but more details were provided by Imerys prior to the start of construction. Substantial soil resources were salvaged during the preparation of the new road footprint and will be used later for reclamation. The pit layback known as "Phase 6" is still underway, which will involve removing overburden from the northern end of the pit over approximately 10 years. As ore

is exposed by the Phase 6 layback, the next phase of future development will start at the south end of the pit, requiring relocation of the on-site mill facility. Reclamation work is taking place at the north end of the site, and as the old North Main pit is backfilled, the final reclaimed surface will be contoured to promote drainage from the area.

Barretts Minerals Inc., Minerals Technologies, Inc. (Talc)

Treasure Mine: In 2017, the HRMB approved a layback expansion within the Treasure Chest Pit that would encompass about 15 acres in the existing pit. This layback would modify the pit topography by deepening the bottom elevation, and it would also contribute more material for backfill on the west side of the adjacent pit. However, the layback is not anticipated to start in the near future.

Regal Mine: A permit amendment application was submitted in March 2018 to expand the Regal Pit (fig. 3) to access more talc at depth. This expansion would necessitate further dewatering in the pit area and mitigation plans for potential impacts to surface water in both Hoffman and Carter Creeks.

Barretts Mill: A series of minor permit revisions were submitted for the excavation of two ponds that contain mill tailings. Ponds F and G were cleaned out and the containment berms were raised in order to increase the tailings storage capacity. The excavated mill tailings were disposed in dry dump areas, adjacent to the active ponds. An optical sorting system was added to the mill facilities in 2018.



Figure 3. North-facing view of the Regal Mine near Dillon, operated by Barretts Minerals Inc. A permit amendment application was submitted to expand the pit to access additional talc reserves, primarily through deepening and layback of the northern half of the pit.

Geyser Mine, Grupo Cementos de Chihuahua (formerly CRH) (Gypsum)

In 2018, all of the CRH operations in Montana were acquired by Grupo Cementos de Chihuahua. An amendment was approved to expand their gypsum mine located to the south of Geyser in Judith Basin County. Mining at the Geyser site occurs based on demand during the year, but anticipated production may increase to 25,000 tons of ore per season. Gypsum ore is hauled by truck to the cement plant located in Trident, approximately 150 mi south of the mine. The amendment increased the permit area by 19 acres to allow the company to mine an area to the east of the current quarry, extending production by approximately 3 years. This eastern extension is located on land administered by the Montana Department of Natural Resource Conservation.

Red Wash Quarry, Garnet USA, LLC (Garnet)

Garnet USA operates the Red Wash site and processing plant located near Alder in Madison County. Historic production in the area relied upon garnets found in alluvial deposits and through reprocessing previously dredged placer tailings. The current operation produces garnets from a bedrock deposit consisting of gar-

net-bearing amphibolite and garnet–quartz–feldspar gneisses containing 10–60% garnet. A permit revision is anticipated in the near future for the southward expansion of the quarry in the “South 80,” to access ore. Upgrades have also occurred around the plant site, including an expansion to walkways and the parking area for haul trucks, and moving the main entrance gate.

Rock Products, Various Companies

There are multiple operating permit applications that have been submitted recently to the HRMB for rock product operations. Pending sites include T.P. Construction near Havre, the Ibex Quarry near Heron, and Homestead Quarry (Kootenai Rocks) and Gordon Jones Ranch, both located south of Harlowton.

E.S. Stone and Structure continues to produce rock from many sites across north-central Montana (fig. 4). Two sites that were approved in 2017 (sites #19 and #20) are located to the north and south of Vaughn, respectively. An amendment was approved in July 2018 for site #21, located in between other permit areas to the south of Harlowton. The permits for Venture Stone and Block Mountain Slate and Stone were finalized upon receipt of the performance bonds for each operation. Venture Stone operations consist of an office and mill site near Vaughn and five rock picking locations to the south–southeast of Great Falls, in Cascade County. Block Mountain Slate and Stone operations consist of seven rock picking and quarry sites near Plains, in Sanders County. A newly permitted site on the far east end of the state is the “Brownfield Ranch” site near Hammond. The site is being operated by Carter County to produce sandstone aggregate for construction and maintenance projects.



Figure 4. A surface rock picking operation by E.S. Stone and Structure near Ulm. Rock from this area is desirable to current markets due to its color and the abundance of moss or lichen growth.

Small Mines and Mineral Exploration in Montana: Regulatory Overview and Examples from the Field

Whitney Bausch and Jake Mohrmann

Environmental Science Specialists, Montana Department of Environmental Quality,

Small Miner and Exploration Program, Helena, Montana

Regulatory Overview

The Small Miner and Exploration Program operates within the Montana Department of Environmental Quality (DEQ) Hard Rock Mining Bureau (HRMB). As a whole, the HRMB regulates hard rock exploration and mining activities in the state of Montana that exceed the definition of recreational mining, and is tasked with administering the Metal Mine Reclamation Act (MMRA—see 82-4-3 of the Montana Code Annotated, MCA). The MMRA outlines three regulatory instruments for hard rock mining and exploration: the Operating Permit (OP), the Small Miner Exclusion Statement (SMES), and the Exploration License.

Operating Permits

Large mines like Montana Resources' Continental Mine, and Sibanye–Stillwater Ltd.'s Stillwater and East Boulder Mines, are operated under OPs. Issuance of an OP is a state action and must undergo an environmental review under the 1971 Montana Environmental Policy Act (MEPA—see 75-1-1, MCA). An environmental review for an OP can be in the form of either an environmental assessment or an environmental impact statement. The permittee must submit a performance bond for reclamation of all proposed mining disturbance to DEQ before commencing operations.

Small Miner Exclusion Statements

Small mines that produce under 5 acres of surface disturbance can operate under an SMES. An SMES is an affidavit certifying that the operator submitting the SMES agrees to a set of rules (82-4-305, MCA) that, if followed, exempt the operator from acquiring an OP. An SMES operator may not hold more than two unreclaimed SMES sites at a time, and those SMES sites must be located at least 1 mi from each other at their closest points.

Acceptance of an SMES affidavit by DEQ is not a state action, and is not subject to an environmental review under MEPA. DEQ holds no performance bond for reclamation of SMES sites, with the exception of placer operations and operations that utilize impoundments to store waste and ore from processing. Unbonded SMES operators are not required to reclaim their sites. A placer SMES can be bonded up to \$10,000 and sites must be reclaimed. A performance bond for an impoundment must equal the State's calculated cost estimate of reclaiming the disturbed land, and the impoundment must be reclaimed.

Exploration Licenses

Exploration for hard rock resources must be conducted under an Exploration License. Issuance of an Exploration License or approval of an amendment to an Exploration License is a State action, and is subject to an environmental review under MEPA. A licensee must submit a performance bond to DEQ for all proposed disturbance, and all disturbance carried out under an Exploration License must be reclaimed within 2 years after the operation ceases.

Small Miner and Exploration Program

The Small Miner and Exploration Program is operated by two DEQ technical staff, with each staff member serving as the main contact for either the north half or south half of Montana. There are approximately 400 active SMES sites in Montana at any one time, with roughly 200 sites located in each half of the state.

SMES operators mine a variety of commodities using a number of methods (fig. 1). Common products and methods include decorative rock and riprap mining in northwest and central Montana that utilize open pits, trenches, and talus collection; aggregate mining in north-central Montana that utilizes open pits; sapphire mining in central Montana and Granite County using underground and placer methods; and metal mining in south-



Figure 1. SMES operations in Montana. Clockwise from top left: a decorative stone quarry in Sander County; entrance to an underground gold operation in Lewis and Clark County; a placer sapphire operation in Lewis and Clark County.

west and south-central Montana utilizing placer and underground methods, as well as reprocessing legacy ore piles (e.g., Golden Sunlight Mine). The only SMES site reclamation requirements are for placer operations.

On average, there are about 140 active Exploration Licenses in the State at any one time, but fewer than 25 active exploration operations are carried out each year. Licensees may keep their license active even if they do not intend to carry out any exploration that year. Modern exploration methods include core drilling, trenching, placer, and underground bulk sampling (fig. 2).

Proposed exploration operations are bonded based on the resulting disturbance to the landscape. Reclamation of exploration operations includes plugging drill holes according to 17.24.106 of the Administrative Rules of Montana and regrading, reseeding, and weed control on all surface disturbances including new roads, drill pads, drill sumps, and exploration trenches. Exploration operations may be inspected prior to and during operations. Reclamation inspections are conducted after operations have ceased in order to ensure that reclamation has been successful, after which a bond may be released back to the operator.

Updated Field Methods: Unmanned Aerial Vehicles (UAVs)

In 2017, the HRMB began using UAVs to collect aerial imagery during field inspections of OP, SMES, and Exploration License sites. The imagery is processed to create aerial maps of each site. This technique is particularly useful for SMES sites because one of the major considerations for SMES sites is total disturbed acreage, which should amount to less than 5 acres. Exploration License and Operation Permit site aerial imagery is used to calculate and update bonds, and track development of site operation and reclamation.



Figure 2. Examples of active exploration projects in Montana. Clockwise from top right: An exploration trench; a core drilling operation; a modern headframe built to access and remove samples from an historic underground shaft.

Part 107 of the Federal Aviation Administration (FAA) regulations requires that all non-hobbyist UAV operators hold a Remote Pilot Airman Certificate with a small unmanned aircraft rating. Currently, three HRMB technical staff hold Remote Pilot Airman Certificates, and routinely use a UAV during site inspections. FAA flight restrictions apply, but the remote location of many SMES and Exploration License sites means that they are largely unaffected by airspace restrictions related to airports, military operations, security, and other factors that restrict or prohibit use of some airspace. A UAV flight is limited to 400 ft above ground surface, and the UAV must be within line of sight of a visual observer throughout the entire flight. HRMB staff use a DJI Phantom 4Pro UAV operated with an iPad.

UAV-collected aerial imagery (figs. 3, 4) has increased the HRMB's ability to transparently and comprehensively regulate the hard rock mining industry. Orthomosaic maps produced from UAV imagery have dramatically improved the accuracy of modern site disturbance calculations. Without updated aerial imagery, the HRMB staff are limited to calculating disturbance acreage based on often-outdated imagery from Google Earth Pro and the U.S. Farm Service Agency National Agricultural Imagery Program. UAV imagery is processed using Pix4D-mapper, which produces orthomosaic maps and three-dimensional models. Three-dimensional site models (fig. 3) are used to create virtual site tours, and calculate cut-and fill volumes. Orthomosaic maps (fig. 4) are also processed in ArcMap to calculate disturbed acreage and produce annotated site maps.



Figure 3. Three-dimensional stone site model rendered by Pix4Dmapper from aerial imagery collected on site with UAV.



Figure 4. High-resolution orthomosaic map rendered by Pix4Dmapper using aerial imagery collected on site with UAV.

Building a Hard Rock Mineral Assessment for the State of Montana

Paul Thale¹ and John J. Metesh²

¹*GIS Manager,*

²*Director and State Geologist,*

Montana Bureau of Mines and Geology, Butte, Montana

Introduction

The Montana Bureau of Mines and Geology (MBMG) is the repository and authority for geologic and mineral information for the state of Montana. The MBMG was established in 1919 at a time of great expansion of mines and mining in Butte and surrounding areas. Archived documents include maps, manuscripts, field notebooks, mine production records, photographs, and many other items related to mining and the geologic history of the State. The MBMG provides information about these archives to the public, mining companies, Federal, State, and local governments, and consultants for a variety of purposes.

The mineral potential of Montana is one aspect of the MBMG's archives that has received renewed attention from many entities in the State. Although certain areas of the State have been studied extensively (Butte, for example), a statewide compilation of mineral assessment has not been produced by government agencies for public or agency use. The MBMG has responded to two separate requests for information regarding mineral potential for the State, and we present some early results of these efforts here.

Motivation for the Study

The MBMG was asked by Senator Jon Tester's office in 2014 to identify areas of mineral potential on Federal lands in southwest Montana, mostly in the Beaverhead–Deerlodge National Forest. Senator Tester was trying to pass the Forest Jobs Recreation Act through Congress in an attempt to bring together timber, mining, and recreation interests to develop a mutually beneficial approach that would allow timber harvest and mining, while also protecting Wilderness Study Areas (WSAs). WSAs exist on both U.S. Forest Service (USFS) and U.S. Bureau of Land Management (BLM) lands, and those on USFS lands were of particular interest.

The MBMG responded to Senator Tester's request by compiling a series of mineral potential maps for areas of southwest Montana. Some of the maps specifically covered wilderness and wilderness study areas (table 1). Many of the map files were small graphics that were included as insets or small-scale maps (i.e., 1:500,000) of broad areas. This presented a problem since these existing map files were not meant to be used as spatially referenced (to real-world coordinates) data products. A decision was made to accept these maps for use in the project since few others existed for these

Table 1. List of publications regarding the U.S. Bureau of Land Management Wilderness Study Areas mineral potential (from U.S. Geological Survey, 1990).

Area Name	USGS Report
Antelope Creek (A)	Bulletin 1722-C
Beaver Meadows	Open File Report 84-0566
Big Horn Tack-On	Bulletin 1723
Blacktail Mountains	Bulletin 1724-B
Burnt Lodge	Bulletin 1722-A
Burnt Timber Canyon	Bulletin 1723
Centennial Mountains	Miscellaneous Field Map 1342-B
Cow Creek	Bulletin 1722-C
Farlin Creek	Bulletin 1724-C
Humbug Spires	Open File Report 80-836
North Fork Sun River	Open File Report 84-0566
Pryor Mountain	Bulletin 1723
Quigg West	Bulletin 1724-D
Ruby Mountains	Bulletin 1724-A
Seven Blackfoot (A)	Bulletin 1722-D
Seven Blackfoot (B)	Bulletin 1722-D
Sheep Creek	Bulletin 1724-
Sleeping Giant	Bulletin 1724-E
Square Butte	Miscellaneous Field Map 1370
Terry Badlands East	Bulletin 1722-B
Terry Badlands West	Bulletin 1722-B

areas.

Staff from Senator Steve Daines' office approached the MBMG in 2017 requesting information similar to that of the Tester project. Senator Daines was working on a bill that would release some U.S. Forest Service WSA lands from consideration as wilderness. MBMG staff worked with geologic consultant Fess Foster to respond to Senator Daines' request. We decided to focus our efforts on a mineral potential assessment of the entire State of Montana, since the earlier project covered a relatively small area of the State (Beaverhead–Deerlodge National Forest; southwest Montana).

Mineral Assessment in Montana

The scope of our project required a broad set of data and a great investment of time and effort. A decision was made to limit the mineral resources considered for this project. We defined hard rock mineral commodities as: aluminum, antimony, arsenic, beryllium, bismuth, cadmium, calcite, chromium, cobalt, copper, fluorite, gold, iridium, iron, lead, magnesium, manganese, mercury, molybdenum, nickel, niobium, palladium, platinum and platinum group elements, rare earth elements, selenium, silver, strontium, talc, tellurium, thallium, tin, tungsten, vanadium, zinc, and zirconium. Barium, quartz, and silica were retained in the compilation because these commodities can be indicators of hard rock mineralization.

The hard rock commodities listed above were considered exclusively because of historic identification, mapping, and research into these resources in Montana. Other industrial mineral resources, such as abrasives, asbestos, clay, coal, diatomaceous earth, dolomite, feldspar, gems, geothermal, graphite, gypsum, kyanite, limestone, marble, mica, nitrogen, sodium, oil shale, pumice, sulphur, sand and gravel, thorium, travertine, vermiculite, and zirconium were deemed impractical for inclusion in our study at this early stage.

We compiled hard rock mineral potential data for all Roadless Areas, USFS Wilderness Study Areas, and BLM Wilderness Study Areas (WSAs) in Montana. Our study examines 254 areas that had hard rock mineral potential (all 214 USFS Roadless Areas, all 9 USFS WSAs, and 31 of the 38 BLM WSAs) and excludes 7 BLM WSAs that did not have hard rock mineral deposits. All data were compiled from sources available to the public, such as U.S. Bureau of Mines, U.S. Geological Survey, and MBMG publications. All Roadless Areas are on USFS lands and were designated by Congress. Note that mineral potential was not compiled for recommended wilderness areas that are designated in individual forest plans. These are informally (versus administratively) designated, and are constantly modified as individual forests update their plans.

All maps depicting mineral potential were incorporated, with the exception of maps showing only geophysical data. In some cases, identical maps appeared in more than one publication. In these situations only one of the maps was incorporated into the compilation to avoid redundancy. Additional descriptions of mineral potential are described in the text of the publications used for this compilation (cited here). Text discussions were not incorporated into this compilation.

Mineral Assessment Studies Maps for Montana

Our compilation produced areas of mineral potential in Montana from existing BLM WSA reports (fig. 1) and USFS reports (fig. 2). These maps are merely presented, and not analyzed or interpreted here. This compilation includes hard rock commodities, both metals and industrial minerals, which occur primarily within the orogenic belts of western and central Montana. The maps that were assembled in this compilation were meant to be used in a modern geographic information system (GIS). Having areas of mineral assessment studies in Montana in a single GIS system allows comparison to other data layers such as administrative boundaries, geology, water resources, existing/historic mines, etc. In particular, Wilderness Study Areas could be compared to identify mineral potential areas. The resulting compilation, however, was not meant to be anything more than a starting point for discussion of mineral potential relative to wilderness, wilderness study areas, and Roadless Areas.

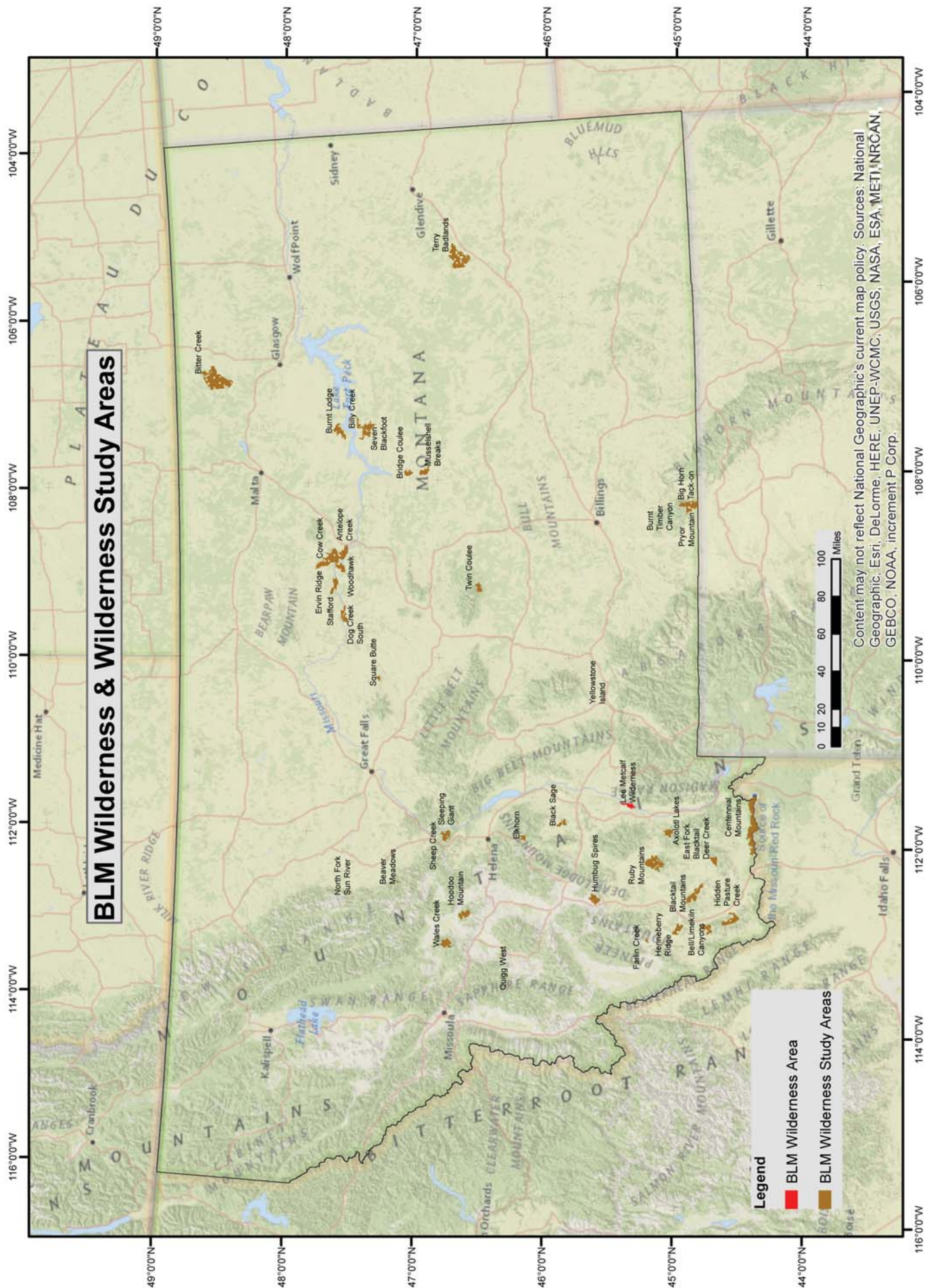


Figure 1. U.S. Bureau of Land Management Wilderness and Wilderness Study Areas in Montana.

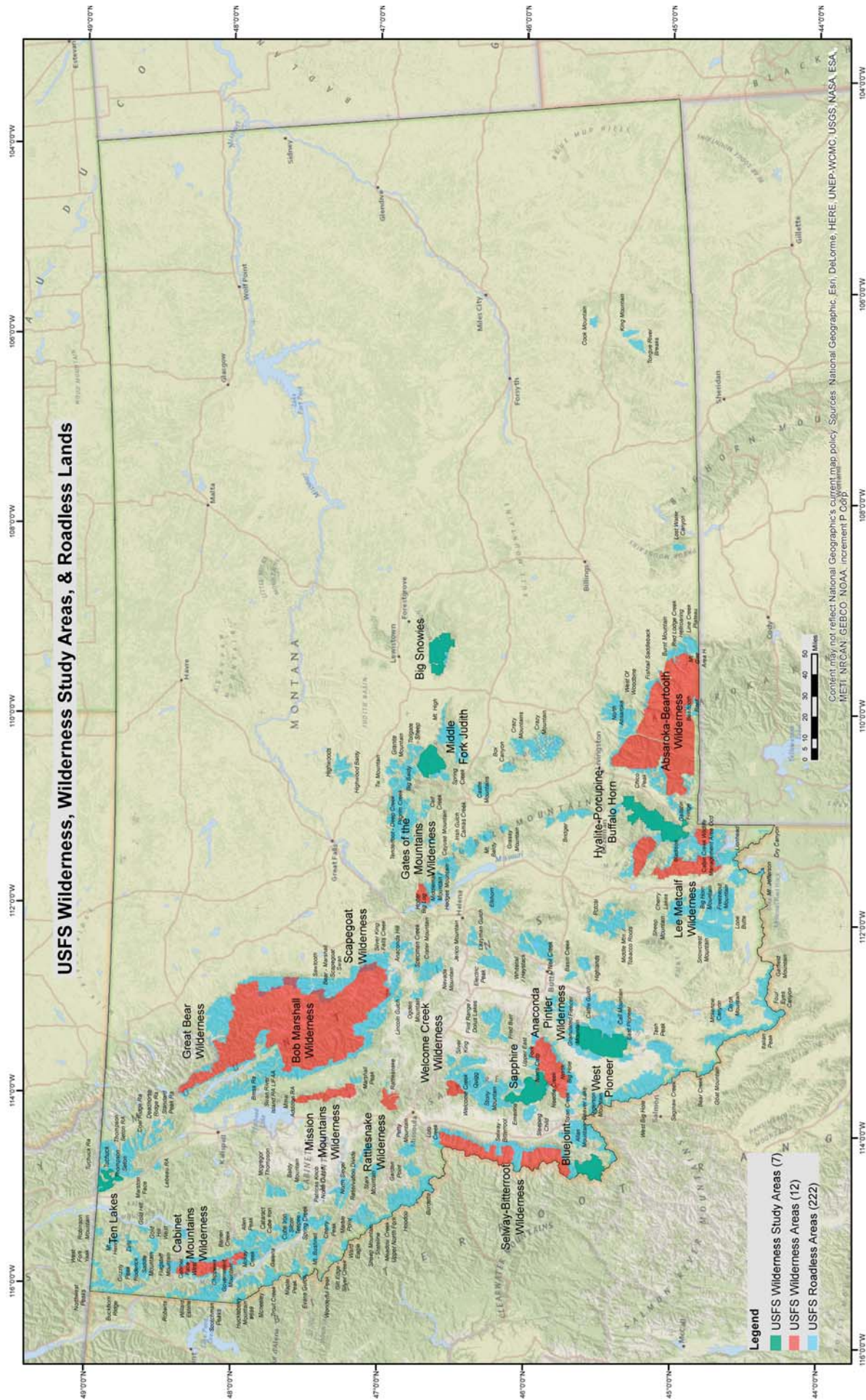


Figure 2. U.S. Forest Service Wilderness, Wilderness Study Areas, and Roadless Lands in Montana.

Publications Compiled in this Project

Individual U.S. Forest Service Wilderness Studies Areas

- Berger, B.R., Snee, L.W., Hanna, W., and Benham, J.R., 1983, Mineral resource potential map of the West Pioneer Wilderness Study Area, Beaverhead County, Montana: U.S. Geological Survey Map 1585-A.
- Greenwood, W.R., Ludington, S., Miller, W.R., Hanna, W.F., Wenrich, K.J., Suits, V.J., and McHugh, J.B., 1990, Mineral resources of the Elkhorn Wilderness Study Area, Broadwater and Jefferson Counties, Montana: U.S. Geological Survey Bulletin 1805, 37 p.
- Lund, K., Rehn, W.R., and Benham, J.R., 1983, Mineral resource potential maps of the Blue Joint Wilderness Study Area, Ravalli County, Montana, and the Blue Joint Roadless Area, Lemhi County, Idaho: U.S. Geological Survey Map MF 1557-A.
- Marsh, S.P., Kropschot, S.J., and Dickenson, R.G., eds., 1984, Wilderness Mineral Potential—Assessment of Mineral-Resource Potential in U.S. Forest Service Lands Studied 1964–1984: U.S. Geological Survey Professional Paper 1300, v. 2, p. 552–1183.

Includes: Blue Joint Wilderness Study Area, Montana; Elkhorn Wilderness Study Area; Flint Creek Range Wilderness Study Area; Middle Fork of the Judith River Wilderness Study Area; Ten Lakes Wilderness Study Area; West Pioneer Wilderness Study Area.

Individual U.S. Forest Service Roadless Areas

- Elliot, J.E., Waters, M.R., Campbell, W.L., and Avery, D.W., 1984, Mineral resource potential and geologic map of the Dolus Lakes Roadless Area, Powell and Granite counties, Montana: U.S. Geological Survey Map 1640-A.
- Elliot, J.M., Wallace, C.E., O'Neill, J.M., Hanna, W.F., Rowan, L.C., Segal, D.B., Zombelman, D.R., Pearson, R.C., Close, T.J., Federspiel, F.E., Causey, J.D., Willett, S.L., Morris, R.W., and Huffsmith, J.R., 1985, Mineral resource potential map of the Anaconda–Pintlar Wilderness and contiguous roadless area, Granite, Deer Lodge, Beaverhead, and Ravalli Counties, Montana: U.S. Geological Survey Map MF 1633-A.
- Lidke, D.J., Wallace, C.A., Antweiler, J.C., Campbell, W.L., Hassemer, J.H., Hanna, W.F., and Close, T.J., 1983, Mineral resource potential map of the Welcome Creek Wilderness, Granite County, Montana: U.S. Geological Survey Map MF 1620-A.
- Marsh, S.P., Kropschot, S.J., and Dickenson, R.G., eds., 1984, Wilderness Mineral Potential—Assessment of Mineral-Resource Potential in U.S. Forest Service Lands Studied 1964–1984: U.S. Geological Survey Professional Paper 1300, v. 2, p. 552–1183.

Includes: Big Snowies Wilderness Study Area and contiguous Roadless areas; Blue Joint Roadless Area; Dolus Lakes Roadless Area; Eastern Pioneer Mountains Roadless Area; Gallatin Divide Roadless Area; Italian Peak and Italian Peak Middle Roadless Areas; Madison Roadless Area; Middle Mountain–Tobacco Root Roadless Area; Mount Henry Roadless Area; North Absaroka study area Roadless; Rattlesnake Roadless Area; Sapphire Wilderness Study Area and contiguous Roadless areas; Scapegoat Wilderness and additions' Bob Marshall and Great Bear Wildernesses and adjacent study areas Roadless; Welcome Creek Wilderness Roadless.

- Mudge, M.R., Earhart, R.L., and Marks, L.Y., 1982, Mineral resource potential of the Reservoir-North and the Deep Creek Roadless Areas, Teton County, Montana, U.S. Geological Survey Open File Report 82-988, p. 13.
- Simons, F.S., and Van Loenen, R.E., 1988, Geochemical maps of the Madison Roadless Area, Madison and Gallatin counties, Montana: U.S. Geological Survey Map MF 1605-A.
- Simons, F.W., Van Loenen, R.W., Moore, S.L., Close, T.J., Dausey, J.D., Willett, S.L., and Rubsey, C.M., 1983, Mineral resource potential map of the Gallatin Divide Roadless Area, Gallatin and Park counties, Montana: U.S. Geological Survey Map MF 1569-A.

Skipp, B., Antweiler, J.C., Kulik, D.M., Lambeth, R.H., and Mayerle, R.T., 1983, Mineral resource potential map of the Italian Peak and Italian Peak Middle Roadless Areas, Beaverhead County, Montana, and Clark and Lemhi counties, Idaho: U.S. Geological Survey Map MF 1601-A.

Smedes, H.W., Hanna, W.F., and Hamilton, M., 1980, Geology and mineral resources of the Humbug Spires Instant Study Area (primitive area and adjacent Roadless areas), Silver Bow County, Montana: U.S. Geological Survey Open File Report 80-836, p. 25.

Multiple U.S. Forest Service Roadless Areas

Mudge, M.R., and Earhart R.L., 1978, Map showing appraisal of mineral resource potential of RARE II proposed Roadless areas in National forests, Montana (exclusive of coal, oil, gas, and construction materials): U.S. Geological Survey Open-File Report 78-972, 2 maps.

Williams, C.E., and Pearson, R.C., 1984, Mineral Resource Potential of National Forest RARE II and Wilderness Areas in Montana: U.S. Geological Survey Open File Report 84-637, 140 p.

Individual U.S. Bureau of Land Management Wilderness Study Areas

Tysdal, R.G., Reynolds, M.W., Carlson, R.R., Kleinkopf, M.D., Rowan, L.C., and Peters, T.J., 1991, Mineral resources of the Sleeping Giant Wilderness Study Area, Lewis and Clark County, Montana: U.S. Geological Survey Bulletin 1724-E, 31 p.

Multiple U.S. Bureau of Land Management Wilderness Study Areas

U.S. Bureau of Mines and U.S. Geological Survey, 1990, Mineral Summaries of Bureau of Land Management Wilderness Study Areas in Montana: Joint Publication, 238 p.

Large Tracts of Public Lands

Carlson, M.H., Zientek, M.L., Causey, J.D., Kayser, H.Z., Spanski, G.T., Wilson, A.B., Van Gosen, B.S., and Trautwein, C.M., 2007, A compilation of spatial digital databases for selected U.S. Geological Survey nonfuel mineral resource assessments for parts of Idaho and Montana: U.S. Geological Survey Open-File Report 2007-1101, 30 p.

Hyndman, P.C., McCulloch, R., Llett, G.W., and Rumsey, C.M., 1993, Availability of federally owned minerals for exploration and development in Western States: Montana: U.S. Bureau of Mines Special Report, 77 p.

Van Loenen, R.E., Siems, D.F., Bankey, V., and Conyac, M.D., 1983, Mineral resource potential map of the Mount Henry Roadless Area, Lincoln County, Montana: U.S. Geological Survey Map MF 1534-D.

Wallace, C.A., Lidke, D.J., Elliott, J.E., Antwieler, J.C., Campbell, W.L., Hassemer, J.H., Hanna, W.F., Banister, D.P., and Close, T.J., 1984, Mineral resource potential map of the Sapphire Wilderness Study Area and contiguous roadless areas, Granite and Ravalli counties, Montana: U.S. Geological Survey Map MF 1469-B.

Wallace, C.A., Lidke, D.J., Kulik, D.M., Campbell, W.L., Antweiler, J.C., and Mayerle, R.T., 1983, Mineral resource potential map of the Rattlesnake Roadless Area, Missoula County, Montana: U.S. Geological Survey Map MF 1235-D.

Water Chemistry Changes in the Berkeley Pit, Butte, Montana

Steve McGrath,¹ Gary Icopini,^{*,2} and Ted Duaime²

¹Analytical Chemist,

²Hydrogeologists,

Montana Bureau of Mines and Geology, Butte, Montana

*Presenting author

Background

The Berkeley Pit Lake in Butte, Montana is a remnant of nearly a century of copper mining by the Anaconda Mining Company and its predecessors. Underground mining in pursuit of precious-metal-enriched vein structures was conducted through the 1940s. As grades of copper declined, more efficient mining methods, such as block-caving and open pit techniques, were adopted. The Berkeley Pit began operation in 1955 to recover lower grade copper ore. The pit eventually consumed around 13% of the 5,600 mi of horizontal haul ways in the historic underground workings of Butte (fig. 1).

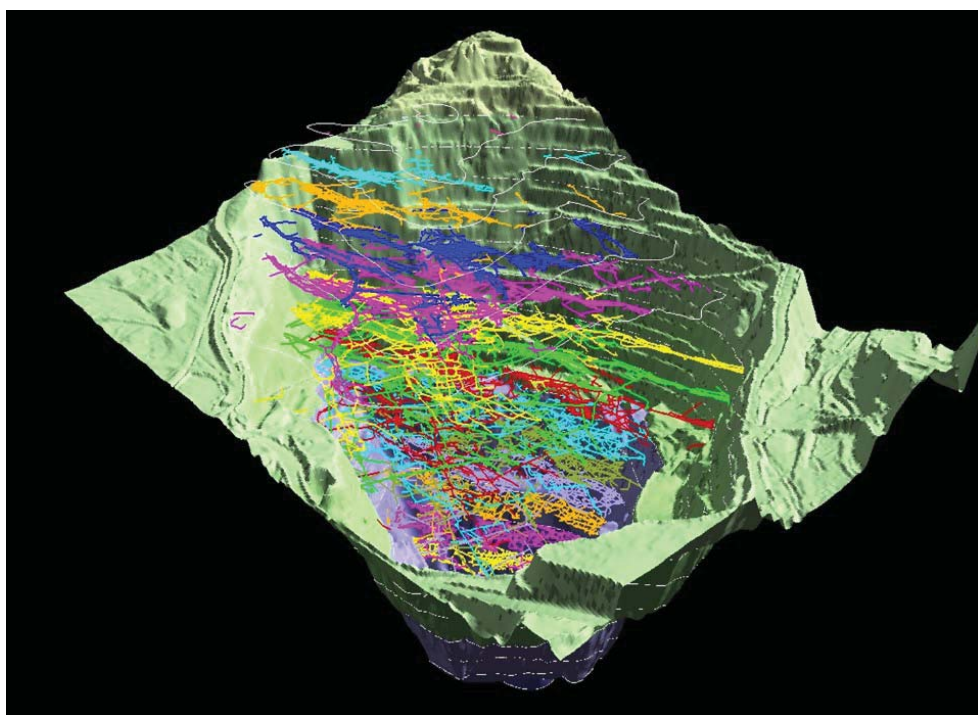


Figure 1. Three-dimensional model of the Berkeley Pit and historic underground workings. The view is from the southwest corner of the pit looking northeast. Colors correspond to levels in the underground workings. From Duaime and others, 2004.

Continuous dewatering of the underground mine workings was necessary for mining to continue. The Anaconda Mining Company, which had been purchased by Atlantic Richfield (ARCO), ceased all mining activity in 1982 and stopped pumping water from the underground workings. The Anaconda Company then established a groundwater monitoring network. Water levels in the mines rose over 1,300 ft in 1982 and another 800 ft in 1983. Meanwhile, contaminated water from Horseshoe Bend drainage (fig. 2) at the base of the tailings dam and other surface-water flows on the mine site were routed into the abandoned Berkeley Pit, and by

1983 the pit lake started to form. That same year the Berkeley Pit and the underground workings became part of the Environmental Protection Agency (EPA) Superfund program because of the potential for toxic heavy metals to contaminate Silver Bow Creek and the Clark Fork River.

Water continues to rise today in the Berkeley Pit, primarily from groundwater influx, including the abandoned underground workings. Surface water from the Horseshoe Bend drainage no longer drains to the Berkeley Pit and is instead diverted by Montana Resources, LLP (MR) for use in active mining in the adjacent Continental Pit. The diverted surface waters must be treated to precipitate metals and neutralize acidity before they can be used in mine operations. The treatment process precipitates metal (oxy) hydroxides in the form of a sludge, which is then discharged to the Berkeley Pit. The only other regular surface-water inputs to the Berkeley pit come from a minor amount of storm drainage and rain. At the same time as the water treat-

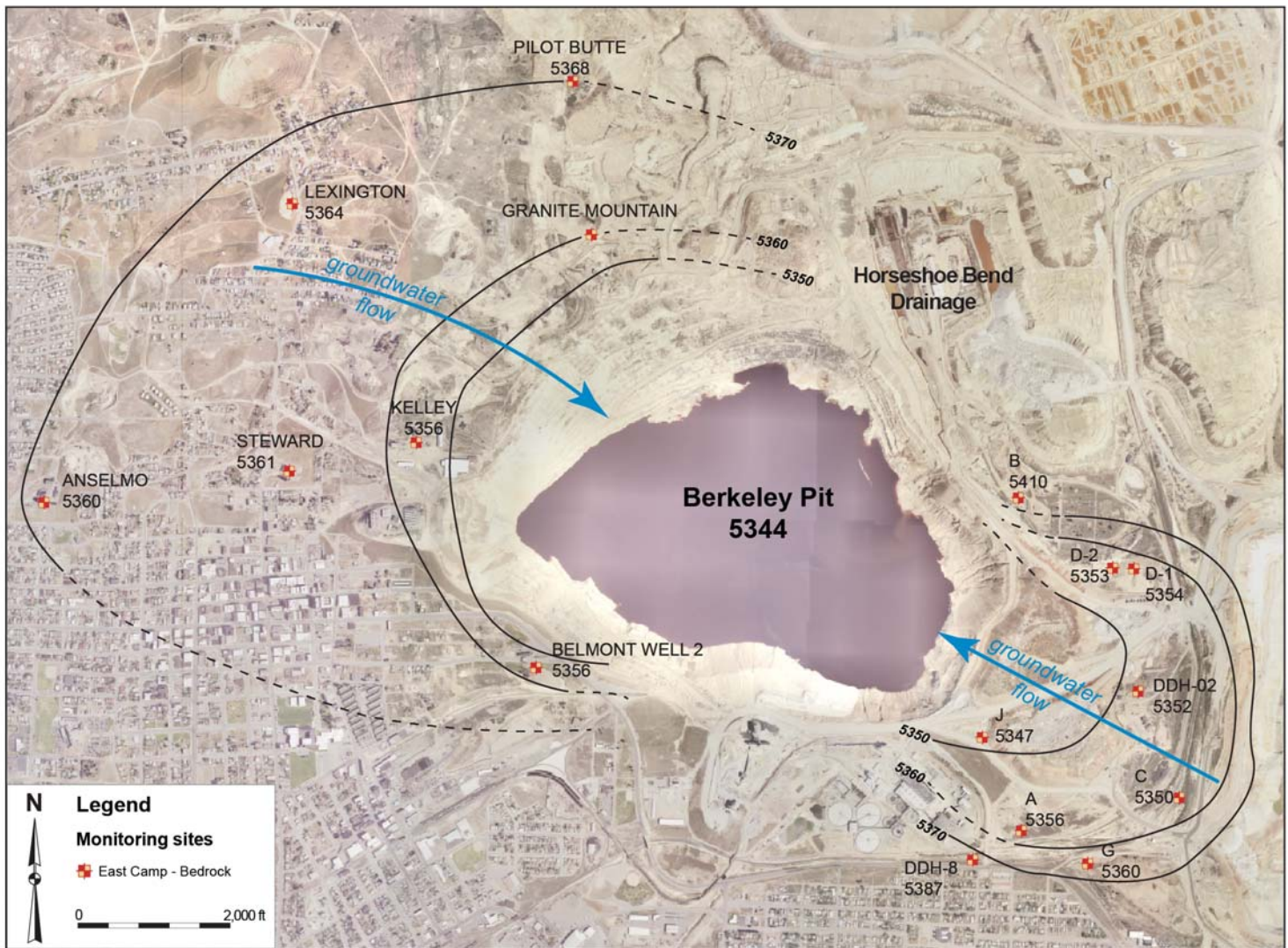


Figure 2. The potentiometric surface of the bedrock aquifer that surrounds the Berkeley Pit (Duaine and others, 2018b). Elevations are in feet above sea level. The Horseshoe Bend Drainage is located in the upper right quadrant of the figure.

ment plant began operation, MR recovered copper from pit water by pumping the water over scrap iron. This continued from 2004 to 2013, but the water was returned to the pit with no net reduction in volume of the pit. The copper recovery recirculated over one entire pit volume during the time it operated.

The Consent Decree (EPA, 2002) established a critical water level (CWL) of 5,410 ft that limited the elevation that points of compliance (POC) wells and mineshafts located near the pit could reach. The decree also stipulated that 2 years prior to water levels in any POC reaching the CWL elevation, treatment and discharge of excess water is required from the pit or nearby mineshafts or wells to prevent water from exceeding the CWL in any POC well or mineshaft. Water in the pit is lower than that in the surrounding mine workings, and therefore all groundwater in the area flows into the pit (fig. 2). As a result of this influx, the CWL will be reached in one of the outlying POC wells or mineshafts before the water in the Berkeley Pit reaches the CWL.

Currently, the Berkeley Pit is over 800 ft deep and contains more than 47 billion gallons of acidic water with high metal concentrations. Until about 2012, the pH of pit water ranged from 2.5 to 2.7 with total dissolved solids (TDS) of 12 g/L. Dissolved Iron (Fe) concentrations ranged from 200 to 1,000 mg/L, zinc (Zn) concentrations were around 600 mg/L, arsenic concentrations were 50 to 1,000 µg/L, and copper (Cu) concentrations were 40–150 mg/L (Duaine and others, 2018a).

Monitoring

The Montana Bureau of Mines and Geology (MBMG) has monitored physical and chemical parameters of the Berkeley Pit water since 1984, as established by the Consent Decree (CD). The CD specified a semi-annual schedule for water-quality parameter measurements and sample collection from multiple depths of pit water. Helicopters were used during the early years of pit sampling because vehicle access to the water was difficult due to severe erosion of the pit walls.

After MR restored vehicle access to the pit water, a pontoon boat was used to haze waterfowl from the lake surface and to monitor the water. Monitoring included depth profiles of water-quality parameters using a Hydro-lab Sonde (fig. 3) that sampled various depths in the water. The water samples were collected in the spring and fall to track changes in the water chemistry and to help understand the evolution of the physical characteristics of the lake.



Figure 3. A pontoon boat that was used to sample Berkeley Pit water until 2013 (Duaine and others, 2018a).

Regular sampling ended abruptly in 2013 when a landslide in the southeast corner of the pit generated a large tsunami-like wave that destroyed infrastructure in the pit. The access ramp and boat dock were damaged, as was the pump system that MR had used to send pit water to their copper recovery operation. Concerns over personnel safety led to a ban of manned boat operations, which effectively suspended sample collection of pit water.

Sampling resumed in 2017 after ARCO and MR commissioned the development of a remotely controlled drone boat (fig. 4) to be designed by the Electrical Engineering Department at Montana Tech in collaboration with the MBMG. The boat is semi-automatous and can automatic-

ly navigate from the shore to a predetermined sampling location. The boat can also be controlled by operators from an observation point on the Berkeley Pit rim (fig. 5). The monitoring system on the boat was designed to



Figure 4. The aquatic drone craft that was developed by Montana Tech and the MBMG for remote sampling of Berkeley Pit water.



Figure 5. Photograph of the drone craft responding to commands sent from operators stationed on the Berkeley Pit rim. Note drone control antenna in the foreground.

record and send water-quality parameter data to operators in real time. After water-quality profiles are collected, sampling depths can be determined to ensure that they were collected at representative depths within the pit water column. Water samples are collected by lowering a hose into the water column that uses a peristaltic pump to transfer the sample into bottles of an ISCO sampler. An additional peristaltic pump purges the sampling pump tubing between samples. Software and hardware developed for the boat sampling equipment allows for control of ISCO sampler from the observation point and real-time monitoring of the sampling process with video observation.

Changes in the Berkeley Pit Lake from 2012 to 2017

After the 2013 landslide, continuous pumping associated with copper recovery ceased and the lake sat undisturbed. Although water chemistry data was not collected from 2013 to 2017, the lake looked markedly different in 2017 than it did in 2003 (fig. 6). Prior to 2013, the Berkeley Pit water had a rusty reddish/brown color with limited light transmittance. After 2017, the Berkeley Pit had become translucent with a bluish/green color.



Figure 6. Berkeley Pit water in 2003 and in 2017 (MBMG).

Pit lake profile data collected before 2013 compared to data collected in 2017 and 2018 reveal that changes in color and light transmittance were caused by changes in physical processes and water chemistry. Temperature, pH, dissolved oxygen, and turbidity profile data collected during 2011/2012 fall and spring sampling are quite different from data collected during 2017/2018 fall and spring sampling (fig. 7). Although the profiles show the influence of wind mixing in the upper 50 ft, the profiles do not show significant stratification of physical or chemical parameters associated with development of temperature or chemical gradients in the water column either before the landslide or after. The lack of stratification prior to 2013 may be associated with continuous circulation of pit water during copper recovery operations (e.g., Tucci and Gammons, 2015). The fall and spring 2013 temperature profiles are nearly identical at depth, both before and after the sampling hiatus. Further, the fall and spring 2013 temperature profiles differ from each other by more than 1°C to depths greater than 600 ft, suggesting that the pit experienced mixing by lake turnover during the winters of both 2011/2012 and 2017/2018.

The contrast between the 2012 pH and dissolved oxygen profiles and the 2017 and 2018 profiles is striking (fig. 7). The pH of the pit water increased by up to 1.5 pH units between the 2012 and 2018 profiles. Dissolved oxygen from the 2018 profile shows a more than threefold increase relative to the 2011 profile. Essentially, the pit has gone from anoxic to oxygenated conditions. Both pH and dissolved oxygen are related to the behavior of iron. Between 2004 and 2013, MR ran the copper recovery operation that continually discharged recycled water

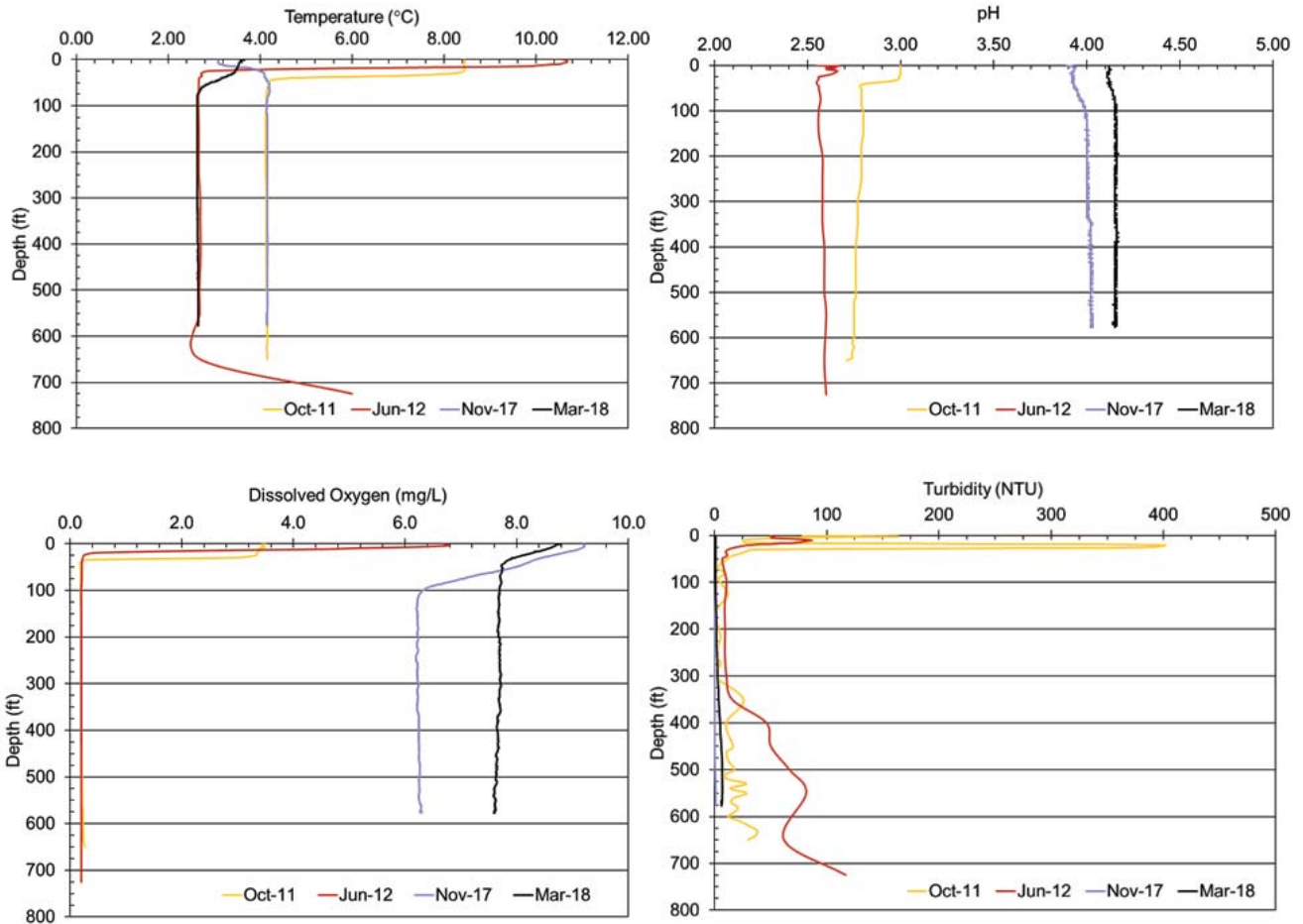
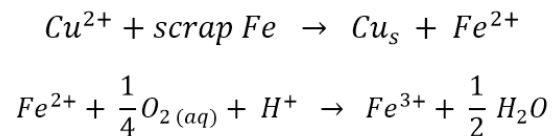
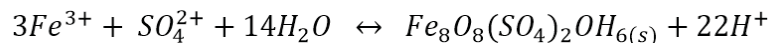


Figure 7. Physical parameter profiles of the Berkeley Pit collected prior to the landslide of 2013 and after sampling resumed in 2017 (Duaine and others, 2018b).

back into the pit. The recycled water contained elevated ferrous iron (Fe^{2+}), which reacts with dissolved oxygen:



The reddish/brown and opaque appearance of the pit in 2003 (fig. 6), and the high turbidity values of the 2011 and 2012 profiles (fig. 7), are reflecting the continuous precipitation of (oxy) hydroxide solids during the period when copper recovery was active. (Oxy) hydroxide precipitation generated hydrogen ions, which acted to maintain a low pH throughout the pit water profile. While copper recovery was underway, continuous circulation of pit water transported Fe^{2+} to the lower depths of the pit, where its reaction with dissolved oxygen depleted the concentration of dissolved oxygen at depth and generated ferric iron (Fe^{3+}). The elevated Fe^{3+} concentration led to precipitation of (oxy) hydroxides of iron, notably schwertmannite (Tucci and Gammons, 2015):



Treatment of metal-laden acidic Horseshoe Bend surface water began in 2003 and produced an average discharge of 0.26 million gallons per day (MGD) of highly alkaline sludge waste into the pit. So, copper recovery and water treatment occurred simultaneously between 2004 and 2013. The combined effect of the two processes is thought to be responsible for decreases in dissolved Fe and As in Berkeley Pit water (fig. 8). Between 2012 and 2017, Fe and As were reduced throughout the pit volume to the point where dissolved As would comply

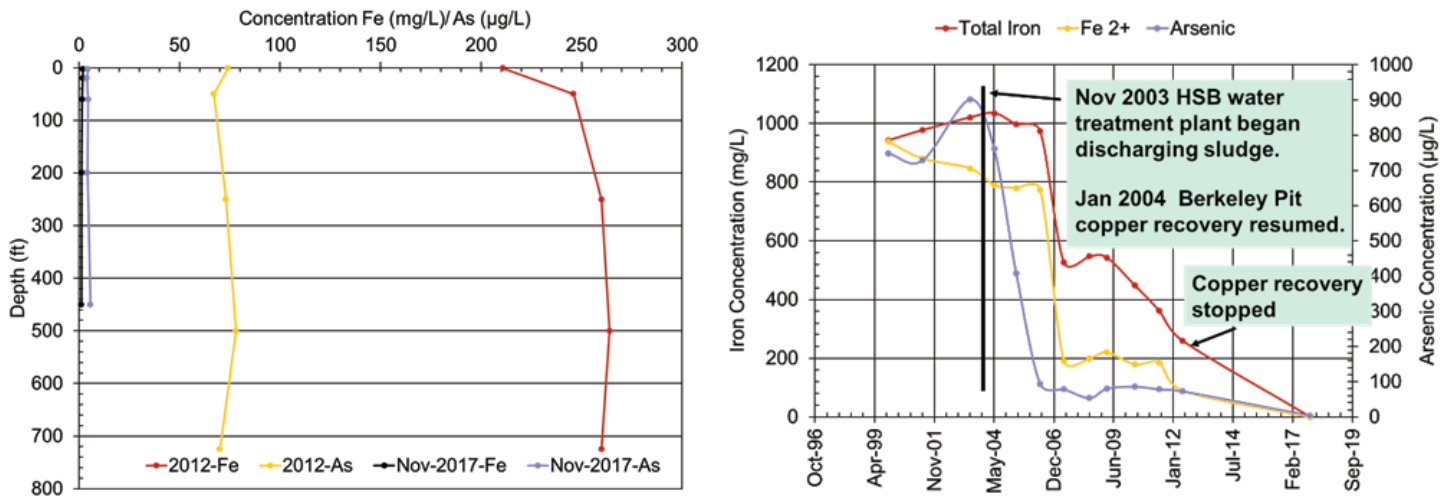


Figure 8. Concentration of dissolved Fe and As profiles in the Berkeley Pit in 2012 and 2017 (left), and concentration of total dissolved Fe, ferrous Fe, and As at 200 ft depth in the Berkeley Pit between 1996 and 2018 (right) (Duaine and others, 2018b).

with the drinking water maximum contaminant level requirement of 10 µg/L (MDEQ, 2017). Samples from the 200 ft depth of the pit water between 1996 and 2018 show that decreases in total dissolved Fe, Fe²⁺, and As occurred during wastewater treatment and copper recovery. While copper recovery ceased in 2013, water treatment sludge discharge is ongoing. When both processes operated, the sludge probably provided sufficient alkalinity to maintain the precipitation reaction equilibrium toward the product side, meaning the amount of (oxy) hydroxide iron solid produced was substantial. These solids have a surface charge that attracts arsenic and it coprecipitates with the solid. After the copper recovery ceased, continued addition of hydroxide sludge neutralized enough acidity to continue depleting Fe by precipitation, and to raise the pH from 2.5 to 4.0.

Conclusions

The recent profiling data indicate that lake turnover occurs in the Berkeley Pit and that no stratification exists except in the upper 100 ft.

Water quality in the Berkeley Pit has improved since 2012:

- **pH** has increased by 1.5 pH units.
- **Fe** concentrations have decreased by two orders of magnitude.
- **As** concentrations have decreased by an order of magnitude.

Both the Fe²⁺ addition from the copper recovery process and the discharge of highly alkaline sludge from the Horseshoe Bend water treatment facility appear to have played a role in reducing the As and Fe concentrations in the Berkeley Pit Lake and in increasing the pH.

References Cited

- Duaine, T.E., Kennelly, P.J., and Thale, P.R., 2004, Butte, Montana: Richest Hill on Earth, 100 years of underground mining: Montana Bureau of Mines and Geology Miscellaneous Contribution 19, 1 sheet, scale 1:9,000.
- Duaine, T.E., Tucci, N.J., and Smith, M.G., 2018a, Butte Mine Flooding Operable Unit water-level monitoring and water-quality sampling 2012 consent decree update, Butte, Montana, 1982–2012: Montana Bureau of Mines and Geology Open-File Report 641, 189 p.
- Duaine, T.E., McGrath, S.F., Icopini, G.A., and Thale, P.R., 2018b, Butte underground mines and Berkeley Pit, water-level monitoring and water-quality sampling, 2017 consent decree update, Butte, Montana, 1982–2017: Montana Bureau of Mines and Geology Open-File Report 700, 187 p.

EPA Consent Decree, 2002, Butte Mine Flooding Operable Unit Consent Decree-02-35-BU-SEH.

MDEQ, 2017, Montana Department of Environmental Quality, Circular DEQ-7 Montana Numeric Water Quality Standards.

Tucci, N.J., and Gammons, C.H., 2015, Influence of copper recovery on the water quality of the acidic Berkeley Pit Lake, Montana: *Environmental Science & Technology* 2015, v. 49, no. 7, p. 4081–4088, doi: 10.1021/es504916n



Petr Yakovlev discusses recent mapping in the Glen 7.5' quadrangle during the Map Chat at the Butte Brewing Company (photo: A. Roth).



Pete Knudsen and Dick Berg at the Montana Tech Mineral Museum (photo: C. McKillips).



Cathy McKillips and Anthony ("Tony") Roth at the Symposium meeting (photo: A. Roth).

Japan Law Twins from the PC Mine, Jefferson County, Montana

Dr. Peter Knudsen

Professor Emeritus, Mining Engineering, Montana Tech, Butte, Montana

The PC Mine is located on the North Fork of Basin Creek about 7 mi northwest of Basin, Montana. Gold in Basin Creek was found probably about 1865, when the upper Basin Creek placers were discovered (Ruppel, 1963). U.S. Bureau of Land Management records show that a 160-acre claim listed as Placer 1453 was patented on July 23, 1884 by Charles Starrett and Jeremiah Hoyt. In 2005, the deposit was mined out and the property sold as a cabin site. The property is privately owned and sample collecting is not permitted.

The PC Mine is in a hydrothermal breccia that Ruppel (1963) mapped as welded tuff of the Elkhorn Mountains volcanic field. The hydrothermal deposit is highly brecciated and has intense silicification and sericitic alteration. Brecciation of the rock formed countless “pockets” (fig. 1) or “vugs” that were perfect environments for crystal growth.

Minerals found in the deposit include quartz, sphalerite, galena, pyrite, muscovite, schorl, sericite, anglesite, anhydrite, and hematite. The rare form of quartz crystal, the Japan Law Twin (fig. 2), makes the PC Mine deposit unique. Japan Law Twins are a geometrical intergrowth of two crystals. A Japan Law Twin is a contact twin, with the c-axes inclined (to each other) at the angle of 84 degrees, 33 minutes.

References Cited

Ruppel, E.T., 1963, Geology of the Basin quadrangle, Jefferson, Lewis and Clark, and Powell Counties, Montana: U.S. Geological Survey Bulletin 1151, 121 p., scale 1:48,000.



Figure 1. An example of a “pocket.” This is the first pocket my wife found, and it yielded nine Japan Law Twins.



Figure 2. Classic heart-shaped Japan Law Twin. The crystal is three-quarters of an inch across.



Acid-sulfate (vuggy silica) alteration at the Hog Heaven Mine (photo: K. Scarberry)



Max at the Cable Mine (photo: P. Hargrave).

The Epithermal Environment in the Yellowstone Hydrothermal System

Peter B. Larson¹ and Jerry Fairley²

¹Professor, School of the Environment, Washington State University, Pullman, Washington

²Professor, Department of Geological Sciences, University of Idaho, Moscow, Idaho

The Yellowstone Caldera, Wyoming, hosts a world-famous hydrothermal system. The hot springs are a pristine natural laboratory that, together with rocks that have been hydrothermally altered by reaction with the hot fluids, provides a unique opportunity to study an active epithermal environment. Surficial activity is manifest in more than 10,000 thermal features located over an area of nearly 6,000 km². A hydrothermal system has been active in the 640,000-year-old Yellowstone Caldera for at least the past 400,000 years (Christiansen, 2001; Larson and others, 2009; Sturchio and others, 1994). Both acid-sulfate (pH < 4) and circumneutral (pH between 6.5 and 7.5) hydrothermal fluids discharge from the active system (Lowenstern and Hurwitz, 2008). Examination of the walls of the Grand Canyon of the Yellowstone River shows shallower kaolinite (acid-sulfate) overlying deeper illite (circumneutral) clay alteration that are products of reaction with the two fluids (fig. 1).

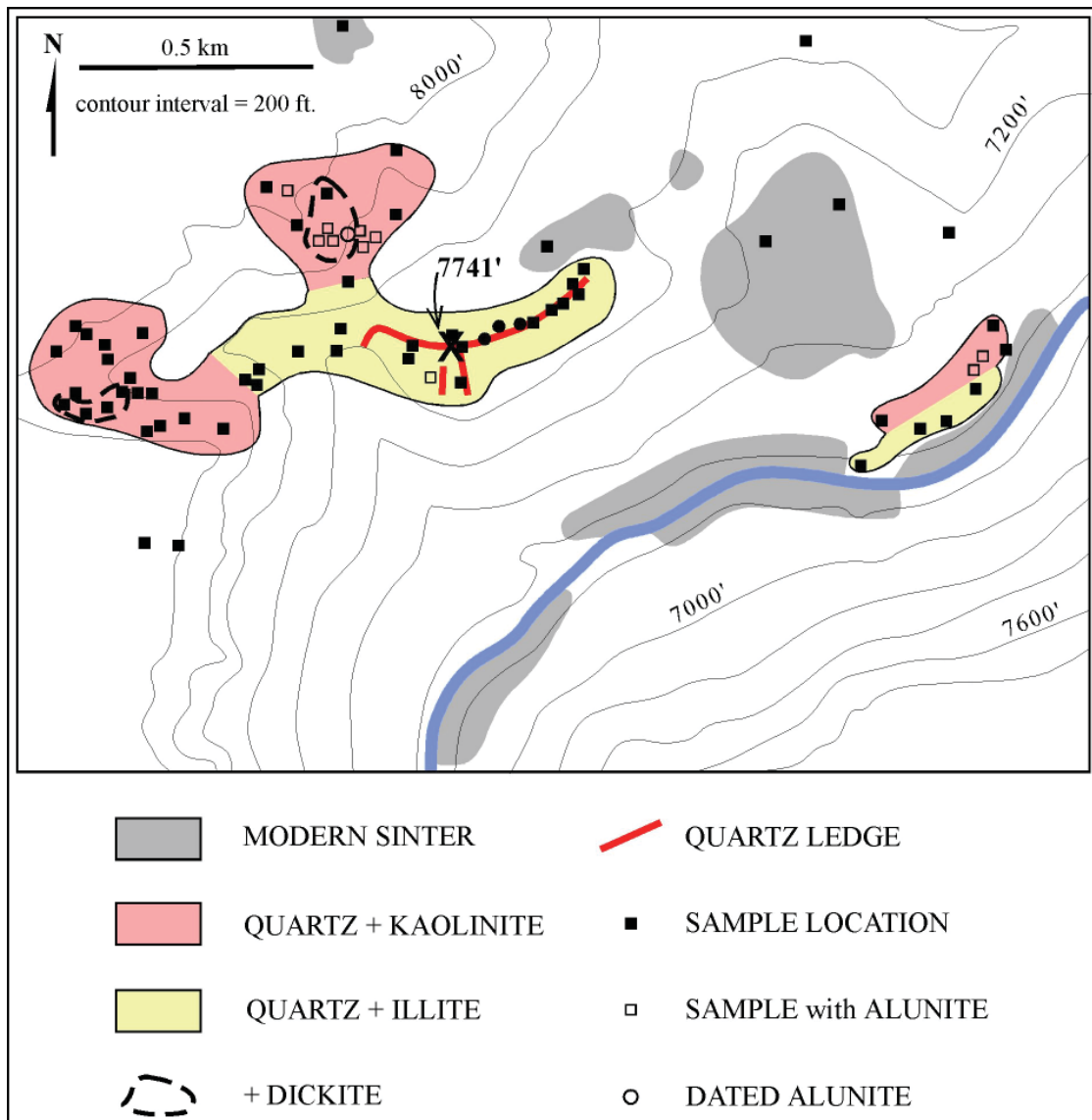


Figure 1. A hydrothermal alteration map of the Sevenmile Hole area, Grand Canyon of the Yellowstone River, Yellowstone Park, WY. Note that kaolinite dominates the clay assemblage in the higher parts of the canyon walls, whereas illite is predominant in the lower canyon walls. Modified from Larson and others (2009).

In the late 1960s, the U.S. Geological Survey drilled about 15 research holes into active Yellowstone hydrothermal areas. The drill holes helped to define the vapor-dominated nature of the Yellowstone hydrothermal system (White and others, 1971). Measurements in these holes provided constraints on temperatures in the shallow subsurface. Generally, the data show that the hot fluids rise along the hydrostatic boiling curve within several hundred meters of the surface (White and others, 1975). Fluid inclusion homogenization temperatures in meter-wide quartz veins deeper in the Grand Canyon of the Yellowstone River also follow the hydrostatic boiling curve (Phillips, 2010). Projecting the curve from these data to the surface suggests that about 100 m has been removed by glaciation and other erosion in the past 140,000 years. Alternatively, the mass of overlying glaciers could have added to the hydrostatic head, and this would then require less erosion since that time. Regardless, altogether the data show that the hydrostatic boiling curve controlled the temperature in upwelling fluids to a depth of at least 500 m, and perhaps to 900 m, below the surface.

Stable isotope analyses of fluids from the active springs (Ball and others, 2006, 2010; Truesdell and others, 1977) show that they follow a boiling trajectory with a slope of about 3 away from the meteoric water line (fig. 2). However, the trend projects back to the meteoric water line to a point well below the zone of modern precipitation in the Yellowstone region (McMillan and others, 2018; Thordsen and others, 1992; Truesdell and others, 1977). These data corroborate the thermal data that show that boiling is important in the history of the hydrothermal fluids discharging at the surface. But the stable isotope data (fig. 2) also suggest that recharge to the system is derived from a meteoric fluid other than modern precipitation. This recharge is most likely derived from an older fluid reservoir.

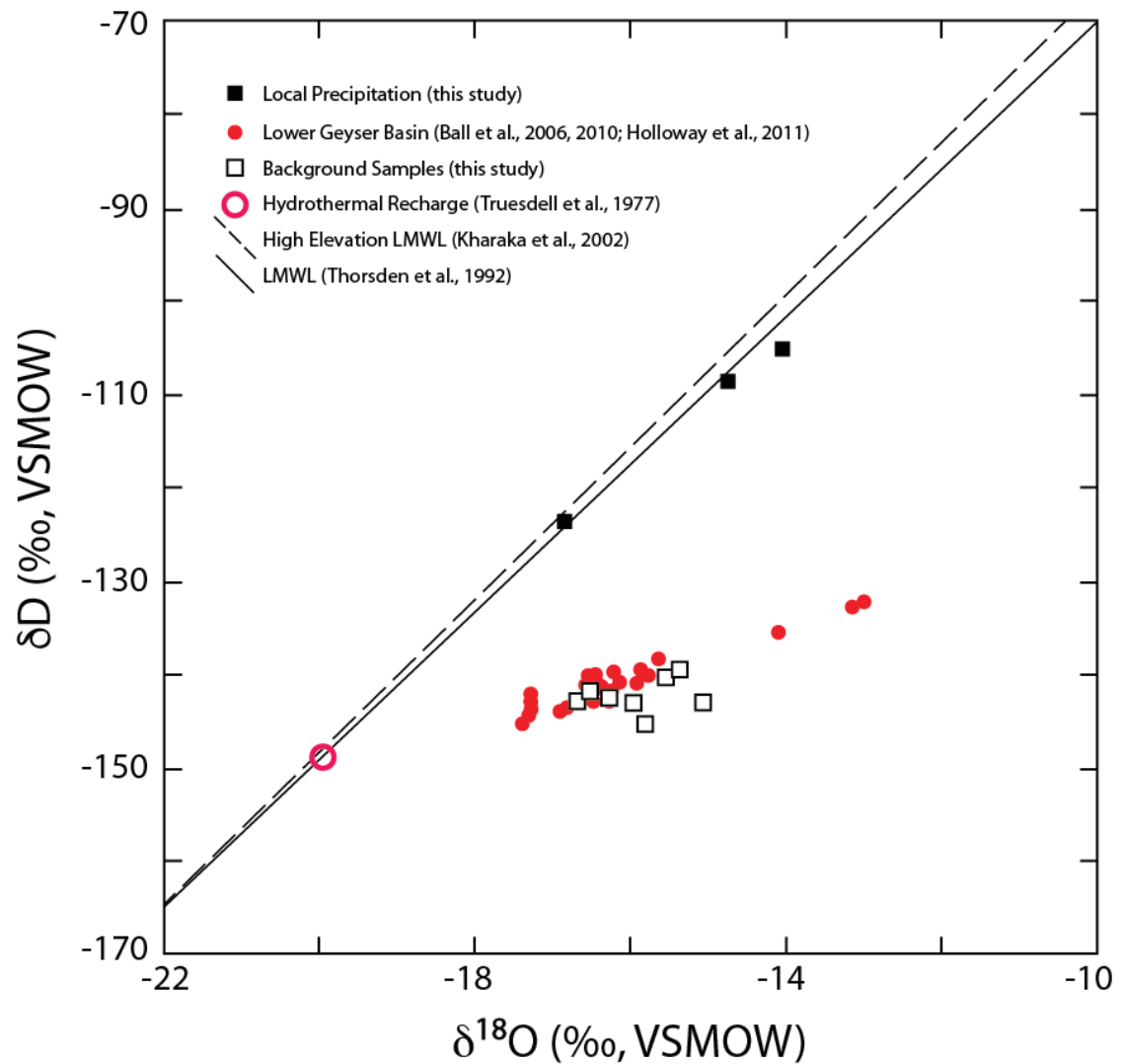


Figure 2. Stable isotope geochemistry of hot spring fluids from the Lower Geyser Basin, Yellowstone Park, WY (from McMillan and others, 2018). The thermal fluid data (Ball and others, 2006, 2010; Holloway and others, 2011; McMillan and others, 2018) lie along a trajectory with a slope of about 3, characteristic of a boiling process. Also shown are the local meteoric water line (Thordsen and others, 1992) and the high-elevation meteoric water line (Kharaka and others, 2002) for the Yellowstone region. Note that the thermal water data project back to the meteoric water line well below the range of modern precipitation (Truesdell and others, 1977), represented here by three analyses (“this study”) from McMillan and others (2018).

Acknowledgments

The research was supported by funding from the National Science Foundation (NSF1250435, PI: Larson, and NSF1250381, PI: Fairley). The work described was performed under permit from the National Park Service.

References Cited

- Ball, J.W., McCleskey, R.B., Nordstrom, D.K., and Holloway, J.M., 2006, Water-chemistry data for selected springs, geysers, and streams in Yellowstone National Park, Wyoming, 2003–2005: United States Geological Survey Open File Report 2006-1339, 137 p.
- Ball, J.W., McCleskey, R.B., and Nordstrom, D.K., 2010, Water-chemistry data for selected springs, geysers, and streams in Yellowstone National Park, Wyoming, 2006–2008: United States Geological Survey Open File Report 2010-1192, 109 p.
- Christiansen, R.L., 2001, The Quaternary and Pliocene Yellowstone Plateau volcanic field of Wyoming, Idaho, and Montana: United States Geological Survey Professional Paper 729-G, 145 p.
- Holloway, J.M., Nordstrom, D.K., Böhlke, J.W., and McCleskey, R.B., 2011, Ammonium in thermal waters of Yellowstone National Park: Processes affecting speciation and isotope fractionation: *Geochimica et Cosmochimica Acta*, v. 75, p. 4611–4636.
- Kharaka, Y.K., Thorsden, J.J., and White, L.D., 2002, Isotope and chemical compositions of meteoric and thermal waters and snow from the greater Yellowstone National Park region: United States Geological Survey Open File Report 02-194.
- Larson, P.B., Phillips, A., John, D., Cosca, M., Pritchard, C., Andersen, A. and Manion, J., 2009, A preliminary study of older hot spring alteration in Sevenmile Hole, Grand Canyon of the Yellowstone River, Yellowstone Caldera, Wyoming: *Journal of Volcanology and Geothermal Research*, v. 188, p. 225–236.
- Lowenstern, J.B., and Hurwitz, S., 2008, Monitoring a supervolcano in repose: Heat and volatile flux at the Yellowstone Caldera: *Elements*, v. 4, p. 35–40.
- McMillan, N., Larson, P., Fairley, J., Mulvaney-Norris, J., and Lindsey, C., 2018, Direct measurement of advective heat flux from several Yellowstone hot springs, Wyoming, USA: *Geosphere*, v. 14, no. 4, <https://doi.org/10.1130/GES01598.1>.
- Phillips, A.R., 2010, An oxygen isotope, fluid inclusion, and mineralogy study of the ancient hydrothermal alteration in the Grand Canyon of the Yellowstone River, Yellowstone National Park, Wyoming: Pullman, Washington State University, M.S. thesis, 132 p.
- Sturchio, N.C., Pierce, K.L., Murrell, M.T., and Sorey, M.L., 1994, Uranium-series ages of travertines and timing of the last glaciation in the northern Yellowstone area, Wyoming–Montana: *Quaternary Research*, v. 41, p. 265–277.
- Thorsden, J.J., Kharaka, Y.K., Mariner, R.H., and White, L.D., 1992, Controls on the distribution of stable isotopes of meteoric water and snow in greater Yellowstone National Park region, USA: *Proceedings of the 7th International Symposium on Water–Rock Interaction*, p. 591–595.
- Truesdell, A.H., Nathenson, M., and Rye, R.O., 1977, The effects of subsurface boiling and dilution on the isotopic compositions of Yellowstone thermal waters: *Journal of Geophysical Research*, v. 82, p. 3694–3704.
- White, D.E., Muffler, L.J.P., and Truesdell, A.H., 1971, Vapor-dominated hydrothermal systems compared with hot-water systems: *Economic Geology*, v. 66, p. 75–97.
- White, D.E., Fournier, R.O., Muffler, L.J.P., and Truesdell, A.H., 1975, Physical results of research drilling in thermal areas of Yellowstone National Park, Wyoming: United States Geological Survey Professional Paper 892, 70 p.



Altered Belt rocks at the Cable Mine (P. Hargrave).



Yvonne and John Metesh (MBMG Director) at the Symposium banquet (photo: A. Roth).

History and Geology of Henderson Gulch, Montana's First Gold Discovery

Ted Antonioli

Geologist, Contact Mining Company, Philipsburg, Montana

Introduction

Henderson Gulch, in northeast Granite County, Montana, is the most productive placer in the Flint Creek watershed (fig. 1). It also has the distinction of having the longest mining life of any placer in Montana, beginning with the earliest documented gold prospecting in the State in 1849, and extending to Chris and Jessica Therriault's mining near the head of the gulch in 2018. The source of the gold is an intrusive-hosted gold and tungsten bearing granodiorite—the Henderson stock—and gold–tungsten veins of the Sunrise district.

Discovery and History of Mining

In the mid-1800s, just as today, the major east–west transportation corridor through Montana ran along the Clark Fork River canyon between Garrison and Missoula. The streams along the corridor, Flint Creek and Gold Creek in particular, became the focus of the first gold prospecting in Montana. While popular historical accounts of the gold rush in Montana focus on Gold Creek, well-informed sources indicate that the first discovery of gold took place in Henderson Gulch, by a party linked to the Hudson's Bay Company. Throughout the early and mid-19th century, western Indian tribes

such as the Salish and Nez Perce made frequent hunting expeditions along trails that led from the Bitterroot and Missoula Valleys to the buffalo hunting grounds east of the Continental Divide. Hudson's Bay traders sometimes accompanied the Native expeditions, and some of them, such as members of the Finlay family, were knowledgeable about gold mining.

Members of a hunting expedition travelling at or near the point along the Mullan Road where it crosses Flint Creek (fig. 1) likely panned the first gold in Montana. These individuals then prospected up Flint Creek and found a place where it would “pay” to mine. The gold discovery was later reported to the Hudson's Bay Company local agent, Angus McDonald, as he reports in his memoirs (McDonald, 1917). McDonald does not list the discoverers by name, but pioneer Jesuit missionary Pierre De Smet later heard of the discovery from an Indian source (Chittenden and Richardson, 1905, p. 1521), and it is reasonable to speculate that some combination of fur traders and Indians found the deposit.

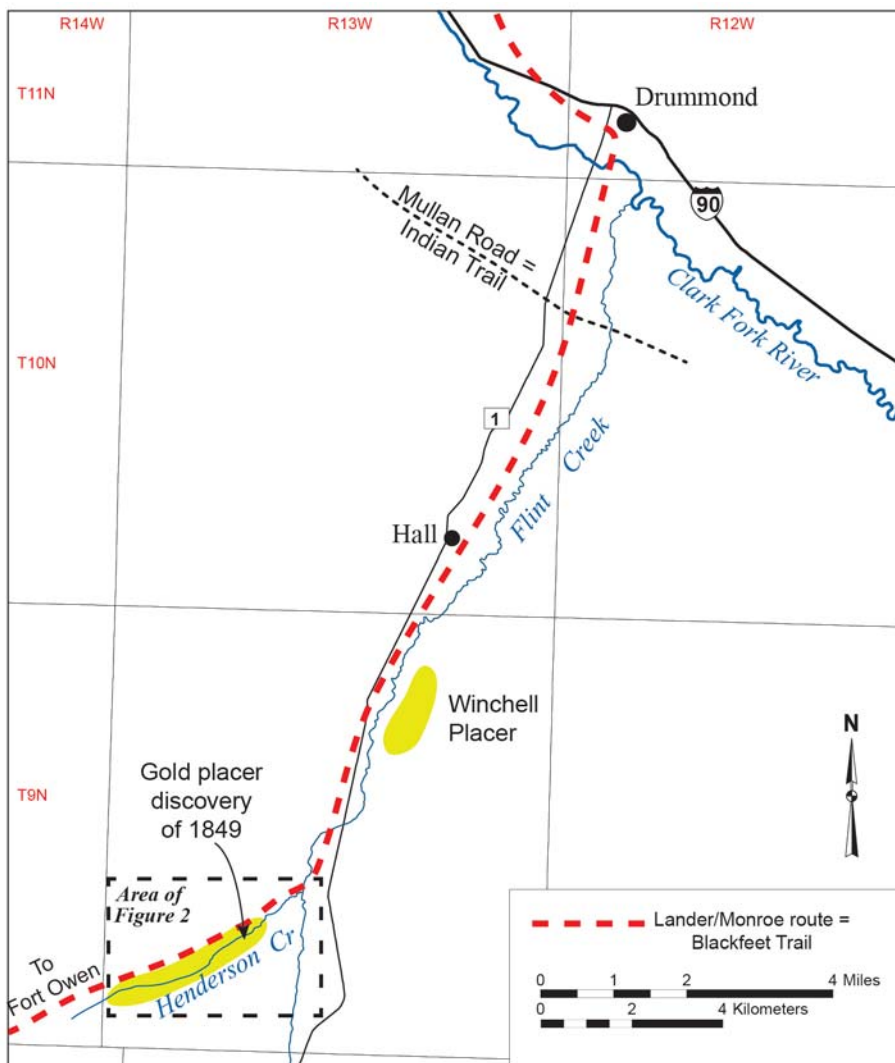


Figure 1. Map of middle 1850s trails and placer gold deposits in the Lower Flint Creek Valley.

A newspaper letter written by pioneer William Graham, a founder of the Montana Historical Society, indicated that the Henderson Gulch discovery occurred in 1849, but was abandoned because of the danger presented by hostile Blackfeet (*The New North-West.*, September 10, 1875). This story is reinforced by information obtained by John Mullan during the course of the Pacific Railroad Survey of 1853–1854 (Stevens, 1860). Mullan was told by his Salish guides that the route to the Bitterroot Valley taken by surveyor F.W. Lander and party, part of which traverses Henderson Gulch, was used by Blackfeet Indians on raiding expeditions. This explains the 16-year delay from discovery to development of the gold deposit in the gulch.

The Flint Creek discovery was known to only a few people, but became regarded as a legendary “El Dorado” as word slowly leaked out to Father Pierre De Smet and others. At least two parties, one led by the Stuart brothers in 1858 and the other by merchant James Harkness in 1862, subsequently prospected in the Flint Creek watershed, but missed the excellent placer ground at Henderson Gulch. The Henderson Gulch deposit became a mine only after 1865, when the Henderson party, an uncle, nephew and unrelated prospector all named Henderson (Domine, 2012), located claims on the best section and then spent the winter digging a ditch to bring water from Willow Creek to mine.

Placer and Lode Geology

An area of early hand workings, identified by stream and bedrock morphology, as well as the location of a water ditch built by the Henderson party, locate the most likely place of the original gold discovery along Henderson Creek (fig. 2). The 1860s era hand workings show up remarkably well on LiDAR imagery (fig. 3). It was an area of “shallow ground,” with only a few feet of overburden atop the bedrock—an ideal place to mine for gold with minimal tools and capital.

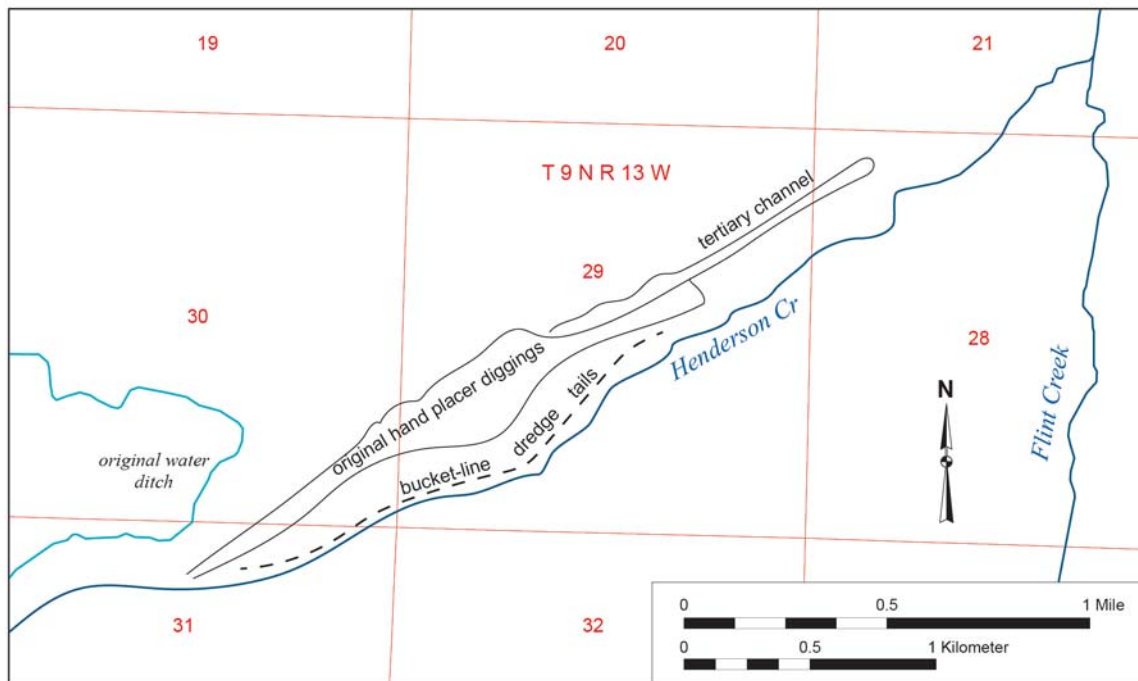


Figure 2. Map of placer mining features in Lower Henderson Gulch.

The auriferous Tertiary placer channel of Henderson Creek (fig. 2) is cut by the modern channel of Flint Creek; however, a bench of placer gravel is also present downstream on the opposite (east) side of Flint Creek (fig. 1). Lyden (1948) proposed that this latter placer, called the Winchell mine or placer (fig. 1) in newspaper articles and J.T. Pardee’s field notes, is actually a continuation of the Henderson Creek placer channel.

In the 1930s, Philipsburg prospectors William and Jake Schneider discovered that the placer gravel of Henderson Gulch contained considerable scheelite, which was recovered as a co-product with gold from a connected bucket-line dredge operation during and after WWII (Hundhausen, 1949). Since scheelite is also present in pan concentrates at the Winchell mine, it is strongly suspected that the Henderson placer originally crossed east

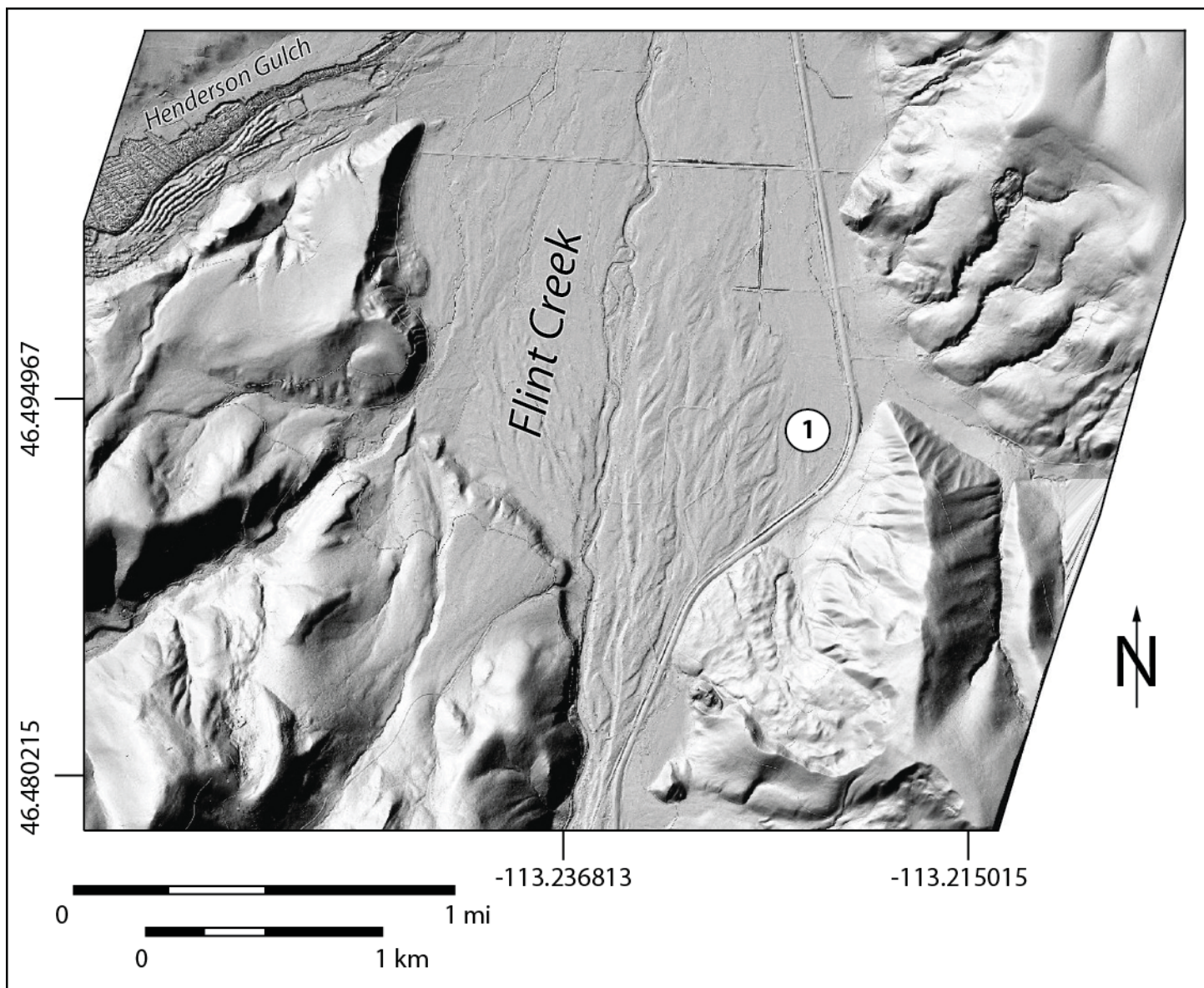


Figure 3. LiDAR image shows the junction of Henderson Gulch with Flint Creek. Henderson Gulch placer deposits are recognized by long rows of dredge tails in the southern part of the gulch, and as a cross-hatched pattern in the hand-worked area in the northern part of the gulch. The LiDAR data were collected by the MT DNRC Water Resources Division, and the image was downloaded from the Montana LiDAR Inventory.

of the future course of modern Flint Creek, and that considerable auriferous gravel has been washed down Flint Creek from the eroded center section of the Tertiary Henderson Gulch placer.

The principal lode shedding gold and tungsten into the placer is a mineralized, 70.1 ± 2.5 Ma Henderson stock, a granodiorite intrusion with a quartz monzonite core, located near the head of the gulch near Sunrise Mountain (Hughes, 1971). The stock is about 2 mi upstream (southwest) of the principal area of hand placer workings. The intrusion contains numerous veinlets with quartz, gold, and scheelite, and veins associated with the exposed intrusive and possibly with buried related intrusions nearby. Native tin occurs in a residual placer developed on top of the Henderson stock (Hundhausen, 1949), and is likely a constituent of the veinlets.

Acknowledgments

This paper was improved by reviews from K. Scarberry and S. Korzeb, and through numerous discussions of the geology with Paul Antonioli.

References Cited

- Chittenden, H., and Richardson, A., 1905, Life, letters, and travels of Father Pierre-Jean DeSmet: New York, Harper, 1624 p.
- Domine, L., 2012, The mettle of Granite County, Book 3: Helena, Mont., KAIOS Books, 343 p.
- Hughes, Jr., G.J., 1971, Petrology and tectonic setting of igneous rocks in the Henderson-Willow Creek Igneous Belt, Granite County, Montana: Houghton, Mich., Michigan Technological University, PhD dissertation.
- Hundhausen, R.J.. 1949, Investigation of Henderson Gulch tungsten deposit, Granite County, Mont: U.S. Dept. of the Interior, Bureau of Mines, 3 p., 11 plates.
- Lyden, C.J., 1948, The gold placers of Montana: Montana Bureau of Mines and Geology Memoir 26, 151 p.
- McDonald, Angus, 1917, A few items of the West: The Washington historical quarterly: Seattle, Wash., Washington University State Historical Society, v. 8, p. 188–229.
- Stevens, Isaac I., 1860, Narrative final report of explorations for a route for a Pacific railroad, near the forty-seventh and forty-ninth parallels of north latitude, St. Paul to Puget Sound: Volume 12, Books 1–2 of U.S. War Dept. Corps of Engineers Report of explorations and surveys from the Mississippi River to the Pacific Ocean in 1853-5.
-



Pleistocene Glacial Lake Missoula shorelines in the Niarada 7.5' quadrangle, northwestern Montana (photo: K. Scarberry).

Three Mines: The Early Career of Joseph T. Pardee

Anne Millbrooke

Historian, Bozeman, Montana

Joseph Thomas (Joe) Pardee (1871–1960) was a Montana lad who became a miner and then a geologist. He is most famous for his geological work on Glacial Lake Missoula. Pardee (1910b) named and described the glacial lake. Later Pardee (1942) interpreted the hills of the Camas Prairie, northwest of Missoula and southwest of Flathead Lake, as ripples from the current of the lake draining catastrophically; this was evidence that Glacial Lake Missoula provided flood waters that scoured eastern Washington into scablands. His mining career is missing from the existing literature, which tends to place him in a minor role in the J. Harlen Bretz story of the Lake Missoula floods and their relation to the channeled scablands (Kelly, 1963; Baker, 2008; Soennichsen, 2008). But Pardee has his own story, one worth telling. The Pardee story includes a decade of mining experience, which helped qualify him for his later career in geology as a Lake Missoula expert and as a mineral resources specialist working for the U.S. Geological Survey.

Pardee was born May 30, 1871, at Salt Lake City, Utah. His parents were James Knox Pardee (1843–1914) and Maria Antoinette (née Lukens) Pardee (1845–1914). From the age of 3, Joe grew up in Philipsburg, Montana (fig. 1A), where his father had mining interests. Joe attended public school in Philipsburg and excelled as a student, routinely meriting mention in the local newspaper as being on the honor roll. At the time Philipsburg, like most communities, did not have a high school; thus Joe Pardee was only 15 years old in September 1886 when he started at the College of Montana, in Deer Lodge. He enrolled in two courses of study, the normal course and the music course. In September of the next year he entered the first class in the new School of Mines at the College of Montana. He continued his music studies while taking the mining courses. Joe returned in September 1888 for his third year at the college and second year in the School of Mines. He majored in Mining Engineering, a 4-year course. But, after his second year as a mining student, he changed schools. In those days students took the prescribed courses of their university and major, and there was no system for transferring credits. Pardee thus enrolled as a special, non-degree-seeking student at the University of California at Berkeley (fig. 1B). He studied chemistry in 1889–1890 and mining in 1890–1891. He completed 5 years of higher education.

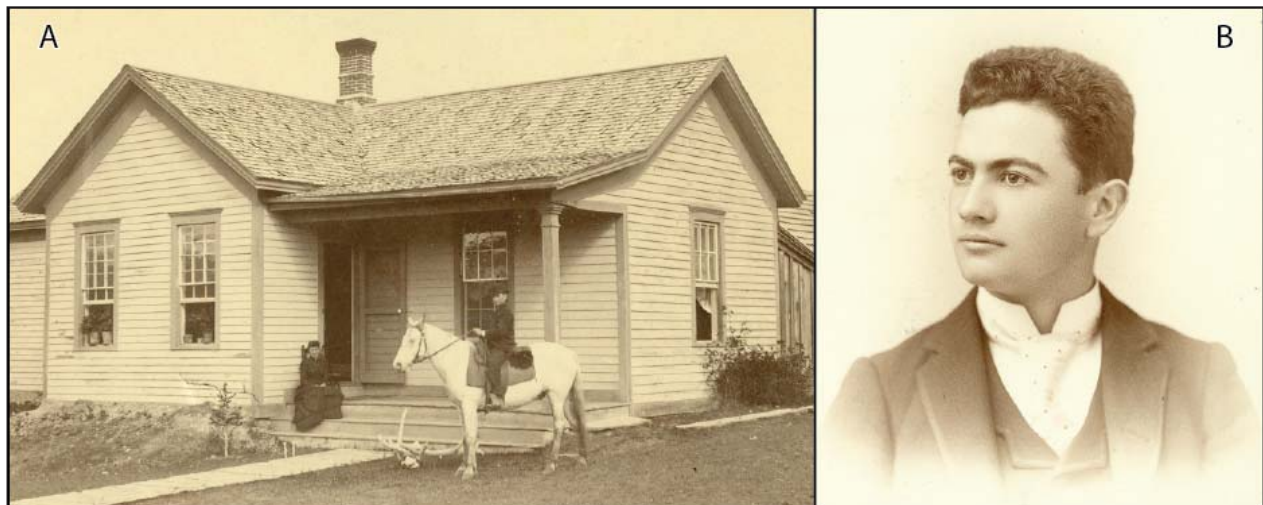


Figure 1. (A) Young Joe Pardee is on a horse named Alamo at the family home in Phillipsburg, Montana, 1883. Photograph from the Pardee Family Collection. (B) After 3 years at the College of Montana in Deer Lodge, Joe Pardee attended the University of California at Berkeley for 2 years, 1889–1891. Photograph from Pardee Family Collection.

Back in Philipsburg, Joe Pardee followed his father, J.K. Pardee, into mining. A Civil War veteran, the elder Pardee had been in the pottery business in Ohio. He and his wife moved to the Salt Lake City area in 1870, and their son Joe was born there the next year. At Little Cottonwood Canyon, J.K. Pardee worked on smelters.

While in Utah, he also got into mining. The Pardee family moved to Philipsburg in the fall of 1874. Joe grew up in a mining camp, where his father had multiple interests in both the mines and the camp. J.K. managed the North-West Company's mining and milling operations for several years, then the Algonquin Company's mines and mill for several years, and later the West Granite Mountain Mining Company's operations for several years. These were silver mines, with gold as a byproduct. J.K. Pardee also organized mining companies, such as the Princeton, Pearl Silver, and East Granite mines in the greater Philipsburg area. He invested in mines beyond the area, such as Iron Mountain on Flat Creek, north of Superior, Montana, and the Fourth of July in the Okanogan district of Washington, and he even explored mining asbestos, lithocarbon, and mineral paint in Texas. He was an organizer of the Philipsburg and Drummond Railroad Company and the Philipsburg Real Estate and Water Company. J.K. Pardee was a big man in Philipsburg. In contrast, young Joe began modestly by opening an assay office in Philipsburg and working at the nearby Granite mining camp. He even took jobs as deputy clerk of the court and deputy county treasurer.

Rock Creek Mining District: Basin Gulch Placers, 1893–1899

Silver became a political question more than a mining activity in the 1890s. The mines of the Western states produced so much silver that inflation became a national problem. The repeal of the Silver Purchase Act, which required the government to purchase silver, prompted mines to cut wages and payrolls, and many mines closed. All that was part of the nationwide Panic of 1893, which ran right into the Panic of 1896. These national depressions hit Philipsburg and other silver mining communities particularly hard. The silver question dominated politics to the extent that the Silver Republicans, including Montana's U.S. Senator Lee Mantle, split from the Republican Party, which supported the gold standard rather than the bimetallism advocated by the Silver Republicans.

In 1893, as the silver mines begin to close, many of the miners in silver districts turned to placer gold. Joe Pardee literally joined local miners going into the hills. He thus was at the beginning of what became the Rock Creek placer rush. Rock Creek was about 15 mi west of Philipsburg. As a boy and now as a young man, Pardee camped and fished along Rock Creek. He acquired claims on Basin, Quartz, and Sapphire gulches (fig. 2), in township 7 north, range 16 west, of the principal baseline and meridian of the state of Montana. All three gulches drained the same Quartz Hill, Basin Gulch as a tributary to Quartz Gulch. In March 1893, Pardee, Sim Shively, H.G. Allen, and G.W. Allen located and claimed the Grover Placer near the mouth of Sapphire (later re-named Cornish) Gulch. They filed their claim in Philipsburg on April 1, 1893. In September, the same foursome filed a nameless 20-acre claim in Basin Gulch. That same month Pardee and John Landers located the Black Pine Placer in the Basin Gulch, and Pardee and Josiah Shull located the Quartz Hill Placer in Basin Gulch.

Claims were close together in Basin Gulch, and claims changed hands. On Basin Creek the Ella was the bottom claim, and the Black Pine was the second claim up. Farther up Basin Gulch were the claims of Sam Watson, Allen F. Spees, and Sim Shively ("Rock Creek Placers," *Anaconda Standard*, June 15, 1893). Jack White had the claim at the head of the gulch. The paystreak was estimated to be over 2 mi in length. Some claims were located on the hillside above the claims straddling the creek, two or three high. Conn Brothers acquired a Basin claim, as did William Glassner. William Hutchinson, known as Poker Bill, and eight partners got into a legal battle with Chas. Kroger and Co. over title to a claim in the gulch. John Landers built a cabin in Basin Gulch, John B. Miller built a cabin at the head of the gulch, and other cabins appeared on claims. For a short time each spring, during the spring runoff, Basin Gulch was a busy place.

Pardee partnered with old-time placer miner John Landers (spelled Landers in newspapers, but Landes in land records), and they mined near the mouth of Basin Gulch. Already in his 60s, Landers had the first claim, the Ella placer at the mouth of Basin Gulch, next to the Eureka Mining Company's Last Chance claim on Quartz Gulch. Pardee had the next claim up Basin, the Black Pine. As partners, each owning a minor share in the other's claim, Pardee and Landers mined claims in lower Basin Gulch (fig. 2). Like most of the miners, the pair began with digging, panning, and using a rocker. But they quickly switched to hydraulic mining; the Eureka company had been the first to use hydraulic equipment on Quartz Hill placers. Mining the Quartz Hill gulches was profitable; in 1894, \$900 to \$2,000 worth of gold per mine was reported. Pardee was not among those

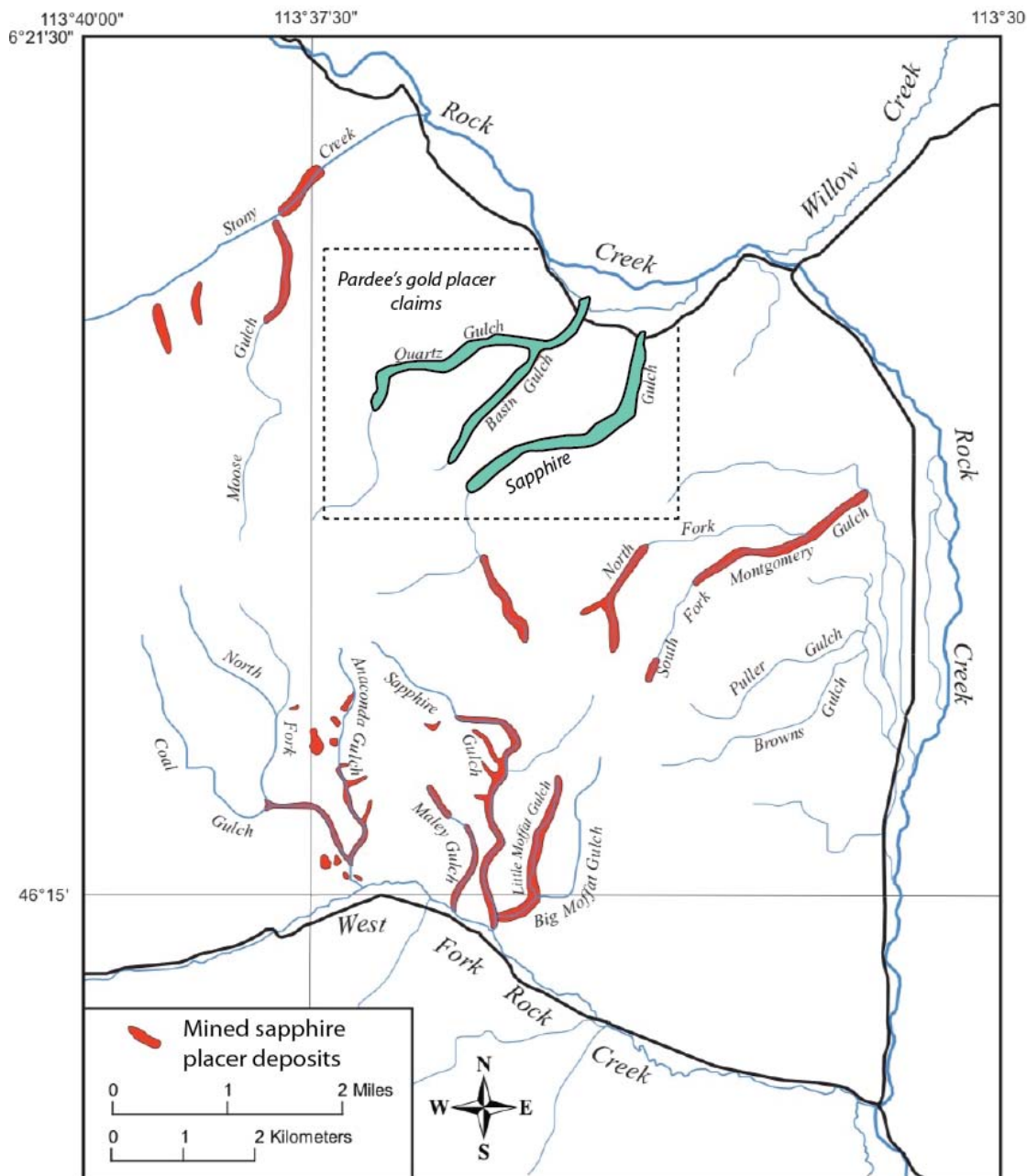


Figure 2. Map of the upper Rock Creek mining district. The region where Pardee had placer claims is shown in green. More recent work in the district has focused on sapphire placer mining (modified from Berg, 2014). Willow Creek Road was the route between Rock Creek in the west and Philipsburg in the east.

reporting to the press, but his partner Landers cleaned up \$1,200 that year (“Among the Ledges,” Philipsburg Mail, August 2, 1894).

Pardee and Landers, adopted hydraulic equipment, as did their mining neighbor Sam Watson, so they could wash more gravel during the mining season. The partners cleaned up about \$4,000 each spring. In fact, in May 1895, the two had already made about \$4,000. They and a few employees had worked quickly because they anticipated a short season due to a water shortage (“Poor Prospects,” Butte Miner, May 29, 1895). Scarce water, just the spring runoff from the mountains, defined their season every year. Preparatory work began in April and washing started in May. In light snow years, the runoff might last only 4 to 6 weeks. The miners routinely collected water at night for use in daytime operations. They built flumes and ditches to bring water to their operations. But the limited water sources still kept the season relatively short. Yet, the Philipsburg Mail reported, “it is a pleasure to pan dirt when the colors show up in the bottom of the pan the size of grains of wheat” (“Rich Gold Section within Granite County,” August 26, 1898).

Claims were located, filed, improved, developed, worked, bought, sold, amended, forfeited, abandoned, and patented in Basin Gulch, as elsewhere. Partial interest in claims routinely changed hands; for example, given the focus of Pardee's mining in Basin Gulch, he in 1895 sold his shares in properties in Sapphire Gulch—1/5 interest in the Grover Placer claim, 1/5 interest in the Sapphire Placer claim, and 1/5 interest in two water rights—for terms masked by the nominal consideration of \$1. In 1894 Pardee and others filed the Sadie claim in Basin Gulch, and in 1895 he was among the filers on the Fraction Placer in Basin Gulch. The same year he purchased the Basin Creek Placer from H.G. Allen and G.W. Spees. He bought the old Admiral Drake lode claims atop Quartz Hill near the heads of all three basins coming off the hill, and he bought the Paul Jones lode on the ridge between Basin and Quartz gulches. In 1896 he sold his interest in the Sim Shively placer and twenty acres atop Quartz Hill. In 1897 Pardee bought out John Landers, who wanted to winter in California and then go to the gold fields in Alaska. Pardee combined the Ella and Black Pines into the Landes claim. He also bought Josiah Shull's 1/2 interest in the Quartz Hill Placer, Shull's 1/3 interest in the Fraction Placer, and Frank Jamison's 1/3 interest in the Fraction. In 1898 he filed the Amended Quartz Hill claim, as an amended location of the Quartz Hill and Fraction placer claims near the head of Basin Gulch, just southwest of Allen and Spees's placer. These are examples of Pardee's mining activities rather than a comprehensive list, which would extend beyond the Basin, Quartz, and Sapphire Gulches.

Pardee lived in Philipsburg, maintained his assay office in the 'burg, and routinely visited and worked his diggings at Basin Gulch. He displayed some of the finest gold nuggets from his diggings in town at Merchants' and Miners' National Bank. He was particularly active in 1899. It had been a snowy winter, so a good season was expected in Basin Gulch. He moved out to his diggings in mid-April to prepare for the spring washing (fig. 3). The Fraction, the Quartz Hill, and the Black Pine had a 30-day season that year, with men working



Figure 3. Joe Pardee, his partner John Landers, and a few hired men worked Basin Gulch placer claims each spring as long as there was sufficient water. An employee named Jackson is at the pipe in this 1896 picture. Photograph from Pardee Family Collection.

open cuts and drift. At Pardee's Basin Creek claim workers dug a ditch 1,500 ft long, 16 in by 20 in. Additionally, Pardee, William Tormey, G.A. Schoonover, Jerry McKinney, and R.T. Gillies filed on the Dream, on the east side of the Amended Quartz Hill claim, and south of the Sim Shively claim. In August, Pardee filed applications for two patents for mining land in Basin Gulch. These applications covered the adjoining claims Landes and Amended Quartz Hill, both of which extended between the Eureka company's Last Chance placer at the lower end and Paul A. Fusz's Shylock placer higher up the gulch. Other neighboring claims at the time were Samuel Clark's "L" Placer, the Conn Brothers' Gold Hill Placer, and Fusz's Shively Placer.

After the 1899 season, Pardee made a big sale to Fusz. Pardee sold both the Landes and Amended Gold Hill, about 34 acres, for \$20,000 ("A Large Placer Deal," Philipsburg Mail, October 13, 1899). (The sum of \$20,000 in 1899 is equivalent to over a half million dollars today.) Before the placer season that year, before enough water flowed for washing, Fusz had purchased the Basin Gulch placer grounds of Allen and Spees, Samuel Watson, and the Conn Brothers ("A Large Placer Deal," Philipsburg Mail, April 7, 1899; and "Mines of Basin Gulch," Philipsburg Mail, April 28, 1899). As president of the Granite-Bi-Metallic Consolidated Mining Company, Fusz was initially interested in lead ore in Basin Gulch; after all, placer gold rushes usually lasted only a

few years, and the lead ore tested high grade. Fusz's employees washed gravel in the gulch during the 1899 season, so he recognized the gold value of the ground in Basin Gulch by the time he purchased the Pardee claims. Despite the gulch having been worked annually since 1893, much of Basin Gulch had not yet been mined due to the water shortage and short season. With the placers purchased from Pardee, Fusz controlled most of the gulch. Frank Grebil and L.C. Johnson's Eureka company still controlled the Last Chance and other Eureka claims. Meanwhile, Allen and Spees still had multiple claims in the neighboring Quartz Gulch.

Pardee had acquired valuable claims in Basin Gulch, as demonstrated by the income he derived from mining, by the sale price, and by subsequent years of mining by others. Fusz pursued the patents that Pardee had applied for, and Fusz applied for other patents. He received patents for the Landes (17.23 acres) and Amended Quartz Hill (16.09 acres) in 1900, the Amended Shively (31.01 acres) in 1901, and the Shylock Placer (13.10 acres) in 1904. With St. Louis investors, Fusz organized the Basin Gulch Syndicate; Fusz was the syndicate's president. The syndicate, in turn, in 1906, incorporated the Basin Gold Mining Company; again Fusz was president. The company mined placer gold in Basin Gulch into the 1920s. It dissolved in 1926 (Basin Mining Company Records, 1903–1925).

Pardee mined Basin Gulch placers in the 1890s. Basin Gulch gave him experience—experience locating, buying, selling, and operating placer ground, alone and with partners. Basin Gulch gave him contacts, notably Samuel (Sam) Watson. Basin Gulch provided him a degree of wealth. With the experience and wealth, he explored other mining opportunities. By the end of 1899 Pardee invested money and expertise in a hardrock mine in northeastern Oregon, and he later entered a mining partnership with Sam Watson.

Greenhorn Mining District: Diadem Lode Mine, 1899–1901

At the end of the 19 century, the Blue Mountains of northeastern Oregon experienced its second mining boom, the first having been in the 1860s. R.L. Farmer, who settled in the area in the early 1860s, and L.M. Barnett, also an early settler, had located the Diadem and Brindle Horse quartz claims on October 6, 1892 ("Oregon's New Eldorado," Sunday Oregonian, March 11, 1900; and Wagner, 1959; fig. 4). These properties at the head of Blue Gulch in the Greenhorn range were in an unorganized mining district sometimes called Robinson-



Figure 4. The discovery hole being worked on the Diadem claim. Within a year, the working mine and mill were built on the Brindle Horse claim just below the Diadem claim, both claims held by the Diadem Gold Mining Company. Photograph from Grant County Library, Oregon.

ville (after an early mining camp), more commonly called Greenhorn (after the newer camp) or Bonanza (after that rich mine about 5 mi away). Farmer and Barnett did assessment work, but neither was a mine operator. They prospected, staked claims, sold claims, and even sought employment at mines. Joe Pardee inspected the property too.

Charles S. Warren of Butte had bonded the Diadem in August 1899. He called the Diadem a “daisy” (“Diadem Is a Daisy,” *Sumpter Miner*, October 18, 1899). Warren, like J.K. Pardee, was a Civil War veteran; Warren’s often-used title of “general” came from a post-war position in the veterans organization Grand Army of the Republic, in which Joe’s father was also an active member. As general manager of the Sumpter townsite syndicate, Warren promoted the town and the entire mining region, which was on a narrow-gauge branch railroad line west of Baker City; a transcontinental line ran through Baker City. Warren had initially planned to lure Portland capitalists into investing in the Diadem, but when money was not transferred in time, the bond expired. Warren invited the Pardees to check out this opportunity in Oregon. Both J.K. and J.T. Pardee went to Sumpter in November 1899. They examined the Diadem property, the two shallow shafts, and the local business environment. They noted the property’s proximity to water and timber, both necessary for mine development. They had the ore tested and liked the results: Gold, silver, copper, and lead ore were in the early samples. They took possession of the property on November 20, 1899, and immediately began development, with Joe Pardee as superintendent of work at the site. They let a contract to Charles Bonner to sink a shaft 80 ft. Anticipating that the Diadem would become a big mine, they happily made the final payment on December 20th. The total cost of the two claims, each 600 ft by 1,500 ft, was \$40,000, as reported in the press. The deed records on file at the Baker County Courthouse recorded a nominal \$1 paid by Joseph T. Pardee to L.M. Barnett and R.L. Farmer and thereafter a nominal \$1 paid by the Diadem Gold Mining Company to Joseph T. Pardee.

The two Pardees and Charles Warren organized a company. They incorporated the Diadem Gold Mining Company on December 18, 1899. According to the articles of incorporation, the new company had capitalization of \$1 million, based on par value of \$1 per share for the usual 1 million shares; these were usual terms for the time. According to the articles of incorporation, the Diadem Gold Mining Company (1899) was:

- “To work, operate, bond, buy, sell, lease, release, local and deal in mines, metals, mineral properties of every kind and description within the United States.
- To bond, buy, sell, lease and hold timber and timber lands and claims.
- To bond, buy, sell, lease, locate and hold ditches, flumes and water rights.
- To construct, lease, bond, buy, sell and operate mills, concentrators, smelters, reduction works and mining machinery of every description.
- To bond, sell, buy, lease, build or operate railroads, ferries, tramways or other means of transporting ores and other minerals, and finally to do anything consistent, proper and requisite for the carrying out of the objects and purposes aforesaid in their fullest and broadest sense.”

Such ambition, or hopes, for a new mining venture were common in the incorporation records of the time.

Charles S. Warren, J.K. Pardee, and Joe Pardee became the company’s trustees to serve until the stockholders’s meeting scheduled for the first Tuesday in October 1900. They were also the company’s officers: Warren, President; J.K. Pardee, Vice President; and Joe, Treasurer. The newly formed Diadem Gold Mining Company undertook development on the property. They began mining on the Diadem claim and soon discovered that the main ledge was on the Brindle Horse or lower claim. The Brindle Horse ledge was about 400 ft lower than the ore on the Diadem claim. J.K. Pardee described the vein as a contact vein “between 200 and 300 ft wide with a serpentine hanging wall and a slate footwall” (“Montanan’s Big Bonanza,” *Weekly Missoulian*, March 9, 1900). That vein shifted the focus of the work to the Brindle Horse part of the Diadem mine property. They installed a hoisting plant with a capacity for a 500-ft deep shaft. During the first summer, under contract, G.W. McCulloch opened an extension. Since that work fouled the air, air pipes were placed in the shaft. In addition to the shaft, they ran levels, initially about 100 ft. A ditch, the “Pardee ditch,” brought the water that was neces-

sary for steampower in the mine and mill. At various times during the first year Joe Pardee, Charles Bonner, and F.F. Grimes acted as the on-site superintendent; Joe had executive authority over the on-site operations. Bonner had mined in Butte and at Iron Mountain, in Montana. Grimes had mined the Speckled Trout near Philipsburg. On June 25, 1900, the first ore from the Diadem reached Sumpter, the railhead for the mines in the surrounding mountains and gulches. That season the narrow-gauge Sumpter Valley railroad carried two Diadem shipments to the Baker City Sampling Works.

Waldemar Lindgren (1901) of the U.S. Geological Survey reported on the Diadem: “The Diadem vein... strikes east–west and is developed by smaller shafts and a tunnel 550 ft long. It is intended to extend the latter 200 ft, giving a vertical depth below the croppings of 425 ft. The gangue is quartz; the principal ore is mineral galena, often in considerable masses, together with a little chalcopyrite. Both are rich in free gold. The vein is claimed to be 20 ft wide, one rich streak assaying \$200 per ton. A shipment of 16 tons in 1900 is reported by the officers of the company to have netted \$1,819.” That was actually two shipments, and, apparently, the only two shipments that year.

Joe Pardee and his father bounced between Oregon and Montana, as did Charles Warren. J.K. Pardee’s history of recurring health problems caught up with him in Sumpter, where the local newspaper reported in the fall of 1900 that his health was “utterly wrecked” (“Talk of the Town,” *Sumpter Miner*, October 3, 1900). These three organizers of the Diadem Gold Mining Company left their respective corporate offices when the stockholders elected new officers late in 1900; Oregon law favored directors who resided in Oregon (“New Diadem Officers,” *Sumpter Miner*, December 5, 1900). The new officers lived in Baker County: J.H. Robbins, President, also mayor of Sumpter; N.C. Richards, Vice President, also an attorney; and Otto Herlocker, Secretary and Treasurer, also assistant cashier at the First Bank of Sumpter. In 1901 advertisements for Diadem stock, J.K. Pardee appeared as “a mining expert well known all over Utah, Idaho and Montana.” The ad quoted his endorsement of the mine: “In all the years I have mined I never saw a prospect that made the showing of the Diadem mine” (“Diadem Gold Mining Company,” advertisement, *Sumpter Miner*, April 17–May 29, 1901). Those advertisements listed only Joe Pardee, not his father, among the major stockholders, but Joe soon left the Diadem to again mine in Montana.

By the end of 1901, both Pardees had left the Diadem, but not because the property lacked potential. Funding became tight and shareholders became vocal. Joe Pardee was used to having more control than the investors in Butte allowed. In 1902 the mine did not resume operations on schedule that season. A representative of Butte investors, who held 700,000 of the 1 million shares, toured the Diadem property in July. He issued a positive report. The Diadem company let a contract to the Sunrise Mining Company, also in the Greenhorn district, to mine and mill Diadem ore. In 1903, now controlled by stockholder Lee Mantle, the Diadem company applied for a patent and contracted with the newly developed Snow Creek mine, just below the Diadem, for mining and milling. Only limited work was done that season. But Snow Creek continued to work the Diadem ore into 1905. That year stockholders became frustrated that continued development had not struck a vein. They refused to pay for further development. That closed the mine. Mantle sued the Diadem Gold Mining Company, the company dissolved, and in May 1906 the court ruled in Mantle’s favor. Both the Diadem and Brindle Horse claims were to be sold at a sheriff’s sale in June to cover the judgment, interest, costs, and accruing costs; in total about \$2000 (“Notice of Sheriff’s Sale,” *Blue Mountain American*, Baker City, Ore., May 19, 1906). As a result, Mantle got control of the now-patented property. But there is no record of the Diadem being mined thereafter.

For its very ordinariness—including its failure to become a major mine, the Diadem is representative of many more mines than the famous mines with big strikes. Joe Pardee got hard rock and corporate mining experience at the Diadem. Two years was enough for him; he returned to hydraulically mining placer gold in Montana. Pardee left financially strong enough to invest in a new mining venture. And he purchased a home in Missoula, a house on East Front Street, with a view of Mount Jumbo and its parallel shorelines of a glacial lake not yet named. Furthermore, the Diadem provided Pardee with local expertise that enabled him to get temporary field assignments in the area with the U.S. Geological Survey in 1908 and 1909, and for his later work on the Sumpter quadrangle.

Three Mile District: Three Mile Placers, 1901–1903

Joe Pardee and Sam Watson, formerly mining neighboring claims in Basin Gulch (fig. 2), formed a partnership to mine placer gold beside Three Mile Creek (fig. 5), northeast of Stevensville, in Ravalli County, Montana. Three Mile Creek flows down the western slope of Cleveland Mountain; it flows from the mountain to the Bitterroot River, which flows north into the Clark Fork of the Columbia River. The Three Mile unorganized mining district on the western slope of the Sapphire Mountains was northwest of Basin–Quartz gulches on the eastern slope of range.

In August 1901, Pardee and Watson began buying claims and water rights along Three Mile Creek, and in September they were locating and relocating claims and water rights in the area. By December they had acquired seven mining claims, with some overlapping boundaries, mostly in Section 24, T. 10 N., R. 19 W., and they added an eighth shortly thereafter:

- Corda, originally located January 2, 1893 and later merged with the Dayton and Freeman;
- Cornucopia, located February 5, 1902, by Joseph T. Pardee and Samuel Watson;
- Dayton and Freeman, originally located November 15, 1884, by Leroy H. Dayton and James Freeman;
- Estella, located September 17, 1901, by Joseph T. Pardee and Samuel Watson;

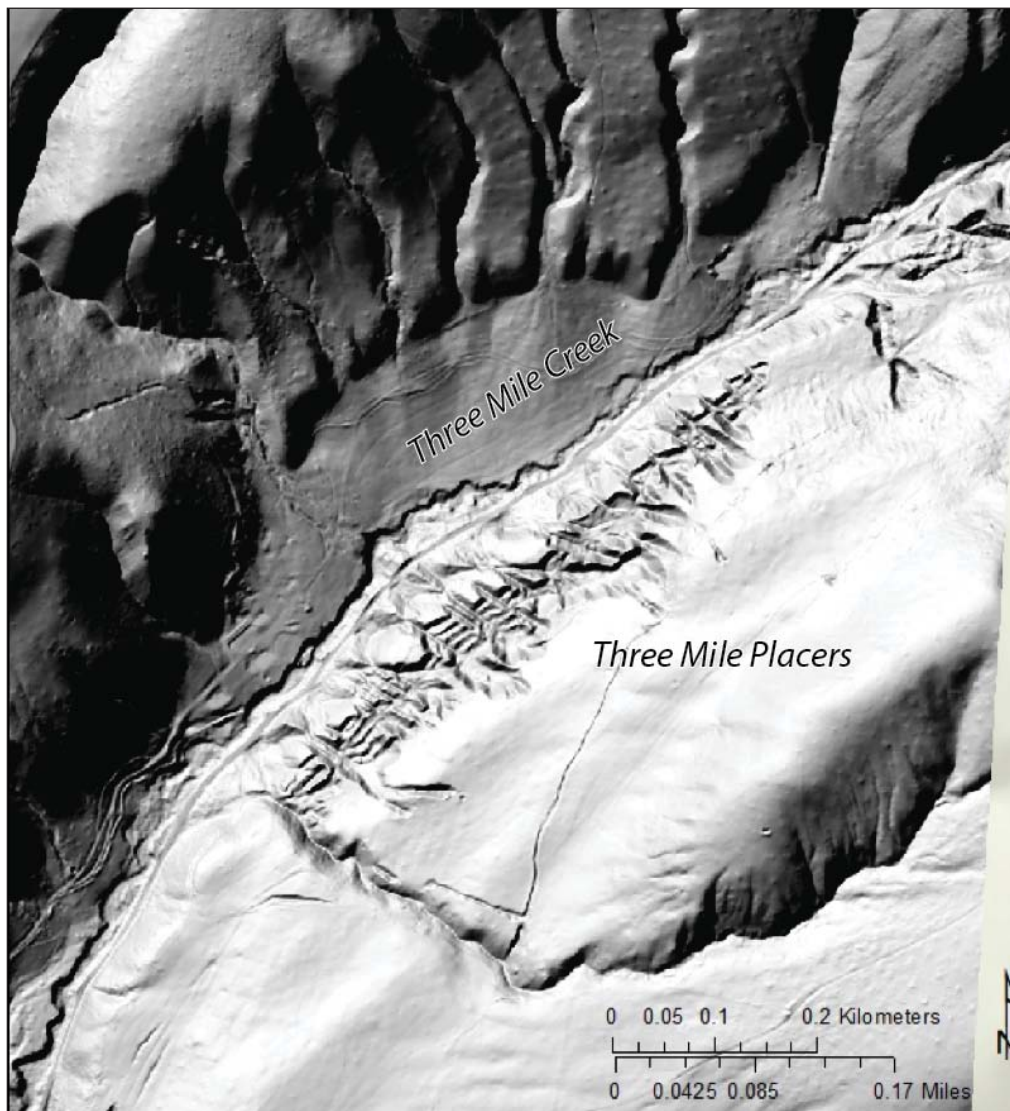


Figure 5. LiDAR map showing the approximately 1-mi scar of the Three Mile placers south of Three Mile Creek. The image was obtained from the Montana LiDAR Inventory and provided to the author by Michael Stickney of the Montana Bureau of Mines and Geology.

- Estella No. 2, located September 17, 1901, by Joseph T. Pardee and Samuel Watson;
- Fausett, located June 4, 1900, by Egbert E. Fausett and J. D. Fausett;
- Fox Quartz Claim, located April 1, 1898, by W. J. Whitmore; and
- Garden City, which had originally been located January 2, 1893 by L.H. Dayton, N.J. Dayton, C.A. Sanders, G.V. Eldridge, W. J. Whitmore, and M. R. Whitmore, and relocated on September 2, 1901, by Joseph T. Pardee and Samuel Watson.

And they filed amended locations for the Fausett and Dayton and Freeman. Also, they bought the Dayton water right and located the Three Mile Creek water right. Most of the claims were south of the creek, but the creek flowed lengthwise down the Estella claim (in R. 18 W.) and the adjoining Dayton and Freeman claim (in R. 19 W.).

Pardee and Watson were on-site working in September, before they finished their acquisition spree. Improvements shown on the Estella plat include a diversion in Three Mile Creek at the upper (eastern) end of the Estella claim and a flume along the creek through the Estella and Dayton and Freeman. One big cut was down to road level next to the creek. A string of cuts were higher up the hillside, along a bench south of the creek (fig. 5). Modest “Chinese walls”—waste rock piled for function—helped direct water down from the bench and provided pathways through waste rock piles; the Chinese walls suggest that at some time Chinese laborers worked on the placers. The exclusionary measures of former years had not removed all Chinese from western mining; in fact, Watson had employed a Chinese laborer at his Basin Gulch mine. Pardee and Watson worked their Three Mile placers with a few hired men and hydraulic equipment in 1902 and 1903.

They also applied for patents on some of the land. Pardee and Watson (fig. 6A) applied for a patent for the Estella, almost 39 acres. They combined the Corda, Dayton and Freeman, Estella No. 2, and Fausett, Garden City into one patent application covering 270 acres; this was the Dayton patent. The Estella patent was granted in January 1905 and the Dayton in June 1909. The delays were due to questions concerning title. The titles of all mining, stone, and forestry claims in former Indian lands in the Bitterroot Valley up from (south of) Lolo Creek had been thrown into question with the realization that the act of Congress that had opened those lands to settlement had failed to open those lands for other types of entry. It took a couple acts of Congress to clarify and affirm the claims to patented lands and unpatented claims. Meanwhile, the State of Montana claimed twenty-some acres of the Pardee and Watson land, a selection duly protested.

Like the Basin Gulch placers, the Three Mile placers required water, so the mining season was also the water season. Three Mile miners had the added challenge of keeping the water clean enough for irrigating fields

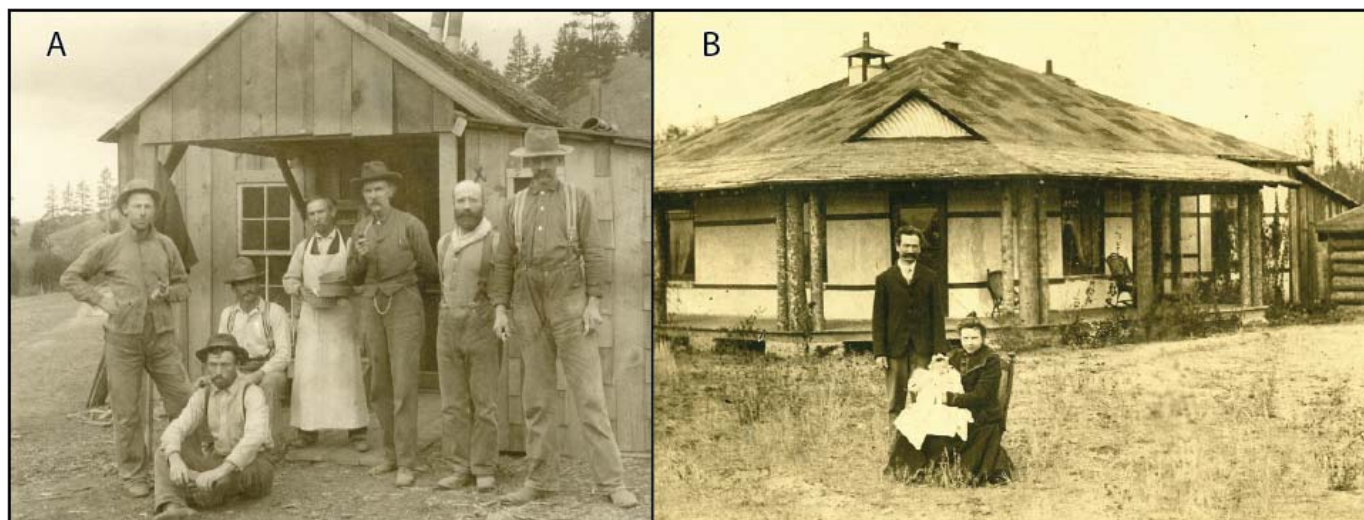


Figure 6. (A) The crew at the Three Mile Placers northeast of Stevensville, Montana. Pardee's partner Sam Watson is the hatless man second from the right. Photograph from Pardee Family Collection. (B) Joe and Ruby Pardee and their daughter Mary Josephine (Mary or Mary Jo) appear in the yard of their home on Three Mile Creek, Stevensville, Montana. Mary was born there in 1905. Photograph from Pardee Family Collection.

and watering livestock downstream; in 1895, a court had issued an injunction stopping the mining at the placer claims because the resulting muddied water was unfit for agricultural use. Pardee and Watson needed water under pressure to hydraulically blast the hillside apart. They built a flume, taking water from upstream. At each open cut on the bench, an earthen- and rock-lined ditch allowed waste water to flow down to the creek.

But the flume did not work as well as anticipated or needed, so Pardee and Watson planned to dam Three Mile Creek, build a reservoir on the creek, and divert water from Rock Creek across the Sapphire Range to Three Mile Creek. The water could also be used to irrigate the Three Mile country. A 40-mi canal-and-flume system and a reservoir would require capital. They found eastern capitalists willing to invest. Pardee and Watson began work on the dam and reservoir in November, but the capitalists also wanted mining ground.

In December 1903, Pardee and Watson sold 320 acres of Three Mile placer land to eastern capitalists and the Western Realty of Missoula (“Mines Sell for a Large Price,” Stevensville Register, December 9, 1903). For \$60,000, W.H. Hammond of Detroit, Michigan, got 3/4 interests in the Cornucopia, Estella, and Dayton and Freeman placers. Hammond’s brother George was president of the Coe Commission in Minneapolis and also a major investor in the Three Mile placers. John A. Scott of Missoula paid \$15,000 for 1/4 interest in each of those claims. Scott also represented additional investors. Pardee and Watson continued building the dam and reservoir on Three Mile Creek. They quit in January due to interference from an investor associated with Western Realty. The placer sale had made Pardee and Watson financially comfortable, and they turned their attentions elsewhere.

The Coe Commission developed the Three Mile placer, installed a Giant type hydraulic, and even did some ground-sluice prospecting above the bench being washed, but the Coe Commission failed. Coe failed due to unrelated stock jobbing. Scott of Missoula organized investors to buy the 3/4 interests from the defunct Coe Commission, and he found investors in Spokane interested in the property and prospects, prospects much bigger than just gold mining. The Bitter Root Placer Irrigation and Power Company, incorporated in Spokane, Washington, in early 1907, acquired the Three Mile placers and water rights. Scott became vice president of the Spokane company. The president, Lachan MacLean, was also president of the Spokane Canal Company. The new owners had big plans and resumed construction of the dam on Three Mile Creek. But the U.S. Department of Interior then ruled against the title to any and all mineral lands on the former Indian lands of the Bitterroot Valley above the Lolo. A.M. Strode of Mullan, Idaho, bought the 3/4 interests in the placers and placed men to work building sluices and flumes for the 1907 mining season. Men mined the placers that season, but in August the venture failed with liens on the property for unpaid wages. Meanwhile, Pardee and Watson divested of their remaining Three Mile mining properties over time.

Conclusion

For several years, Pardee was in a career transition. While exploring new opportunities, Pardee traveled to Butte, Spokane, and other cities. In March 1904 Pardee purchased land on Three Mile country, down the creek a few miles from the placer diggings. That September, he married Ruby Estelle Schoonover, of Philipsburg; they had known each other for years. Joe and Ruby settled on Three Mile Creek (fig. 6B). Their daughter Mary Josephine Pardee (Mary or Mary Jo) was born there in 1905. A view from his house and from along Three Mile Road, looking southeastward, is Cowell Buttes. Horizontal lines of trees and shrubs mark the beaches of Glacial Lake Missoula. Joe Pardee sketched the buttes in August 1908, and he used that sketch in his 1910 article on Glacial Lake Missoula.

Meanwhile, Pardee took a job as professor and director of music at the Stevensville Training School for a year and advertised private music lessons the next year. While in Philipsburg in the summer of 1908, he spent a couple of weeks as a volunteer helping a U.S. Geological Survey team working around the Flint Creek Valley; William Harvey Emmons and Frank Cathcart Calkins used Pardee’s unpublished 1892 topographic map and his local expertise in their work on the Philipsburg quadrangle (Emmons and Calkins, 1913). In August 1908 Pardee accepted a temporary, seasonal job with the federal agency, which sent him to northeastern Oregon to report on mining prospects there. The Geological Survey published his report on “Faulting and Vein Structure in the Cracker Creek Gold District, Baker County, Oregon” (Pardee, 1909). The following year the Geological Survey

again hired him as a temporary on field assignment. This time he wrote a report on the “Placer Gravels of the Sumpter and Granite Districts, Eastern Oregon” (Pardee, 1910a). His article on “The Glacial Lake Missoula” appeared in the May–June 1910 issue of *The Journal of Geology* (Pardee, 1910b).

By the time Pardee received his notice of appointment as Junior Geologist with the U.S. Geological Survey, dated July 11, 1910, he had a good education from the College of Montana and the University of California, he had 10 years of experience mining, he had completed two temporary assignments for the federal survey, and he had three geology publications. Despite lacking the doctorate credential then common among new junior geologists, he was well qualified for the position of a mineral resources expert. He remained with the Geological Survey until forced by federal regulations to retire at the age of 70.

References

- Baker, V.R., 2008, The Spokane flood debates: Historical background and philosophical perspective: Geological Society of London Special Publications 301, p. 33–50.
- Basin Mining Company Records, 1903–1925, Record group MC 311: Montana Historical Society Research Center Archives, Helena.
- Berg, R.B., 2014, Sapphires in the southwestern part of the Rock Creek sapphire district, Granite County, Montana: Montana Bureau of Mines and Geology Bulletin 135, 86 p.
- Diadem Gold Mining Company Articles of Incorporation, December 18, 1899, Oregon State Archives, Salem, Ore.
- Emmons, W.H., and Calkins, F.C., 1913, Geology and ore deposits of the Philipsburg quadrangle, Montana: U.S. Geological Survey, Professional Paper 78.
- Kelly, M.P., 1963, Memorial to Joseph Thomas Pardee: Geological Society of America Bulletin 74, no. 5, p. 39–42.
- Lindgren, W. , 1901, The Gold Belt of the Blue Mountains, *in* Twenty-second Annual Report of the Director of the United States Geological Survey, 1900–1901, Part 2: Ore Deposits, p. 551–776.
- Pardee, J.T., 1909, Faulting and vein structure in the Cracker Creek gold district, Baker County, Oregon: Bulletin of the U.S. Geological Survey 380, p. 85–93.
- Pardee, J.T., 1910a, Placer gravels of the Sumpter and Granite districts, Eastern Oregon: Bulletin of the U.S. Geological Survey 430-A, p. 59–65.
- Pardee, J.T., 1910b, The Glacial Lake Missoula: *Journal of Geology*, v. 18, no. 4, p. 376–386.
- Pardee, J.T., 1942, Unusual currents in Glacial Lake Missoula, Montana: Geological Society of America Bulletin 53, p. 1569–1600.
- Soennichsen, J., 2008, Bretz’s flood: The remarkable story of a rebel geologist and the world’s greatest flood: Seattle, Wash., Sasquatch Books.
- Wagner, N.S., 1959, Mining in Baker County, 1861 to 1859: Ore-Bin (Oregon Department of Geology and Mineral Industries), v. 21, no. 3 (March 1959): p. 21–27.



Anne Millbrooke and Bruce Cox at the Cable Mine field trip overview (photo: P. Hargrave).



Mike Garverich reads a book at the Montana Tech Mineral Museum (photo: C. McKillips).

The Mineral Display at the 1893 World's Fair: How Montana Became Known as the Treasure State

Michael J. Gobla

Engineer, U.S. Department of the Interior, Bureau of Reclamation, Denver, Colorado

Montana has several nicknames, including The Treasure State, and more recently Big Sky Country and The Last Best Place; however, none of these are official names. The State has an official motto, “Oro y Plata,” which is Spanish for “gold and silver.” The nickname “The Treasure State” originates from 1892, and most people assume that it is a self-proclaimed boast of the vast mineral wealth found in the State. Montana was a mining powerhouse in 1892, with its great production of silver, gold, and copper, and its citizens enjoyed the highest per capita income of any state in the nation. Julian Ralph, a journalist from New York City, called Montana the Treasure State, but mineral wealth was only a small part of the consideration for the name.

The name “Treasure State” grew out of the excitement generated by the 1893 Chicago World's Fair (Columbian Exposition) commemorating the 400th anniversary of the voyage of Christopher Columbus to the New World. Planning to celebrate the Columbus anniversary began in the late 1880s at a time when fairs were very popular. A desire to do the fair on a grand scale led to a competition between New York and Chicago to be the host, causing the Federal Government to step in and decide the matter. Congress announced that they would provide up to \$1.5 million to support the fair, including construction of a Federal building at the fairgrounds. Chicago was selected by the lawmakers, swayed by a pledge that Chicago citizens would immediately provide \$5 million in cash along with a promise to raise another \$5 million, outbidding New York. With the Federal Government involved, it was decided to delay the fair until 1893. Harpers Magazine, a big supporter of the Columbian Exposition, hired Julian Ralph in 1891 to write an introductory book about Chicago and the Columbian Exposition. Harpers published the book a few months before the fair opened (Ralph, 1893). Mr. Ralph also wrote a 16-page article titled “Montana: The Treasure State” (Ralph, 1892), providing details about Montana treasure that included its extensive cattle herds; vast agricultural lands; numerous mines, mills, and smelters; its modern cities; great rivers; and awesome scenic beauty. Mr. Ralph's article was noticed by a few Montana newspapers who published brief summaries of it and suggested the name was a fitting one and should be adopted. In 1892, final preparations for Montana's mineral display for the Fair were ongoing across the State, and the notion of showing the world that Montana was indeed the Treasure State took hold.

Prize Winning Displays

Mine owners in Montana Territory sent spectacular mineral exhibits to fairs and expositions to promote investment in the region. The displays evolved over time from a collection of ores and gold nuggets like those sent to the Centennial Exhibition in Philadelphia in 1876, to grand displays filled with high-grade specimens of gold, silver, and copper ores, metal ingots, gems, coal, and building stones from throughout Montana. Senator W.A. Clark was a leading proponent who, along with a few of Montana's other millionaires, contributed cash to ensure the mineral displays were the best that could be assembled. Fine cabinetry was constructed to house the mineral specimens. Clark persuaded other individuals, banks, and mining companies to loan their best specimens to the exhibition effort and he convinced the State legislature to pay for shipping the displays. By the late 1890s, Montana was renowned for putting on the best mining and mineral exhibits in the nation.

One of the early elaborate displays was at the World's Industrial and Cotton Centennial Exposition held at New Orleans, Louisiana from December 1884 to May 1885 (fig. 1). Representing Montana Territory were John S. Harris of Helena as Commissioner and William A. Clark of Butte as the alternate representative. The display included a fortune in gold dust and nuggets, on loan from various banks and leading mine owners of the territory. Specimens of crystalline gold from the Atlantic Cable mine in Deer Lodge County were the most impressive feature of the Montana exhibit. The gold was described as a sight to behold. It was valued at \$10,000 based upon its estimated gold content, an incredible 500 oz of contained gold. The Montana exhibit grew in scope over the next few years as it made its way to other fairs around the nation, and it was even sent to the Paris Expo in 1889.



Figure 1. A portion of the Montana exhibit at the 1884 World's Industrial and Cotton Centennial Exposition at New Orleans, Louisiana (Photograph from the Montana Historical Society collection).



Figure 2. The Mining and Minerals Building at the Chicago World's Fair cost \$265,000 to erect.



Figure 3. The Montana State building at the Chicago World's Fair cost \$50,000 and was paid for by the State legislature.

The World's Fair in Chicago was somewhat unique in that an entire 6-acre building was devoted to Mining and Minerals (fig. 2), which had not been done before. Past World fairs had dedicated buildings for arts, industrial equipment, and agricultural products, with the remaining buildings being put up by nations.

Montana went all out for their display at the Columbian Exposition, held in 1893 in Chicago. Montana put up a building costing \$50,000 (fig. 3), but it was the mineral exhibit that was the outstanding achievement. Montana had 538 separate contributions of ores, nuggets, gems, building stones, and smelter products from across the state (Handy, 1893). Madison County sent rich gold and silver ores from nearly every mine. An incredible boulder of silver ore weighing 4,557 lbs (about 2.2 tons) was contributed from the Bi-Metallic mine in Granite County (figs. 4, 5). Mr. Cameron was persuaded to loan his collection of gold crystals from the Atlantic Cable mine in Deer Lodge County and a special secure case was constructed to display them. Many photographs of the mines, mills, and smelters of Butte were exhibited. The Anaconda Company sent ore samples from the Anaconda, Wake Up Jim, High Ore, Green Mountain, and Mountain Consolidated mines. Many of the Anaconda Company's samples contained large amounts of native silver. Clark contributed samples from the Gagnon, Mountain View, and East and West Colusa mines. The Butte & Boston Company exhibited ores from the Original, Gambetta, and Stella mines and two fine wire silver specimens from the Wapelo mine. The Parrot Silver and Copper Company exhibited copper at all stages of manufacturing from ore to ingots and wire. The Lexington mine exhibited various ores along with crystals of quartz, sphalerite, wire silver, pyrite, and interpenetrating crystals of transparent gypsum. Included in the Lexington display was a tin pail encrusted with gypsum crystals. The Alice and Moulton mines contributed silver ore with its characteristic pink rhodochrosite and rhodonite matrix. A cluster of large rhodochrosite crystals found in the Moulton mine were exhibited by Mrs. J.K. Clark. The total weight of ores and smelter products was over 50,000 pounds, including bullion displayed in



Figure 4. The entrance to the Montana Mining Exhibit at the 1893 World's Fair. Note the 2.2-ton silver ore boulder from the Bi-Metallic mine at the entrance (Engineering and Mining Journal, 1893).



Figure 5. This boulder of silver ore was photographed at the Bi-Metallic mine at Granite, Montana just prior to shipping to the Columbian Exposition in Chicago. Rich in ruby silver, it was estimated to contain more than 2,000 oz of silver.

piles like cord wood. Other states sent impressive displays, as did many foreign nations. The Mining and Minerals Building housed the greatest display of gold, silver, and rich ore specimens ever collected, with the Montana display exceeding all of its peers.



Figure 6. Montana's Silver Justice statue at the Columbian Exposition.

an unsuccessful campaign to stop the nation from removing silver as backing for U.S. currency.

Silver Statues

To make the display even more memorable, Montana presented its "Silver Justice" statue (fig. 6). It was the most remarkable exhibit at the Fair. The 9-ft silver statue consisted of Justice carrying a two-edged sword and a scale poised atop a globe resting upon a silver Montana eagle. Justice was modeled in the Greek style with her eyes wide open. The scale contained coins of silver on one pan balanced by coins made of gold in the other.

Although the gems and gold specimens were most remarkable, it was the statue that made the big impression with the public. Only the Colorado display with its Silver Queen statue came close to the grandeur of the Montana exhibit. The Colorado "Silver Queen" statue (fig. 7),

had the head carved from a boulder of native silver (the largest single piece of native silver ever mined) that had recently been recovered from the Molly Gibson mine at Aspen, Colorado. The western states were trying to advertise the importance of silver to their economies in 1893. The lavish displays were part of

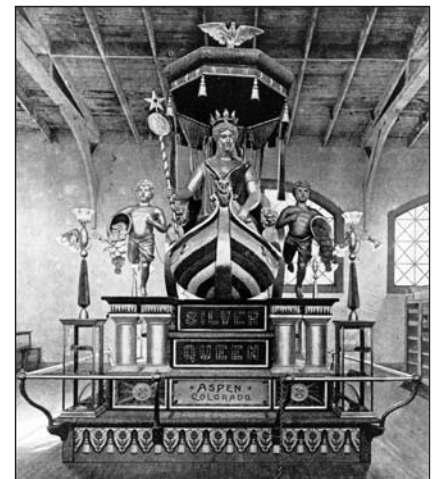


Figure 7. The Silver Queen in the Colorado mineral exhibit at the Columbian Exposition in 1893.

The Montana statue of “Justice” was made from \$75,000 worth of silver resting upon a \$225,000 gold platform (Engineering and Mining Journal, 1893). The entire metal casting was supported by a slab of mineral-bearing rock, giving the exhibit a total height of 15 ft (State Board of World’s Fair Managers, 1893a,b). It was cast by the American Bronze Company of Chicago for a fee of \$3,750, and the sculptor, Mr. Park, received \$10,000 for the effort. It contained 60,000 oz of silver from the mines of Senator William A. Clark and former Governor Samuel T. Hauser, the largest amount of silver used in a single object. The gold was on loan from the Mrs. McAdow’s Spotted Horse mine at Maiden, Montana. The statue was the most popular exhibit; most of the 27 million visitors to the fair went to see the famous silver statue. Souvenir booklets, photographs, and a water-color print (fig. 8) were popular items, and it was featured in several books about the fair (fig. 9).

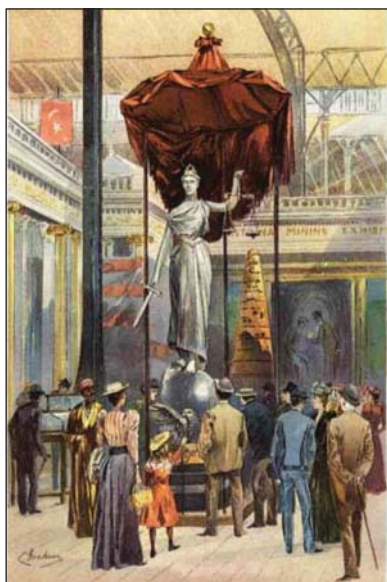


Figure 8. Print of artist’s watercolor drawing of the Montana Silver Justice was a popular souvenir of the 1893 World’s Fair.



Figure 9. A view showing the Silver Justice statue and some of the mineral cases in the Montana Exhibit, as depicted in a souvenir book about the fair.



Figure 10. Advertisement from a Kansas City, Missouri department store (Kansas City Daily Journal, March 12, 1895, p. 3).

The Chicago company that cast the statue took possession of it with the intent of sending it on tour around the country. They offered to send an equivalent amount of silver and gold back to the Montana owners of the metal. The Montana Statue Company objected to the deal. They had paid the expenses for creation of the statue and claimed part ownership of it. An agreement was worked out and an equivalent amount of silver was returned to Clark and Hauser in Montana. Mrs. McAdow continued to loan out the gold base to the Montana Statue Company.

The silver statue was sent out on a tour of the country. It first went to a New York City department store. The statue typically was exhibited for a few weeks at each location. After New York it made appearances at fairs and department stores all over the nation (fig. 10). In December 1894 it was back in Chicago at a department store, when there was an unsuccessful attempt to steal it. Afterwards, five armed guards were posted night and day at the Chicago store for the remainder of the visit. The tour continued until it reached Topeka, Kansas in 1903, when a \$1,000 dispute arose over the contract with the Montana Statue Company to display it in a Topeka department store. The judge appointed a receiver and had it removed from the Topeka store, boxed up, and stored in the basement of a local building. The McAdow gold base was returned, but the silver statue sat in the basement for 6 years as the dispute played out in the court. Finally, agreements were reached on how to divide up the value and settle the debts. In November 1903, it was sent to Omaha, Nebraska and melted down. The Omaha smelter paid \$40,000 for the recovered silver. Although Montana was not successful in its efforts to retain government support for the price of silver, its silver statue impressed the nation and the grandeur of its mineral exhibit confirmed the fitting nature of its name as the Treasure State.

References

- Handy, M.P., 1893, The official directory of the World's Columbian Exposition, May 1 to October 30th, 1893: A reference book:Chicago, W. B. Conkey Company.
- Ralph, Julian, 1892, Montana: The Treasure State: Harper's New Monthly Magazine, Vol. LXXXV, June, 1892, p. 90–106.
- Ralph, Julian, 1893, Harper's Chicago and The World's Fair: New York, Harper & Brothers, 244 p.
- Engineering and Mining Journal, 1893, Mining at The Columbian Exposition, August 19, p. 186–189.
- State Board of World's Fair Managers, 1893a, Montana, history, resources, possibilities: State Board of Managers for Montana, 64 p.
- State Board of World's Fair Managers, 1893b, Montana exhibit at the World's Fair and a description of the various resources of the State mining, agriculture and stock-growing: Butte, Mont., Intermountain Print, 64 p.
-



Mike Gobla and Stan Korzeb at the Montana Tech Mineral Museum (photo: C. McKillips).



The student poster session at Montana Tech (photo: A. Roth).



Book sale at the Montana Tech Mineral Museum (photo: C. McKillips).

Magmatic Processes that Produce Porphyry Copper Deposits: From Batholith Formation to Anhydrite, Apatite, and Zircon Mineralogy

John H. Dilles

*Professor of Geology, College of Earth, Ocean and Atmospheric Sciences
Oregon State University, Corvallis, Oregon*

Porphyry copper (Cu ± Mo ± Au) deposits today provide much of the world's newly mined copper (>65%), molybdenum (>90%), and gold (>35%), as well as numerous minor metals (Re, Te). Individual deposits contain as much as 10 Bt of sulfide ores with up to 1 wt.% Cu, 0.04 wt.% Mo, and 1 g/t Au. The ores are produced by hot hydrothermal fluids (700–300°C) derived from granitic magmas. Oxidized arc magmas (oxidation states of NNO+1 to +3) are commonly enriched in sulfur, chlorine, water and metals, and are therefore favorable to

formation of porphyry and epithermal Cu-Au-Mo-Ag ores. Ore-forming magmas record these characteristics via their petrology and mineral compositions. In particular, studies of the sulfur content of apatite and the rare earth element (REE) composition, in particular the Eu_N/Eu^*_N , of zircon provide useful petrologic indications of ore-forming magmas.

Anhydrite ($CaSO_4$) has been reported in a number of arc volcanoes, and attests to high contents of oxidized sulfur in these magmas. At high temperature, the magmatic silicate melt can dissolve large amounts of sulfate under oxidized conditions, but at low temperature sulfur solubility is negligible (<100 ppm at <750°C). Cooling magmas may store sulfur as anhydrite, which then breaks down upon magmatic volatile (water) saturation to add SO_2 to these parental ore fluids (fig. 1). Recent reconnaissance studies have identified anhydrite inclusions in apatite in several ore-forming porphyry samples, which suggests this may be a widespread phenomenon and source of sulfur to these ores.

Where anhydrite is not present, sulfur-rich apatite also has the potential to record high sulfur contents of magmas and, by inference, anhydrite saturation. Anhydrite is very soluble in aqueous solutions and is rarely preserved in crystalline igneous rocks. Therefore, anhydrite may have been lost both during magmatic degassing and during later weathering or rain water leaching. High sulfur apatites have been recognized in several porphyry copper magmas, and offer a robust way to discern high sulfur contents of magmas (Streck and Dilles, 1998).

Zircon is a robust accessory mineral that is present in many granitoids, intermediate-silicic volcanic rocks, and clastic sedimentary deposits that are derived from these rock types. Both ion microprobe (SHRIMP) and laser ablation-ICP-MS methods provide U/Pb age and trace element compositional “fingerprinting” for zircon. Both rare earth elements Ce and Eu (Ce^{3+} vs Ce^{4+} and Eu^{2+} and Eu^{3+}) are incorporated into zircon, and potentially record oxidation state of the magma (fig. 2). A more strongly oxidized condition is recorded by a greater positive Ce anomaly (Ce_N/Ce^*_N , i.e., chondrite-normalized) or the smaller negative Eu anomaly as recorded by a larger value of Eu_N/Eu^*_N , but the former is difficult to measure compared to the latter.

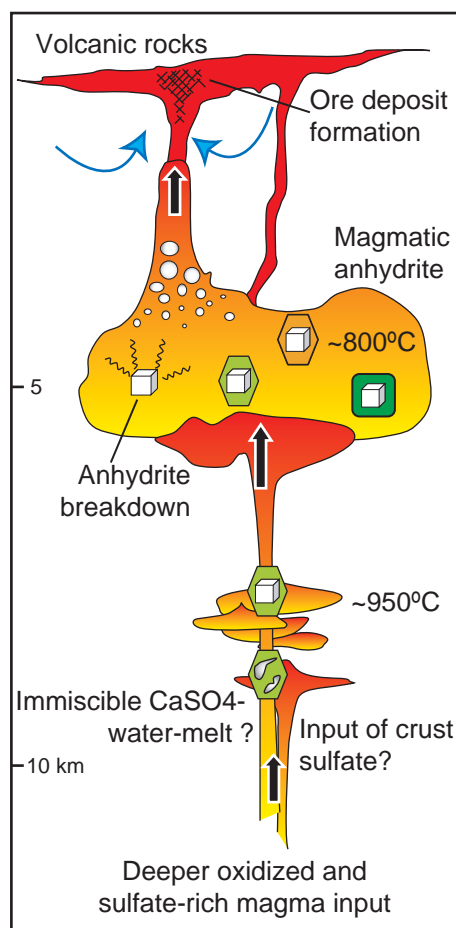


Figure 1. Schematic illustration of magmatic middle and upper crustal magma emplacement, illustrating the deep input of $CaSO_4$ -bearing melt or anhydrite in andesite magma into an upper crustal evolving dacite magma chamber containing anhydrite (modified from Yanacocha, Peru, Au-Cu epithermal-porphyry deposits, of Chamberfort and others, 2008). As dacite cools it saturates with water-rich volatiles that rise to become ore-forming fluids, anhydrite breaks down via the reaction $CaSO_4$ (anhy) \leftrightarrow CaO (m) + SO_2 (v) + $0.5O_2$ (v) that adds sulfur to the fluids and oxidizes both magma and fluids.

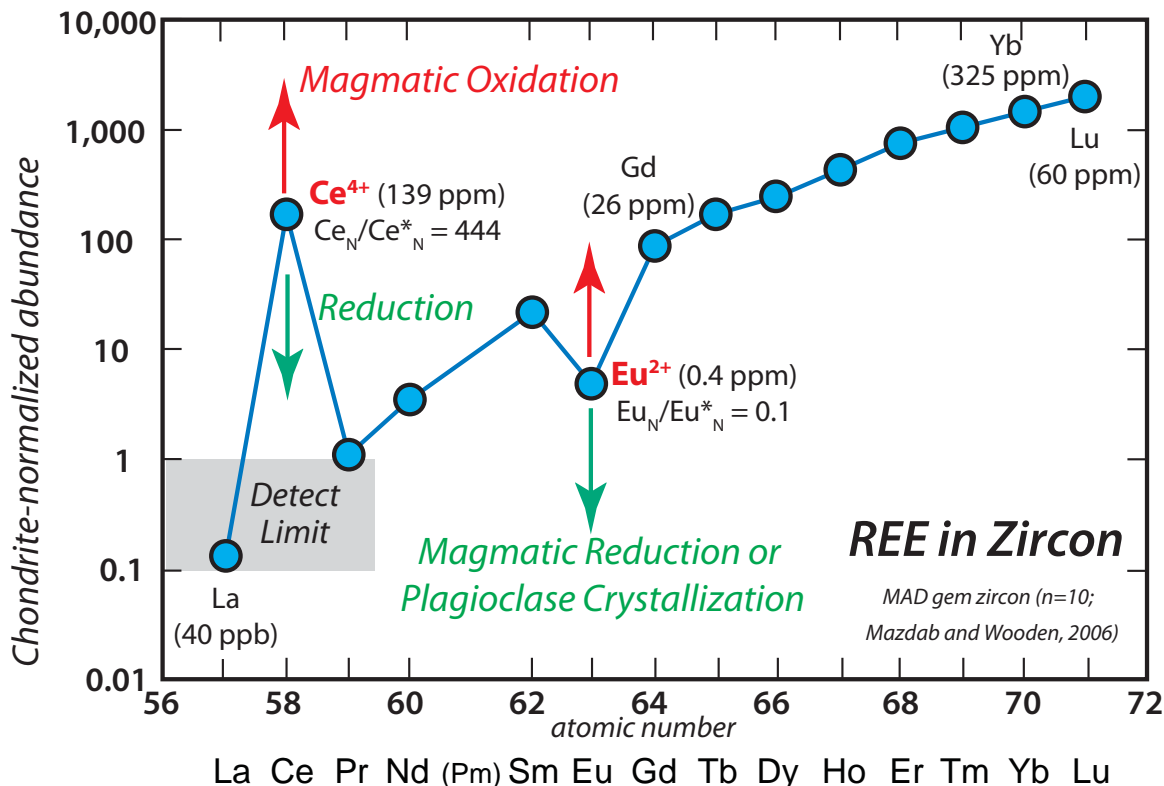


Figure 2. Typical rare earth element pattern of zircon (normalized to chondrite; see Mazdab and Wooden, 2006, for normalization procedure), illustrating the Ce and Eu anomalies and how they record magmatic oxidation state and the amount of plagioclase crystallization.

SHRIMP data indicate that arc magmatic rocks are characterized by zircon with relatively high U/Th >0.6, high Sc/Yb >1, and relatively low Ti (<20 ppm) compared to MORB and mantle plume settings. Our zircon database from Cordilleran plutons indicates that both pre-ore and post-ore non-mineralized granitoids from porphyry Cu districts are similar to typical arc magmatic rocks. The Ti-in-zircon temperatures range widely and generally decrease from core to rim; correspondingly, the Hf content increases, REE and Y contents and Th/U ratio decrease, and the europium anomaly (Eu_N/Eu^*_N) becomes more negative.

Mineralizing granitoid melts lacking zircon likely separated from lower- to middle-crustal source regions at low temperature (850–800°C) and ascended with low (<10 vol.%) crystal contents. These magmas were strongly oxidized and both water- and sulfur-rich. Commonly, the ore-related porphyries have characteristic low Ti-in-zircon temperatures (750 to 650°C) and a small negative europium anomaly ($Eu_N/Eu^*_N >0.4$; fig. 3). The latter attests to high water content and suppression of plagioclase crystallization similar to high Sr/Y of whole rock. As Ti-in-zircon temperature decreases, Eu_N/Eu^*_N is constant or increases, REE and Y contents decrease by a factor of ca. 10, and the middle REE/heavy REE ratio decreases. These effects are attributed to <760°C crystallization of titanite. The distinctive small negative Eu_N/Eu^*_N of mineralized porphyries during crystallization at near solidus temperatures of 750–650°C is a complex process; oxidation of melt (Eu^{2+} to Eu^{3+}) via degassing of SO_2 -rich ore fluids (Dilles and others, 2015; fig. 1) and titanite crystallization both cause an increase in Eu_N/Eu^*_N , whereas crystallization of observed Na-plagioclase causes a decrease.

Therefore, reconnaissance analyses to determine the S-content of apatite and Eu_N/Eu^*_N of zircon rims from granites and clastic sedimentary rocks derived from granitic terranes may provide fingerprints of prospective plutons.

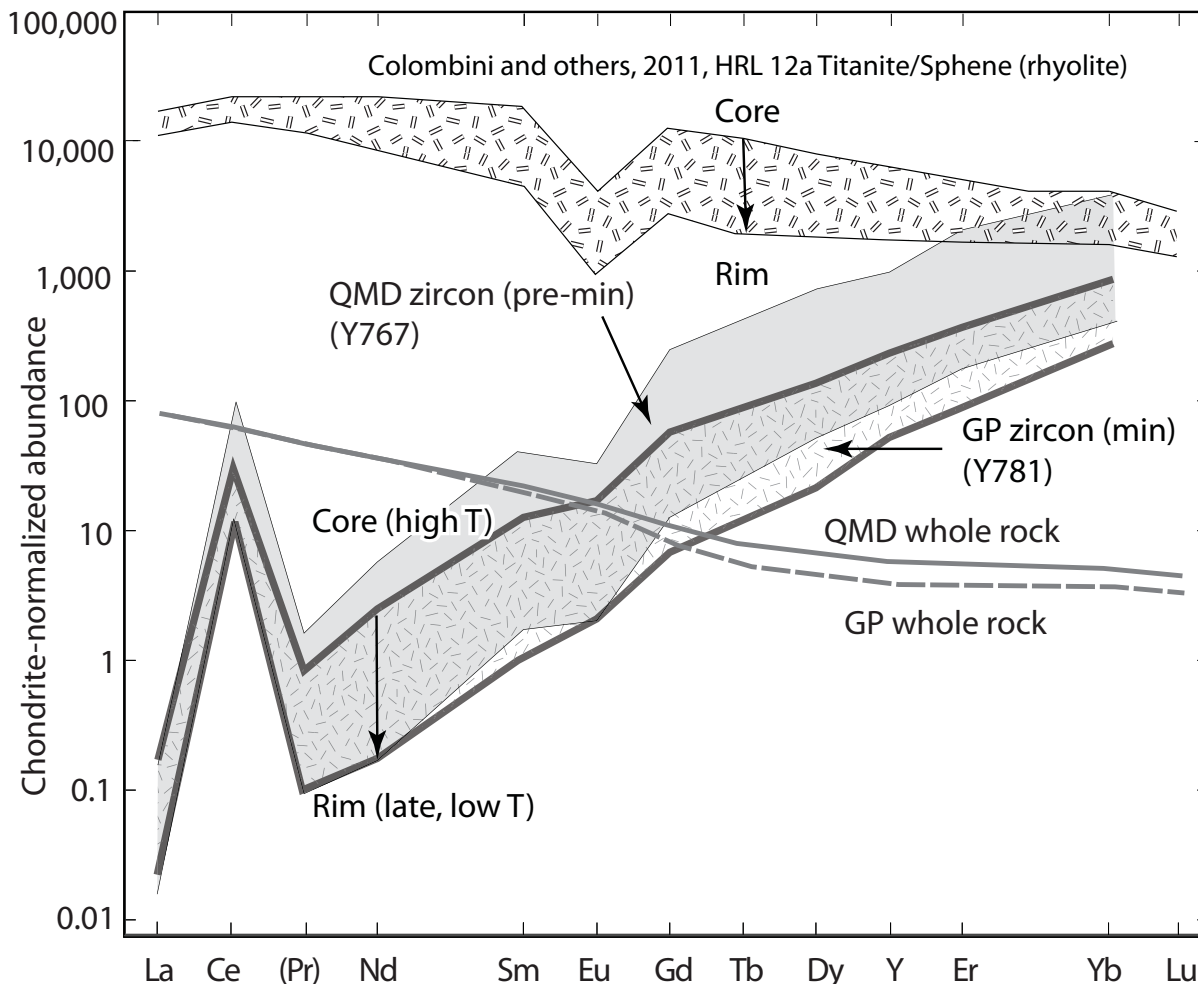


Figure 3. Rare earth element (REE) pattern of zircon from the Yerington batholith, Nevada (from Dilles and others, 2015). Early, non-mineralized McLeod Hill quartz monzodiorite (QMD, Y767) has a modest negative Eu anomaly and a convex upward pattern, whereas a late mineralizing granite porphyry dike of the Luhr Hill granite (GP, Y781) has a very small Eu anomaly ($Eu_N/Eu_N^* \sim 0.8$) and an almost flat REE pattern. The reduction of REE contents and flattening of the REE pattern of both the melt and zircon is likely caused by low temperature ($<860^\circ\text{C}$) crystallization of titanite (sphene), which takes up abundant REE and particularly the middle REEs.

References

- Chambefort, I., Dilles, J.H., and Kent, J.R., 2008, Anhydrite-bearing andesite and dacite as a source for sulfur in magmatic-hydrothermal mineral deposits: *Geology*, v. 36, p. 719–722.
- Colombini, L.L., Miller, C.F., Gualda, G.A.R., Wooden, J.L., and Miller, J.S., 2011, Sphene and zircon in the Highland Range volcanic sequence (Miocene, southern Nevada, USA): Elemental partitioning, phase relations, and influence on evolution of silicic magma: *Mineralogy and Petrology*, v. 102, p. 29–50.
- Dilles, J.H., Kent, A.J.R., Wooden, J.L., Tosdal, R.M., Koleszar, A., Lee, R.G., and Farmer, L.P., 2015, Zircon compositional evidence for sulfur-degassing from ore-forming arc magmas: *Economic Geology*, v. 110, p. 241–251.
- Mazdab, F.K., and Wooden, J.L., 2006, Trace element analysis in zircon by ion microprobe (SHRIMP-RG): Technique and applications: *Geochimica et Cosmochimica Acta Supplement*, v. 70, p. 405.
- Streck, M.J., and Dilles, J.H., 1998, Sulfur evolution of oxidized arc magmas as recorded in apatite from a porphyry copper batholith: *Geology*, v. 26, p. 523–526.



Road into the Cable Mine (photo: P. Hargrave).



The book sale at the Montana Tech Mineral Museum (photo: C. McKillips).

An Overview of Mesozoic Magmatism in Montana

Kaleb C. Scarberry and Petr V. Yakovlev

Geologists, Montana Bureau of Mines and Geology, Butte, Montana

Introduction

North American Cordilleran arc magmatism began around 225 Ma, prior to break up of the supercontinent Pangea (Coney, 1972; Miller and Snoke, 2009; Dickinson and others, 1988). Pyroclastic air-fall deposits from silicic eruptions settled in the Western Interior of the United States, in shallow marine and continental settings inland and west of the Cordilleran arc. In Montana, ash deposits came from vents located along the continental margin (the Sierra Nevada Batholith) and the continental interior (the Idaho and Boulder Batholiths) (Christiansen and others, 1994).

Mesozoic igneous rocks in Montana were emplaced between about 120 Ma and 66 Ma and include batholiths, plutons, volcanic fields, epiclastic volcanic sedimentary aprons, and pyroclastic ash beds (bentonite). Magmatism beginning in the Mesozoic continued into the Cenozoic. Most workers agree that: (1) batholiths and plutons formed in and adjacent to an evolving thrust wedge during Late Cretaceous contractional deformation (Tilling and others, 1968; Hamilton, 1988; Lageson and others, 2001); (2) batholiths, plutons, and related volcanic rocks are a record of Cordilleran arc magmatism (Rutland and others, 1989; Saleeby and others, 1992; Gaschnig and others, 2011); (3) uplift and deep erosion removed volcanic tops from many batholiths and plutons; and (4) collectively, these processes contributed to the production and distribution of lode gold systems and stream placer deposits throughout southwestern Montana (Foster and Childs, 1993; Lyden, 1948).

Batholiths and Plutons

Mesozoic intrusions in Montana occur primarily within and adjacent to the Helena structural salient (fig. 1) and include large batholiths and smaller plutons. The Idaho, Boulder, and Pioneer Batholiths are the major intrusive centers in Montana. Smaller batholiths, such as the Philipsburg, Mount Powell, and Tobacco Root Batholiths, are satellite masses to the major intrusive centers.

Volcanic Deposits

Stratovolcanoes, lavas, ash-flow tuffs, and air fall deposits formed throughout the North American Cordillera during Mesozoic arc magmatism (Yonkee and Weil, 2015). In Montana, a volcanic belt established itself west of the Western Interior Seaway during the Late Cretaceous (Robinson Roberts and Kirschbaum, 1995). The products of Mesozoic volcanic activity occur as volcanic fields, epiclastic volcanic deposits, and bentonite beds that are interstratified with fine-grained marine sediments. Epiclastic deposits (fig. 2) consist predominantly of volcanic rock fragments produced during eruptions and reworking of volcanic deposits by surface processes. Collectively, the volcanic deposits record the formation, uplift, and erosion and redistribution of a broad Mesozoic volcanic plateau.

Volcanic Fields

Volcanic deposits are notorious for their significant lateral variation in thickness and texture, which makes them difficult to regionally correlate. We make an attempt at correlating these deposits in Montana using results from published studies (fig. 2). Primary volcanic deposits include basaltic–andesite lava flows and breccia, water-lain tuff, rhyolite tuff and breccia, rhyolite–dacite ignimbrites, and dacite lavas and flow-dome complexes. The best exposures of these sequences occur in the Adel Mountain Volcanic Field, the Bannack Volcanic Field, the Elkhorn Mountains Volcanic Field, and Sliderock Mountain Volcano (figs. 1, 2). Interstratified with the volcanic fields are epiclastic volcanic deposits including reworked tuff, mudflows, and isolated channels of volcanic sands and conglomerate.

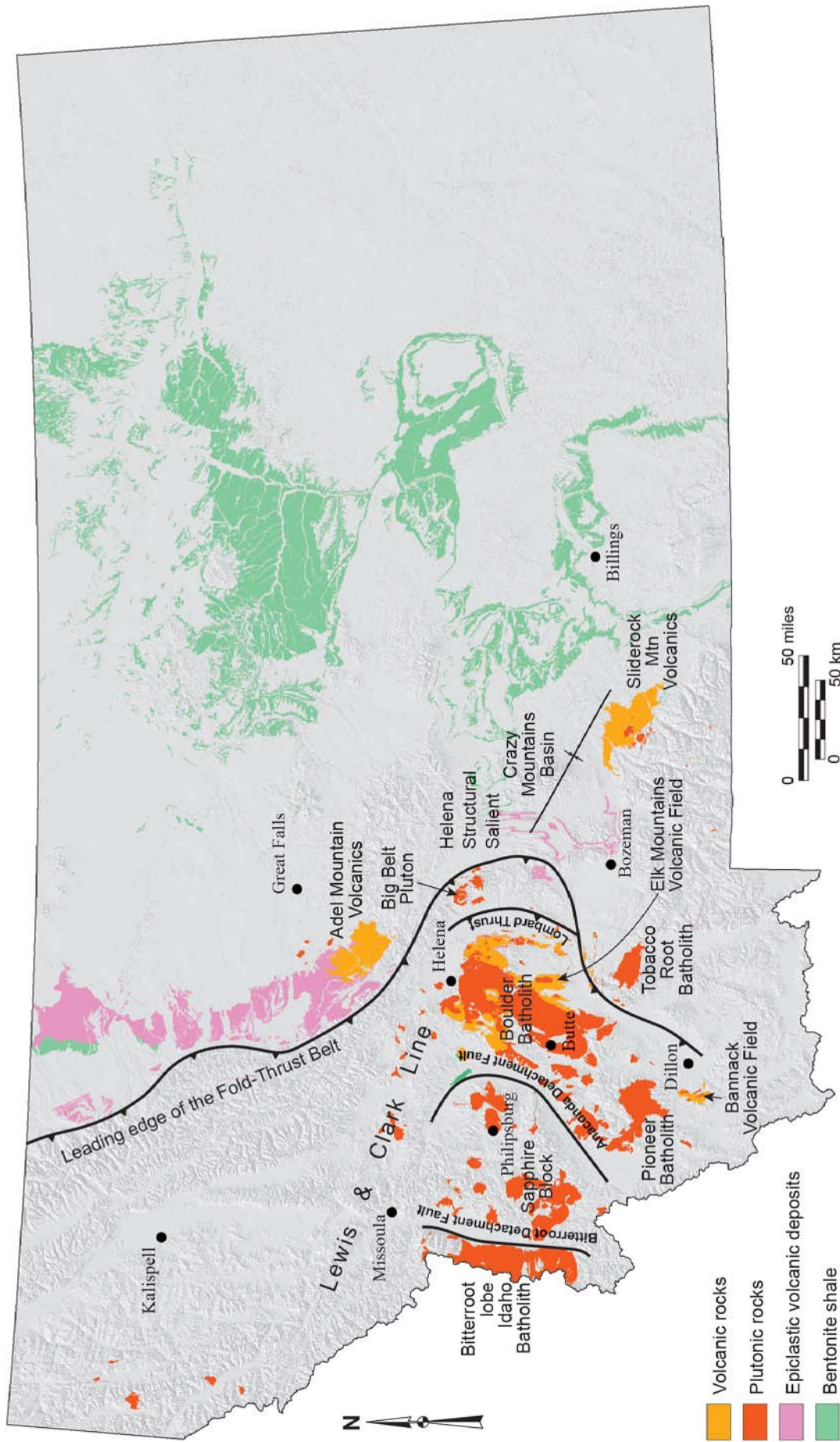


Figure 1. Type and distribution of Mesozoic igneous deposits in Montana (after Vuke and others, 2007). Note that bentonite deposits form relatively thin beds that are interstratified with thick shale successions. For a more precise description of the distribution of bentonite beds in Montana the reader is referred to Berg (1986).

MESOZOIC VOLCANIC ROCKS IN MONTANA

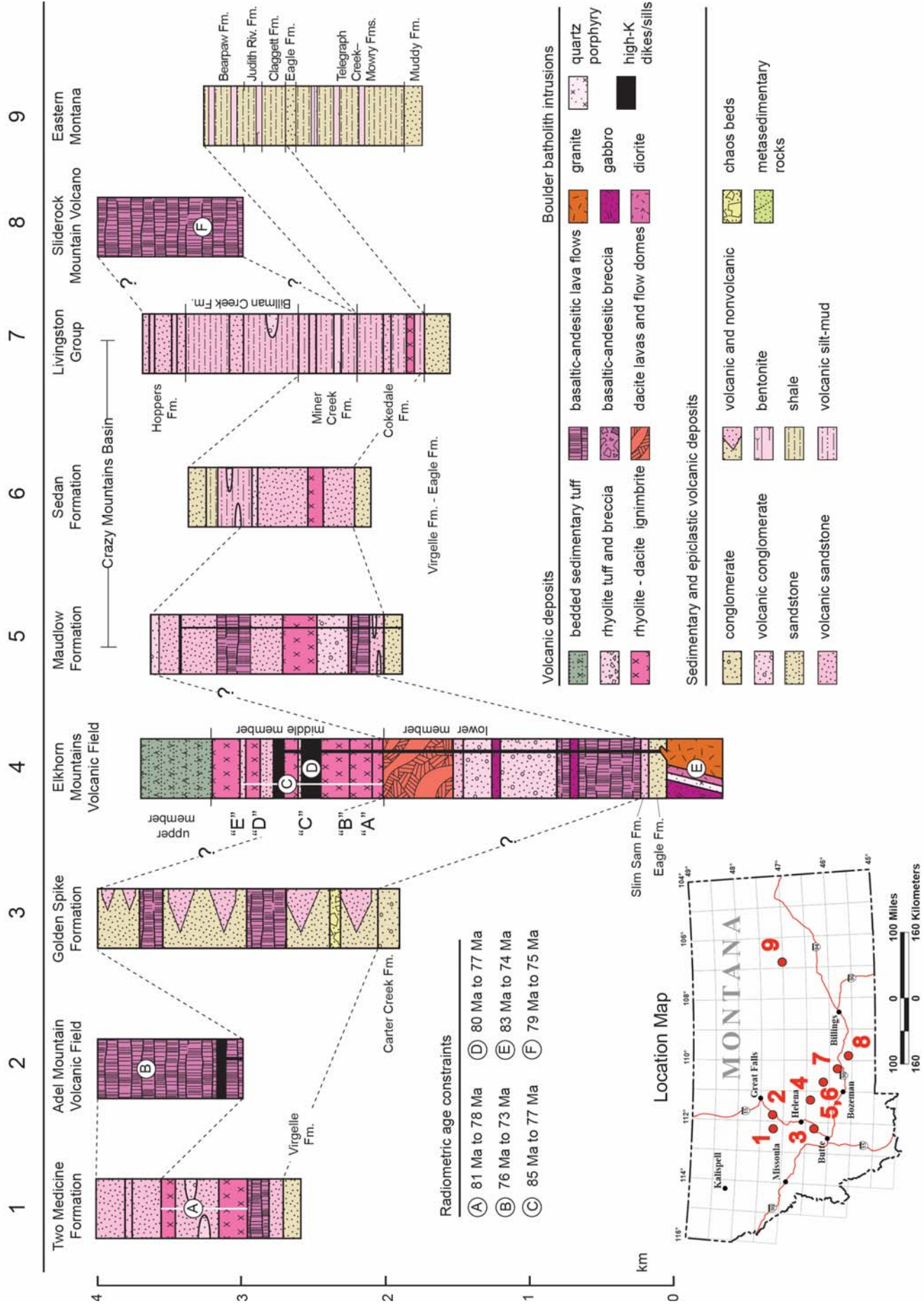


Figure 2. Composite lithostratigraphic sections. Dashed lines show reasonable age correlations based on published work on sections 1–9: (1) Schmidt (1978); (2) Harlan and others, 2005; (3) Gwinn and Mutch (1965); (4) This section is schematic and a composite of work by Prostka (1966), Olson and others (2016), Becraft and others (1963), DeWitt and others (1996), Scarberry (2016) and Korzeb and others (2018); (5 and 6) Skipp and McGrew (1977); (7) Roberts (1963, 1972); (8) du Bray and Harlan (1998); (9) Knechtel and Patterson (1956).

Epiclastic Volcanic Deposits

Epiclastic volcanic deposits occur outwards from the volcanic fields, mainly east of the leading edge of the Fold–Thrust Belt and Helena structural salient (fig. 1), where they are interstratified with lavas and tuffs. Almost all of the epiclastic sequences rest with slight unconformity over marine and marginal marine sandstone and conglomerate of the Virgelle Formation in western Montana, and the Eagle Formation in central and eastern Montana (fig. 2; see Vuke and others, 2007). Continental epiclastic sequences become increasingly fine-grained and water-laid from west to east (fig. 2), reflecting a change from continental deposition to coastal and marine deposition within the Western Interior Seaway.

Bentonite Deposits

Large reserves of industrial quality bentonite are interstratified with fine-grained, largely marine shales in eastern Montana (fig. 2; Knechtel and Patterson, 1956; Roberts, 1963; Berg, 1969). Bentonite is a volcanic ash deposit that has altered to montmorillonite due to sedimentary and chemical processes. A total of 24 bentonite beds that range in thickness from 15 m to 5 cm occur in a 1,500 m section of shale that was deposited between 96 and 75 Ma in eastern Montana (Knechtel and Patterson 1956; Vuke and others, 2007). The volcanic fields and epiclastic deposits in western and central Montana are correlated with bentonite beds in the uppermost 0.5 km of Mesozoic shales in eastern Montana (fig. 2; Skipp and McGrew, 1977). Ash altered to bentonite in the oldest shales came from volcanic activity related to the Sierra Nevada and Idaho Batholiths to the west (Christiansen and others, 1994). Mesozoic sediments in western Montana also contain bentonite deposits (e.g., Walker, 1987; Roberts and Hendrix, 2000; Foreman and others, 2008) that are not as extensive as those in eastern Montana.

Suggestions for Future Research

Several fundamental questions remain for future researchers to address. In particular, the age, distribution, geometry, and emplacement history of plutons and batholiths in Montana is unresolved. For example, did Mesozoic plutons and batholiths form during contractional deformation, extensional deformation, both contractional and extensional deformation, or maybe during a slab failure event that marked the transition in style of deformation? Additionally, opportunities for student research projects that focus on correlating epiclastic sequences with adjacent volcanic fields (fig. 2) are near limitless.

References Cited

- Becraft, G.E., Pinckney, D.M., and Rosenblum, S., 1963, Geology and mineral deposits of the Jefferson City Quadrangle, Jefferson and Lewis and Clark Counties, Montana: U.S. Geological Survey Professional Paper 428, 101 p.
- Berg, R.B., 1969, Bentonite in Montana: Montana Bureau of Mines and Geology Bulletin 74, 34 p.
- Christiansen, E.H., Kowallis, B.J., and Barton, M.D., 1994, Temporal and spatial distribution of volcanic ash in Mesozoic sedimentary rocks of the western interior: An alternative record of Mesozoic magmatism, *in* Mesozoic systems of the Rocky Mountain Region, USA, Caputo, M.V., Peterson, J.A., and Franczyk, K.J., eds, p. 73–94.
- Coney, P.J., 1972, Cordilleran tectonics and North America plate motion: *American Journal of Science*, v. 272, p. 603–628.
- DeWitt, E., Foord, E.E., Zartman, R.E., Pearson, R.C., and Foster, F., 1996, Chronology of Late Cretaceous igneous and hydrothermal events at the Golden Sunlight gold–silver breccia pipe, southwestern Montana: U.S. Geological Survey Bulletin 2155, 48 p.
- Dickinson, W.R., Klute, M.A., Hayes, M.J., Janecke, S.U., Lundin, E.R., McKittrick, M.A., and Olivares, M.D., 1988, Paleogeographic and paleotectonic setting of Laramide sedimentary basins in the central Rocky Mountain region: *Geological Society of America Bulletin*, v. 100, p. 1023–1039.
- du Bray, E.A., and Harlan, S.S., 1998, Geology, age, and tectonic setting of the Cretaceous Sliderock Mountain Volcano, Montana: U.S. Geological Survey Professional Paper 1602, 19 p.

- Foreman, B.Z., Rogers, R.R., Deino, A.L., Wirth, K.R., and Thole, J.T., 2008, Geochemical characterization of bentonite beds in the Two Medicine Formation (Campanian, Montana), including a new $^{40}\text{Ar}/^{39}\text{Ar}$ age: *Cretaceous Research*, v. 29, p. 373–385.
- Foster, F., and Childs, J.F., 1993, An overview of significant lode gold systems in Montana, and their regional geologic setting: *Exploration Mining Geology*, v. 2, p. 217–244.
- Gaschnig, R.M., Vervoort, J.D., Lewis, R.S., and Tikoff, B., 2011, Isotopic evolution of the Idaho Batholith and Challis Intrusive Province, northern US Cordillera: *Journal of Petrology*, v. 52, p. 2397–2429.
- Gwinn, V.E., and Mutch, T.A., 1965, Intertongued Upper Cretaceous volcanic and nonvolcanic rocks, central-western Montana: *Geological Society of America Bulletin*, v. 76, p. 1125–1144.
- Hamilton, W.B., 1988, Laramide crustal shortening, *in* Interaction of the Rocky Mountain Foreland and the Cordilleran Thrust Belt, Schmidt, C.J., and Perry Jr., W.J., eds., *The Geological Society of America Memoir* 171, p. 27–39.
- Harlan, S.S., Snee, L.W., Reynolds, L.W., Mehnert, H.H., Schmidt, R.G., and Irving, A.J., 2005, ^{40}Ar – ^{39}Ar and K-Ar geochronology and tectonic significance of the Upper Cretaceous Adel Mountain Volcanics and spatially associated Tertiary igneous rocks, northwestern Montana: *U.S. Geological Survey Professional Paper* 1696, 29 p.
- Knechtel, M.M., and Patterson, S.H., 1956, Bentonite deposits in marine Cretaceous Formations, Hardin District, Montana and Wyoming: *U.S. Geological Survey Bulletin* 1023, 116 p.
- Korzeb, S.L., Scarberry, K.C., and Zimmerman, J.L., 2018, Interpretations and genesis of Cretaceous age veins and exploration potential for the Emery mining district, Powell County, Montana: *Montana Bureau of Mines and Geology Bulletin* 137, 49 p.
- Lageson, D., Schmitt, J., Horton, B., Kalakay, T., and Burton, B., 2001, Influence of Late Cretaceous magmatism on the Sevier orogenic wedge, western Montana: *Geology*, v. 29, p. 723–726.
- Lyden, C.J., 1948, The gold placers of Montana: *Montana Bureau of Mines and Geology Memoir* 26, 152 p.
- Miller, R.B., and Snoke, A.W., 2009, The utility of crustal cross sections in the analysis of orogenic processes in contrasting tectonic settings, *in* Miller, R.B., and Snoke, A.W., eds., *Crustal cross sections from the Western North American Cordillera and elsewhere: Implications for tectonic and petrologic processes: Geological Society of America Special Paper* 456, p. 1–38.
- Olson, N.H., Dilles, J.H., Kallio, I.M., Horton, T.R., and Scarberry, K.C., 2016, Geologic map of the Ratio Mountain 7.5' quadrangle, southwest Montana: *Montana Bureau of Mines and Geology EDMAP* 10, scale 1:24,000.
- Prostka, H.J., 1966, Igneous geology of the Dry Mountain quadrangle, Jefferson County, Montana: *U.S. Geological Survey Bulletin* 1221-F, scale 1:24,000.
- Roberts, A.E., 1963, The Livingston Group of south-central Montana, *in* *Short papers in geology and hydrology: U.S. Geological Survey Professional Paper* 475-B, p. B86–B92.
- Roberts, A.E., 1972, Cretaceous and Early Tertiary depositional and tectonic history of the Livingston area, southwestern Montana: *U.S. Geological Survey Professional Paper* 526-C, 113 p.
- Roberts, E.M., and Hendrix, M.S., 2000, Taphonomy of a petrified forest in the Two Medicine Formation (Campanian), northwest Montana: Implications for Palinspastic restoration of the Boulder Batholith and Elkhorn Mountains Volcanics: *PALAIOS*, v. 15, p. 476–482.
- Robinson Roberts, L.N., and Kirschbaum, M.A., 1995, Paleogeography of the Late Cretaceous of the western interior of middle North America—Coal distribution and sediment accumulation: *U.S. Geological Survey Professional Paper* 1561, 115 p.

- Rutland, C., Smedes, H., Tilling, R., and Greenwood, W., 1989, Volcanism and plutonism at shallow crustal levels: The Elkhorn Mountains Volcanics and the Boulder Batholith, southwestern Montana, *in* Henshaw, P., ed., Volcanism and plutonism of western North America; v. 2, Cordilleran volcanism, plutonism, and magma generation at various crustal levels, Montana and Idaho, Field trips for the 28th International Geological Congress: American Geophysical Union, Monograph, p. 16–31.
- Scarberry, K.C., 2016, Geologic map of the Wilson Park 7.5' quadrangle, southwestern Montana: Montana Bureau of Mines and Geology Geologic Map 66.
- Schmidt, R.G., 1978, Rocks and mineral resources of the Wolf Creek area, Lewis and Clark and Cascade Counties, Montana, U.S. Geological Survey Bulletin 144, 91 p.
- Saleeby, J.B., Busby-Spera, C., Oldow, J.S., Dunne, G.C., Wright, J.E., Cowan, D.S., Walker, N.W., and Allmendinger, R.W., 1992, Early Mesozoic tectonic evolution of the western U. S. cordillera, *in* Burchfiel, B.C., Lipman, P., and Zoback, M.L., eds., The Cordilleran Orogen: Conterminous U.S.: Boulder, Colorado, Geological Society of America, 107 p.
- Skipp, B., and McGrew, 1977, The Maudlow and Sedan Formations of the Upper Cretaceous Livingston Group on the west edge of the Crazy Mountains Basin, Montana, U.S. Geological Survey Bulletin 142 2-B, 68 p.
- Tilling, R.I., Klepper, M.R., and Obradovich, J.D., 1968, K-Ar ages and time span of emplacement of the Boulder batholith, Montana: American Journal of Science, v. 266, p. 671–689.
- Vuke, S.M., Porter, K.W., Lonn, J.D., and Lopez, D.A., 2007, Geologic map of Montana: Montana Bureau of Mines and Geology Map 62A, scale 1:500,000.
- Walker, S.C., 1987, The nature and origin of bentonites and potassium bentonites, northwestern Montana: Missoula, University of Montana, M.S. thesis, 33 p.
- Yonkee, W.A., and Weil, A.B., 2015, Tectonic evolution of the Sevier and Laramide belts within the North American Cordillera orogenic system: Earth Science Reviews, v. 150, p. 531–593.



Stretching lineations and sheath folds in rheomorphic rhyolite ignimbrite from the Elkhorn Mountains volcanic field (photo: K. Scarberry).

Late Cretaceous Magmatism and Upper Crustal Shortening within the Bannack Volcanic Field, Southwest Montana

Jesse G. Mosolf

Geologist, Montana Bureau of Mines and Geology, Butte, Montana

Introduction

The historic ghost town of Bannack holds an important position in Montana's mining and political history, most notably as the first capital of the Montana Territory soon after placer gold was discovered in Grasshopper Creek in 1862 (Geach, 1972; Sassman, 1941; Shenon, 1931). While Bannack is best known for its rich ore deposits and colorful mining history, the region's geology is important to understanding thrust-belt kinematics and contemporaneous magmatism in southwest Montana. Late Cretaceous volcanic units composing the Bannack Volcanic Field are deformed by contractional structures that are in turn intruded by late-stage subvolcanic rocks. These tectonomagmatic relationships provide an exceptional opportunity to constrain the timing and style of upper crustal faulting and synorogenic magmatism in the Bannack area. This paper presents preliminary results of field mapping and accompanying U-Pb zircon dating of magmatic units composing the Bannack Volcanic Field. These results are used to reconstruct the region's eruptive history, coeval folding and faulting, and the

emplacement of post-deformational intrusions and related mineral deposits.

Geologic Setting

The Bannack Volcanic Field is located in the Armstead Hills approximately 24 km (15 mi) west of Dillon, Montana (fig. 1). The geologic setting of the Bannack area is a composite of several tectonic elements including the leading edge of the fold-thrust belt within the southwestern Montana reentrant, a Late Cretaceous magmatic arc, extensive Tertiary magmatism of the Dillon Volcanic Field, and numerous Cenozoic extensional structures and associated sedimentary basins. The oldest rocks in the Bannack 7.5' quadrangle (fig. 2) include Proterozoic–Paleozoic sedimentary rocks that are variably metamorphosed and strongly deformed by contractional structures. Late Cretaceous synorogenic sedimentary strata of the Beaverhead Group (Johnson, 1986; Azevedo, 1993) are intercalated with volcanic and subvolcanic rocks of the Bannack Volcanic Field that together rest on a regional unconformity cutting the older Paleozoic strata (Lowell, 1965; Ruppel and others, 1993). Contractional structures are locally overprinted by Cenozoic extensional structures; the Muddy-Grasshopper detachment is the most prominent extensional fault in the area and places poorly consolidated Tertiary deposits of the Medicine Lodge beds

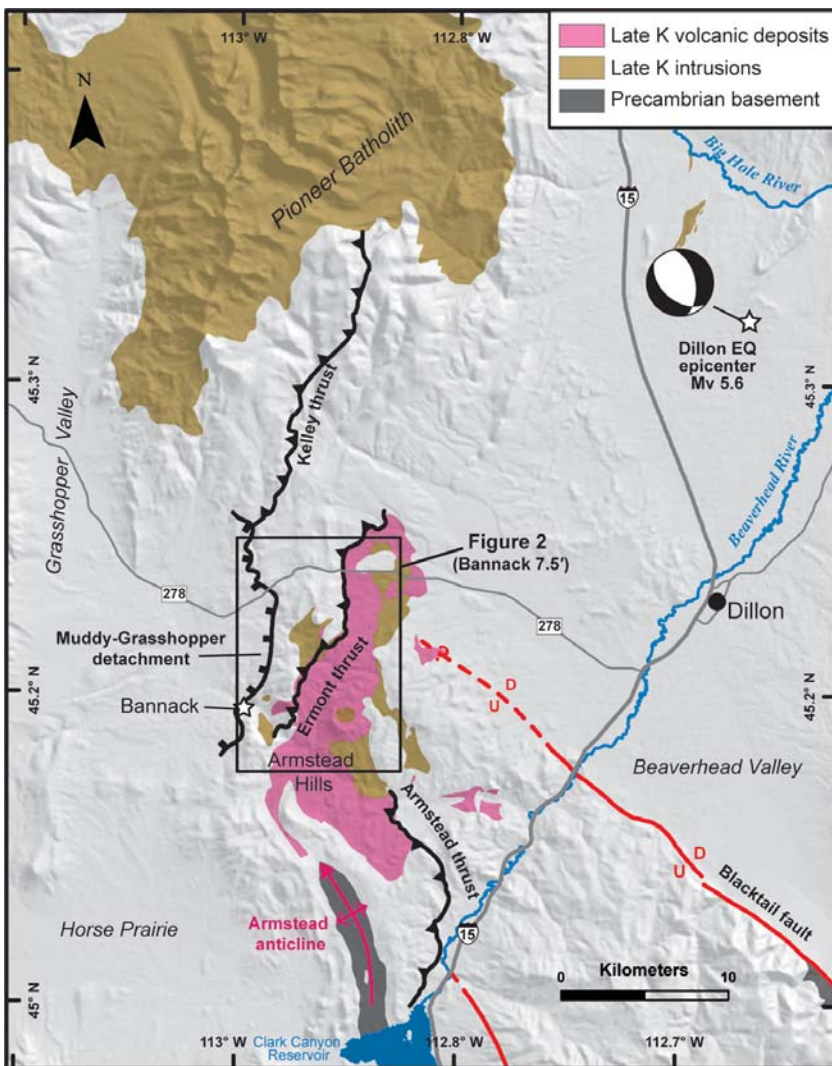


Figure 1. Simplified geologic map showing the major tectonic structures and the distribution of Late Cretaceous igneous rocks and Archean crystalline basement in the Bannack area. The epicenter and focal mechanism for the 2005 Dillon earthquake and boundary of the Bannack 7.5' quadrangle are also shown. Basemap is a shaded digital elevation model (DEM) hillshade.

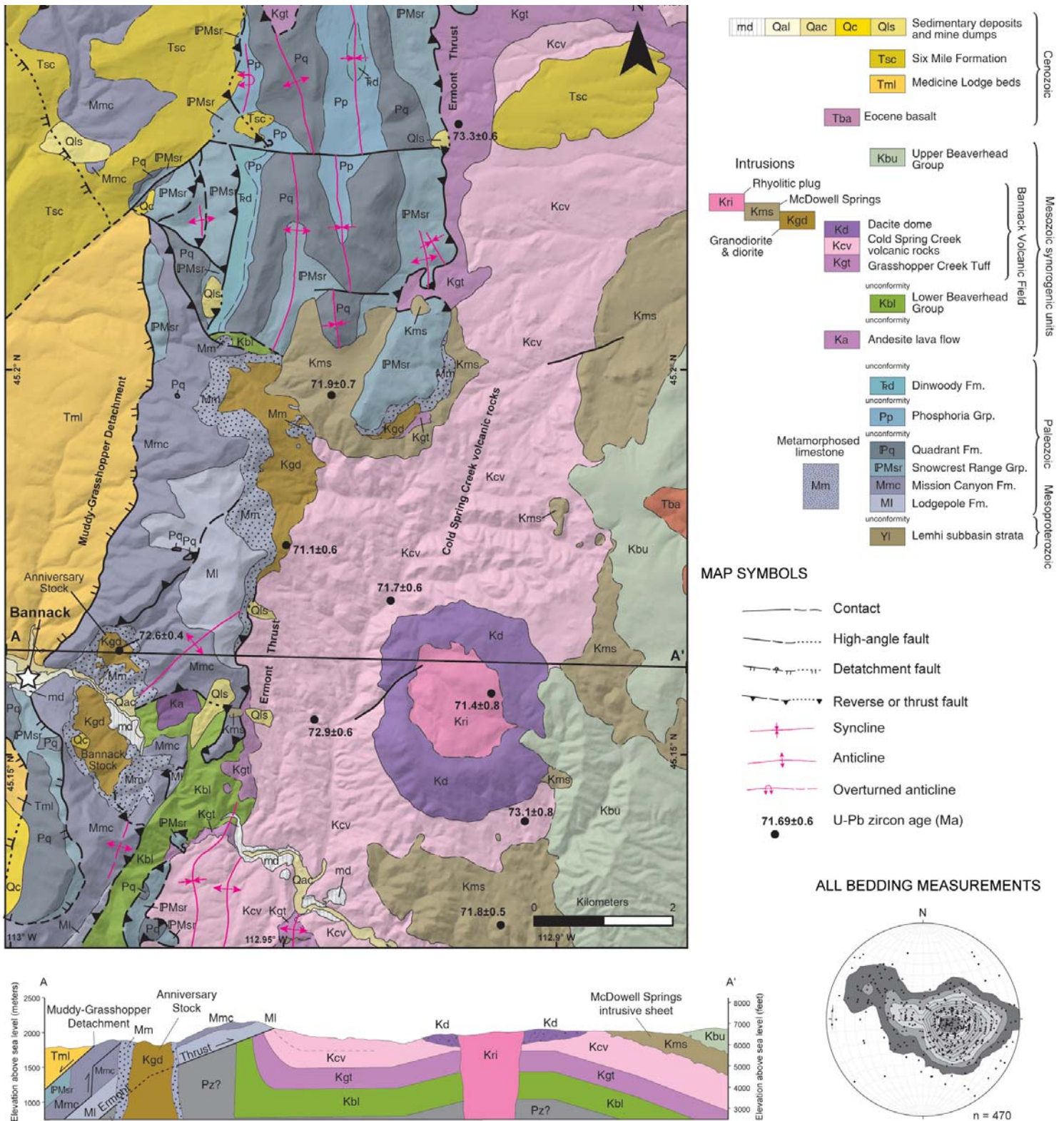


Figure 2. Simplified geologic map, correlation diagram, and interpretive cross section from the Bannack 7.5' quadrangle. Stereonet is lower-hemisphere projection of poles to all bedding measurements in the quadrangle. The map figure was simplified from 1:24,000 scale field mapping that is anticipated to be published at the MBMG (Mosolf, in preparation).

against Paleozoic strata. Sedimentary deposits of the Miocene Six Mile Creek Formation occur throughout the area, obscuring the Muddy-Grasshopper detachment in the northern part of the study area.

Methods

Field Mapping

The Bannack 7.5' quadrangle was mapped during one field season (Mosolf, in preparation) with reference to previous mapping and research in the region by Lowell (1965), Meyer (1980), Thomas (1981), Coryell (1983), Johnson (1986), Ivy (1988), Pearson and Childs (1989), Ruppel and others (1993), Vandenburg and others (1998), and Kalakay (2001). A 1:24,000 scale topographic base and high-resolution satellite imagery were utilized for field mapping. Volcanic and subvolcanic rocks were divided and mapped after Ivy (1988); stratigraphic divisions were based upon volcanic facies, stratigraphic architecture, and geochemical and geochronological information (fig. 3). Field sheets were scanned and georegistered in ArcGIS; the geology was then digitized using the NCGMP09 geodatabase template, a cartographic standard jointly formulated by the U.S. Geological Survey and the Association of American State Geologists. A geologic map, interpretive cross section, correlation diagram, and unit names are shown in figure 2. A brief description of the magmatic units is provided in the following sections; see Coryell (1983), Johnson (1986), and Ruppel and others (1993) for descriptions of the Proterozoic–Mesozoic sedimentary and metasedimentary units.

U-Pb Zircon Geochronology

Zircons were separated from 1–2 kg of rock at the Montana Bureau of Mines and Geology's mineral separation laboratory using standard density and magnetic separation techniques. Approximately 100–200 representative zircon grains were hand selected per sample and set in a 2.5 cm epoxy grain mount. Scanning electron microscopy cathodoluminescence (SEM-CL) and laser ablation inductively coupled plasma mass spectrometry (LA-ICPMS) were performed on at least 30 zircon grains per sample at the University of California–Santa Barbara Geochronology Center. An additional ~30–70 grains were analyzed for samples with significant inheritance. The raw data were processed with Iolite (Paton and others, 2011). The Excel plugin Isoplot (Ludwig, 2000) was used to plot the U-Pb data and calculated weighted mean ages. Weighted mean $^{206}\text{Pb}/^{238}\text{U}$ ages are reported in table 1 and figures 2 and 3; age uncertainties are 2σ .

Late Cretaceous Synorogenic Units of the Beaverhead Group and Bannack Volcanic Field

Volcanic deposits of the Bannack Volcanic Field are intercalated with synorogenic sedimentary sequences of the Beaverhead Group (fig. 3). The Lower Beaverhead Group consists of coarse alluvial fan deposits composed mainly of detritus eroded from Mississippian limestone units (e.g., Madison Group). U-Pb detrital zircon ages from the Lower Beaverhead Group support a maximum depositional age of ~78 Ma (Laskowski and others, 2013), and an andesite lava at the base of the lower Beaverhead Group yielded a U-Pb zircon age of 79.3 Ma (Murphy, 2000; Murphy and others, 2002). These volcano-sedimentary sequences preserve growth strata in the footwall of the Ermont Thrust near Grasshopper Creek, and therefore record the onset of local contractional deformation ca. ~78–80 Ma. The Grasshopper Creek Tuff (Kgt; 73.3 Ma), the oldest formal unit of the Bannack Volcanic Field, overlies the Lower Beaverhead Group and is composed of highly silicified and zeolitized crys-

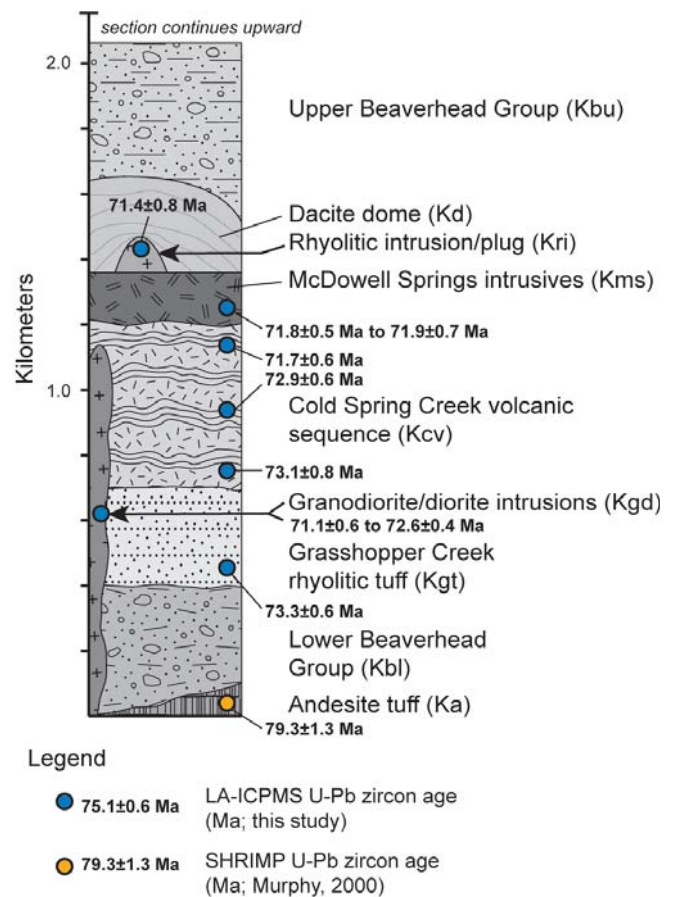


Figure 3. Schematic stratigraphic column of the Bannack Volcanic Field that is based on geologic map relationships and was not measured in the field. Map unit abbreviations as in figure 2.

Table 1. U-Pb zircon geochronology.

Sample	Unit	Lithology	Latitude (°N)	Longitude (°W)	Age (Ma)	2 σ (Ma)	MSWD
DN-60	Kgd	diorite intrusion	45.177	112.950	71.1	0.6	0.5
DN-52	Kgd	diorite intrusion (Anniversary Stock)	45.163	112.980	72.6	0.4	2.0
DN-55	Kms	granodiorite intrusion	45.128	112.911	71.8	0.5	0.6
DN-62	Kms	granodiorite intrusion	45.197	112.942	71.9	0.7	1.1
DN-57B	Kri	rhyolite plug	45.158	112.912	71.4	0.8	0.4
DN-63	Kcv	dacite lava flow	45.170	112.931	71.7	0.6	1.4
DN-59	Kcv	andesite lava flow	45.155	112.945	72.9	0.6	1.8
DN-56	Kcv	dacite lava flow	45.141	112.906	73.1	0.8	0.7
DN-66	Kgt	ash-flow tuff	45.232	112.918	73.3	0.6	1.8

Note: Reputed ages are the weighted mean of $^{206}\text{Pb}/^{238}\text{U}$ ages obtained for each sample (MSWD is the mean square of weighted deviates). Age uncertainties are $\pm 2\sigma$. Zircon separates were prepared at the Montana Bureau of Mines and Geology and analyzed by LA-ICPMS at the University of California, Santa Barbara. Datum used for sample coordinates is World Geodetic Survey 1984 (WGS84).

tal–lithic tuff intervals interpreted to be pyroclastic flow deposits (Pearson and Childs, 1989). The Cold Spring Creek volcanic unit (Ivy, 1988) overlies the Grasshopper Creek Tuff and comprises a complex, inter-tonguing sequence of vent proximal volcanic breccias, andesite–dacite lava flows (73.1–71.7 Ma; 68.1–60.6 wt. % SiO_2), and pyroclastic flow deposits. The waning stages of volcanism in the Bannack area were marked by the extrusion of a dacite lava dome (66.9–64.1 wt. % SiO_2) and associated rhyolitic volcanic plug (71.4 Ma), and the emplacement of numerous diorite–granodiorite intrusions (72.6–71.1 Ma; 64.1–56.9 wt. % SiO_2), including the McDowell Springs intrusions and the Anniversary and Bannack plutons. Volcanic and subvolcanic intervals composing the Bannack Volcanic Field generally exhibit high-potassium, calc-alkaline geochemical trends, and are enriched in incompatible elements (Ivy, 1988). Most of the samples dated in this study contained a significant number of inherited zircons with the majority of their respective U-Pb ages spanning ~2.7–1.7 Ga (Mosolf, in preparation), indicating that parental melts assimilated evolved crustal rocks similar in age to crystalline basement rocks exposed in the core of the nearby Armstead anticline (fig. 1; Coryell, 1983; Mueller and others, 2012). The Upper Beaverhead Group unconformably rests on the Bannack volcanic sequences and consists of conglomeratic deposits dominated by Proterozoic quartzite clasts that were likely eroded from thrust sheets in the hinterland. Detrital zircon ages from these deposits indicate a maximum depositional age of approximately 71.6 Ma (Laskowski and others, 2013).

Structural Geology

Contractional Structures

The Ermont thrust fault is the most prominent contractional structure in the map area, placing Paleozoic sedimentary units over Late Cretaceous synorogenic sedimentary strata and intercalated volcanic deposits of the Lower Beaverhead Group and Bannack Volcanic Field, respectively. The fault gently dips westward in the north part of the map area, forming a hanging wall flat above truncated footwall strata. Here, the hanging wall strata are deformed by a series of north–northwest-oriented folds and associated tear faults (fig. 2). To the west, the dip of the Ermont fault is interpreted to steepen to 40° in the subsurface, forming a footwall ramp beneath west-dipping imbricate thrust faults in the hanging wall (Kalakay, 2001). The surface trace of the fault shows it to steepen to 30–40° southward near the town of Bannack, where it is obscured by Late Cretaceous intrusions and appears to merge with the Armstead fold-thrust system to the south (Coryell, 1983). Large slabs of Paleozoic strata rest on Late Cretaceous units east of the main surface trace of the Ermont thrust fault and are interpreted to be klippen isolated from the main allochthon, suggesting the fault had a minimum heave of ~2.3 km. The

fault dips eastward beneath the klippen, indicating the Ermont thrust is either folded or has been rotated by an unrecognized listric normal fault located to the east (Kalakay, 2001). U-Pb zircon ages from synorogenic volcanic sequences and cross-cutting intrusions constrain movement on the Ermont thrust fault between approximately 79.3 and 71.69 Ma (this study; Murphy, 2000; Kalakay, 2001), with fault slip slowing or ceasing prior to the emplacement of granodiorite and diorite intrusions (72.61–71.09 Ma) that exhibit no evidence of solid-state deformation. The Beaverhead Group rests unconformably on folded Mississippian strata in the footwall of the Ermont thrust, indicating the Bannack area was exhumed and underwent significant erosion prior to or during movement on the fault.

Extensional Structures

The Muddy-Grasshopper detachment fault likely inverts an imbricate fault or fault ramp structurally linked to the Ermont thrust fault. The fault dips 30° to the west along its northern trace, placing poorly consolidated Tertiary sedimentary deposits in the hanging wall against Paleozoic strata in the footwall. The fault progressively steepens to approximately 60° south of Bannack, paralleling the geometry of imbricate thrust faults. The timing of fault movement is poorly constrained but was likely synchronous with the deposition of proximal alluvial fan and debris flow deposits composing the Medicine Lodge beds during Eocene–Oligocene time (Janecke and others, 1999). Middle Miocene sedimentary deposits of the Six Mile Creek Formation on-lap the detachment and are not deformed, obscuring the northern trace of the fault. A northeast-striking normal fault places Medicine Lodge beds against the Six Mile Creek Formation, indicating extensional faulting occurred in the area since the Miocene.

Mineralization

The principal lode deposits in the quadrangle consist of replacement bodies in skarn derived from metamorphism of limestone near its contact with Late Cretaceous intrusions (Pearson and Childs, 1989). The ore bodies are tabular, pipe-like, irregular, and sometimes vein-like. The primary ore consists of gold-bearing quartz and pyrite with various skarn minerals including garnet, diopside, vesuvianite, specularite, and magnetite (Shenon, 1931). Minor amounts of chalcopyrite, galena, and sphalerite occur locally. The chief lode mines in the Bannack district included the Golden Leaf, Excelsior, Hendricks, and Gold Bug. The Golden Leaf was the largest mine and produced about 75,000–125,000 oz of gold between the 1860s and 1955 (Pearson and Childs, 1989). The principal mines of the Blue Wing district, about 1 mi north of the town of Bannack, included the New Departure mine and the Blue Wing, Whopper, and Bannack Chief mines, later known as the Kent Group (Sassman, 1941). Placer gold and silver mined along Grasshopper Creek was likely sourced from these lode deposits.

Discussion and Conclusions

Preliminary geologic mapping and radiometric age results from the Bannack Volcanic Field provide temporal constraints on local magmatism and coeval contractional deformation. U-Pb dating of detrital zircon from synorogenic sedimentary deposits of the Lower Beaverhead Group and an underlying andesite lava indicate that magmatism and coeval shortening in the Bannack area were underway no later than ca. ~78–80 Ma. The Lower Beaverhead Group rests on an unconformity truncating deformed Paleozoic rocks and is composed of alluvial fan-type deposits that preserve growth strata locally. These stratigraphic relationships suggest that the Bannack area underwent significant exhumation and related erosion prior to or during local crustal shortening and movement on the Ermont thrust fault. Deformed volcanogenic units of the Bannack Volcanic Field record magmatism and coeval contractional deformation that continued until ca. ~72 Ma. These volcanic and volcanic-clastic sequences are dominantly vent-proximal deposits, comprising lava flows and intrusions exhibiting enriched calc-alkaline trends (Ivy, 1988; Mosolf, in preparation). Volcanic activity likely occurred in an intra-arc setting and parental melts were greatly modified by the melting or partial melting and assimilation of evolved crust. Large granodiorite–diorite stocks intrude and cross-cut the Ermont thrust and show little to no evidence of solid-state deformation, together suggesting movement on the fault had slowed or ceased by ~72 Ma. Emplacement of these late stage intrusions marked the waning stages of magmatism within the Bannack Volcanic Field, and was contemporaneous with crystallization of the southern Pioneer batholith (~71–72 Ma).

References

- Azevedo, P.A., 1993, Tectono-sedimentary evolution of a Late Cretaceous alluvial fan, Beaverhead Group, southwestern Montana: Bozeman, Montana State University, M.S. thesis, 137 p., 2 sheets.
- Coryell, J.J., 1983, Structural geology of the Henneberry Ridge area, Beaverhead County, Montana: College Station, Texas A&M University, M.S. thesis, 126 p.
- Geach, R.D., 1972, Mines and mineral deposits (except fuels), Beaverhead County, Montana: Montana Bureau of Mines and Geology Bulletin 85, 194 p., 3 sheets.
- Ivy, S.D., 1988, Source, evolution, and eruptive history of the Cold Spring Creek volcanics, Beaverhead County, Montana: Corvallis, Oregon State University, M.S. thesis, 132 p.
- Janecke, S.U., McIntosh, W.C., and Good, S.C., 1999, Testing models of rift basins; structure and stratigraphy of an Eocene-Oligocene supradetachment basin, Muddy Creek half graben, southwest MT: Basin Research, v. 11, p. 143–165.
- Johnson, L.M., 1986, An overlap zone between a Laramide Rocky Mountain foreland structure and Sevier-style thrust structures near Bannack, Montana: Missoula, University of Montana, M.S. thesis, 47 p., 2 sheets, scale: 1:24,000.
- Kalakay, T.J., 2001, The role of magmatism during crustal shortening in the retroarc fold and thrust belt of southwest Montana: Laramie, University of Wyoming, Ph.D. dissertation, 204 p.
- Lowell, W.R., 1965, Geologic map of the Bannack-Grayling area, Beaverhead County, Montana: U.S. Geological Survey Miscellaneous Geologic Investigations Map I-433, scale 1:31,680.
- Laskowski, A.K., DeCelles, P.G., and Gehrels, G.E., 2013, Detrital zircon geochronology of Cordilleran retroarc foreland basin strata, western North America: *Tectonics*, v. 32, p. 1027–1048.
- Ludwig, K.R., 2000, User's manual for Isoplot/Ex version 2.4: A geochronological toolkit for Microsoft Excel: Berkeley Geo-chronological Center, Special Publication No. 1a.
- Meyer, J.W., 1980, Alteration and mineralization of the Grasshopper prospect, Beaverhead County, Montana: Tucson, University of Arizona, M.S. thesis, 91 p.
- Mosolf, J., in preparation, Geologic map of the Bannack 7.5' quadrangle, Beaverhead County, Montana: Montana Bureau of Mines and Geology Open-File Report, 1 sheet, 1:24,000 scale.
- Mueller, P., Mogk, D., and Wooden, J., 2012, Age and composition of crystalline basement in the Armstead anticline, southwestern Montana: *Northwest Geology*, v. 41, p. 63–70.
- Murphy, J.G., 2000, Geochronology of late synkinematic plutons in the Sevier fold and thrust belt, SW Montana: Gainesville, University of Florida, M.S. thesis, 105 p.
- Murphy, J.G., Foster, D.A., Kalakay, T.J., John, B.E., and Hamilton, M., 2002, U-Pb zircon geochronology of the Eastern Pioneer Igneous Complex, SW Montana: *Magmatism in the foreland of the Cordilleran fold and thrust belt: Northwest Geology*, v. 31, p. 1–11.
- Paton, C., Hellstrom, J., Paul, B., and Woodhead, J., 2011, Iolite: Freeware for the visualization and processing of mass spectrometric data: *Atomic Spectrometry*, v. 26, p. 2508–2518.
- Pearson, R.C., and Childs, J.F., 1989, Field trip guide, roadlog, and summary of Cretaceous volcanic geology, Dillon to Bannack, Beaverhead County, Montana: *Northwest Geology*, v.18, p. 36–59.
- Ruppel, E.T., O'Neill, J.M., and Lopez, D.A., 1993, Geologic map of the Dillon 1° x 2° quadrangle, Idaho and Montana: U.S. Geological Survey Miscellaneous Investigations Series Map I-1803-H, scale 1:250,000.
- Sassman, O., 1941, Metal mining in historic Beaverhead: Bozeman, Montana State University, M.A. thesis, 310 p.
- Shenon, P.J., 1931, Geology and ore deposits of Bannack and Argenta, Beaverhead County, Montana: Montana Bureau of Mines and Geology Bulletin 6, 80 p.

Thomas, G.M., 1981, Structural geology of the Badger Pass area, southwest Montana: Missoula, University of Montana, M.S. thesis, 58 p., 1 sheet, scale: 1:24,000.

Vandenburg, C.J., Janecke, S.U., and McIntosh, W.C., 1998, Three-dimensional strain produced by >50 my of episodic extension, Horse Prairie basin area, SW Montana, U.S.A.: *Journal of Structural Geology*, v. 20, p. 1747–1767.



Boris the Cave Bear harasses conference participants during the book sale at the Montana Tech Mineral Museum (photo: C. McKillips).



The ore bin at the Cable Mine (photo: P. Hargrave).



The Meet and Greet at the Montana Tech Mineral Museum (photo: C. McKillips).

Orbicular Alteration at the Clementine Porphyry Copper Prospect of Southwest Montana: Defining the Edges of Advective Flow in the Porphyry Copper Paradigm

George H. Brimhall

Principal Geologist and Managing Member, Clementine Exploration LLC, Wise River, Montana

The Need to Explore for Deep Subsurface Porphyry Copper Deposits

Over the next 26 years, the projected increase in world requirements for copper will necessitate mining more copper than was mined in all prior human history (Schaffer, 2018). Junior exploration companies are expected to account for about 70 percent of the discoveries (Schaffer, 2018). It is now widely accepted that opportunities to discover shallow orebodies have diminished significantly throughout much of the world (Wood, 2016). Hence, there is a compelling need to abandon a predominantly surface to near-surface target approach and embrace instead deep exploration, thus placing a serious challenge on junior exploration companies. Particularly daunting is the fact that (1) the discovery rate of major orebodies had been falling from the early 1970s onward, while expenditures have continued to rise, and (2) the depth of discovery was mostly 200 to 300 m or less and has largely remained the same up to now (Schodde, 2013). Wood and Hedenquist (2019) assert that overall, “exploration efforts since 2010 have been wealth destructive.” A pressing need has existed for a decade or more for a decisive change in how the search for new orebodies is designed, funded, and implemented. This is a daunting challenge, as many types of ore bodies with their tops located 500 to 1,000 m or more below surface are unlikely to exhibit the obvious signs on the surface that have guided past geological mapping that is the pivotal activity of exploration. An effective exploration strategy for junior exploration companies is required to map and describe new surficial geological evidence of deep mineralization sufficiently compelling for major companies to enter into partnerships to support the requisite deep drilling of targets. The current paradigm for porphyry copper deposits (Sillitoe, 2010; fig. 1) is based in part on two papers published almost half a century ago by Lowell and Guilbert (1970) and Gustafson and Hunt (1975). Sillitoe and others (2016) summarized the current discovery climate: “in the past decade, deep exploration for porphyry copper deposits completely concealed beneath extensive lithocaps has become increasingly common as near-surface mineralization becomes scarcer, but with rare exceptions there have been few successes.” This raises the question as to what features, besides lithocaps, may prove to be more effective guides to locating the porphyry copper hypogene mineralization center? In this study we focus on orbicular textural features beneath the lithocap in both the porphyry to epithermal transition and the deeper porphyry level (fig. 1). In addition to the Bingham district, where Atkinson and Einaudi (1978) logged mineralized orbs in core, orbs have been described, though not mapped, at three deposits in Chile: Caspiche, La Escondida, and El Hueso (Sillitoe and others, 2013); Cajamarca in Peru; Morenci and Fortitude Copper Canyon in the U.S.; Cananea in Mexico; and Oyu Tolgoi in Mongolia (Marco Einaudi, written commun., 2019). This paper describes our fieldwork at the pre-drilling phase to map and interpret extensive orbicular alteration as part of lateral zoning at the Clementine prospect, a possible new deep porphyry copper system in Montana. The intent is to develop within the porphyry copper paradigm a powerful and predictive mapping tool for better locating the center and defining the edges of hypogene hydrothermal fluid flow that has evaded recent exploration efforts searching beneath lithocaps.

The Connection between Base Metal Vein Systems and Porphyry Deposits

Our approach to exploration at Clementine focuses on the observation that Cordilleran base metal vein systems exposed on the surface may have genetically related porphyry copper deposit root zones amenable to underground mining methods. The relation between polymetallic veins and porphyry-style mineralization was first brought to light by Meyer (1965) in the Butte District of Montana. During the past few decades (Bendezú and Fontbote, 2009), extensive mining and exploration in mature vein districts have revealed that some of these polymetallic ores can be the shallow expression of porphyry-Cu-(Au, Mo) and/or skarn mineralization centers (e.g., Quiruvilca, Noble and McKee, 1999; Yauricocha, Alvarez and Noble, 1988; Magma, Manske and Paul, 2002; Vinchos, Farfán Bernales, 2006; Morococha, Bendezú, 2007; Catchpole and others, 2008; and Kouz-

manov and others, 2008). Fontboté and Bendezú (2009) further highlighted the connection between Cordilleran polymetallic vein deposits and Butte-type veins and replacement bodies, and grouped them into a deposit class in porphyry copper systems.

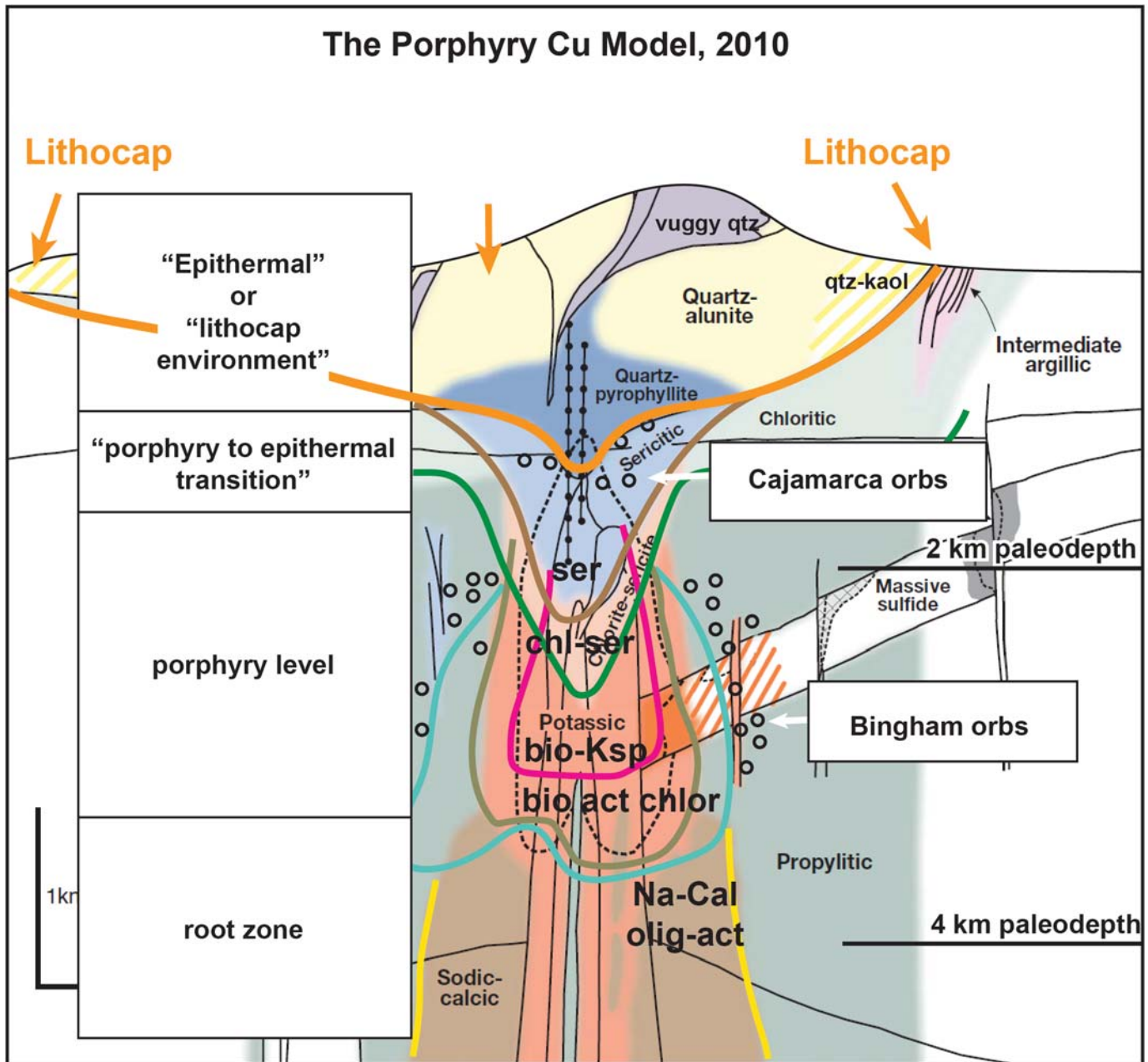


Figure 1. The porphyry copper model modified from Sillitoe (2010). The lithocap is shown with peripheral strata-bound advanced argillic alteration surrounding a central hypogene silicic core with structurally controlled high sulfidation sulfides with sericitic alteration extending to depth into the porphyry level. The porphyry Cu level has concentric alteration zones that transition outwards from central chlorite-sericite, to biotite-K-feldspar, biotite, actinolite, and finally to a chlorite outer shell. Orbicular alteration at Bingham described in Atkinson and Einaudi (1978) are related to the deeper porphyry level while orbs at Cajamarca, Peru occur at the porphyry to epithermal transition (Nobel and others, 2011).

Preparing for 21st Century Mining Methods and Implications for Exploration Strategy

Concurrent with the shift to deeper exploration, there has been an evolution of mass mining technology away from open pit to underground bulk mining techniques that are both economic and more deserving of a social license. Final approval for development nowadays involves much more than economics alone, even on private lands. While underground mining, especially with paste backfill, drastically reduces both subsidence and surface storage of voluminous waste rock and has relatively minor surface expression, public perception and

concerns about the outfall of past mining practices continue to influence attitudes about mining in Montana and even threaten the future of the industry in the U.S. Of particular concern in Montana is water quality, both in the short and long term, given the importance of its blue ribbon-quality freshwater fisheries and their economic and natural value to the State's citizens and active outdoor community. The mine life cycle must address the full range of concerns, from formulating a suitable scientific exploration target, discovery drilling, engineering design, economic planning, and earning a social license with all stakeholders, to ensuring that the environmental quality of the mined land surface and hydrological system be maintained day to day and ultimately be restored in perpetuity as a healthy ecosystem.

Selecting Drilling Targets

While porphyry copper exploration targets are very large, drill targeting is challenging as it must address three major aspects of how the Cordilleran vein system on the surface relates to the deeper porphyry copper deposit.

(1) Finding the porphyry copper center

As yet unexposed deep porphyry copper deposits are the primary exploration target, using the overlying Cordilleran vein systems and wall rock alteration patterns as guides to what mineralization may occur below. The characteristics of an exposed Cordilleran vein system vary considerably in this model. The nearby ore deposits at Butte provide perhaps the best example of a high-grade, zoned base metal vein network descending into older, fracture-controlled, disseminated copper and molybdenum ore (fig. 2; Brimhall, 1977, 1979, 1980; Brimhall and Ghiorso, 1983). The plan map of the 2800 mine level of the Butte District (Brimhall, 1979) shows how the vein system only partially overlaps the deep porphyry copper system. The Main Stage veins are zoned such that the Badger (B) and Anselmo (A) produced mostly zinc, while the Lexington (X) produced mostly manganese, and the Mt. Con (C), Kelley (K), Leonard (L), Steward (S), and Belmont (Bt) produced mostly copper. Hence, search for deep porphyry copper deposits relies on exploring below the copper-rich portions of the Cordilleran vein system because drilling beneath the peripheral zinc, lead, and silver veins may entirely miss the porphyry copper center. Only in the Leonard (L) area is there advanced argillic alteration with high sulfidation state covellite–chalcocite–enargite mineral assemblages that could be considered as having some of the attributes of a lithocap. Instead, elsewhere in the district completely unaltered fresh Butte granite occurs at the surface between the large high-grade vein alteration envelopes.

(2) Predicting the potential size of the porphyry copper target

The second complication relates to the potential size of the porphyry copper target. We followed an intriguing suggestion that the porphyry systems with the highest contained copper are a “closed system” as described by Oyarzun and others (2001) that did not vent, or out-gas. Sillitoe (2010) reaffirmed the importance of this containment factor in por-

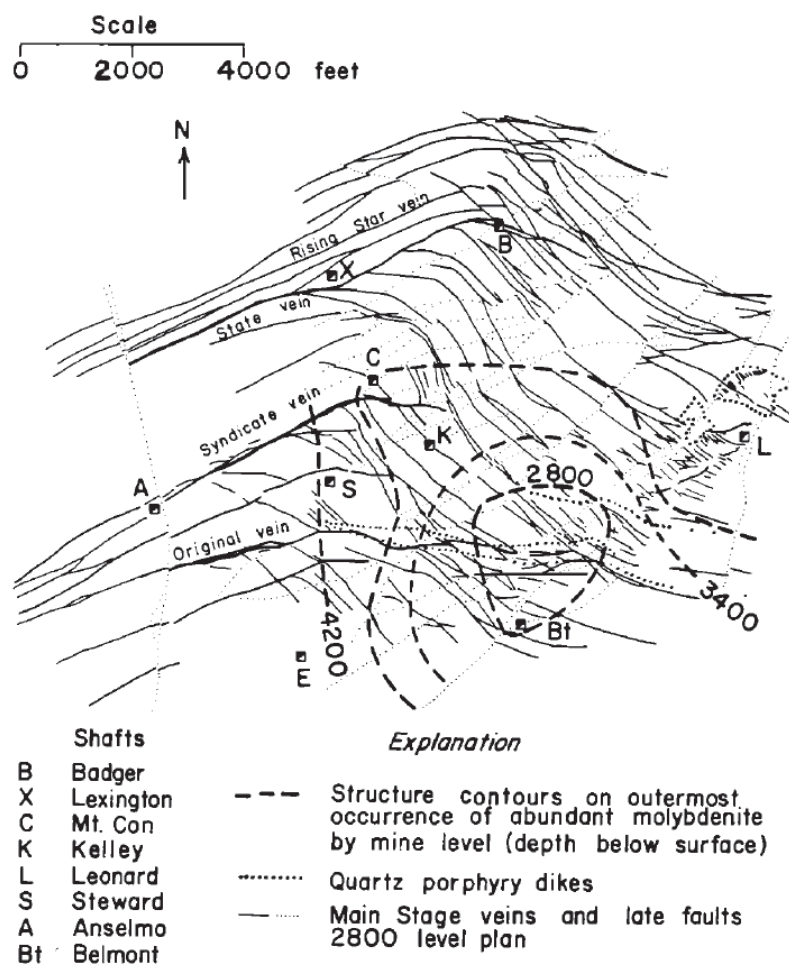


Figure 2. 2800 mine level plan map of the Butte District (Brimhall, 1979) showing structure contours on the outermost occurrence of abundant molybdenite. Main Stage veins are shown, as are their production shafts.

phyry ore formation in the largest scale systems. Finally, another key factor to consider in gauging the potential size of a deep porphyry copper target in early stage exploration is its likely dimensions in plan view. Any and all discernible features that can be systematically mapped are potentially useful in estimating the dimensions of the possible porphyry system at depth. However, we show here that orbicular alteration offers unique insights as to both the center of the hypogene system sought and its likely size.

(3) Relying on observations rather than models: Extending the porphyry copper paradigm

Applying exploration models for porphyry copper deposits developed in Arizona (Lowell and Guilbert, 1970; John and others, 2010), or Chile (Gustafson and Hunt, 1975), to new territory can invite interpretive shortcomings. Especially concerning is the fact that most of the models describe systems where the pre-mine landscape surface intersected midway down into the well-mineralized part of the cylindrical porphyry copper deposit column, which can extend as far down from the paleosurface as 7 or 8 km (John and others, 2010). Stated differently, geological knowledge applied in exploration often reflects a clear proximity to economically mineable ore rather than to the less well known tops of the systems, which may in fact depart distinctly from the highly mineralized portions at depth.

The Location of the Clementine Prospect

Given the prevailing wisdom regarding clustering (Oyarzun and others, 2001; Tosdal and Richards, 2001), our target selection was based on searching as close to the Butte ore deposit as possible using a regional tectonic model in combination with maps of active and historic mining districts (Brimhall and Marsh, 2017). Our search focused on areas where the closed system model described by Oyarzun and others (2001) and Sillitoe (2010) would apply as a key element in the generation of large porphyry copper deposits. Subsurface containment of magmas and early stage hydrothermal fluids is a central part of our exploration strategy, much like the stratigraphic and structural anticlinal traps explored in the petroleum industry. However, instead of searching for a porous and permeable reservoir rock for hydrocarbons, we search for intact stratigraphic traps providing containment for porphyry copper mineralization without dissipative metal loss upwards into more permeable zones in an open system. Within this context, we also search for systems where the early hydrothermal footprint is largest and, presumably, indicative of a significant porphyry copper deposit at depth. These constraints are tempered by the realization that in a fold and thrust belt, once an early stage of porphyry mineralization forms, later through-going mineralized veins are likely to develop, as with the syntectonic Main Stage vein system at Butte, which extend up above the protore and serve as guides to mineralization at depth. The nearby Pioneer Mountains have a long history of base and precious metal production useful in our regional search. Historic mining districts extend southward from Butte to Quartz Hill and end at Bannack. We sought to put Butte and the nearby deposits of the Pioneer Mountains into as broad a regional tectonic context as possible to glean useful knowledge as to controls on ore deposition. Hildenbrand and others (2000) summarized the distribution of ore deposits in the western United States in relation to regional crustal structures and showed Butte and Bingham situated along the frontal Sevier age thrust fault. The historic mines of the Pioneer Mountains in Montana south of Butte occur along a single, north-south-trending, regional anticlinal hinge of the frontal (easternmost) anticline of the Cordilleran fold and thrust belt of Sevier (Late Cretaceous) age. Many deposits, including Quartz Hill and Heccla, occur within domal structures illustrating structural and stratigraphic containment. We focused our fieldwork on the former Divide District, which had no prior history of metal production but occurs at a suggestive gap in the string of inactive mines in the Pioneer Mountains. Most importantly, through mapping we recognized a doubly plunging anticlinal fold, indicative of stratigraphic and structural containment of subsurface magmatic and hydrothermal fluids.

Geological Mapping of the Clementine Prospect

Given that much of the Divide Creek District where the Clementine prospect is located is steep terrane up to 9,200 ft high at Mount Fleecer, with dense timber below the alpine zone and largely inaccessible except on foot, GPS-supported digital mapping methods were a necessity (Brimhall and Vanegas, 2001; Brimhall and others, 2002, 2006). Much of the mapped area has a very poor rock exposure, both under tree canopy and on open grassy hillslopes. However, tree root heave mounds provide sufficiently good rock fragment samples that map-

ping inferred geological formation contacts is possible. Only through accurate digital mapping was it possible to map small outcrops and accurately correlate them spatially so that distinct linear belts of similar lithologies and alteration zones could be discerned. Of particular importance to our exploration strategy was discovery of a vein gossan system that provides the key evidence of Cordilleran polymetallic mineralization that might be followed to depth to find a porphyry copper deposit.

The geological mapping done over seven field seasons, from 2011 through 2018, is shown in figure 3 at a scale of 1:30,000. The prospect is in a nappe window into the Lewis Overthrust, and occurs below the Grasshopper Thrust Fault (Fraser and Waldrop, 1972) but above the frontal thrust to the east described by Ruppel (1993) and Ruppel and others (1993). While the anticline intruded by the Big Hole River (Mount Fleecer Pluton) is also shown on the Dillon 2° sheet of Ruppel and others (1993) and the more detailed 30' x 60' Butte

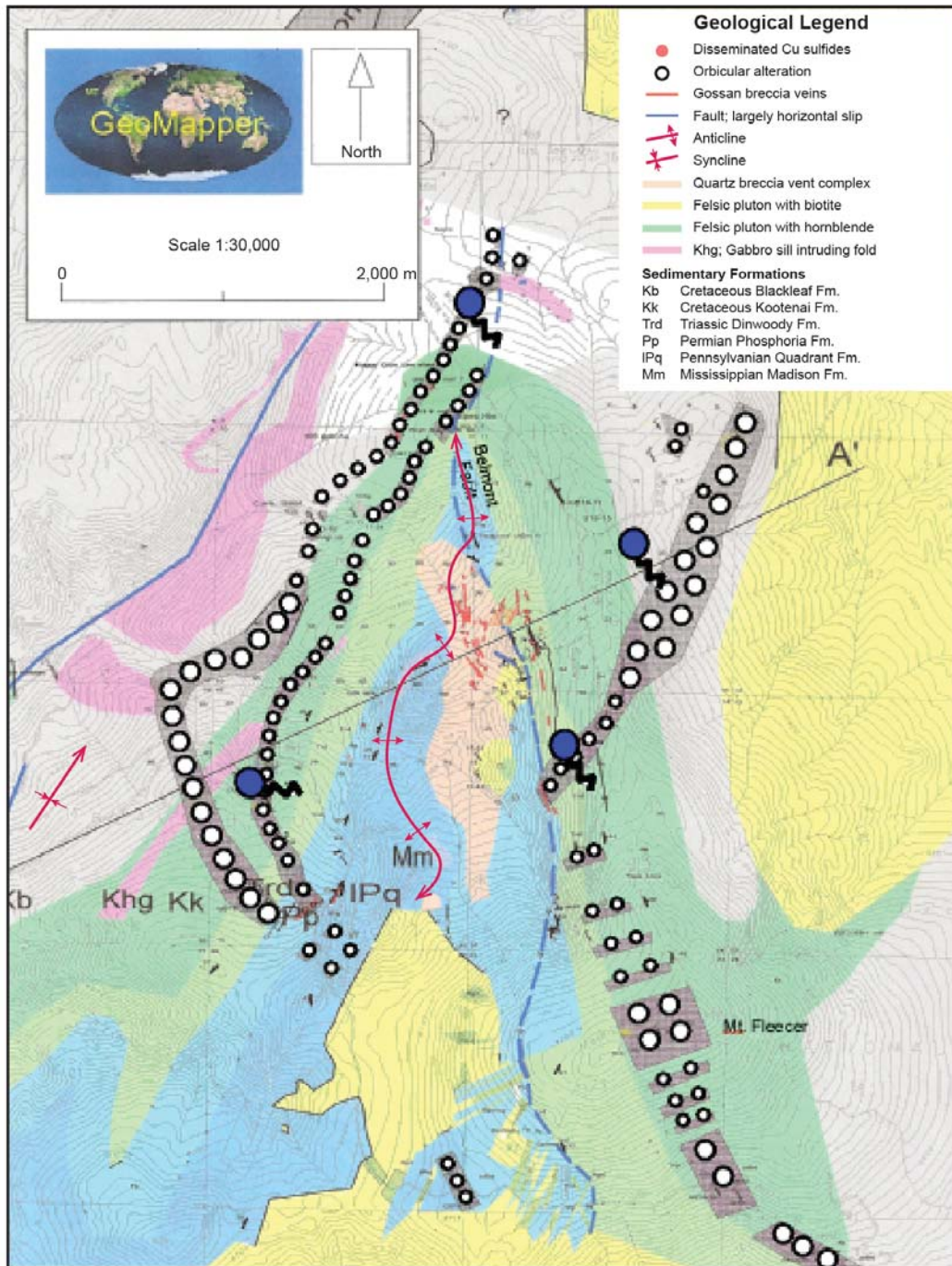


Figure 3. Bedrock geological plan map based on fieldwork from 2011 through 2018. Formation abbreviations are: Mm (Mississippian Madison), IPq (Pennsylvanian Quadrant), Trd (Triassic Dinwoody), Kk (Cretaceous Kootenai), Khg (hornblende gabbro sills), and Kb (Cretaceous Blackleaf). Four groundwater-derived springs are shown with blue circles.

South sheet of McDonald and others (2012), we have added significant new detail that leads us to interpret the structure as a mineralized and altered, syntectonic, frontal thrust, fault-bend anticline. At the anticlinal core, Mississippian Madison limestone outcrops. The Pennsylvanian Quadrant, Permian Phosphoria, and Triassic Dinwoody Formations occur in sequence above the Madison Limestone, farther away from the north-south-trending axial plane. The uppermost stratigraphic units are the Cretaceous Kootenai and overlying Blackleaf Formations. A gabbroic sill intrudes the west flank of the anticline and can be found on the eastern side of the anticline, displaced by the north-south right lateral Belmont Fault, which has a displacement of 500 to 600 ft. The lateral displacement is consistent with observed fault slickensides with a pitch of 20°. Conglomerate beds in the Blackleaf Formation were also mapped east of this fault, confirming the right lateral sense and magnitude of displacement.

Styles of Alteration

The most obvious district-scale features superimposed on the bedrock anticline are distinctive, continuous tabular zones of orbicular alteration (fig. 4) that extend over 6 km north-south and 2.5 km east-west on both sides of the anticline (fig. 3). Orbicular alteration is the outermost feature of the Clementine prospect and was discovered only through systematic digital mapping. While approaching the Clementine prospect, unaltered sedimentary lithologies were found within the Blackleaf and Kootenai Formations on the flanks of the anticline. Farther inside the anticline however, orbs occur up to 3 cm in diameter that commonly have remnants of their original green-colored silicate mineral filling. The most intact orbs we found and thin sectioned are filled with actinolite, quartz, calcite, titanite (sphene), and other minerals. Like the gabbro sills and conglomerate beds, the orbicular zones are displaced right laterally by the Belmont Fault. The orbicular rocks outcrop, unlike the siliclastic diopside-bearing hornfels units in the footwall, and form what few outcrops occur in this area, under tree canopy and thin alpine soil cover.

One notable feature of the orbicular alteration is that all of the observed groundwater-derived springs (fig. 3) in the Mount Fleecer Area emanate nearby orbicular zones as at Tub Springs, Fleecer saddle, along the Parker



Figure 4. Orbicular wall rock alteration consisting of orbs lined with actinolite in fresh samples up to about 1 in diameter also containing sparse disseminations of chalcopyrite, pyrrhotite, and ilmenite in the rock matrix. Sample from the west side of the Clementine anticline above the Parker Mine. Orbs are often now voids where the original mineral filling has disappeared. Egg crate insert shows lines formed by intersecting planes.

Mine road on the west side of the anticline, and on the east side of the anticline. We interpret the close association of springs with the orbicular zones as being due to the relatively low permeability of both the dense hornfels rocks immediately below the orbicular zones and the orb zones themselves forcing water that infiltrated unaltered formations at higher elevations back up to the surface. Given that this area is very dry after the spring snowmelt has run off, all four of these springs constitute the principal water supply for the cattle that graze there in the summer under U.S. Forest Service rangeland permitting. There are only three watering tanks mapped in the entire area, and all three are fed by springs emanating from orbicular zones. The only other springs, which are significantly smaller, occur near the trace of the Belmont Fault. On their southern terminus, the northern plutons of the Big Hole River (Fleecer Mountain) intrusion seem to intrude the orbicular zones. Similarly, on the northern end, the plutons of the southern end of the Boulder Batholith cut off the orbicular

zones.

Description of the Orbicular Zones: The Outer Ring of Wall Rock Alteration

Inside the core of the anticline in the footwall of the orbicular zones, the alteration is best described as widespread diopside hornfels that are differentially developed spatially. Of particular importance is the fact that the orbicular alteration zones have fresh, unaltered, sedimentary rock formations in their hanging walls and diopside hornfels on their footwalls that are metasomatic products of hydrothermal alteration. This transition implies that outward and upward convective fluid flow coursed up through the hornfels facies and ceased where the orbicules developed in the uppermost distal parts of the Clementine convective system. This regional spatial coincidence of orbicules exactly at the upper and outer limit of visible fractures is central to our interpretation of orb formation in low permeability upper reaches and to advancing understanding of the porphyry copper paradigm in terms of vertical and lateral zoning. The importance of the orbicular alteration in the context of porphyry copper ore formation is strengthened by the fact that orbicules have been previously observed and meticulously described at the world-class copper deposit at Bingham Utah. Tabular bodies of hydrothermal, orbicular, wall rock alteration similar to those in the Clementine prospect have been described in the contact aureole at Carr Fork, Bingham, by Atkinson and Einaudi (1978), and around breccia pipes at Cananea, Mexico, by Meinert (1982). At Clementine, the orbicular alteration alters multiple rock formations over a 6 km strike length. The formations affected at the surface include the Pennsylvanian Quadrant, Permian Phosphoria, Triassic Dinwoody, Cretaceous Kootenai, and Cretaceous Blackleaf Formations. Our mapping documents disseminated chalcopyrite and pyrrhotite associated with the orbicular zone, making the genetic parallel with Carr Fork extremely close. Furthermore, we have now recognized that the primary mineral lining the orbicular cavities at Clementine is in fact actinolite, which is consistent with the current porphyry copper model (fig. 1).

Breccias, Veins, and Plutons

Inside the tabular orbicular zone bands on both sides of the axial plane of the anticline, just west of the Belmont fault, is a large breccia complex that is 2.2 km north–south and 500 m wide. This zone contains Quadrant, Phosphoria, Dinwoody, and Kootenai Formations cut by north–south-trending, steep, tabular bodies of breccia consisting of angular fragments of quartzite in a matrix of pure milled quartz. The rock contains about 98 percent silica. Within the boundaries of the barren breccia is a smaller system of north–south-striking, mineralized-matrix, breccia-vein gossans extending over a strike length of 900 m. These mineralized breccias have iron contents up to 32 percent and represent oxidized sulfide veins, and constitute compelling evidence of Cordilleran polymetallic base metal mineralization. Near the southeast side of the copper-barren breccia complex, two new plutons have been mapped (fig. 3). The northern felsic pluton has disseminated sulfides and is highly altered. An adit, now caved, was collared in the pluton and heads eastward. The mine dump, however, contains diorite fragments typical of another pluton to the south that is completely fresh and has both fresh biotite and hornblende along with unaltered sphene.

The geometric center of the mineralization is the vein system shown in figure 3 as thin red lines, west of the Belmont Fault. East of the Belmont Fault, quartz-rich veins outcrop with a considerable strike length and obvious surface manifestation, which apparently drew historic attention to this area. Two trenches east of the Belmont Fault have rocks that assay up to 1,190 ppm copper and have colloform silica chalcedony. These silica-rich veins have been offset right laterally along the Belmont Fault. With the offset restored northward, they become the northern end of the vein gossan system on the west side of the fault.

The centrality of the vein system to the district as a whole is confirmed by surface contouring of the tabular orbicular zones, which have gentle outward dips and form a cupola in three dimensions. Mapping to date shows a general co-axiality of the orbicular alteration, the centrally located vein gossan system, and an altered pluton nearby with old workings, including the adit mentioned, as well as a shaft and two trenches east of the Belmont Fault.

Knowledge of the three-dimensional shape of the orbicular zones gained through surface contouring provides guidance in construction of an interpretive vertical cross section (fig. 5), which is based entirely on surface

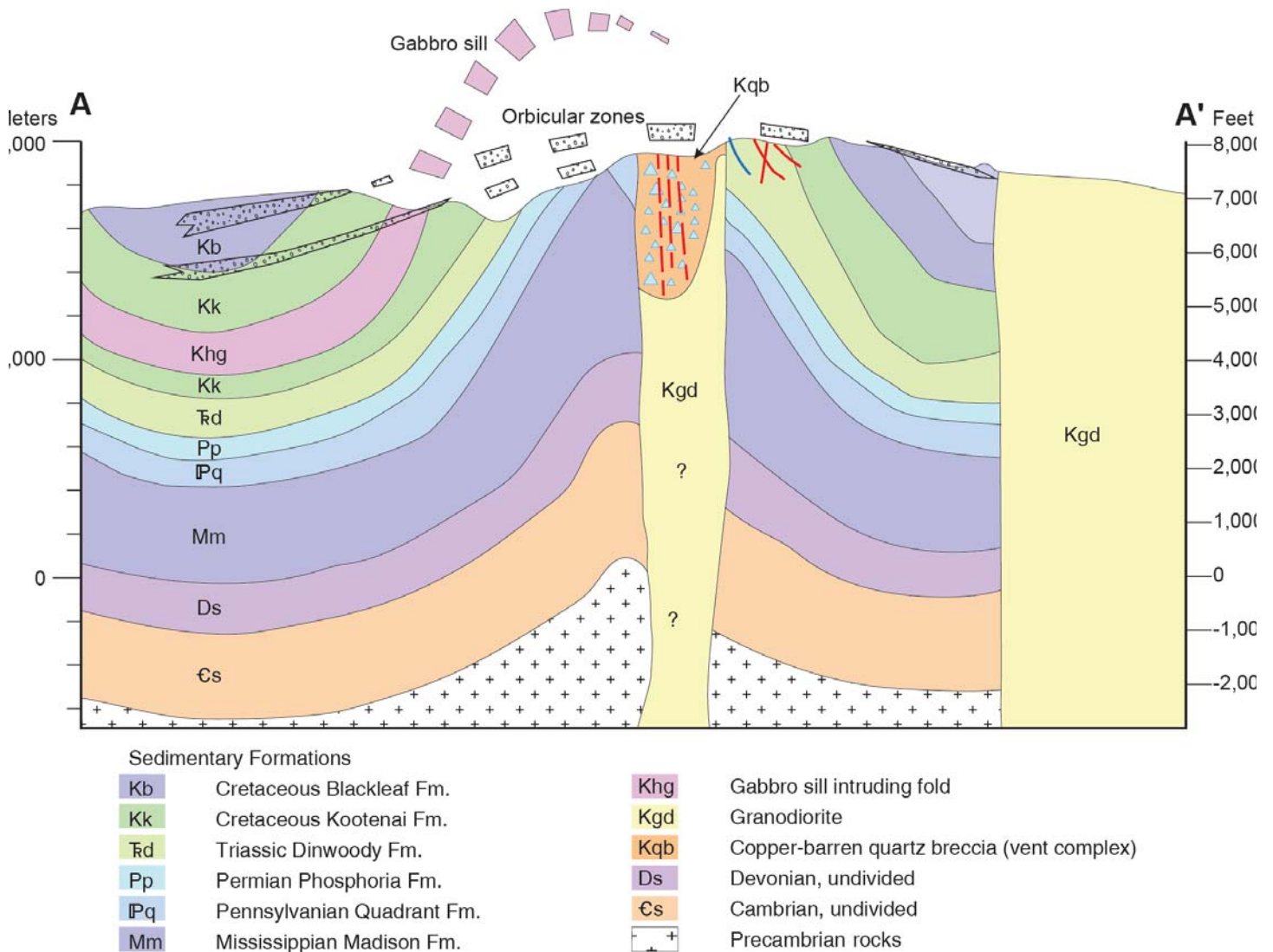


Figure 5. Interpretive vertical geological cross section of Clementine based entirely upon: (1) surface digital geological mapping and (2) approximate formation thickness. Notice the gentle outward dips of the orbicular zones and their upward closure near the present surface. Also, notice that the copper-barren breccia, with quartzite fragments occurring along the axial plane of the anticline, plots in the vertical vicinity of the orbicular zone projection. We interpret this to mean that fragmentation of the Quadrant was related to formation of the steeply dipping, tabular copper-barren breccia zones.

geological mapping shown in figure 3. Structure contouring and surface fitting using Surfer shows that the top of the orbicular zones probably occurred just east of the vein gossan system and altered felsic pluton, and intersects the folded sedimentary strata near the apical crest at the level of the Pennsylvanian Quadrant Formation projected upwards. We view the dominance of Quadrant quartzites in the copper-barren breccias and the projected position of the orbicular zone in the cross section as not accidental. The Quadrant Formation may have been ideally situated to fracture in the axial zone of the fold where, above a neutral surface, extension-related fragmentation is expected. Hence the breccias are dominated by locally derived, mono-mictic, Quadrant clasts.

Formation of the Orbicular Zones: Defining the Edges of Advective Flow in the Porphyry Copper Paradigm

Given our observations at Clementine that the tabular orb bodies occur right at the top of observed fracture networks with unaltered sedimentary formations above and hydrothermally altered hornfels below, our attention is drawn to crack tips on the upper edge of the convective halo and what changes occur there with regards to advection, diffusion, and reaction. These are the essential types of solute transport involved in ore genesis and wall rock alteration. Here we inspect what each of these terms mean in order to understand our field observations and to better understand the structural front represented by the continuous tabular orbicule cupola, extending 6 km

in plan view. Understanding orb growth quantitatively supports our goal of significantly advancing the porphyry copper paradigm in terms of developing mapping tools to: (1) help locate the center of hydrothermal convection and (2) estimate the size of the likely mineralization system.

Throughout the formation of porphyry copper deposits, advective flow of hydrothermal solutions dominates transport of aqueous species, including ions and aqueous complexes being carried in solution or in gaseous form. Advective transport of solutes via a moving fluid is responsible for vein and veinlet formation. The other two major processes to consider in metasomatism, besides advection, are diffusion and reaction. These are responsible for the development of alteration envelopes parallel to the veins and veinlets controlling advective transport. In general, since alteration envelopes are parallel to the veins, diffusion happens normal to the veins by aqueous species migrating from areas of higher concentration to areas of lower concentration within a stationary pore fluid rather than by fluid pressure differences controlled by temperature gradients, as in convection.

The analytical expression relating changes in rock composition over time to advective transport, diffusion, and chemical reaction in one direction, x , are given in equation 1 (Garzón-Alvarado and others, 2012). Equation 1 is a statement of conservation of mass coupled with diffusion and reaction.

$$\text{Equation 1:} \quad \begin{array}{cccc} (1) & (2) & (3) & (4) \\ \frac{\partial C_i}{\partial t} = & - \frac{v \partial C_i}{\partial x} + & \frac{D_i \partial^2 C_i}{\partial x^2} - & \frac{\partial q_i}{\partial t} \end{array}$$

In equation 1, C_i is concentration of aqueous solute (i) in water, t is time, v is pore or crack water flow velocity, x is distance, and D_i is the diffusion coefficient of (i). Term (1) is the change in solute composition over time; term (2) represents advective transport, which depends upon fluid velocity and goes down the concentration gradient; term (3) represents diffusive transport involving the curvature of the concentration gradient; and term (4) is the change in concentration in the solid mineral phases due to the sum of all chemical reactions.

Given the field observation at Clementine that the orbicular features occur at the outer extremity of hornfels and microveinlets, we assert here that the position occupied by the orbs is where advective transport slowed sufficiently that diffusional processes dominated in the absence of active fluid advection, as in the center of the district where veins occur. Additionally, the roughly spherical shapes of the orbs, in contrast to planar veins with parallel alteration envelopes, appears to be a radial-diffusive phenomena.

The relative importance of advective transport and diffusion are expressed by the Peclet number (Pe). Pe is a class of dimensionless numbers relevant in the study of transport phenomena in a continuum. It is defined to be the ratio of the rate of advection of a solute by the flow to the rate of diffusion (Huysmans and Dassargues, 2005). Dividing the advective term (2) above in equation 1 by the diffusive term (3) and substituting L for the variable x gives equation 2:

$$\text{Equation 2:} \quad P_e = v \frac{L}{D}$$

L is called the Characteristic Length and is given by the ratio of volume to surface area in the case of spherical structures like the Clementine orbs. For a sphere with radius r , the volume is given by $4/3\pi r^3$ and the surface area by $4\pi r^2$ so that $L = r/3$. The orbs have a radius of approximately 3 cm, so L is about 1 cm, making P_e equal to v/D . If we assume that the value of P_e was about 1, implying that the orbs formed at the edge of the convection system where diffusion was as equally important as advection, we can estimate the approximate flow velocity as $v = D$ in this case. Empirical values of diffusion coefficients D for sandstones show 3×10^{-8} cm²/sec as typical (Boving and Grathwohl, 2001). The distance traveled by the fluid over the time span of 1 year would then be 3×10^{-8} cm/sec times 3.15×10^7 sec, or 9.45×10^{-1} cm, or only about 1 cm per year. This markedly slow rate of fluid migration compared with the kilometric size of porphyry copper deposits is consistent with our assertion that the orbicular zone represents the outermost and uppermost advance of fracture-controlled fluid advection. Since we see in thin section that the orbs often have narrow quartz veinlets entering them, we view orb formation as being a crack-tip growth feature from both the one-dimensional conduits formed at crack intersec-

tions and planar cracks. Spherical orbs and elongate tubular orbs formed from crack intersections and individual cracks, respectively.

When the Peclet number P_e has a value of 1, then the advective flow rate, v , is equal to the diffusion coefficient or diffusivity D , which is a very small number for rocks. This implies that the fluid flow rate is similarly very, very slow. Advective flow rates on this order clearly indicate that the orbs formed as the very upper and outer edge of the convective fluid flow halo. As advective flow slowed dramatically, the orbicular zones were frozen as hydrothermal relicts created largely in place by diffusive processes and local chemical reactions. The orb front is a mappable textural change in rock fabric even in areas with poor exposure. We have observed orbs in a variety of sedimentary rock types that have one attribute in common: clastic rocks with intergranular porosity. Diffusion took place through the pore fluid medium, making orb growth possible. In other rock types lacking intergranular porosity, for example igneous rocks with interlocking grains, we suspect that orbs could be lacking or at least substantially smaller in size, perhaps occurring as splotches.

Conclusions

This report describes mapping distal wall rock alteration features likely to be encountered early on in exploration mapping as the outermost ring of concentric alteration and sparse disseminated chalcopyrite mineralization. Combining field observation on the Clementine prospect with first principle analysis of known solute transport mechanisms, we show that the district-wide orbicular alteration represents the outer edge of hydrofractured stockworks where advective flow slowed considerably and spherical orbs formed by diffusion from the uppermost crack tips or crack intersections. The utility of orb cupolas as a targeting tool then stems from the fact that orbicular zones mark the position of a key hydrodynamic boundary: the upper and outer edge of the mineralized fracture permeability network. Orb alteration makes this subtle physical feature macroscopically visible and contributes a powerful mapping tool in lithologies where orbs are likely to form in sedimentary rocks with connected pore space rather than interlocking grains. At Clementine the continuously exposed strike length of 6 km of the orbicular zones implies a remarkable continuity and large scale of the fracture network at depth. We view the large dimensions and axially symmetric disposition of the orbicular alteration, base metal vein system, and plutons at Clementine as a positive sign of a deeper and potentially large-scale porphyry copper–molybdenum deposit, possibly within reach by drilling to depths of several thousand feet. In that context, mineralized orbicular alteration is shown to be an important factor in porphyry copper exploration for closed system, confined, magmatic-hydrothermal systems, which are most likely to form large ore bodies. Orb zone mapping is a high-impact endeavor significantly enlarging the target size in early stage exploration. It is hoped here that by describing orb cupolas and discerning their origin in a sound, process-based understanding accessible through mapping and quantitative reasoning, our ideas are anchored within a framework sufficiently compelling to now formally include orb zoning to the porphyry copper model. More broadly, while lithocaps, vein systems, and breccia complexes offer useful targeting information in searching for deep porphyry copper bodies, these structurally controlled types of mineralization reflect very high-fracture permeability, usually developed relatively late in a district, and may vary from minor to major features of a new prospect. What can be much more telling about the size and proximity below the present land surface to infer possible ore masses below are the tabular orbicular alteration zones with disseminated copper sulfides. We publish this work in the hope that it will help to modify the current perception of excessive risk in greenfields exploration relative to the work in mature districts where low discovery rates have prevailed.

Acknowledgments

First and foremost, I thank my wife Mary Jane Brimhall for her abiding artful support and help from our early years in Butte to the inception of Clementine Exploration. William Atkinson and Marco Einaudi provided photographs of diamond drill core from the Carr Fork area of the Bingham District and insightful conversation of orbicular alteration. Kaleb Scarberry and Colleen Elliott provided reviews of this manuscript. Jerry Zieg and Sergio Rivera provided reviews and comparisons with Chilean porphyry copper deposit geology and exploration for new blind ore deposits. Ed Rogers has been a steadfast field companion in challenging terrains for a decade. Ray Morley, Dan Kunz, and Doug Fuerstenau are thanked for their ongoing enthusiastic commentary and

support. Jay Ague has provided vital discussion about the lack of orbs in metamorphic rocks. Dick Berg, Chris Gammons, and Colleen Elliott of Montana Tech and the Montana Bureau of Mines and Geology continue to provide insightful scientific dialogue and access to laboratory equipment. Maya Wildgoose, Russell McArthur, and David Belt are thanked for helping in mapping in fill portions of the orbicular zones.

References Cited

- Alvarez, A.A., and Noble, D.C., 1988, Sedimentary rock-hosted disseminated precious metal mineralization at Purísima Concepción, Yauricocha district, central Peru: *Economic Geology*, v. 83, p. 1368–1378.
- Atkinson, W., and Einaudi, M.T., 1978, Skarn formation and mineralization in the contact aureole at Carr Fork, Bingham, Utah: *Economic Geology*, v. 75, p. 1326–1365.
- Bendezú, R., 2007, Shallow polymetallic and precious metal mineralization associated with a Miocene diatreme-dome complex: The Colquijirca district of the Peruvian Andes: Geneva, Switzerland, University of Geneva, *Terre & Environment*, v. 64, 221 p.
- Bendezú, R., and Fontboté, L., 2009, Cordilleran epithermal Cu-Zn-Pb-(Au-Ag) mineralization in the Colquijirca District, Central Peru: Deposit-scale mineralogical patterns: *Economic Geology*, v. 104, p. 905–944.
- Boving, T.B., and Grathwohl, P., 2001, Tracer diffusion coefficients in sedimentary rocks: Correlation to porosity and hydraulic conductivity: *Journal of Contaminant Hydrology*, v. 53, p. 85–100.
- Brimhall, G.H., 1977, Early fracture-controlled disseminated mineralization at Butte, Montana: *Economic Geology*, v. 72, p. 37–59.
- Brimhall, G.H., 1979, Lithologic determination of mass transfer mechanisms of multiple stage porphyry copper mineralization at Butte, Montana: Vein formation by hypogene leaching and enrichment of potassium-silicate protore: *Economic Geology*, v. 74, p. 556–589.
- Brimhall, G.H., 1980, Deep hypogene oxidation of porphyry copper potassium-silicate protore: A theoretical evaluation of the copper remobilization hypothesis: *Economic Geology*, v. 75, p. 384–409.
- Brimhall, G.H., and Ghiorso, M.S., 1983, Origin and ore-forming consequences of the advanced argillic alteration process in hypogene environments by magmatic gas contamination of meteoric fluids: *Economic Geology*, v. 78, p. 73–90.
- Brimhall, G.H., and Vanegas, A., 2001, Removing science workflow barriers to adoption of digital geological mapping by using the GeoMapper universal program and visual user interface, *in* D.R. Soller, ed., *Digital Mapping Techniques'01–Workshop proceedings*: U.S. Geological Survey Open File Report 01-223, p. 103–114.
- Brimhall, G.H., Vanegas, A., and Lerch, D., 2002, GeoMapper program for paperless field mapping with seamless map production in ESRI ArcMap and GeoLogger for drill-hole data capture: Applications in geology, astronomy, environmental remediation and raised relief models, *in* D.R. Soller, ed., *Digital Mapping Techniques'02–Workshop Proceedings*: U.S. Geological Survey Open File Report 02-370, p. 141–151.
- Brimhall, G.H., Dilles, J., and Proffett, J., 2006, The role of geological mapping in mineral exploration in wealth creation in the minerals industry: Special Publication 12, Anniversary Publications of the Society of Economic Geologists, p. 221–241.
- Brimhall, G.H., and Marsh, B.D., 2017, Nature of the mineralization and alteration at the Clementine porphyry copper prospect in the northern Pioneer Mountains of southwest Montana: Montana Bureau of Mines and Geology Open-File Report 699, p. 55–58.
- Catchpole, H., Bendezú, A., Kouzmanov, K., Fontboté, L., and Escalante, E., 2008, Porphyry-related base metal mineralization styles in the Miocene Morococha district, central Peru: Society of Economic Geologists–Geological Society of South Africa 2008 Conference, Johannesburg, July 05–06, Programs and Abstracts, p. 54–57.

- Farfán Bernal, C., 2006, Modelo de Prospección Geológica de Yacimientos Minerales en Rocas Carbonatadas, Región de Pasco-Mina Vinchos: Unpublished M.Sc. thesis, Lima, Peru, Universidad Nacional Mayor San Marcos, 50 p.
- Fontboté, L., and Bendejú, R., 2009, Cordilleran or Butte-type veins and replacement bodies as a deposit class in porphyry systems: Society of Geology Applied to Ore Deposits Meeting, 10th Biennial, Townsville, Australia, Proceedings, p. 521–523.
- Fraser, G.D., and Waldrop, H.A., 1972, Geologic map of the Wise River quadrangle, Silver Bow and Beaverhead Counties, Montana: U.S. Geological Survey Geologic Quadrangle Map GQ-988, scale 1:24,000.
- Garzón-Alvarado, D., Galeano, C., and Mantilla, J., 2012, Computational examples of reaction–convection–diffusion equations solution under the influence of fluid flow: Applied Mathematical Modeling, v. 36, p. 5029–5045.
- Gustafson, L., and Hunt, J.P., 1975, The porphyry copper deposit at El Salvador, Chile: Economic Geology, v. 70, p. 857–912.
- Hildenbrand, T.G., Berger, B.R., Jachens, R.C., and Ludington, S.D., 2000, Regional crustal structures and their relationship to the distribution of ore deposits in the Western United States, based on magnetic and gravity data: Economic Geology, v. 95, p. 1583–1603.
- Huysmans, M., and Dassargues, A., 2005, Review of the use of Péclet numbers to determine the relative importance of advection and diffusion in low permeability environments: Hydrogeology Journal, v. 13, p. 895–909.
- Kouzmanov, K., Ovtcharova, M., von Quadt, A., Guillong, M., Spikings, R., Schaltegger, U., Fontboté, L., and Rivera, L., 2008, U-Pb and $^{40}\text{Ar}/^{39}\text{Ar}$ constraints for the timing of magmatism and mineralization in the giant Toromocho porphyry Cu-Mo deposit, central Peru: Congreso Peruano de Geología, 14th, Lima, Peru, Proceedings.
- John, D.A., Ayuso, R.A., Barton, M.D., Blakely, R.J., Bodnar, R.J., Dilles, J.H., Gray, Floyd, Graybeal, F.T., Mars, J.C., McPhee, D.K., Seal, R.R., Taylor, R.D., and Vikre, P.G., 2010, Porphyry copper deposit model, chap. B of Mineral deposit models for resource assessment: U.S. Geological Survey Scientific Investigations Report 2010–5070–B, 169 p.
- Lowell, J.D., and Guilbert, J., 1970, Lateral and Vertical alteration-mineralization zoning in porphyry ore deposits: Economic Geology, v. 65, p. 373–408.
- Manske, S.L., and Paul, A.H., 2002, Geology of a major new porphyry copper center in the Superior (Pioneer) district, Arizona: Economic Geology, v. 97, p. 197–220.
- McDonald, C., Elliott, C.G., Vuke, S.M., Lonn, J.D., and Berg, R.B., 2012, Geologic map of the Butte South 30' x 60' quadrangle, southwestern Montana: Montana Bureau of Mines and Geology Open-File Report 622, 1 sheet, scale 1:100,000.
- Meyer, C., 1965, An early potassic type of wall-rock alteration at Butte, Montana: American Mineralogist, v. 50, p. 1717–1722.
- Meinert, L., 1982, Skarn, manto, and breccia pipe formation in sedimentary rocks of the Cananea mining district, Sonora, Mexico: Economic Geologists, v. 77, p. 919–949.
- Noble, D.C., and McKee, E.H., 1999, The Miocene metallogenic belt of central and northern Perú: Society of Economic Geologists Special Publication 7, p. 155–193.
- Noble, D.C., Vidal, C.E., Miranda, M., Walter Amaya, A., and McCormack, J.K., 2011, Ovoidal- and mottled-textured rock and associated silica veinlets and their formation by high-temperature outgassing of sub-jacent magma, in Steininger, R., and Pennell, B. eds., Great Basin Evolution and Metallogeny, Symposium, May 14–22, 2010, Volume II: Geological Society of Nevada, p. 795–812.

- Oyarzun, R., Marquez, A., Lillo, J., Lopez, I., and Rivera, S., 2001, Giant versus small porphyry copper deposits of Cenozoic age in northern Chile: Adakitic versus normal calc-alkaline magmatism, *Mineralia Deposita*, v. 36., p. 794–798.
- Ruppel, E.T., O’Neill, J.M., and Lopez, D.A., 1993, Geologic map of the Dillon 1 degree x 2 degree quadrangle, Idaho and Montana: U.S. Geological Survey Miscellaneous Investigation Series 1803-H.
- Ruppel, E.T., 1993, Cenozoic tectonic evolution of southwest Montana and east-central Idaho: Montana Bureau of Mines and Geology Memoir 65, p. 1–31.
- Schaffer, R., 2018, Crisis in discovery; Improving the business paradigm for mineral exploration: *Mining Engineering*, May Issue, p. 26–27.
- Schodde, R., 2013, Long term outlook for the global exploration industry: Geological Society of South Africa, Geo Forum Conference, Gloom or Boom?, Johannesburg, 2–5 July 2013, Oral Presentation.
- Sillitoe, R.H., 2010, Porphyry copper systems: *Economic Geology*, v. 105, p. 3–41.
- Sillitoe, R.H., Tolman, J., and van Kerkvoort, G., 2013, Geology of the Caspiche porphyry gold–copper deposit, Maricunga belt, northern Chile: *Economic Geology*, v. 108, p. 585–604.
- Sillitoe, R.H., Burgoa, C., and Hopper, D.R., 2016, Porphyry copper discovery beneath the Valeriano lithocap, Chile: *SEG Newsletter*, no. 106, July 2016, p. 1, 15–20.
- Tosdal, R.M., and Richards, J.P., 2001, Magmatic and structural controls on the development of porphyry Cu+ or -Mo+ or -Au deposits: *Reviews in Economic Geology*, v. 14, p. 157–181.
- Wood, D., 2016, We must change exploration thinking in order to discover future orebodies: *SEG Newsletter*, no. 105, p. 16–18.
- Wood, D., and Hedenquist, J., 2019, Mineral exploration: Discovering and defining ore deposits: *SEG Newsletter*, no. 116, p. 1, 11–22.
-



Panoramic of the Cable Mine site (photo: A. Roth).



The Map Chat at the Butte Brewing Company (photo: A. Roth).



View south into Browns Meadow, and the Kofford Ridge 7.5' quadrangle (photo: K. Scarberry).

Assessing the Potential for New and Economic Polymetallic Deposit Types within the Stillwater Complex, Montana

Craig Bow,¹ Michael Johnson,² Justin Modroo,^{*,3} Mike Ostenson,² and Michael Rowley⁴

¹Chief Geologist, ²Geologist, ³Geophysicist, ⁴President and CEO,
Group Ten Metals, Vancouver, BC
**Presenting author*

The Stillwater Igneous Complex of south-central Montana (fig. 1) is a 2.7 Ga layered magmatic intrusion that has a rich mining history, beginning in 1883 with the discovery of high-grade nickel and copper associated with the Mouat prospects on the eastern portion of the Basal Series. Chromite was first discovered in the 1890s; wartime efforts (1918, 1941–1943, and 1953–1961) produced chrome from the “G” chromitite layer of the Ultramafic Series at three different mines. In the 1950s, U.S. Steel focused exploration on the older, banded iron formation country rock. Many companies had explored the Basal Series for nickel and copper in the 1960s and 1970s, including Amax, Anaconda, Freeport, Lindgren, and Platinum Fox. PGEs were discovered in the 1930s, and subsequently recognized to occur in the lower chromitites (“A” and “B”) by the late 1960s. The first PGE bulk sample came from the Janet 50 pegmatoidal bronzitite target, located near the contact between the Banded and Ultramafic Series. Exploration drilling intercepted the J-M Reef in 1972, and by 1974 exploration focused on what was to become one of the highest-grade PGE deposits in the world. The Stillwater mine opened in 1986, and the East Boulder and Blitz mines followed in 2002 and 2017, respectively. The Picket Pin Horizon (“Reef-Type” target located within the Middle-Banded Series) was discovered and explored in the late 1970s and 1980s. This horizon exhibited elevated PGEs along the 20-km strike of surface exposure. In the 1980s, bonanza grade gold with PGEs and Ni-Cu was discovered in a chromitite hosted shear zone on the western flank of Chrome Mountain.

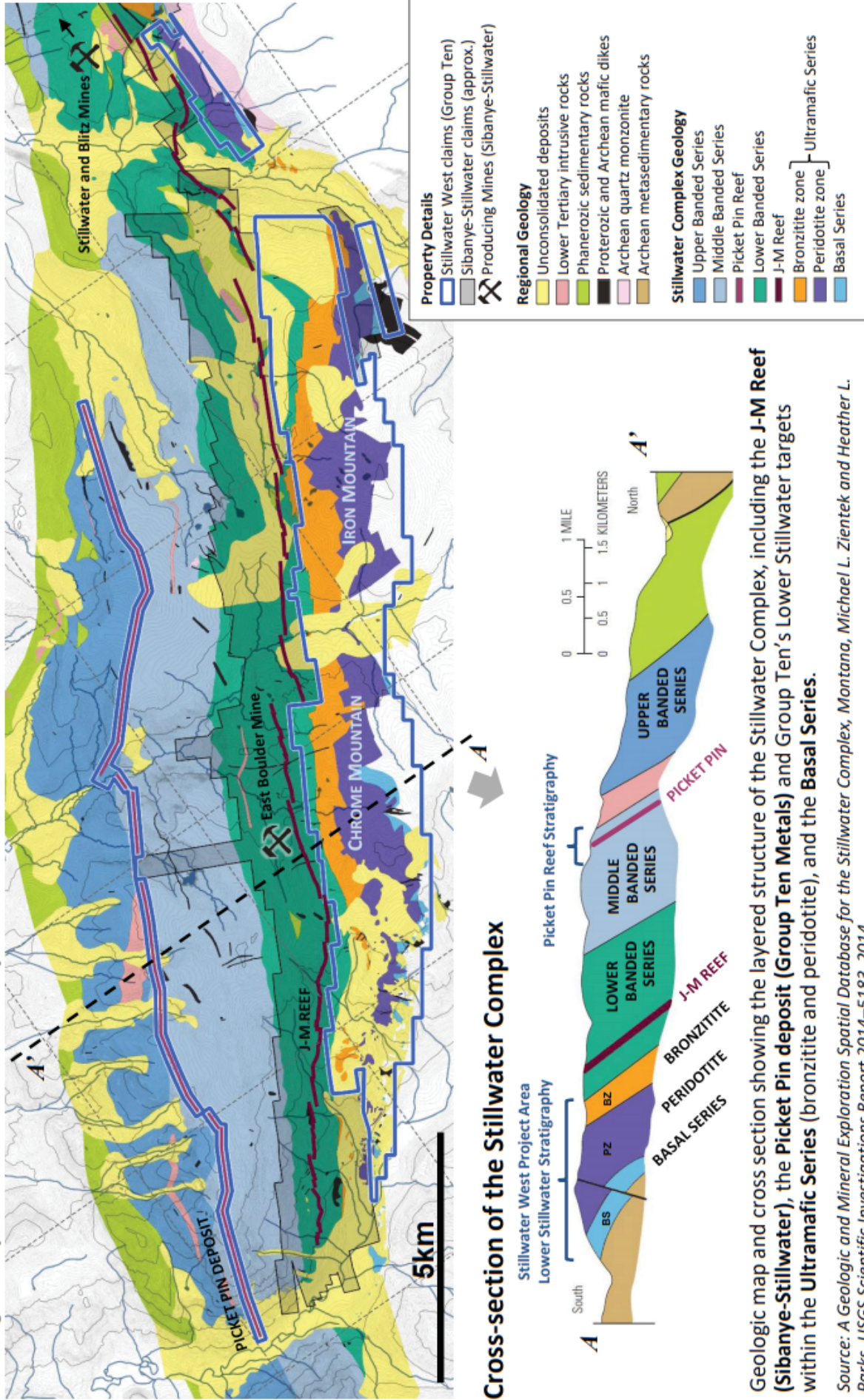
Renewed exploration efforts in the 1990s and 2000s added to the growing exploration database, including the discovery of a new PGE-Ni-Cu mineralization type associated with disseminated and schlieren type chromite over broad stratigraphic intervals within the Ultramafic Series on Chrome Mountain (2007–2008). Cobalt was also recognized in significant concentrations associated with the PGE-Ni-Cu mineralization. In the early 2010s, Stillwater Mining Company acquired the Mouat Ultramafic and Basal Series claims, indicating an interest in exploration outside of the J-M Reef. During 2017, Sibanye Gold purchased Stillwater Mining Company for \$2.2B, at the same time Group Ten Metals acquired the adjacent claims, consolidating the lower Stillwater complex and much of the non-J-M Reef and Mouat targets.

Group Ten Metals’ extensive historical database includes 215 drill holes totaling over 28,000 m, 14,000+ soil samples, 200+ rock samples, an airborne magnetic and EM (DIGHEM) survey, ground geophysics, and extensive surface geology mapping. Our data indicate the potential for a much larger mineralized system than has been previously recognized in this underexplored part of the Stillwater Complex (figs. 2, 3).

Group Ten Metals is targeting two different deposit types in the Stillwater Complex. The first target is high-grade Reef-Type PGE-Ni-Cu deposits, like the J-M Reef and analogous Bushveld Merensky and UG2 Reefs, represented by the Picket Pin Horizon and the A and B chromitites. The second target type is large-scale “Platreef-Style” PGE-Ni-Cu deposits that consist of magmatic-hosted sulfide mineralization within the Ultramafic and Basal Series. These deposits are the geological equivalent of the Bushveld’s Platreef succession, which host Ivanhoe’s Flatreef PGE-Ni-Cu discovery and Anglo American’s four Mogalakwena mines. Re-logging of the 2007–2008 Chrome Mountain holes identified a new “hybrid” unit in which bronzite cumulate and olivine cumulate rocks host disseminated and schlieren type chromite. These host rocks are complexly textured on a variety of scales with sharp domain boundaries, indicating the potential for previously unrecognized magmatic breccias. This hybrid unit is characterized by pegmatoidal textures, an abundance of intercumulus plagioclase, and persistent levels of sulfides (trace–3%). Fieldwork in 2018 has also discovered outcrop 1 km east of the 2007 hybrid discovery zone, with pegmatoidal bronzitite hosting disseminated and schlieren type chromite within a magmatic breccia that is similar to the hybrid zone. Discordant or intrusive dunites are recognized in

Stillwater West PGE-Ni-Cu Project – District Geology

Geologic map of the Stillwater Complex



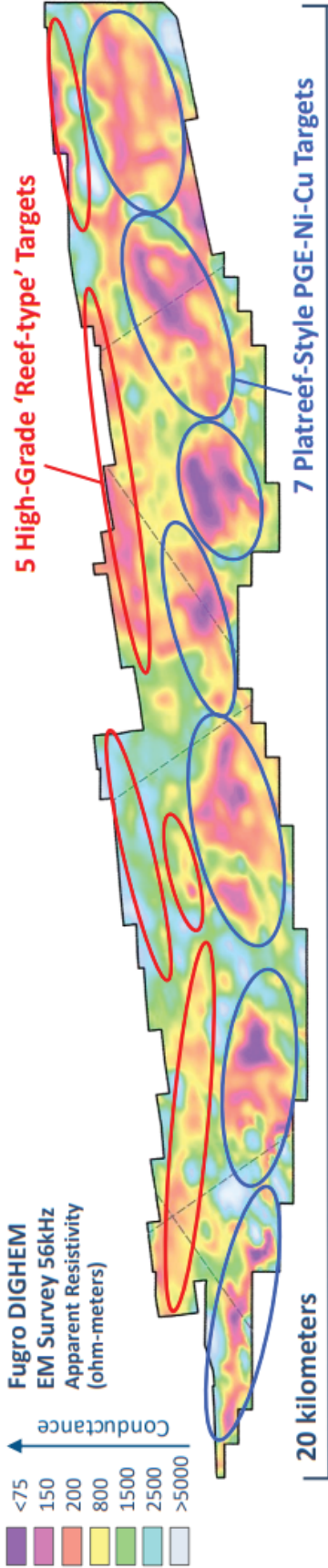
Geologic map and cross section showing the layered structure of the Stillwater Complex, including the J-M Reef (Sibanye-Stillwater), the Picket Pin deposit (Group Ten Metals) and Group Ten's Lower Stillwater targets within the Ultramafic Series (bronzite and peridotite), and the Basal Series.

Source: A Geologic and Mineral Exploration Spatial Database for the Stillwater Complex, Montana, Michael L. Zientek and Heather L. Parks, USGS Scientific Investigations Report 2014-5183, 2014.

Figure 1. Geologic map and cross section showing the layered structure of the Stillwater Complex. Modified from Zientek and Parks (2014).

Stillwater West PGE-Ni-Cu Project – Airborne EM Survey Results

12 major multi-kilometer geophysical conductor targets across 20 kilometer strike



- Results of 1,914 line-km Fugro DIGHEM (EM) Survey:**
- 12 major geophysical conductive anomalies on main claim block
 - Five main **Reef-type target areas** 1.5 to 5km long with potential for multiple higher-grade PGE 'Reef-type' deposits
 - Seven broad **Platreef-style PGE-Ni-Cu +/- Cr sulphide target** areas 2 to 4 km long with potential for large-scale magmatic sulphide-hosted PGE-Ni-Cu deposits +/- Cr
 - Strongest conductors may be characteristic of large bodies of massive to extensively disseminated sulphides and correspond with overlapping highly elevated palladium, platinum, gold, nickel, copper and chromium values in soils
 - Geophysical and geochemical signatures **show potential for a much larger mineralized system than has been previously recognized in this under-explored part of the Stillwater Complex**

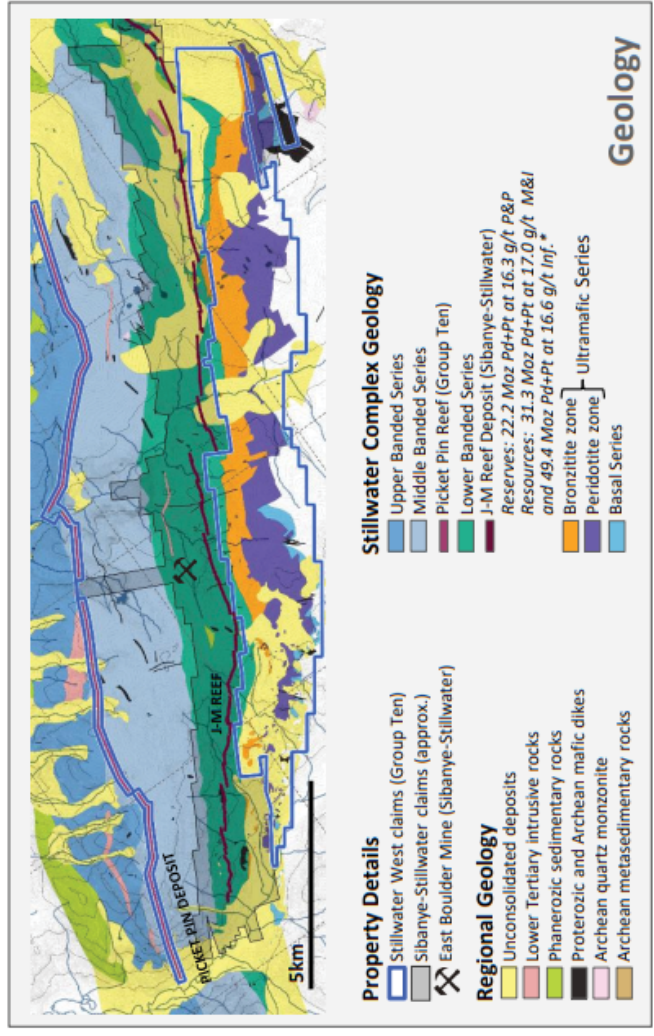


Figure 2. Group Ten's Stillwater West PGE-Ni-Cu project Airborne EM Survey Results has identified 12 major multi-kilometer geophysical conductor targets across 20 km strike.

Stillwater West PGE-Ni-Cu Project – Soil Geochemistry

Highly anomalous precious and base metal values cover >18 km strike in lower Stillwater Stratigraphy

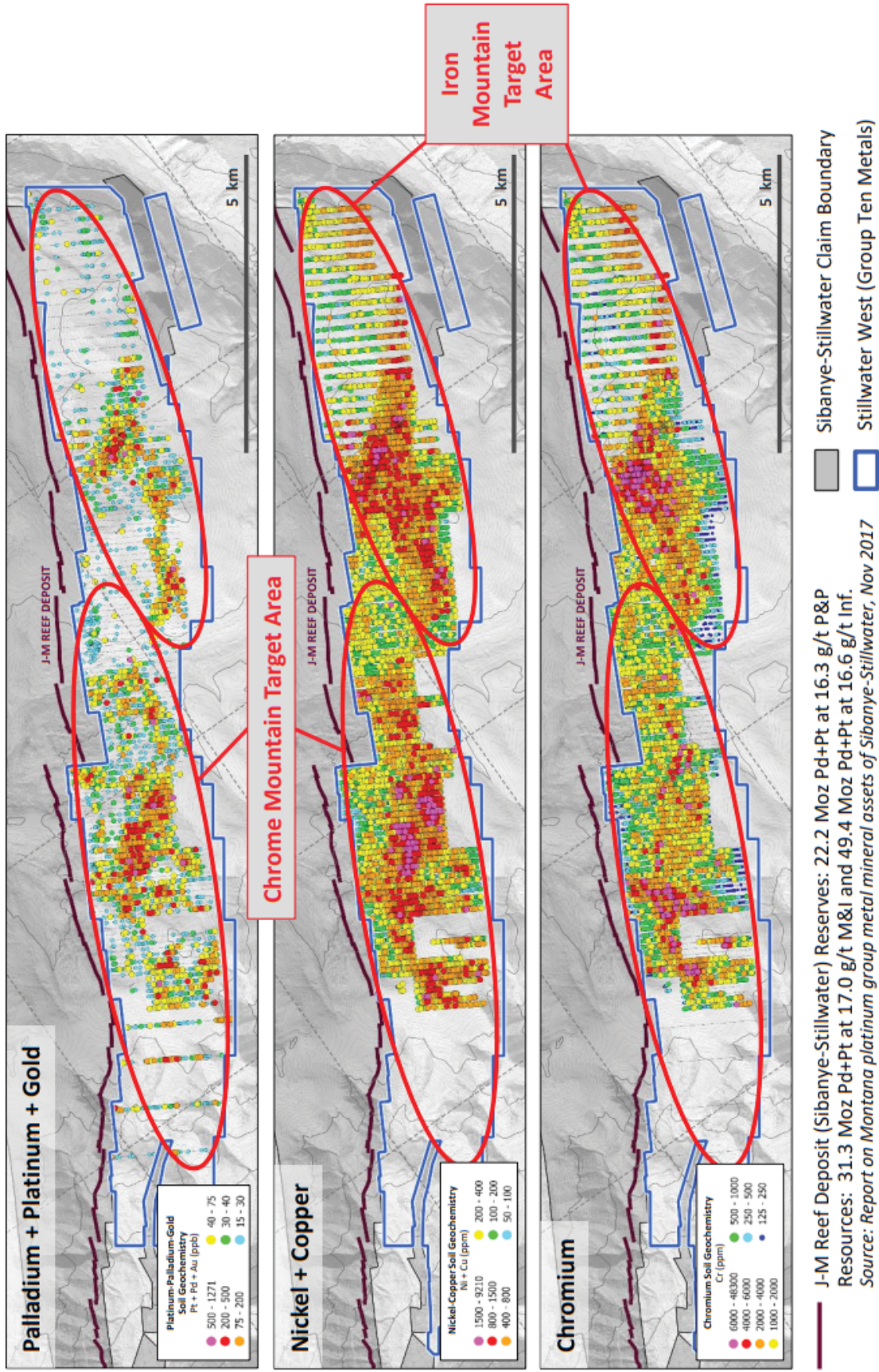


Figure 3. Group Ten's Stillwater West PGE-Ni-Cu project soil geochemistry results show highly anomalous precious and base metal values cover >18 km strike in lower Stillwater stratigraphy.

outcrop on both Chrome and Iron Mountains, where some samples containing disseminated chromite also exhibit elevated PGEs.

The Basal Series is also of interest because of the historical data and Ni and Cu resource estimates. The deposits from the eastern portion of the Basal Series indicate no elevated PGEs, while the middle and western portions have consistent PGE enrichment associated with net texture and massive base metal sulfides. Xenoliths and rafts of country rock (hornfels and iron formation) are mineralized proximal to the contact with the Stillwater Complex. Country rocks could have hosted Ni and Cu sulfide mineralization prior to Stillwater emplacement, and at this time it is unknown how the different country rocks affected mineralization and the overall cumulate processes.

The recognition of a Platreef setting in the Stillwater district is an exciting development that brings the potential for large, bulk-mineable polymetallic deposits to this iconic, mineral-rich district.

References

Zientek, M.L., and Parks, H.L., 2014, A geologic and mineral exploration spatial database for the Stillwater Complex, Montana: U.S. Geological Survey Scientific Investigations Report 2014-5183.



John Childs (left) and Bruce Cox (right) dust off dump rocks at the Cable Mine (photo: P. Hargrave).



Banquet at the Butte Brewing Company (photo: A. Roth).



The Meet and Greet at the Montana Tech Mineral Museum (photo: C. McKillips).

Precious Metal Mineralogy, S-Isotopes, and a New LA-ICP-MS Date for the Easton and Pacific Lode Mines, Virginia City District, Montana

Chris Gammons,¹ Jesse Mosolf,² and Simon R. Poulson³

¹Professor, Department of Geological Engineering, Montana Tech, Butte, Montana

²Geologist, Montana Bureau of Mines and Geology, Butte, Montana

³Professor, Department of Geological Sciences and Geological Engineering, University of Nevada–Reno, Reno, Nevada

Introduction

The placer deposits of Alder Gulch and tributaries in the Virginia City district, Madison County, Montana, produced an estimated 2.475 million oz of gold between 1863 and 1963 (Shawe and Wier, 1989). This makes the area by far the richest gold placer district in Montana, and one of the richest per kilometer of stream length in the U.S. The district also contains dozens of historic lode mines (fig. 1), the majority of which are quartz or quartz-carbonate veins that cut Archean metamorphic rock. However, in comparison to the placers, gold production from the lode deposits of the Virginia City district has been modest (171,000 oz Au, >2 million oz Ag; Shawe and Wier, 1989). This disparity makes the source for the Alder Gulch placers a topic of considerable interest and debate. In the current study, we present new mineralogical findings, reconnaissance sulfur-isotope data, and radiometric dates for mineralized veins at the Easton and Pacific lodes (fig. 1), the largest historic bedrock producers in the district.

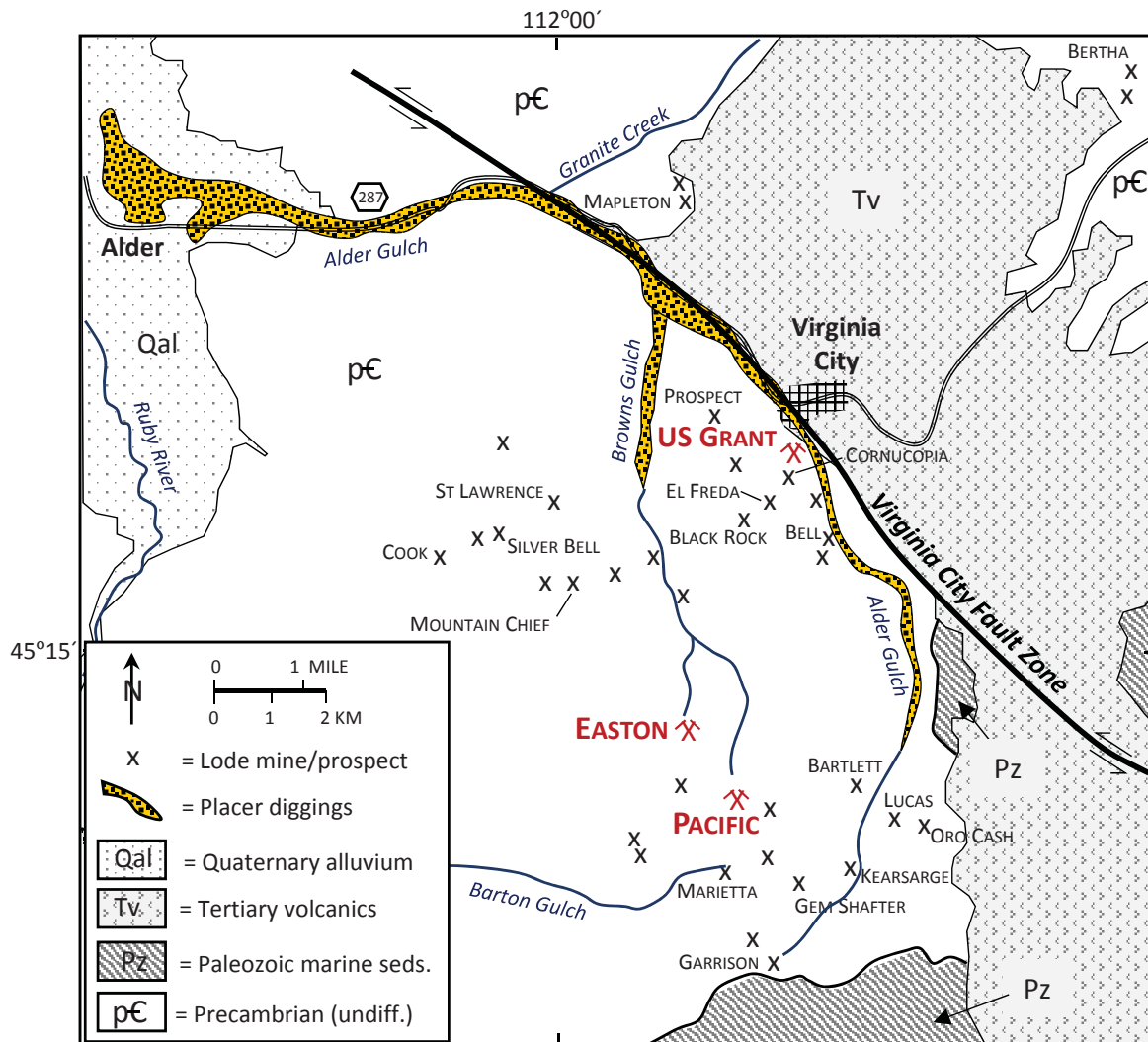


Figure 1. Generalized geologic map of the Virginia City district (after Shawe and Wier, 1989, and Ruppel and Liu, 2004).

The geology and ore deposits of the Virginia City district have been studied by many previous workers, including Winchell (1914), Lorain (1937), Lockwood and others (1991), Wier (1982), Cole (1983), Shawe and Wier (1989), Lockwood (1990), Barnard (1993), Eimon (1997), Despotovic (2000), and Ruppel and Liu (2004). At the time of this writing, the Easton, Pacific, and US Grant mines (fig. 1) are being mined intermittently at a small scale. Archean basement rock consists of tightly folded and highly metamorphosed biotite- and hornblende-schist, quartzo-feldspathic gneiss, and amphibolite that is intruded by numerous granite-pegmatite dikes that contain conspicuous, pink K-feldspar. Radiometric dating by Wier (1982) and Cole (1983) indicate a Proterozoic age (1.57 to 1.9 Ga) for the granite-pegmatite dikes, which suggests they may have formed during the Big Sky Orogeny, a major deformational and high-grade metamorphic event that affected the Tobacco Root Mountains at approximately 1.7 Ga (Harms and others, 2004). Paleozoic sedimentary rocks crop out in the southern part of the district, near the head of Alder Gulch (fig. 1), but are comparatively unmineralized. The Precambrian/Paleozoic rocks are unconformably overlain by Tertiary volcanic deposits east and north of Virginia City, which are also unmineralized. Small intrusive plugs of presumed Tertiary age and unspecified composition have been mapped in the vicinity of the Black Rock mine (Shawe and Wier, 1989). Early workers referred to a body of aplite of presumed late Cretaceous age near the Easton and Pacific mines as the Browns Gulch Stock. This igneous mass was later reinterpreted (Eimon, 1997; Ruppel and Liu, 2004) as being part of the system of granite dikes and pegmatites that occur elsewhere in the Virginia City district. Transecting the district is the Virginia City Fault Zone (VCFZ), a major NW-trending structure with a complex geologic history (fig. 1) akin to similar NW-trending structures that cut Precambrian terrain in the Tobacco Root and Highland Mountains (Ruppel and Liu, 2004).

Precious-metal-bearing veins and lodes in the Virginia City district have two dominant orientations. Most of the lodes strike N. 50 E. to N. 70 E. (e.g., Kearsarge, Marietta, US Grant, Silver Bell), while the Easton–Pacific and Mapleton lodes strike N. 35 W. to N. 60 W. A majority of the veins are rich in pyrite, sphalerite, and galena, with uncommon chalcopyrite. Some of the lodes reportedly contain Au-Ag tellurides (Winchell, 1914), although there are no detailed published studies of the precious metal mineralogy. Previous workers (see summary in Shawe and Wier, 1989) noted a general increase in Ag/Au ratio in the lodes from values <1 to the southeast (e.g., Kearsarge, Oro Cash; fig. 1) to values >50 to the northwest (e.g., Cook, Silver Bell; fig. 1). The Easton–Pacific lodes have Ag/Au ratios between 10 and 50. Lockwood (1990) reported reconnaissance fluid inclusion data from the Pacific Mine in which homogenization temperatures (not pressure-corrected) ranged from 175 to 275°C, and salinities from 3 to 12 wt% NaCl_{eq}. Also, the ratio of illite to smectite in argillically altered wallrock was used to estimate hydrothermal temperatures around 250°C. Lockwood (1990) proposed that the Easton–Pacific lodes formed at depths corresponding to the epithermal–mesothermal transition.

Methods

Several samples of high-grade ore from the Pacific mine pit (fig. 2) were obtained from the mine owners in 2015 for petrographic study. Additional samples of mineralized rock were collected from mine dumps and ore



Figure 2. The Pacific Mine Pit, looking south (June 9, 2017, photo taken by Jon Rice). Note the east-dipping granite-pegmatite dikes and sills exposed in the east wall (left side of photograph), and the crumbly, oxidized schist exposed in the west wall. Hand samples were collected from the “high grade stockpile” in the foreground, on the left side of the photograph.

stockpiles during follow-up visits to the Easton and Pacific mines in June and September of 2017. Sulfide-rich samples were slabbed and made into polished plugs for optical and SEM-EDS examination. A LEO 1430VP SEM with an EDAX Apollo 40 detector (ZAF corrected) was used at the Center for Advanced Mineral and Metallurgical Processing laboratory at Montana Tech. In total, approximately 30 polished plugs were prepared and examined optically, and 6 were selected for SEM work.

Eleven $\delta^{34}\text{S}$ analyses of sulfide minerals collected from dumps at the Easton and Pacific mines were performed at the University of Nevada–Reno. Sample preparation followed the methods of Giesemann and others (1994), and measurements were obtained from a Eurovector elemental analyzer interfaced to a Micromass IsoPrime isotope ratio mass spectrometer (IRMS). Results are given in the usual delta ($\delta^{34}\text{S}$) notation relative to the Vienna Canon Diablo Troilite (VCDT) standard and have estimated uncertainties of $\pm 0.2\%$.

Two whole rock samples (Pac 1 and Pac 6) containing *in situ* hydrothermal xenotime were mounted in epoxy resin mounts and polished to expose the inner portion of xenotime overgrowths on zircon. The xenotime overgrowths were then imaged to reveal compositional zoning and to guide U-Pb spot locations; X-ray elemental maps of xenotime were acquired using a Cameca SX-100 electron probe micro-analyzer (EPMA) at the University of California–Santa Barbara (UCSB). The samples were subsequently analyzed on a laser-ablation inductively coupled plasma mass spectrometer (LA-ICPMS) at the UCSB geochronology center following methods modified from Cottle and others (2013), Kylander-Clark and others (2013), and Briggs and Cottle (2018). Data reduction was carried out using Iolite (Paton and others, 2011), and the Isoplot Excel plugin (Ludwig, 2012) was used to plot U-Pb data and to calculate a weighted mean age.

Results

Ore and Gangue Mineralogy

Based on material examined from the dumps and ore stockpiles at the Easton and Pacific mines, the most common sulfide minerals in the lodes are pyrite, sphalerite, and galena, with lesser amounts of chalcopyrite and trace Au/Ag minerals. Pyrite is ubiquitous, and forms coarse crystals that were later sheared and partially replaced by other sulfide and gangue minerals. Sphalerite is Fe-poor (< 1 mole % FeS, based on SEM-EDX). The gangue, a mixture of milky-gray quartz, pearly-white carbonate (dolomite-ankerite), and barite, also shows textures that suggest repeated breaking and recementing of the veins. Whereas barite is a scarce gangue mineral overall (based on the rocks examined in this study), some barite-bearing samples were also rich in electrum and Ag-telluride minerals. Siderite was found as small, euhedral grains coating late-stage vugs and cracks. The carbonate minerals (dolomite, siderite) are locally associated with Ag-tellurides (hessite and cervelleite), and electrum (fig. 3). Based on SEM-EDX analyses ($n = 7$), cervelleite has a consistent formula near $\text{Ag}_{3.7}\text{Cu}_{0.3}\text{TeS}$. Electrum ranges in composition, often becoming more gold-rich around the rims (fig. 3F). Most of the coarser, unaltered electrum grains had $X_{\text{Au}} = 0.63$ to 0.69 . Small grains of pearceite were also observed, two of which contained up to 7.1 wt. % Te, which suggests partial solid solution with the rare mineral benleonardite ($\text{Ag}_8(\text{Sb,As})_2\text{Te}_2\text{S}_3$). Two small grains of uytenbogaardtite (Ag_3AuS_2) were found, one of which was rimmed by native silver (fig. 3B). Whereas the silver is thought to be supergene, the other Au/Ag minerals are most likely hypogene, or late hypogene. The irregular-shaped mineral in the upper right corner of figure 3F has the approximate formula: $(\text{Ag,Au,Cu})_9\text{Te}_2\text{S}_3$. If this formula is correct, it would represent a new mineral; more precise electron microprobe data are needed to confirm the composition.

Polished sections of hydrothermally altered pink granite at the Easton and Pacific mines (fig. 4A) also proved to be mineralogically interesting. The pink phase is close to pure KAlSi_3O_8 and is thought to be primary igneous K-feldspar. Patches of pyrite intergrown with hydrothermal quartz and dolomite cut the K-feldspar. A number of accessory minerals were observed near the border of the veins, including zircon (ZrSiO_4), xenotime (YPO_4), rutile (TiO_2), monazite (REE-PO_4), and rhabdophane (hydrous REE-PO_4). The zircon and rutile crystals are well-shaped and occur in clusters unusual for an igneous rock, suggesting a hydrothermal origin. Many of the zircons have overgrowths of xenotime (fig. 5A), one of which was used for U-Pb dating (fig. 6). Rhabdophane occurs as masses of fine-grained, feathery aggregates in close association with pyrite, and is almost certainly of hydrothermal origin. One micrometer-sized grain of a U-Ti-bearing mineral (probably brannerite, UTi_2O_6) was observed next to rutile.

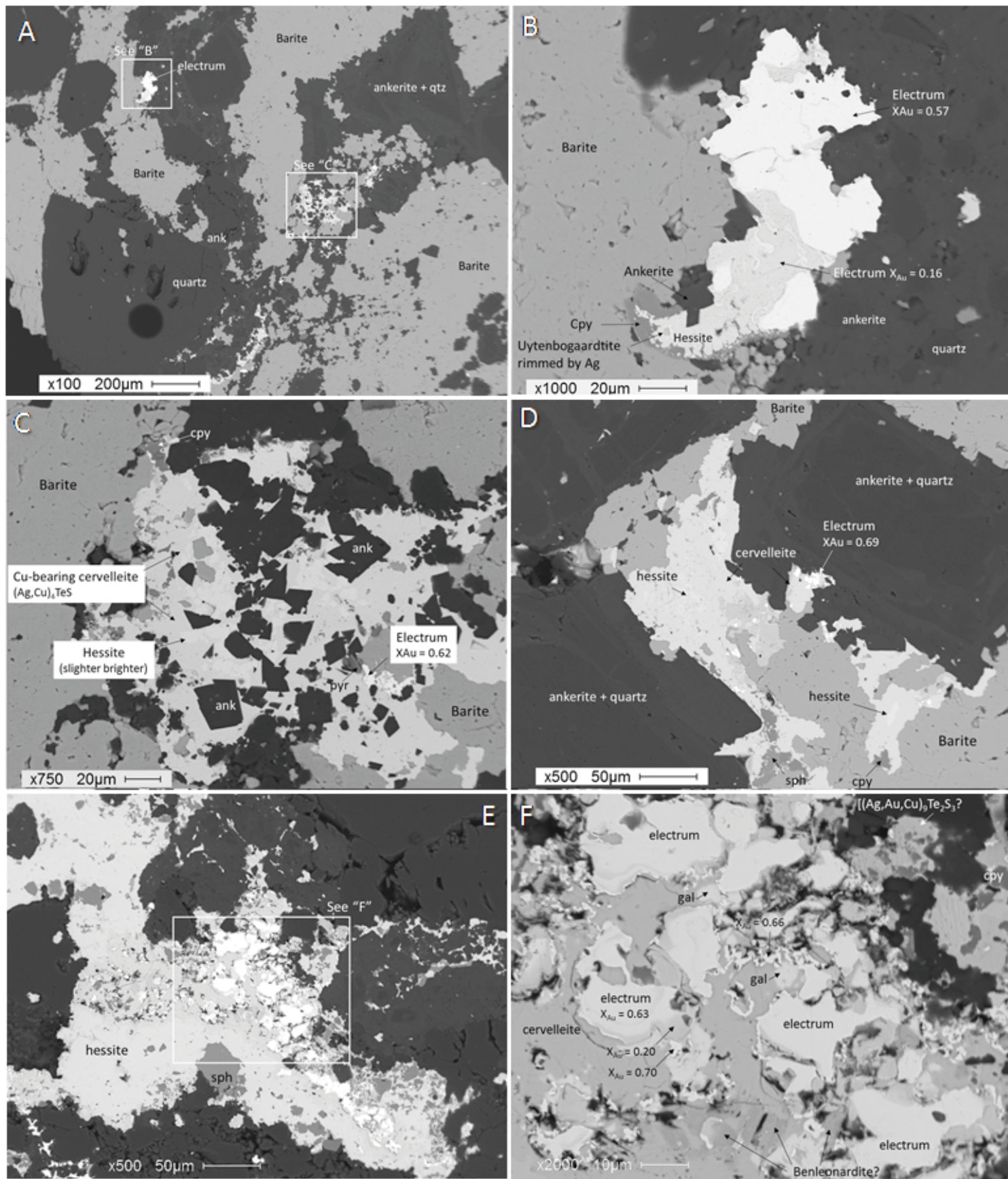


Figure 3. SEM-BSE images of rich Au/Ag ore from the Pacific Pit. (A) General view of quartz–barite–ankerite gangue. (B) Close up showing electrum of two different compositions with minor chalcopyrite (cpy), hessite, and uytenbogaardite (Ag_3AuS_2). (C and D) Complex intergrowths of cervelleite, hessite, barite, and ankerite with minor pyrite (pyr), chalcopyrite, sphalerite (sph), and electrum. (E and F) Intergrowths of hessite and cervelleite with abundant zoned electrum grains, minor galena (gal), benleonardite, and an unknown mineral with possible formula $(\text{Ag,Au,Cu})_9\text{Te}_2\text{S}_3$.

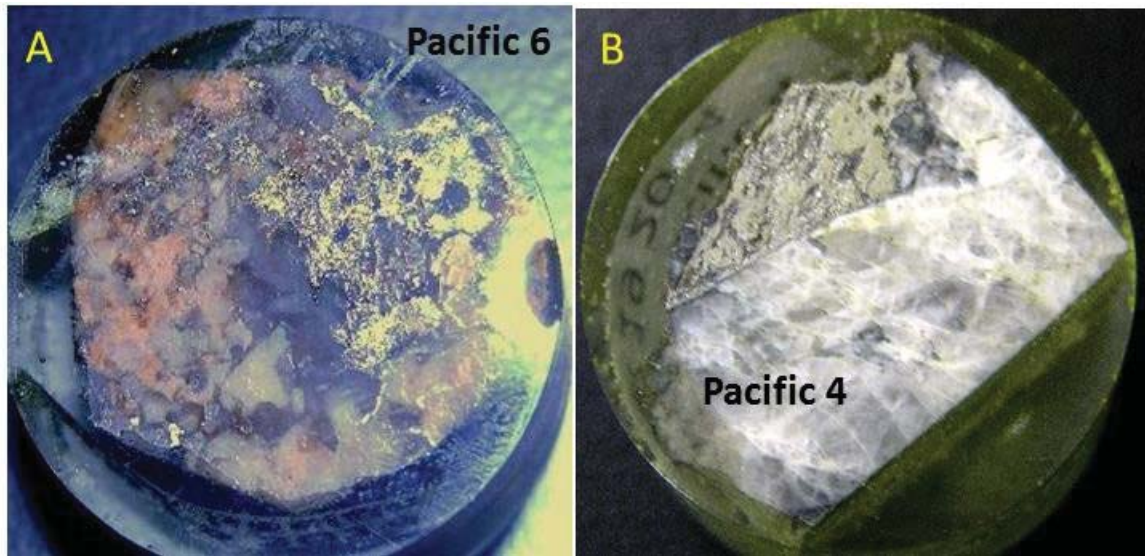


Figure 4. Photographs of polished plugs. (A) Pyrite and other gangue minerals cutting pink granite. (B) A typical vein of quartz-carbonate-pyrite that shows evidence of repeated breaking and recementing. Width of specimen is 1 inch in both photos.

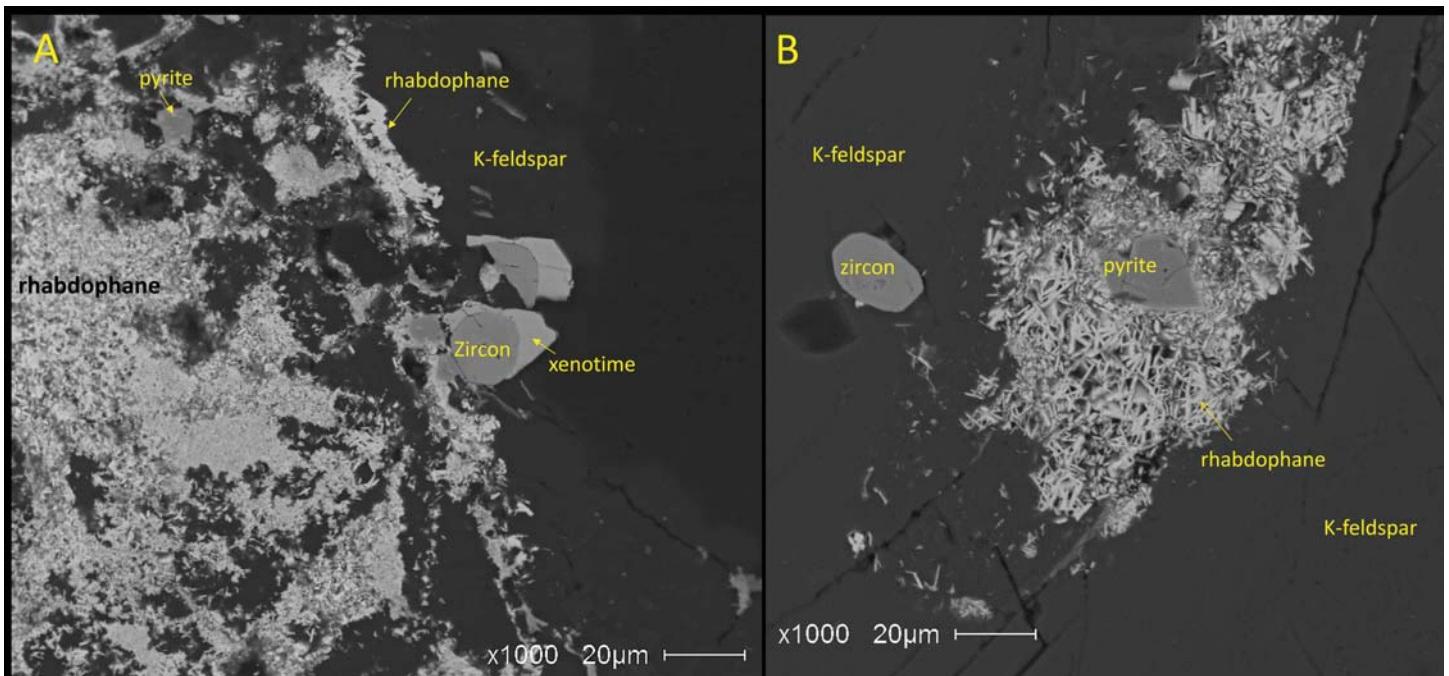


Figure 5. Accessory minerals (hydrothermal?) found in the altered pink granite wallrock (fig. 4A) from the Pacific Mine. The xenotime crystal overgrowing zircon in "A" was dated by U-Pb. See figure 6.

Sulfur Isotopes

Sulfur-isotope analyses for sulfide minerals from the Easton and Pacific mines are all very light, in the range of -13.6 to -17.4‰ (table 1). Possible reasons for the strongly negative S-isotope signature are discussed below. Attempts to estimate temperature based on the S-isotope separation between coexisting mineral pairs gave mixed results. Using fractionation factors from Kajiwra and Krouse (1971), the pyrite-galena pair from Pacific sample P3 gives a temperature of 287°C, in close agreement with a temperature of 293°C for the pyrite-chalcopyrite pair from Easton sample E4. However, the other mineral pairs (table 1) gave calculated temperatures that are clearly too high, in the range of 501 to 613°C. For samples PX and PZ, the poor result could be attributed to the small isotopic separation between pyrite and sphalerite at equilibrium, coupled with the $\pm 0.2\%$ analytical error in the S-isotope analyses. The anomalous result for the pyrite-galena pair from sample E4 could represent isotopic disequilibrium. For example, the galena may have formed after the pyrite, and may have scavenged some S from the preexisting pyrite.

Table 1. S-isotope data for sulfide minerals from the Easton and Pacific mines.

Sample No.	Mine	Mineral	$\delta^{34}\text{S}$, ‰VPDB	Estimated Temperature Based on $\delta^{34}\text{S}$ of Mineral Pairs	
E2	Easton	pyrite	-13.6		
E4	Easton	pyrite	-13.7	pyrite-cpy	pyrite-galena
		chalcopyrite	-15.1		
E1258	Easton	galena	-15.1	293°C	(613°C)
		chalcopyrite	-14.7		
P3	Pacific	pyrite	-13.9	pyrite-galena	
		galena	-17.4	287°C	
PX	Pacific	pyrite	-15.0	pyrite-sphalerite	
		sphalerite	-15.1	(1458°C)	
PZ	Pacific	pyrite	-14.3	pyrite-sphalerite	
		sphalerite	-14.8	(501°C)	

U-Pb Ages of Hydrothermal Xenotime

Thirty-six *in situ* xenotime spot analyses were acquired. These data generally exhibit high $^{207}\text{Pb}/^{206}\text{Pb}$ ratios that are attributed to common Pb. All but the most highly discordant analyses (discordance >50%, $n = 11$) were regressed on a Tera-Wasserburg plot anchored to theoretical common Pb ($^{207}\text{Pb}/^{206}\text{Pb} = 0.84$; Stacey and Kramers, 1975), which yielded a lower intercept age of 100.6 ± 3.3 Ma (fig. 6). A weighted mean age of 100.7 ± 1.9 Ma was calculated from the individual $^{206}\text{Pb}/^{238}\text{U}$ spot ages with a ^{207}Pb based correction (Andersen, 2002; Stacey and Kramers, 1975). Considering that the regressed and weighted mean ages are well within error, we interpret the acquired U-Pb age data to be a reliable and accurate proxy of the crystallization age of hydrothermal xenotime.

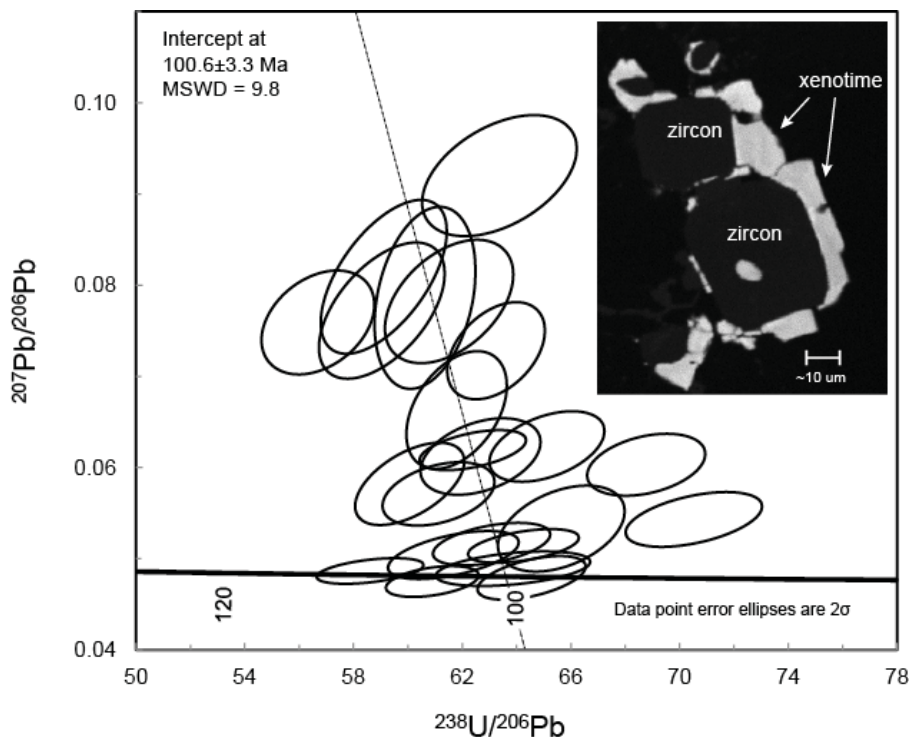


Figure 6. Tera-Wasserburg plot of U-Pb xenotime data with <50% discordance. Inset is an x-ray elemental map that shows the distribution of dysprosium in xenotime.

found in these deposits, including benleonardite and Cu-bearing cervelleite (Spry and Thieben, 1996).

The isotopically light sulfide minerals from the Easton–Pacific lodes (table 1) are distinctly anomalous when compared to $\delta^{34}\text{S}$ values of most calc-alkaline porphyry-hydrothermal systems that tend to cluster near upper-mantle values of 0‰ (Ohmoto and Rye, 1979). The most common source of isotopically light S in the crust is organic-rich black shales that contain pyrite formed by bacterial sulfate reduction. However, the igneous

Discussion

The ore-mineral assemblage documented in this study raises the possibility that the Easton–Pacific veins, and possibly other lode deposits in the Virginia City district, may be genetically similar to telluride-rich precious-metal deposits associated with late Cretaceous to Tertiary alkaline magmatism in Montana and central Colorado (Thieben and Spry, 1995; Jensen and Barton, 2000). Other examples of these deposits in Montana include the Golden Sunlight and Mayflower mines in the Whitehall District (Porter and Ripley, 1985; Spry and others, 1996; Spry and Thieben, 1996), the Zortman–Landusky mines in the Little Rocky Mountains (Wilson and Kyser, 1988), and the Gies mine in the Judith Mountains (Zhang and Spry, 1994). Some of the same rare telluride minerals reported in this study were

and high-grade metamorphic rocks of the Archean basement in the Virginia City district would seem an unlikely place to harbor deep, metamorphosed sediments of this type.

In contrast to calc-alkaline porphyries, recent studies have shown that gold-rich porphyry-epithermal mineralization related to alkalic magmatism often contains sulfide minerals that are isotopically light (Deyell and Tosdal, 2005; Wilson and others, 2007). Wilson and others (2007) attributed the negative $\delta^{34}\text{S}$ signatures to isotopic exchange between dissolved sulfide and sulfate in magma-derived fluids that are strongly oxidized ($\text{SO}_2 \gg \text{H}_2\text{S}$). The Golden Sunlight deposit, which is underlain by a porphyry-Mo-Cu system of alkalic affinity (Spry and others, 1996), contains isotopically light pyrite in the range of -5 to -12‰ (Porter and Ripley, 1985; Gnanou, 2018). However, to our knowledge, no previously described porphyry-epithermal system worldwide contains sulfide minerals with $\delta^{34}\text{S} < -12\text{‰}$. The range of $\delta^{34}\text{S}$ from the Easton and Pacific mines, -13.6 to -17.4‰, may represent an extreme endmember of the process argued by Wilson and others (2007). Otherwise, the light $\delta^{34}\text{S}$ values are difficult to explain.

The U-Pb age of 100 ± 3 Ma for hydrothermal xenotime from the Pacific mine (fig. 6) is also difficult to explain. Although the age supports a Cretaceous mineralizing event in the Virginia City district, it is about 20 m.y. older than any of the other igneous rocks in the region. Individual plutons in the Boulder and Tobacco Root Batholiths range in age from about 80 to 75 Ma (Mueller and others, 1996; Lund and others, 2002) and overlap with eruption ages for the Elkhorn Mountains volcanic field. Although it is tempting to dismiss our 100 Ma age because it came from a single mineral grain, Hammarstrom and others (2002) reported a $^{40}\text{Ar}/^{39}\text{Ar}$ date of 120.2 ± 0.7 Ma for hydrothermal sericite from the Kearsarge mine (fig. 1), located roughly 3 km southeast of the Pacific mine. Hammarstrom and co-authors were also perplexed by their mid-Cretaceous age determination. Aleinikoff and others (2012) reported ages of 104 to 93 Ma for xenotime overgrowths on Precambrian xenotime cores from the Cu-Co ore deposits of the Blackbird district in central Idaho. The 100 Ma age reported here also overlaps with 98 to 68 Ma igneous rocks described in the Atlanta lobe of the Idaho Batholith (Gaschnig and others, 2010), and a new U-Pb age of 105.2 ± 0.5 Ma that was obtained from a trachyte in the Pioneer Mountains, located about 70 km west of the Virginia City mining district (J. Mosolf, written commun., 2018). It is possible that hydrothermal activity in the Virginia City district took place as a distal expression of deformation and magmatism centered further west. It is also possible that the Virginia City district has experienced multiple episodes of hydrothermal alteration and mineralization spread over a very long period of geologic time, from the Precambrian to the Cenozoic.

Conclusions

This paper has documented a tellurium-rich, precious-metal mineral assemblage from the Easton and Pacific Mines, two of the largest lode-gold producers in the Virginia City district. Associated pyrite, sphalerite, and galena have isotopically light $\delta^{34}\text{S}$ values that are difficult to explain given the setting of the deposits in amphibolite-grade metamorphic rocks of the Wyoming Craton. Hydrothermal xenotime overgrowths on zircon from the Pacific Mine yielded a U-Pb age of 100 ± 3 Ma, which is older than documented late Cretaceous intrusive and volcanic activity described elsewhere in southwest Montana. Could there have been a previously overlooked magmatic-hydrothermal event in southwest Montana dating to the mid-Cretaceous? More detailed ore-deposit studies coupled with radiometric dating are needed to confirm or refute this idea.

Acknowledgments

We thank Matt Moen for supporting the initial petrographic study of rocks from the Easton–Pacific area, and for permission to visit the field sites. We also thank Gareth Seward and Andrew Kylander-Clark for technical support at UCSB’s EPMA and LA-ICPMS facilities. Montana Tech graduate students Dustin Jensen and Francis Grondin helped with the project. The manuscript was improved by the reviews of Kaleb Scarberry and Stan Korzeb. Partial funding came from the Montana Tech Stan and Joyce Lesar Endowment, and the U.S. Geological Survey National Cooperative Geologic Mapping Program, award number G17AC00257.

References Cited

- Aleinikoff, J.N., Slack, J.F., Lund, K., Evans, K.V., Fanning, C.M., Mazdab, F.K., Wooden, J.L., and Pillers, R.M., 2012, Constraints on the timing of Co-Cu+Au mineralization in the Blackbird district, Idaho, using SHRIMP U-Pb ages of monazite and xenotime plus zircon ages of related Mesoproterozoic orthogneisses and metasedimentary rocks: *Economic Geology*, v. 107, p. 1143–1175.
- Andersen T., 2002, Correction of common lead in U-Pb analyses that do not report ^{204}Pb : *Chemical Geology*, v. 192, p. 59–79.
- Barnard, F., 1993, District-scale zoning patterns, Virginia City, Montana, USA: 96th National Western Mining Conference, Colorado Mining Association (Denver), Reprint 93-29, 19 p.
- Briggs, S.I., and Cottle, J.M., 2018, Accessory mineral petrochronology reveals 30 m.y. of partial melting during the separation of Zealandia from eastern Gondwana: *Lithosphere*, v. 11, no. 1, p. 169–189.
- Cole, M.M., 1983, Nature, age, and genesis of quartz-sulfide-precious metal vein systems in the Virginia City mining district, Madison County, Montana: M.S. thesis, Bozeman, Montana State University, 63 p.
- Cottle, J.M., Burrows, A.J., Kylander-Clark, A., Freedman, P.A., and Cohen, R.S., 2013, Enhanced sensitivity in laser ablation multi-collector inductively coupled plasma mass spectrometry: *Journal of Analytical Atomic Spectrometry*, v. 28, p. 1700–1706.
- Despotovic, P., 2000, Geology and geochemistry of Au-Ag-mineralization in the Virginia City mining district (VCMD), Montana, U.S.A: Berlin, University of Berlin, M.S. thesis, 101 p.
- Deyell, C.L., and Tosdal, R.M., 2005, Alkaline Cu-Au deposits of British Columbia: Sulfur isotope zonation as a guide to mineral exploration: British Columbia Geological Survey, Geologic Fieldwork 2004, Paper 2005-1, p. 191–208.
- Eimon, P. I., 1997, The economic geology of Montana's Virginia City mining district: *Society of Economic Geology Newsletter*, no. 28, January, 1996, 6 p.
- Gaschnig, R.M., Vervoort, J.D., Lewis, R.S., and McClelland, W.C., 2010, Migrating magmatism in the northern US Cordillera: in situ U-Pb geochronology of the Idaho batholith: *Contributions to Mineralogy and Petrology*, v. 159, p. 863–883.
- Giesemann, A., Jager, H.J., Norman, A.L., Krouse, H.P., and Brand, W.A., 1994, On-line sulfur-isotope determination using an elemental analyzer coupled to a mass spectrometer: *Analytical Chemistry*, v. 66, p. 2816–2819.
- Gnanou, H., 2018, Mineralogy and sulfur isotope geochemistry of the Apex and Bonanza prospects at the Golden Sunlight Mine, Montana: Butte, Montana Tech, M.S. thesis, 78 p.
- Hammarstrom, J.M., Van Gosen, B.S., Kunk, M.J., and Herring, J.R., 2002, Gold-bearing quartz veins in the Virginia City mining district, Madison County, Montana: *Northwest Geology*, v. 31, p. 12–43.
- Harms, T.A., Brady, J.B., Burger, H.R., and Cheney, J.T., 2004, Advances in the geology of the Tobacco Root Mountains, Montana, and their implications for the history of the northern Wyoming province: *Geological Society of America, Special Paper 377*, p. 227–243.
- Jensen, E.P., and Barton, M.D., 2000, Gold deposits related to alkaline magmatism: *SEG Reviews*, v. 13, p. 279–314.
- Kajiwa, Y., and Krouse, H.R., 1971, Sulfur isotope partitioning in metallic sulfide systems: *Canadian Journal of Earth Sciences*, v. 8, p. 1397–1408.
- Kylander-Clark, A.R., Hacker, B.R., and Cottle, J.M., 2013, Laser-ablation split-stream ICP petrochronology: *Chemical Geology*, v. 345, p. 99–112.
- Lockwood, M.S., 1990, Controls on precious-metal mineralization, Easton-Pacific vein, Virginia City mining district, Madison County, Montana: Socorro, New Mexico Institute of Mines and Technology, M.S. thesis.

- Lockwood, M.S., Campbell, A.R., and Chavez, W.X. Jr., 1991, Evolution of mineralizing fluids, Virginia City mining district, Montana: Geological Society of America Abstracts with Programs, v. 23, no. 4, p. 43.
- Lorain, S.H., 1937, Gold lode mining in the Tobacco Root Mountains, Madison County, Montana: U.S. Bureau of Mines, Information Circular 6972, 74 p.
- Ludwig, K.R., 2012, User's manual for Isoplot 3.75: A Geochronological Toolkit for Microsoft Excel: Berkeley Geochronology Center Special Publication 5, 75 p.
- Lund, K., Aleinikoff, J., Kunk, M., Unruh, D., Zeihen, G., Hodges, W., DuBray, E., and O'Neill, J., 2002, Shrimp U-Pb and $^{40}\text{Ar}/^{39}\text{Ar}$ age constraints for relating plutonism and mineralization in the Boulder batholith region, Montana: Economic Geology, v. 97, p. 241–267.
- Mueller, P. A., Heatherington, A.L., D'Arcy, K.A., Wooden, J.L., and Nutman, A.P., 1996, Contrasts between Sm-Nd whole-rock and U-Pb zircon systematics in the Tobacco Root batholith, Montana: Implications for the determination of crustal age provinces: Tectonophysics, v. 265, p. 169–179.
- Ohmoto, H., and Rye, R.O., 1979, Isotopes of sulfur and carbon, in Barnes, H.L., ed., Geochemistry of Hydrothermal Ore Deposits, 2nd ed.: New York, John Wiley & Sons, Chapter 10, p. 509–567.
- Paton, C., Hellstrom, J., Paul, B., and Woodhead, J., 2011, Iolite: Freeware for the visualization and processing of mass spectrometric data: Atomic Spectrometry, v. 26, p. 2508–2518.
- Porter, E.W., and Ripley, E.M., 1985, Petrologic and stable isotope study of the gold-bearing breccia pipe at the Golden Sunlight Deposit, Montana: Economic Geology, v. 80, p. 1689–1706.
- Ruppel, E.T., and Liu, Y., 2004, The gold mines of the Virginia City mining district, Madison County, Montana: table Montana Bureau Mines Geology Bulletin 133, 79 p.
- Shawe, D.R., and Wier, K.L., 1989, Gold deposits in the Virginia City–Alder Gulch district, Montana: U.S. Geological Survey Bulletin 1857-G, p. G12–G19.
- Spry, P.G., Paredes, M.M., Foster, F., Truckle, J.S., and Chadwick, T.H., 1996, Evidence for a genetic link between gold–silver telluride and porphyry molybdenum mineralization at the Golden Sunlight Deposit, Whitehall, Montana; fluid inclusion and stable isotope studies: Economic Geology, v. 91, p. 507–526.
- Spry, P.G., and Thieben, S.E., 1996, Two new occurrences of benleonardite, a rare silver–tellurium sulphosalt, and a possible new occurrence of cervelleite: Mineralogical Magazine, v. 60, p. 871–876.
- Stacey, J., and Kramers, J.D., 1975, Approximation of terrestrial lead isotope evolution by a two- stage model: Earth and Planetary Science Letters, v. 26, p. 207–211.
- Thieben, S.E., and Spry, P.G., 1995, The geology and geochemistry of Cretaceous-Tertiary alkaline igneous rock-related gold-silver telluride deposits of Montana, USA, in Pašava, J., Kříbek, B., and Zák, K., eds., Mineral deposits: From their origin to their environmental impacts: A.A. Balkema, Rotterdam, p. 199–202.
- Wier, K.L., 1982, Maps showing geology and outcrops of part of the Virginia City and Alder quadrangles, Madison County, Montana: U.S. Geological Survey, Miscellaneous Field Studies Map MF-1490.
- Wilson, M.R., and Kyser, T.K., 1988, Geochemistry of porphyry-hosted Au–Ag deposits in the Little Rocky Mountains, Montana: Economic Geology, v. 83, p. 1329–1346.
- Wilson, A.J., Cooke, D.R., Harper, B.J., and Deyell, C.L., 2007, Sulfur isotopic zonation in the Cadia district, southeastern Australia: Exploration significance and implications for the genesis of alkalic porphyry gold–copper deposits: Mineralium Deposita, v. 42, p. 465–487.
- Winchell, A.N., 1914, Mining districts in the Dillon quadrangle, Montana, and adjacent areas: U.S. Geological Survey Bulletin, v. 574, 191 p.
- Zhang, X., and Spry, P.G., 1994, Petrological, mineralogical, fluid inclusion, and stable isotope studies of the Gies gold–silver telluride deposit, Judith Mountains, Montana: Economic Geology, v. 89, p. 602–627.



Altered rock at the Cable Mine (photo: P. Hargrave).

New Investigations of the Economic Geology of the Historic Elkhorn Mining District, Jefferson County, Montana

Alexander H. Brown,¹ Chris Gammons,² and Simon R. Poulson³

¹M.S. Student, Department of Geological Engineering, Montana Tech, Butte, Montana

²Professor, Department of Geological Engineering, Montana Tech, Butte, Montana

³Professor, Department of Geological Sciences and Geological Engineering, University of Nevada–Reno, Reno, Nevada

Despite the Elkhorn mining district being one of the largest historic silver producers in the state of Montana, very little modern work has been done on ore deposits in the district. Most production of silver and lead occurred in the late 19th century and was derived from a single galena-rich carbonate replacement deposit (CRD). Modern exploration has delineated significant gold-rich skarn deposits that are currently idle. A low-grade porphyry Mo-Cu deposit is also present in the middle of the district. Here we present a study of the Elkhorn District using ore microscopy, fluid inclusion analysis, and sulfur isotope data in an effort to better understand the genetic links among the CRD, skarn, and porphyry mineralizing systems.

Geology, Mineralization, and Mining History

The town and mining district of Elkhorn are located south and at the base of the Elkhorn Mountains, east of Boulder, in Jefferson County, Montana. The district geology is characterized by a window of deformed Paleozoic and mid-Proterozoic sedimentary rocks that are overlain by the late Cretaceous Elkhorn Mountains volcanic field and then cut by Late Cretaceous intrusions (fig. 1). Within the district, Cretaceous intrusive rocks are, from

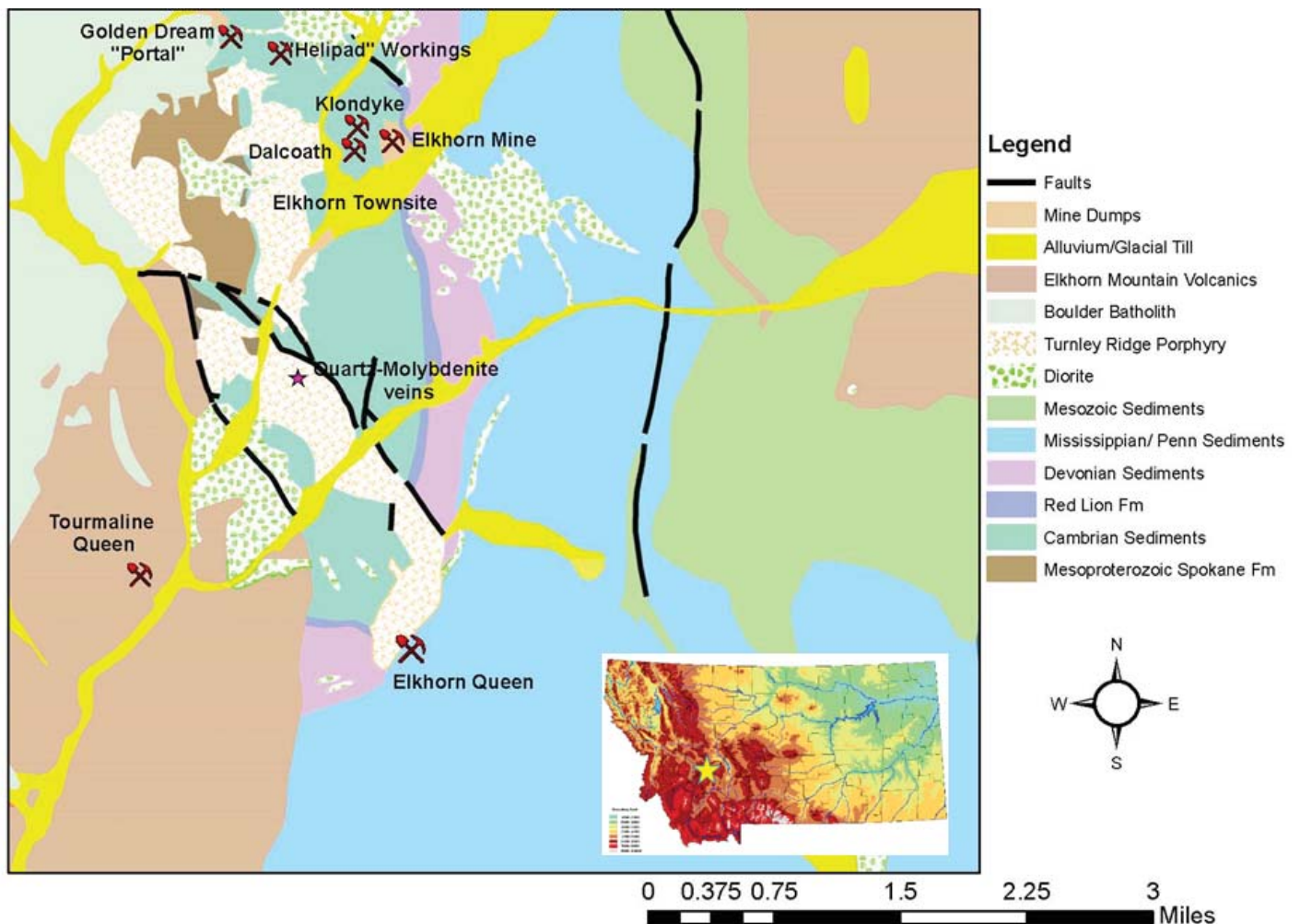


Figure 1. Geology and location of the Elkhorn mining district. Geology adapted from Reynolds and Brandt (2006).

oldest to youngest, diorite to gabbro stocks of Black Butte, East Butte, and Cemetery Ridge, the granitic porphyry of Turnley Ridge, and the granitic Butte Pluton of the Boulder Batholith. The Paleozoic and mid-Proterozoic metasedimentary rocks strike north–south and dip to the east in the vicinity of the mines in the district.

Geologic and mineral deposit studies at Elkhorn were performed by Weed (1901), Knopf (1913a,b), Pardee and Schrader (1933), Klepper and others (1957), Roby and others (1960), Senter (1976), Steefel (1982), Steefel and Atkinson (1984), Everson and Read (1992), and Tucker (2008). Hydrothermal mineralization includes: (1) porphyry Mo-(Cu) mineralization in the Turnley Ridge stock; (2) gold-rich skarn deposits; (3) Ag-Pb-Zn CRDs; and (4) base- and precious-metal tourmaline-bearing breccia pipes. Most historic production has come from CRD deposits at the main Elkhorn Mine (fig. 1). More recent exploration and development, continuing to this day, has focused on a number of gold-rich skarn deposits, and some small-scale mining occurred in the late 1990s.

The history of mining at Elkhorn is summarized here from information reported by Weed (1901) and Gray (1998). Prospecting began in 1868 when Peter Wys arrived at Elkhorn Creek and stayed after discovering promising rock samples. Wys is credited with discovering ore at Elkhorn, although he died suddenly in 1872, rumored to have been murdered by his partner, Simmons. In 1875, George Benjamin discovered argentiferous galena at what would later become the Elkhorn mine. A five stamp mill arrived in town by 1881, when George Benjamin sold his mining claim for \$200 to the ambitious and resourceful A.M. Holter. Under new ownership, the Elkhorn mine (fig. 2) became one of the largest producers of silver in the world for a short time. Eventually, two stamp mills were constructed at the Elkhorn mine, and production continued along an inclined shaft to the 2300 level (1,975 ft depth), which made the mine the deepest in Montana at the time. The Elkhorn mine ran continuously from 1875 to 1899, when it was sold and the tailings were reprocessed. The Elkhorn mine operated intermittently until the 1930s, and other surrounding mines in the district remained productive until 1953. In total, the Elkhorn mining district produced 20,023 oz of gold, 14,789,492 oz of silver, 148,361 lbs of copper, 14,004,780 lbs of lead, and 2,845,221 lbs of zinc. Zinc and copper production was not recorded prior to 1902.

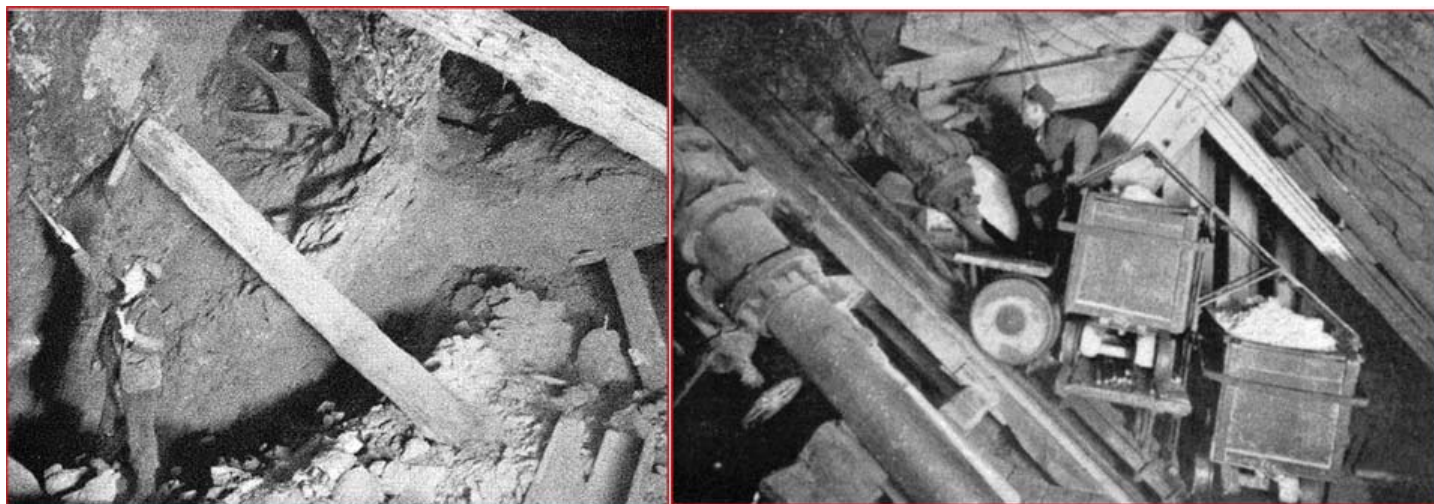


Figure 2. The South stope and inclined shaft at the Elkhorn mine (photos from Weed, 1901).

Mine Properties Sampled in This Study

The Elkhorn district is interesting because it displays many different types of hydrothermal mineralization within a relatively small area. The Turnley Ridge stock contains low-grade, porphyry-type Mo-Cu mineralization (Senter, 1976; Steefel, 1982), and Steefel and Atkinson (1984) proposed that the composite stock also influenced most skarn and CRD mineralization in the district. We sampled molybdenite-bearing quartz veins from the Turnley Ridge stock that are exposed along the old railroad grade about a mile south of the townsite.

Skarn deposits are prevalent in the Elkhorn district. The Golden Dream (aka: Sourdough or Golden Curry; fig. 2) is the most developed of the skarn deposits, and contains a pyrrhotite-rich exoskarn. Everson and Read (1992) reported a resource of 1.3M tonnes at 6.5 g/t Au for the Golden Dream, which remains open at the NE

and SW entrances. We sampled stockpiled ore at the mine portal. We also sampled exoskarn exposed at the surface in a small open pit roughly 300 m east and uphill of the Golden Dream portal. This site is referred to as the “Helipad” (fig. 1) in this study, and is probably the Heagen deposit described by Everson and Read (1992).

Southeast of the Golden Dream, we sampled two small skarn deposits from the Dalcoath (aka Hard Cash) and Klondyke mines (fig. 2), which had locally high gold content associated with bismuth minerals, according to Weed (1901). Unlike the Golden Dream mine, skarns at the Dalcoath and Klondyke contained only minor amounts of sulfide minerals. Everson and Read (1992) described gold-rich skarn deposits at the East Butte and Carmody mines, but these deposits are mainly defined by drilling and were not sampled.

Carbonate-replacement Ag-Pb-Zn mineralization at the Elkhorn mine (aka: Holter; fig. 3) formed as stratabound lenses and breccias within the contact zone between Cambrian dolomite (marble) of the Pilgrim Formation and shale (hornfels) of the overlying Red Lion Formation (fig. 4). McClernan (1976, 1983) suggested that the Elkhorn mine could be a Mississippi-Valley Type (MVT) deposit. Although mine dump material consisted mainly of non-mineralized, buff-colored dolomitic marble, we managed to collect several rock samples that contained coarse sulfides (pyrite, galena, sphalerite, and sulfosalts).

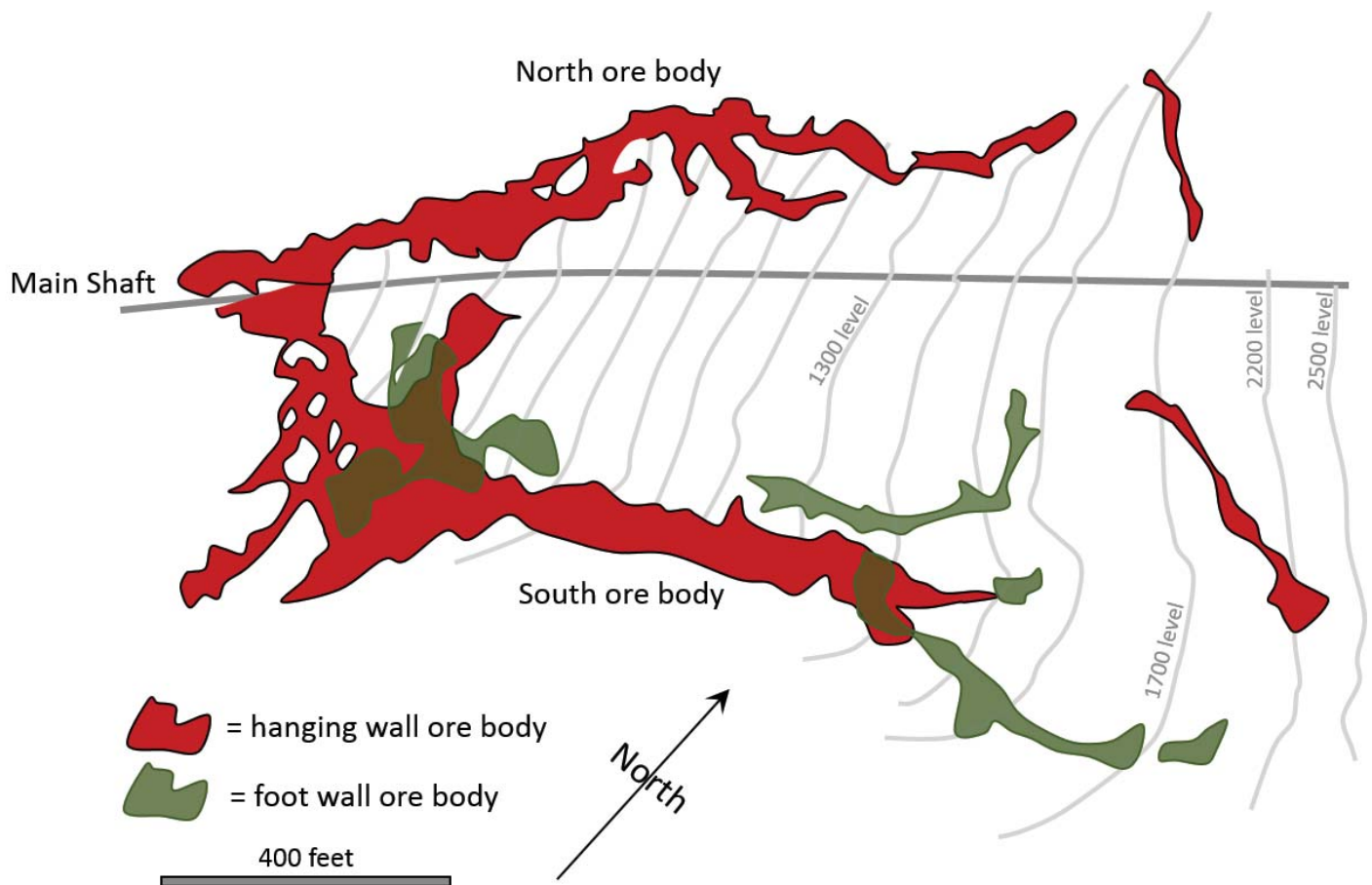


Figure 3. Plan map of the historic Elkhorn Mine (redrawn from Weed, 1901).

The Elkhorn Queen and the Tourmaline Queen mines in the southern part of the district (fig. 1) targeted tourmaline-bearing breccia pipes and were mined for gold and silver, as well as Cu-Pb-Zn (at Elkhorn Queen). Senter (1976) described the ore body at the Elkhorn Queen as an elliptical-shaped quartz-porphry ore pipe in contact with hornfels of the Three Forks shale. We sampled the dumps at the Elkhorn Queen mine.

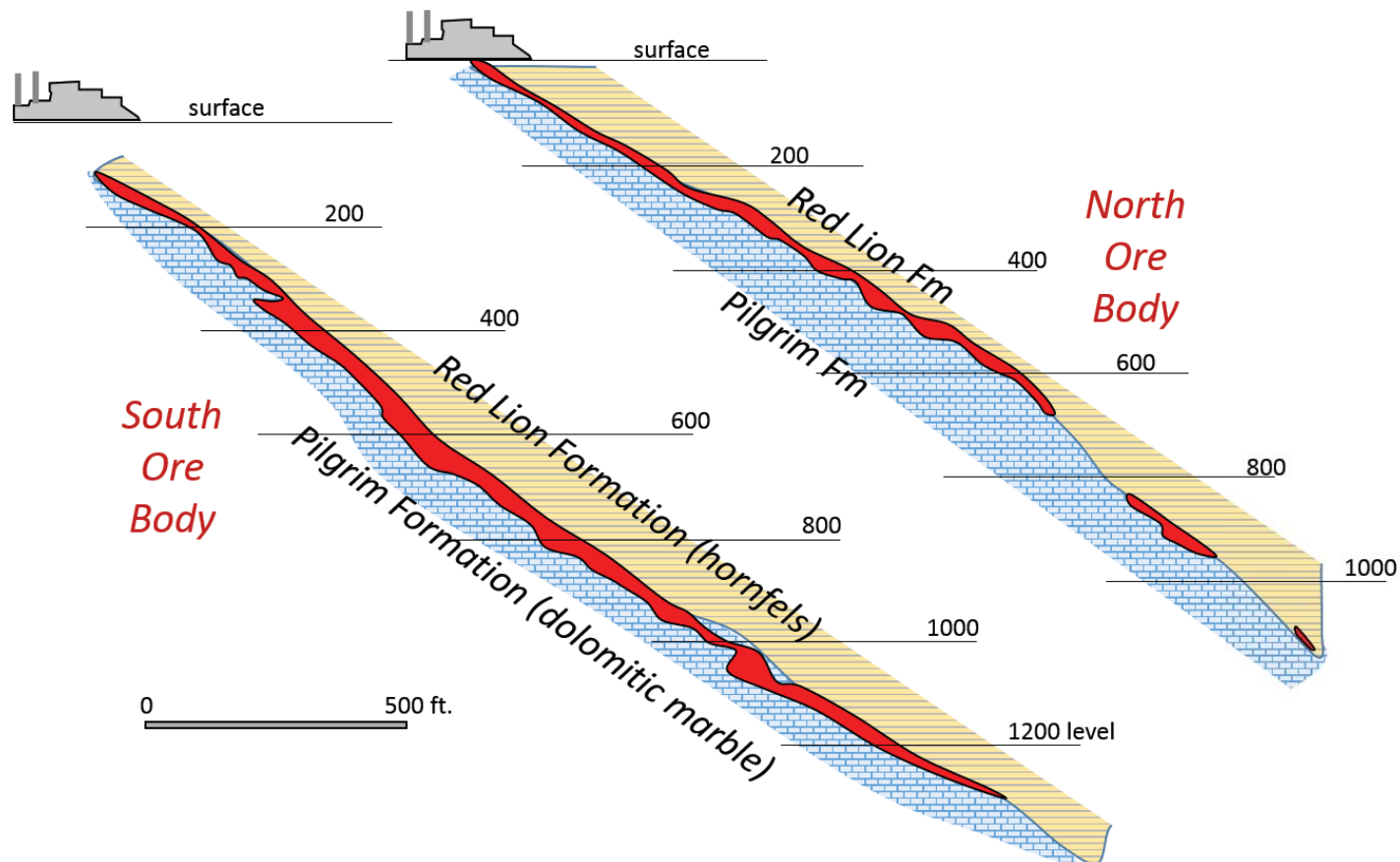


Figure 4. Schematic cross sections through the historic Elkhorn mine showing the geology of the hanging wall ore bodies (redrawn from Weed, 1901).

Laboratory Methods

Samples of ore and gangue minerals were set in 1-in-diameter epoxy mounts and polished. All samples were examined using reflected light microscopy and some were examined using scanning electron microscopy energy dispersive spectroscopy (SEM-EDS). A LEO 1430VP SEM with an EDAX Apollo 40 detector (ZAF corrected) was used at the Center for Advanced Mineral and Metallurgical Processing laboratory at Montana Tech. For fluid inclusion analysis, the polished epoxy mounts were superglued to a glass slide, sliced thin, and then repolished. Small chips with usable fluid inclusions were then analyzed using a Fluid Inc., USGS-style heating/freezing stage. Heating rates during measurement of ice-melting temperatures (T_m) and vapor bubble homogenization temperature (T_h) were roughly $2^\circ\text{C}/\text{min}$ and $10^\circ\text{C}/\text{min}$, respectively. Measurements were repeated to ensure accuracy and reproducibility.

Sulfide-mineral separates from several of the mine dump and stockpile samples were sent to the University of Nevada–Reno for S-isotope analysis. Sample preparation followed the methods of Giesemann and others (1994), and S-isotope measurements were performed using a Eurovector elemental analyzer interfaced to a Micromass IsoPrime isotope ratio mass spectrometer (IRMS). Results are given in the usual delta ($\delta^{34}\text{S}$) notation relative to Vienna Canon Diablo Troilite (VCDT) and have estimated uncertainties of $\pm 0.1\%$.

Results: Mineralogy

Hypogene minerals identified in the skarn deposits examined (Golden Dream, Helipad, Dalcoath, Klondyke; fig. 1) include pyrite, pyrrhotite, arsenopyrite, chalcopyrite, magnetite, bismuthinite, tetradymite ($\text{Bi}_2\text{Te}_2\text{S}$), cosalite ($\text{Pb}_2\text{Bi}_2\text{S}_3$), native bismuth, small amounts of galena and sphalerite, and trace gold in a gangue of diopside, andradite garnet, hedenbergite, vesuvianite, actinolite, epidote, calcite, dolomite, and minor quartz. Although the Golden Dream and Helipad skarns contain a much higher percentage of Fe-Cu-sulfides, similar ore and gangue minerals were found in all of the Au-rich skarn deposits. At Dalcoath and Klondyke, gold of high fineness ($X_{\text{Au}} > 0.85$) is closely associated with tetradymite and bismuthinite (figs. 5, 6, 7). One grain of jonassonite (AuBi_5S_4)

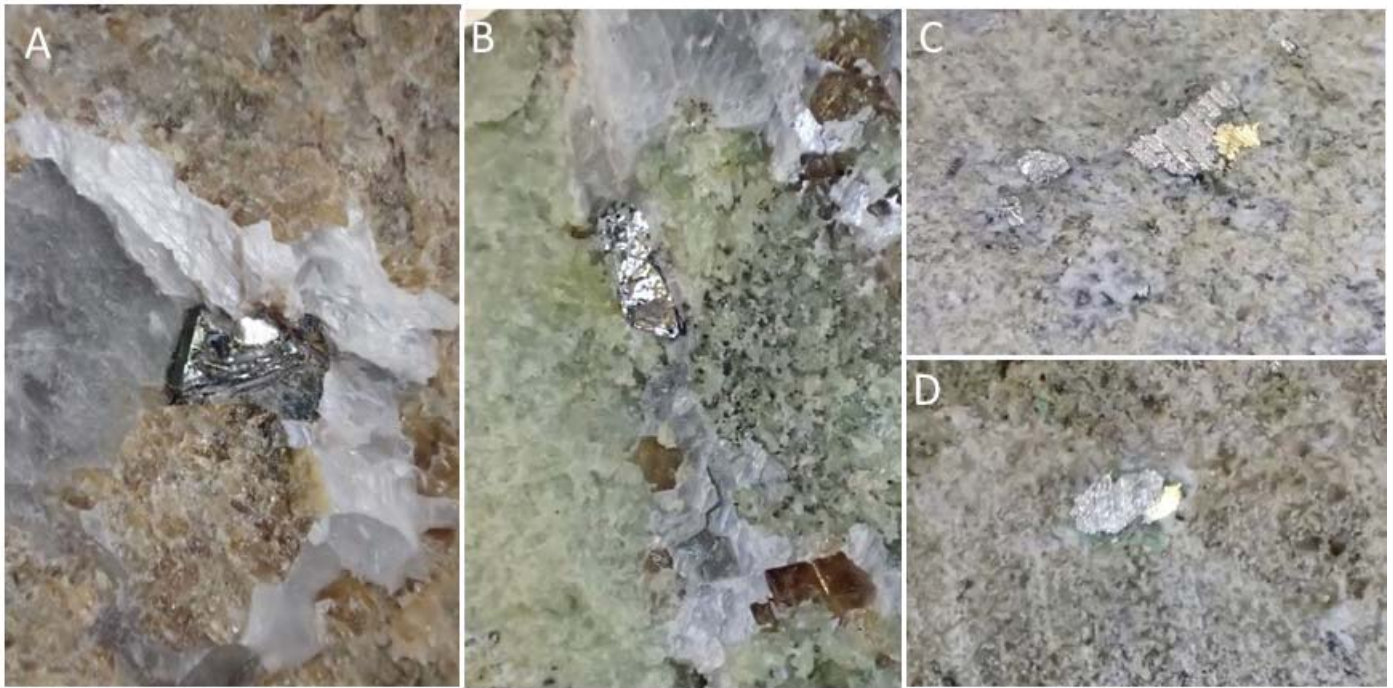


Figure 5. Photographs of samples from the Dalcoath skarn deposit; (A) tetradymite with calcite and andradite; (B) bismuthinite with calcite, andradite, and diopside; (C and D) visible gold attached to Bi-minerals (sawn but unpolished surfaces). Photos taken by Nick Allin. Width of photos is 1 cm in A and B and 0.5 cm in C and D.

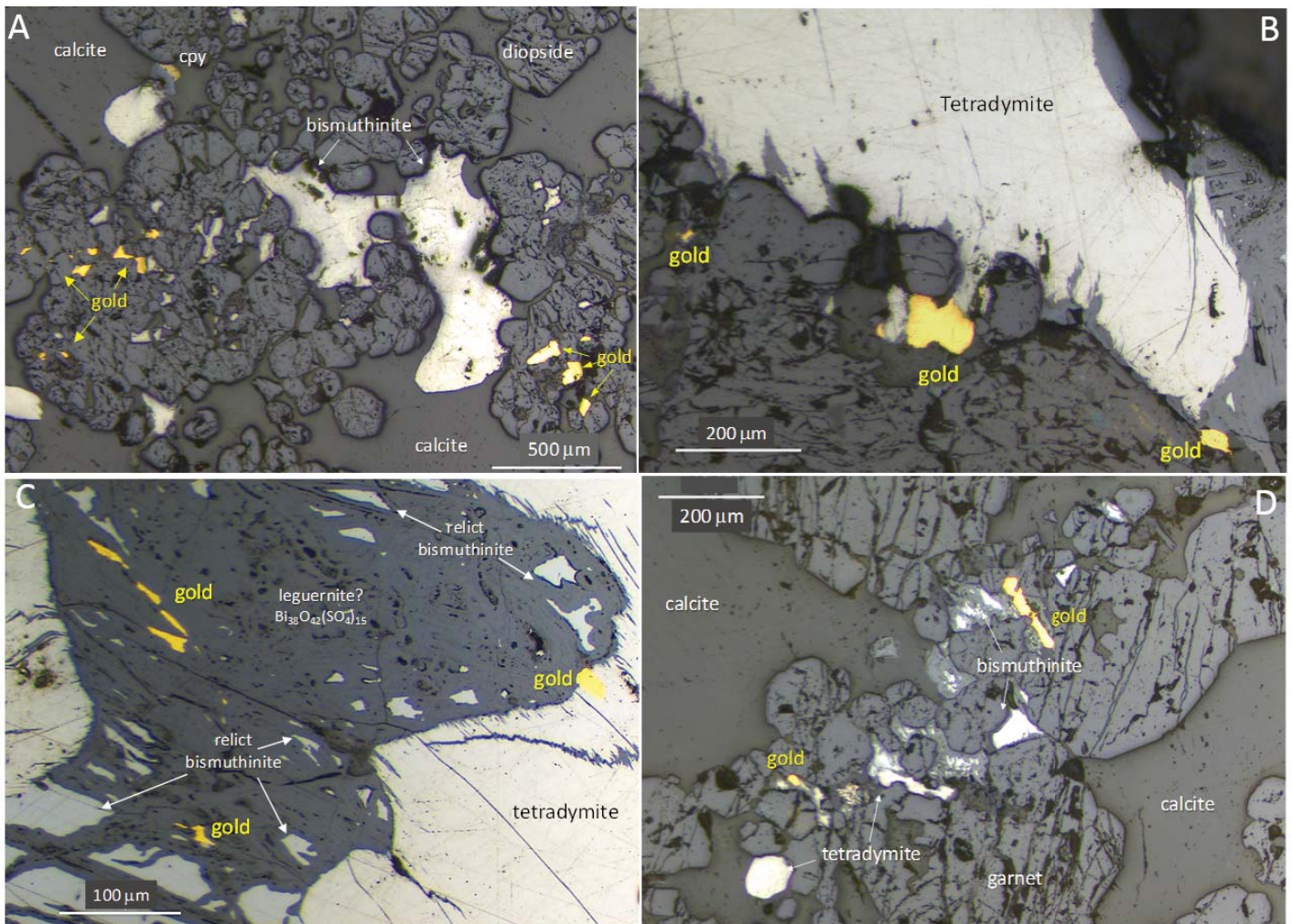


Figure 6. Reflected light photographs of Bi-minerals and gold from the Dalcoath skarn.

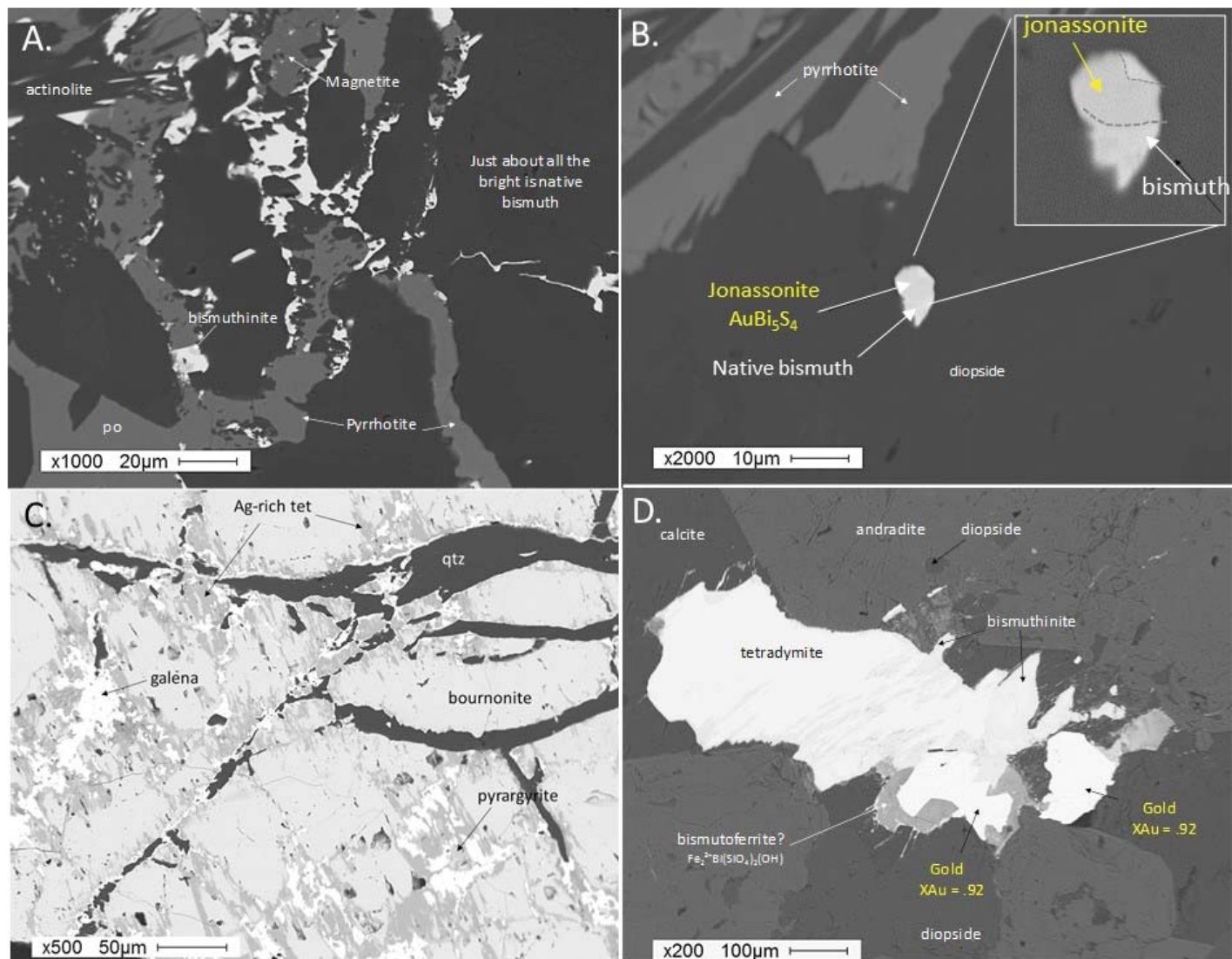


Figure 7. SEM-BSE photographs of select samples: (A) sulfide-rich skarn from the Golden Dream mine showing abundant native bismuth with pyrrhotite, magnetite, bismuthinite, and actinolite; (B) close-up of a small grain of jonassonite intergrown with native Bi, also from Golden Dream; (C) Ag-rich sample from the main Elkhorn mine shows complex intergrowths of bournonite, galena, pyrargyrite, and Ag-rich tetrahedrite; (D) Dalcoath sample with native gold associated with tetradymite and bismuthinite.

was found intergrown with native bismuth in the Golden Dream skarn (fig. 7B). Based on SEM-EDS analysis, the primary Bi-minerals are weathering to a mixture of smirnite (Bi_2TeO_5), bismutite ($\text{Bi}_2\text{O}_2\text{CO}_3$), and leguerrite ($(\text{Bi}_{38}\text{O}_{42}(\text{SO}_4)_{15})$). Violet-brown axinite (Fe-Al-boro-silicate) occurs as late veins and pods in the skarns, notably in endoskarn developed in diorite on the south side of Black Butte.

Samples from the old Elkhorn mine contained abundant, coarse-grained galena (presumably Ag-rich) ± sphalerite and pyrite, and lesser amounts of bournonite, pyrargyrite, and Ag-bearing tetrahedrite (see fig. 7C) in a gangue of calcite + quartz. Although supergene acanthite, silver, and cerargyrite (AgCl) were important silver ore minerals at the Elkhorn mine (Weed, 1901), only trace amounts of secondary acanthite (Ag_2S) and native silver were found in this study. Samples from the Elkhorn Queen mine were rich in coarse, euhedral arsenopyrite along with pyrite, galena, sphalerite, and chalcopyrite, in a gangue of quartz + fine-grained tourmaline. Molybdenite-bearing quartz veins from the Turnley Ridge intrusion contained minor amounts of chalcopyrite and pyrite.

Fluid Inclusions

Heating and freezing runs were performed on doubly polished sections of calcite from the Dalcoath Au-skarn and sphalerite and quartz from the main Elkhorn mine. The Dalcoath calcite analyzed was closely associated with Bi-minerals and gold and most of the fluid inclusions were water-rich, moderately sized bubbles that

were up to 40 μm (figs. 8A, 8B). Several inclusions displayed a double bubble at room temperature, indicating the presence of $\text{CO}_2(\text{l})$. Final homogenization temperatures ranged between 175° and 309°C, and averaged near 250°C for quartz and sphalerite from the Elkhorn mine, and near 275°C for calcite from Dalcoath (fig. 9). Salinities ranged between 6.1 and 7.7 wt% NaCl_{eq} for Elkhorn, and 4.1 to 13.1 wt% NaCl_{eq} for Dalcoath. Several fluid inclusions in a calcite chip from Dalcoath contained two transparent, cubic daughter minerals (figs. 8C, 8D). The larger daughter minerals, presumed to be halite, dissolved at temperatures of 227 to 240°C, indicating salinities of 33–34 wt% NaCl . These anomalously high saline inclusions may have formed by the boiling of a less saline fluid.

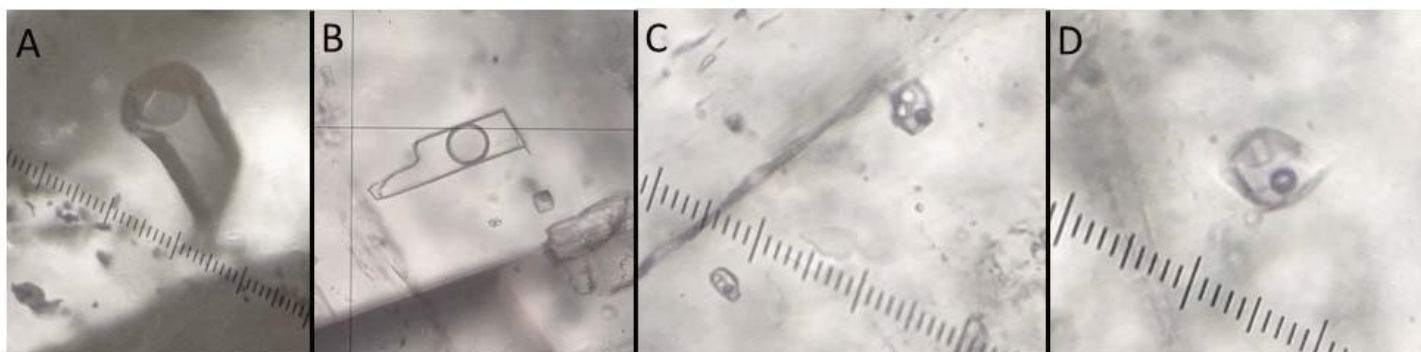


Figure 8. Photographs of fluid inclusions: (A) large, primary inclusion in sphalerite from the Elkhorn mine; (B) liquid-rich inclusion in calcite from Dalcoath; (C and D) Fluid inclusions from Dalcoath with multiple salt daughter minerals. Width of small ticks in photos is 2.5 μm .

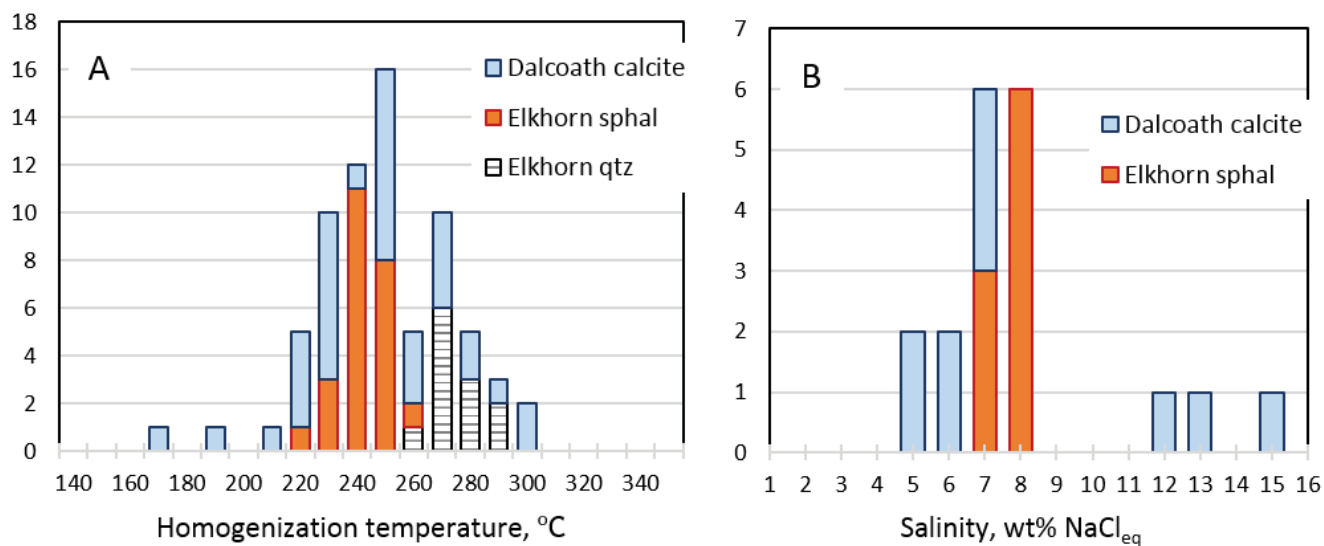


Figure 9. Histograms showing (A) homogenization temperatures, and (B) salinities of fluid inclusions.

Sulfur Isotopes

The S-isotope composition of 24 mineral separates from samples collected at different locations in the Elkhorn district are summarized in table 1. Half of the samples came from dumps at the historic Elkhorn mine. The other samples were collected at the Elkhorn Queen, Golden Dream, the Helipad areas, and from quartz–molybdenite veins that cut the Turnley Ridge porphyry. The two molybdenite samples (table 1) were distinctly lighter (-2.6, +0.1‰) compared to the other samples, which clustered between +3.8 and +7.9‰ (fig. 10).

The $\delta^{34}\text{S}$ values of coexisting sulfide mineral pairs can be used as a geothermometer, provided the two minerals formed at equilibrium. Temperatures were calculated for mineral pairs from the Elk-5b, Elk-8b, Elk-10, and Elk-8a samples obtained from the Elkhorn mine (table 2). The Δ symbols in table 2 refer to the difference in stable isotopic composition of two sulfide minerals in the same hand sample, and T is the calculated temperature based on published stable isotope fractionation factors (see footnotes to the table). Calculated temperatures ranged from 298° to 468°C. However, because each S-isotope analysis has an uncertainty of $\pm 0.1\%$, there is

Table 1. Stable isotope data for sulfide minerals from the Elkhorn district.

Sample	Location	Mineral	$\delta^{34}\text{S}$, ‰	Sample	Location	Mineral	$\delta^{34}\text{S}$, ‰
ELK-5b	Elkhorn Mine	pyrite	6.9	ELK-77	Helipad	arsenopyrite	3.9
ELK-5b	Elkhorn Mine	sphalerite	6.0	ELK-12	Elk Queen	arsenopyrite	7.1
ELK-5b	Elkhorn Mine	galena	3.8	ELK-12	Elk Queen	galena	5.6
ELK-5a	Elkhorn Mine	sphalerite	6.0	EQ-1	Elk Queen	pyrite	7.6
ELK-8b	Elkhorn Mine	pyrite	7.0	EQ-1	Elk Queen	sphalerite	7.9
ELK-8b	Elkhorn Mine	sphalerite	6.4	EQ-2	Elk Queen	pyrite	5.6
ELK-8b	Elkhorn Mine	galena	3.9	EQ-2	Elk Queen	galena	4.3
ELK-8a	Elkhorn Mine	pyrite	6.2	EQ-3	Elk Queen	pyrite	4.4
ELK-8a	Elkhorn Mine	galena	4.2	EQ-3	Elk Queen	galena	4.2
ELK-10	Elkhorn Mine	sphalerite	6.5	ELK-51	Golden Dream	pyrrhotite	5.8
ELK-10	Elkhorn Mine	galena	4.4	TR-1	Railroad cut	molybdenite	0.1
ELK-77	Helipad	pyrite	4.6	TR-2	Railroad cut	molybdenite	-2.6

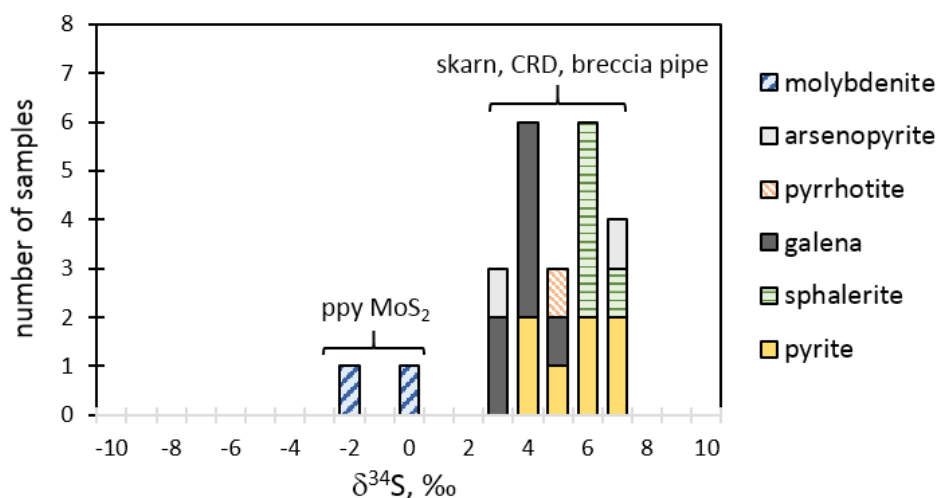


Figure 10. S-isotope compositions of sulfide minerals from all mines examined in the Elkhorn district.

considerable error in the calculated temperatures, especially for the pyrite–sphalerite pairs. It is possible that some of the outlying data, such as Elk 8a (table 1), represent two sulfides that formed out of equilibrium or at different times. A simple average of all of the temperature estimates in table 2 is 354°C, which is possibly the best estimate of the temperature of formation of sulfides at the old Elkhorn Mine.

Overall, the S-isotope data gave estimated temperatures of formation that are about 100°C higher than the fluid inclusion homogenization results (fig. 9A). This temperature difference can be used to estimate the pressure and depth of sulfide mineral formation. Based on phase diagrams presented in Roedder and Bodnar (1997), an offset of this magnitude corresponds to a pressure of trapping of approximately 1.5 kbar and a depth of formation of about 5 km for CRD mineralization at the Elkhorn mine, assuming a typical lithostatic gradient of 3.5 km/kbar. More fluid inclusion work and stable isotope geothermometry would be needed to further refine this estimate.

Table 2. Results of S-isotope geothermometry calculations.

Sample	$\Delta_{\text{pyr-sph}}$	$\Delta_{\text{pyr-gal}}$	$\Delta_{\text{sph-gal}}$	$^1T_{\text{pyr-sph}}$	$^1T_{\text{pyr-gal}}$	$^2T_{\text{sph-gal}}$
Elk-5b	0.9	3.1	2.2	304°C	322°C	336°C
Elk-8b	0.6	3.1	2.5	433°C	322°C	298°C
Elk-10			2.1			350°C
Elk-8a		2.0			468°C	

Using fractionation factors from: ¹Kajiwra and Krouse, 1971; ²Li and Liu, 2006

Discussion

One of the main objectives of this study was to see if new mineralogical, fluid inclusion, and S-isotope data could help determine whether or not the various mineral deposit types in the Elkhorn district are genetically related. For example, Steefel and Atkinson (1984) suggested that all of the mineralization in the district is zoned around the Turnley Ridge stock, with an inner porphyry Mo-Cu zone, a proximal Au-rich skarn zone, and a distal Ag-Pb-Zn CRD zone. However, the S-isotope data collected in this study show a significant difference in $\delta^{34}\text{S}$ values between the porphyry-Mo veins of the Turnley Ridge intrusion (-2.6 to +0.1) and the other deposit types in the Elkhorn district (+3.8 to +7.9‰). This raises the possibility that the skarn and CRD mineralization at Elkhorn have little to do with the Turnley Ridge porphyry, and are more closely related to emplacement of the Butte Granite or the older diorites. In fact, Everson and Read (1992), citing evidence based on drilling, concluded that gold-skarn mineralization in the district is more closely related to the diorite intrusions and the Butte Granite than to the Turnley Ridge porphyry.

Overall, the results of this study do not support the idea of McClernan (1976, 1983) that mineralization at the historic Elkhorn mine formed as an MVT deposit. Typically, MVT deposits show a wide range in $\delta^{34}\text{S}$ of sulfides (often exceeding 10‰), and contain fluid inclusions that are lower in temperature (< 200°C) and higher in salinity (10 to 30 wt% NaCl). Most MVT deposits also have a lower Ag content compared to the Elkhorn mine. The range of Ag grades and fluid inclusion homogenization temperatures displayed for Elkhorn (fig. 11) plots far from the classic MVT or “Irish-type” deposits, and closer to some well-known Ag-Pb-Zn carbonate-replacement deposits, such as Leadville (Colorado), Lavrion (Greece), and Deer Trail (Utah). If one were to replot the data for Elkhorn using the estimated temperature of formation as opposed to the fluid inclusion homogenization temperatures, the Elkhorn district would shift closer to La Providencia, a large CRD deposit in Spain.

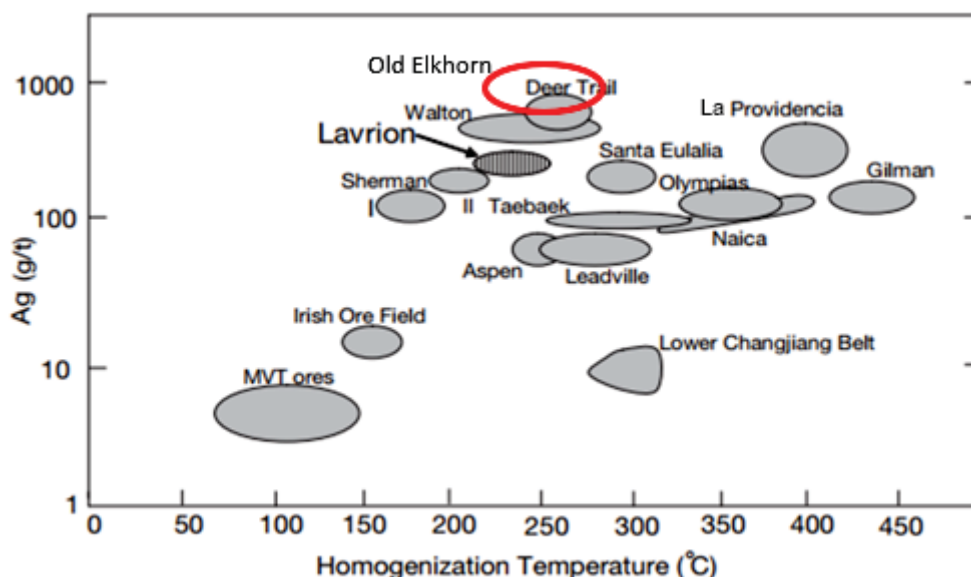
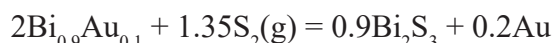


Figure 11. Plot of Ag grade vs. fluid inclusion homogenization temperatures for MVT deposits, “Irish-type” deposits, and carbonate-replacement Pb-Zn-Ag deposits worldwide, with addition of the historic Elkhorn Mine. (Adapted from Bonsall and others, 2011.)

The close association of gold with Bi-minerals (bismuthinite, tetradyomite, native Bi) in the skarn deposits examined in this study could possibly be explained by the “bismuth-scavenging” model of Tooth and others (2008). At temperatures above the melting temperature of elemental Bi (roughly 250°C), droplets of liquid bismuth could effectively scavenge gold from hydrothermal solutions by forming an Au-Bi alloy. At lower temperatures, this Au-Bi alloy could react with S_2 and/or Te_2 in retrograde fluids to form bismuthinite and tetradyomite, forcing gold into the elemental state. The reaction of interest could be written this way:



Textures shown in many of the photographs in figures 5, 6, and 7 support this type of retrograde reaction for the gold skarns of the Elkhorn district.

Acknowledgments

This study began as a semester project for a graduate class at Montana Tech. We thank Nick Allin, Francis Grondin, Garrett Hill, and Jon Szarkowski for helping with data collection. Chris Frank (Montana Tunnels) shared information and provided access to the Golden Dream property. We also thank Gary Wyss (Montana Tech, CAMP) for help with the SEM-EDS analyses, and Kaleb Scarberry and Stan Korzeb for suggestions and edits. Partial funding for this study came from the Stan and Joyce Lesar Endowment.

References

- Bonsall, T.A., Spry, P.G., Pangiotis, C.H., Stylianos, T., St. Seymour, K., and Melfosa, V., 2011, The geochemistry of carbonate-replacement Pb-Zn-Ag mineralization in the Lavrion District, Attica, Greece: Fluid inclusion, stable isotope, and rare earth element studies: *Economic Geology*, v. 106., p. 619–651.
- Everson, C.I., and Read, J.J., 1992, Gold skarn deposits of the Elkhorn district, Jefferson County, Montana: AIME-SME Annual Meeting, Preprint 92-105, 6 p.
- Giesemann, A., Jager, H.J., Norman, A.L., Krouse, H.P., and Brand, W.A., 1994, On-line sulfur-isotope determination using an elemental analyzer coupled to a mass spectrometer: *Analytical Chemistry*, v. 66, p. 2816–2819.
- Gray, D.M., 1998, Cultural resource inventory and assessment for East Butte and Dickman Mills, Elkhorn, Montana. Montana Department of Environmental Quality Mine Waste Cleanup Bureau. GCM Services, tDAR id: 325520.
- Kajiwarra, Y., and Krouse, H.R., 1971, Sulfur isotope partitioning in metallic sulfide systems: *Canadian Journal Earth Sciences*, v. 8, p. 1397–1408.
- Klepper, M.R., Weeks, R.A., and Ruppel, E.T., 1957, Geology of the southern Elkhorn Mountains, Jefferson and Broadwater Counties, Montana: U.S. Geological Survey Professional Paper 292.
- Knopf, A., 1913a, Ore deposits of the Helena mining region, Montana: U.S. Geological Survey Bulletin 527, 143 p.
- Knopf, A., 1913b, A magmatic sulphide ore body at Elkhorn, Montana: *Economic Geology*, v. 8, p. 323–336.
- Li, Y., and Liu, J., 2006, Calculation of sulfur isotope fractionation in sulfides: *Geochimica et Cosmochimica Acta*, v. 70, p. 1789–1795.
- McClerman, H.G., 1976, Recent lead and sulfur isotope data from southwestern Montana: *Economic Geology*, v. 71, p. 1599–1600.
- McClerman, H.G., 1983, Lead-zinc-silver deposits in carbonate host rocks in Montana: Mississippi Valley Type?, *in* Kisvarsanyi G., Grant, S.K., Pratt, W.P., and Koenig, J.W., eds., *International Conference on Mississippi Valley Type Lead-Zinc Deposits*, University of Missouri-Rolla, p. 516–525.
- Pardee, J.T., and Schrader, F.C., 1933, Metalliferous deposits of the greater Helena mining region, Montana: U.S. Geological Survey, Bulletin 842, 318 p.
- Reynolds, M.W., and Brandt, T.R., 2006, Preliminary geologic map of the Townsend 30' by 60' quadrangle, Montana: U.S. Geological Survey Open-File Report 2006-1138.
- Roby, R.N., Ackerman, W.C., Fulkerson, F.B., and Crowley, F.A., 1960, Mines and mineral deposits (except fuels) of Jefferson County, Montana: Montana Bureau of Mines and Geology Bulletin 16, 120 p.
- Roedder, E., and Bodnar, R.J., 1997, Fluid inclusion studies of hydrothermal ore deposits, *in* Barnes, H.L., ed., *Geochemistry of Hydrothermal Ore Deposits*, 3rd ed.: New York, John Wiley & Sons, p. 657–698.
- Senter, L.E., 1976, Geology and porphyry molybdenum mineralization of the Turnley Ridge Stock in the Elkhorn mining district, Jefferson County, Montana: Cheney, Eastern Washington University, M.S. thesis, 91 p.

- Steefel, C.I., 1982, Porphyry mineralization in the Elkhorn district, Montana: Boulder, University of Colorado, Boulder, M.S. thesis.
- Steefel, C.I., and Atkinson, W.W., 1984, Hydrothermal andalusite and corundum in the Elkhorn District, Montana: *Economic Geology*, v. 79, p. 573–579.
- Tooth, B., Brugger, J., Ciobanu, C., and Liu, W., 2008, Modeling of gold scavenging by bismuth melts coexisting with hydrothermal fluids: *Geology*, v. 36, p. 815–818.
- Tucker, C.S., 2008, The Old Elkhorn Mine: Rocks and minerals, v. 83, January/February, p. 20–33.
- Weed, W.H., 1901, Geology and ore deposits of the Elkhorn mining district, Jefferson County, Montana: U.S. Geological Survey Annual Report, v. 22, p. 399–510.
-



Old house in the Kofford Ridge 7.5' quadrangle (photo: K. Scarberry).



Oxide gossan at the Hog Heaven Mine, Kofford Ridge 7.5' quadrangle (photo: K. Scarberry).



Lithic tuff of the Hog Heaven Volcanic Field in the Kofford Ridge 7.5' quadrangle (photo: K. Scarberry).

Advances in Precious-Metal Mineral Exploration at Broadway Gold's Cu–Au Madison Project in the Silver Star Mining District, Montana

Phil Mulholland¹ and Thomas Smeenk²

¹Chief Geologist, Broadway Gold Mining Ltd., Whitehall, Montana

²Chief Executive Officer, Broadway Gold Mining Ltd., Oakville, Ontario, Canada

In fall 2017, Broadway Gold Mining Ltd. announced a late porphyry discovery at its 100%-owned Madison Copper–Gold Project, located in the Silver Star Mining District. Broadway has documented a well-mineralized, 2-mi-long trend of geological, geophysical, and geochemical anomalies at Madison. Current exploration is focused on four high-priority targets: (1) jasperoid skarn (Cu-zone); (2) epidote skarn (Au); (3) massive sulfide (Au); and (4) Cu–Au porphyry.

Many techniques were used to identify the new porphyry discovery. While most were conventional, the geological model assembled was comprehensive and tailored to pursue a porphyry deposit on an ambitious timetable. The geologic model incorporates an understanding of the porphyry–skarn model, the district and regional geology (Montana and western USA), examination of the geologic environment, soil and rock chip geochemistry, geologic mapping, geophysical surveys, and drilling. Results from all methods were integrated and used to determine the location of the porphyry system (fig. 1).

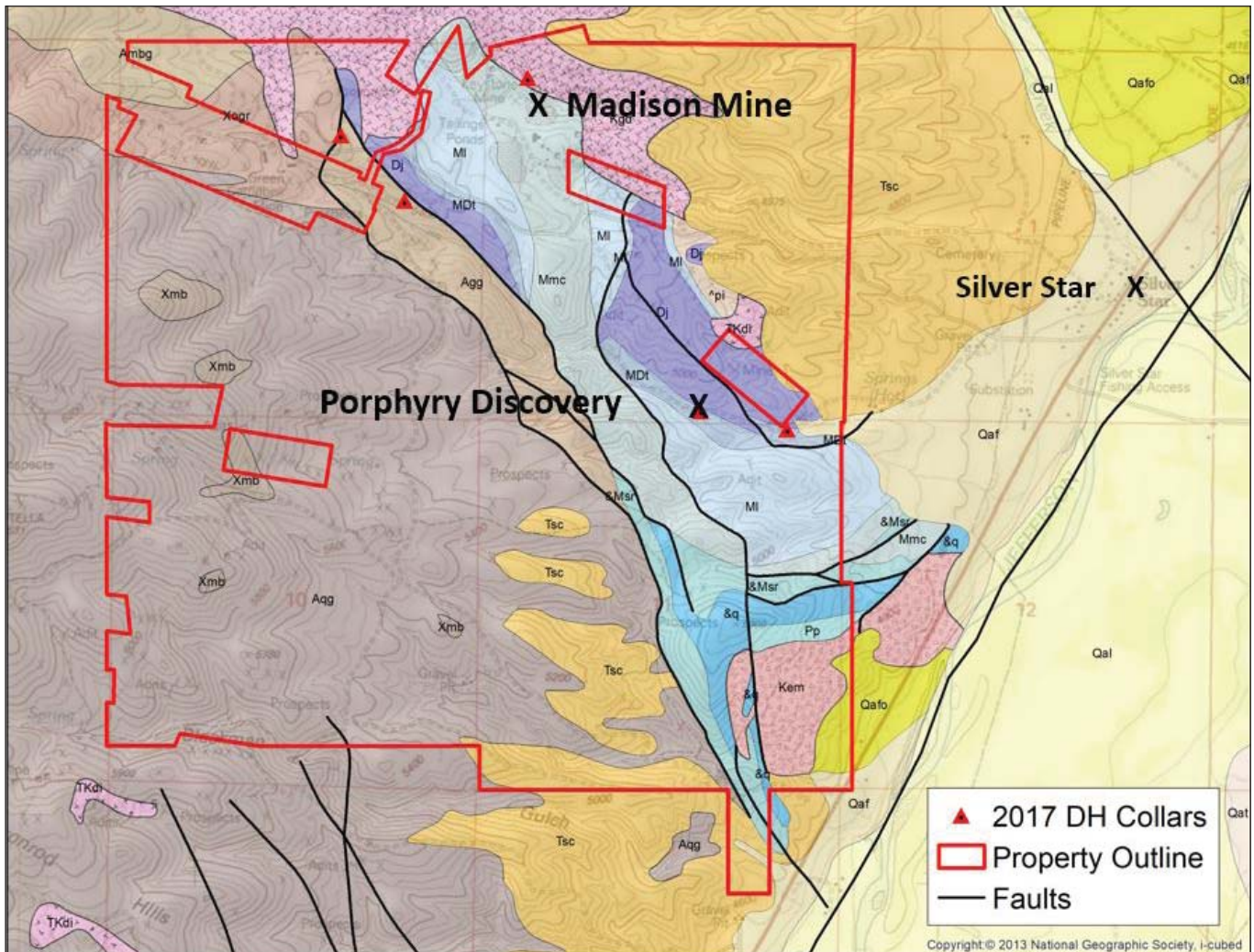


Figure 1. Geologic setting of the Madison Cu–Au project located 2 mi west of Silver Star, Montana. Xmb, Archean metamorphic rocks in brown; Cp, Cambrian Pilgrim Fm; Dj, Devonian Jefferson Fm; MDt, Devonian–Mississippian Three Forks Shale; Mm, Mississippian Madison Group; Pp, Pennsylvanian–Permian meta-sediments; Kem, Cretaceous Elkhorn Mountains Volcanics; Kgdr, Cretaceous Rader Creek Granodiorite; Qa, Quaternary Gravels; Ts, Tertiary Sediments. Modified from Foote (1987) and McDonald and others (2012).

District-scale skarns and base-metal veins, like those described at the Madison Cu–Au project (e.g., Sotendahl, 2012), are common features of large porphyry systems worldwide. Whereas our porphyry exploration program is focused on partnering with a major producer, the work completed on the skarn deposits has focused on building a resource base geared for near-term and small-scale production.

Skarns associated with porphyry deposits, and their respective ore ratios, are described by Forster and Downes (2008), which is helpful as a means to vector into a forward-thinking statement about Broadway Gold's asset. Skarn deposits are an expression of deeper porphyry deposits, and while they carry higher grade ore, they also have fewer tons with respect to lower grade porphyry systems that contain 5 to 66 times more tons of ore. Typically, the skarn portion of the system is thought of as the “tip of the iceberg.” For example, recognition of skarn alteration helped focus exploration at Cadia toward the largest porphyry system in Australia (Forster and Downes, 2008).

History of Exploration and Rationale for Current Work

Previous exploration in the Silver Star district (fig. 1) suggested the presence of a deep porphyry system as the source of skarn mineralization based on the occurrence of altered and mineralized intrusive rocks in drill core from historic drill holes. Nonetheless, the focus of historic drill programs through the 1980s was for the Au potential of the oxidized skarn mineralization, while the porphyry potential remained untested. Of 116 historic drill holes, only six reached a vertical depth in excess of 492 ft (150 m), with only one reaching a maximum depth of 814 ft (248 m).

Broadway's management team identified the Silver Star district as an exciting opportunity because the area was underexplored. Further, the company's small-miner's exclusion permit allowed bulk sampling of Madison's underground workings. Strategic considerations that elevated Madison from an exploration project to a potential mining operation included: availability of power and water, the presence of a major road (Montana Hwy 41) near its eastern boundary, and the mine's proximity to local contract mills, which would reduce capital requirements for building and permitting a milling facility to treat the ore.

An early phase of work at the Madison Mine required rehabilitating the underground workings so that the exploration team could access and systematically sample the workings. Underground rehabilitation also created a safe environment for new drilling. A multidimensional exploration program began in fall 2016 that involved: geologic mapping, rock chip and soil sampling, a ground-based magnetics survey, and an Induced Polarization/Resistivity (IP/R) survey. All efforts were focused on defining a deep Cu–Au porphyry system.

Exploration Program

Statistically significant mineralization in rock samples is defined as 1,000 ppm or greater concentration of Cu, Pb, Zn and Mn, 10 ppm or greater Ag and Mo, and 1 ppm or greater Au. Background mineralization is defined as <1,000 ppm Cu, Pb, Zn, and Mn, <10 ppm Ag and Mo, and less than 1 ppm Au.

Table 1. Background and statistically significant multiple elements in rock samples.

Elements	Background Occurrences	Statistically Significant Occurrences
Au	464	89
Ag	510	40
Cu	489	61
Mo	460	90
Mn	400	150
Pb	513	37
Zn	367	58

In 2016, 60 surface samples were collected from historic dumps on the property. Detailed rock descriptions were recorded for each sample and locations were marked by GPS. Cu values exceeded 1,000 ppm in 17 of the 60 samples, with high concentrations of 24,100; 14,800; 12,400; and 10,800 ppm (equivalent to 2.41, 1.48, 1.24, and 1.08 wt. percent, respectively). A total of 28 of the 60 samples returned Au values that exceeded 0.1 ppm with high concentrations of 16.15, 13.75, 11.1, and 9.91 ppm (equivalent to 16.15 g/t, 13.75 g/t, 11.1 g/t, and 9.91 g/t).

In 2017 and 2018, additional rock and soil samples were collected; to date, 571 rock samples and 1,457 soil samples have been examined from the Madison property. Assay results (tables 1 and 2) indicate several coincident multi-el-

ement anomalies that are consistent with porphyry-based mineralization.

Soil anomalies consist of coincident Au, Ag, Cu, Mo, Mn, Pb and Zn (table 2). Five regions on the Madison property show relatively high gold concentrations that overlap with soil anomalies (fig. 2). Four of these regions are consistently anomalous in the elements that are commonly associated with the upper levels of porphyry deposits (fig. 2, black ellipses), while the other anomalous area is probably due to historic contamination (fig. 2, yellow ellipse).

Seventeen intrusive rock samples were collected from surface exposures and drill core (holes C17-22, 23, 24, and 27) for whole-rock trace element geochemical analysis. Most of the samples plot in the Adakite-like magma field, which is distinguished from calc-alkaline arc magmas by elevated Sr/Y and lower Y content (fig. 3). Adakite-like signatures are associated with economic porphyry-style Cu-Au-Mo ore deposits

Table 2. The number of statistically significant soil samples that reported above the numerical average for the sample set, and the low to high values in the soil anomalies.

120 Samples (g per tonne)	Average	Samples	Low	High
Au	0.022	24	0.0285	0.203
Ag	0.131	29	0.131	14.65
Cu	28.8	11	45.2	87.2
Mo	0.756	15	1.1	7.92
Mn	898	29	910	6530
Pb	50	16	66	1515
Zn	124	21	124.5	779

1,457 Samples (ppm)	Average	Samples	Low	High
Au	0.041	242	0.001	3.81
Ag	0.281	243	0.006	14.65
Cu	282	266	1.64	3,700
Mo	2.31	264	0.06	143.5
Mn	571	345	68.2	13,550
Pb	47	230	1.31	>10k
Zn	152	208	15.8	12,400

Madison Project Au-in-soil Geochem Map

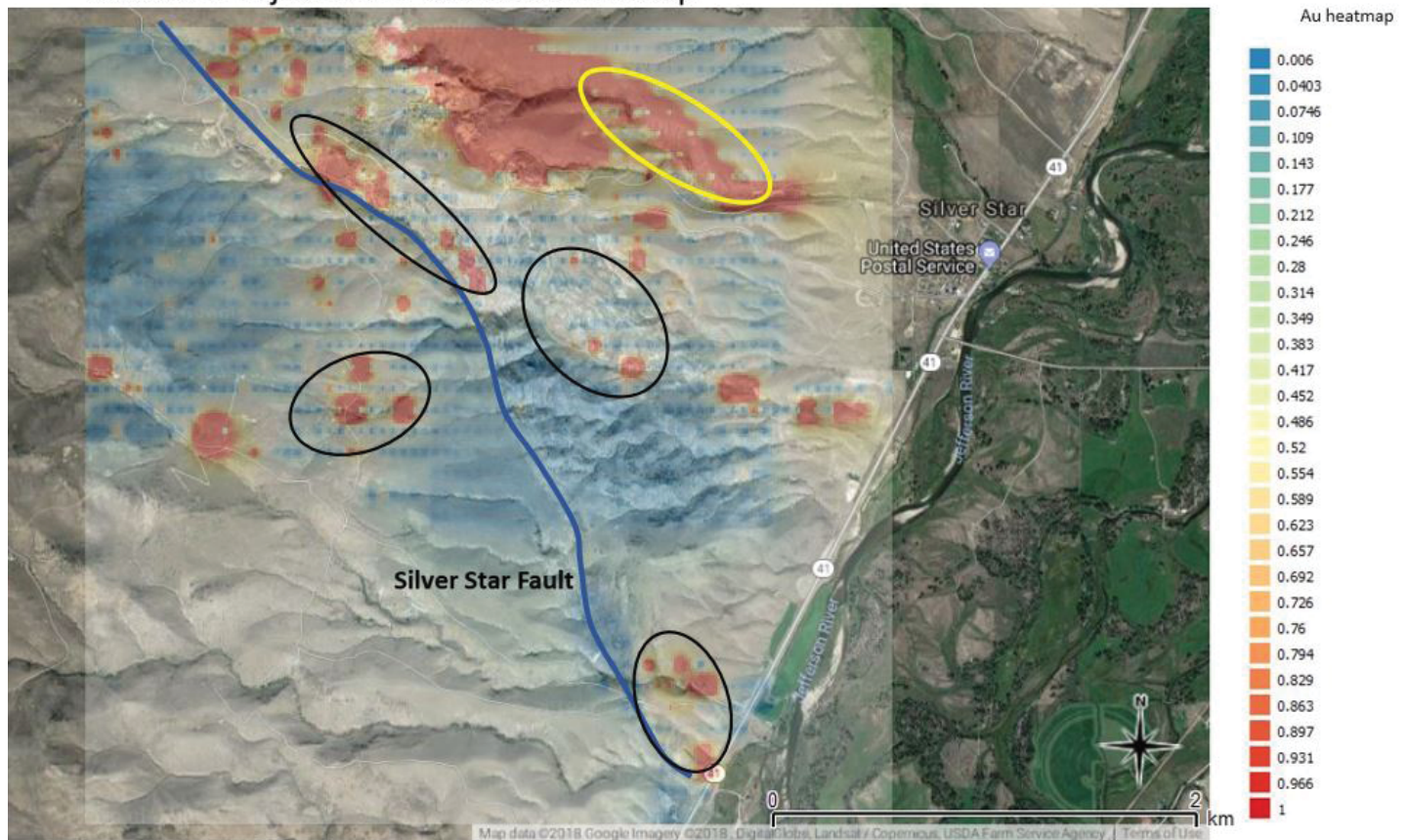
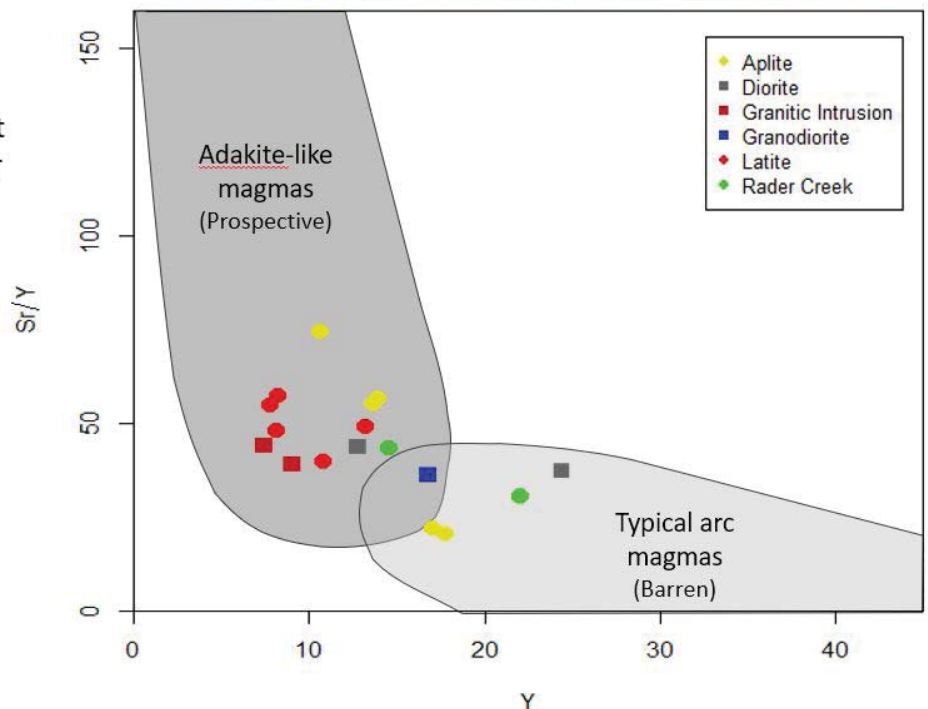


Figure 2. Heatmap illustrates the spatial occurrence of Au-in-soil (ppm) with overlapping regions of multi-element anomalies (Au, Ag, Cu, Mo, Mn, Pb, and Zn) shown as ellipses. Note that the high Au values in ppm near the top of the map are red to brown colors, whereas blue colors correspond with low Au values. The yellow ellipse probably coincides with historic mining-related contamination.



Whole Rock Geochemistry

- Magmas emplaced in the lower crust stay partially molten long enough for repeated cycles of replenishment. This allows for the accumulation of magmatic H₂O and eventually volatile saturation.
- High magmatic water content and high pressure fractionation encourages hornblende crystallization and suppresses plagioclase. This will increase the Sr/Y ratio as the magma evolves
- Low Y and high Sr/Y ratio suggests a deep hydrous source and has potential to form large deposits



19

Figure 3. Sr/Y ratios from whole-rock analysis (ALS lab Vancouver) of Cretaceous igneous rocks at the Madison Cu–Au project. Magma type fields are defined from work by Kolb and others (2013); Loucks (2014) and Rohrlach and Loucks (2005).

worldwide. A retrospective analysis of rock-chip and soil geochemistry data, collected by our field team, found similar Adakite-like Sr/Y ratios.

Geochemical modeling of all existing Sr/Y data from the property identified several patches with statistically significant Sr/Y anomalies located along a 1.5-mi section of the Silver Star Fault characterized by strong structural deformation and mineralization (fig. 4). The Sr/Y dataset includes 571 rock chip and 1,468 soil samples collected across prospective areas of the property. Laboratory duplicates, blanks, and standard samples confirm good analytical and sampling quality control by both ALS labs of Vancouver, British Columbia and the ground team.

Geophysical Program

Robert S. (“Bob”) Middleton, P. E., and his crew conducted a geophysical survey across the Madison Project during the winter months of 2017. Nine lines of deep (IP/R) data were collected over an area that hosts complex Au-Cu skarns and jasperoid vein systems. Data collected for this survey included: IP, chargeability, resistivity, and metal factor. Middleton reported that chargeability works best for identifying skarn mineralization because of its high sulfide and magnetite content. Middleton interpreted the results of his geophysical program and prepared a report, “Analysis of a Deep Induced Polarization (IP) Survey for Broadway Mining’s Madison Project” that concluded the Madison skarn system is underlain by a felsic intrusion or porphyry.

Drilling

Broadway initiated a multi-phased drilling program in January 2017. The Phase I and II drilling were designed to verify known Cu and Au mineralization that was identified during historic drill programs prior to Broadway purchasing the property. The drilling programs also tested for potential Cu and Au mineralization extensions at depth and west of the modern underground workings. An eleven-hole Phase III drilling program was proposed to evaluate the newly identified geophysical and geochemical anomalies.

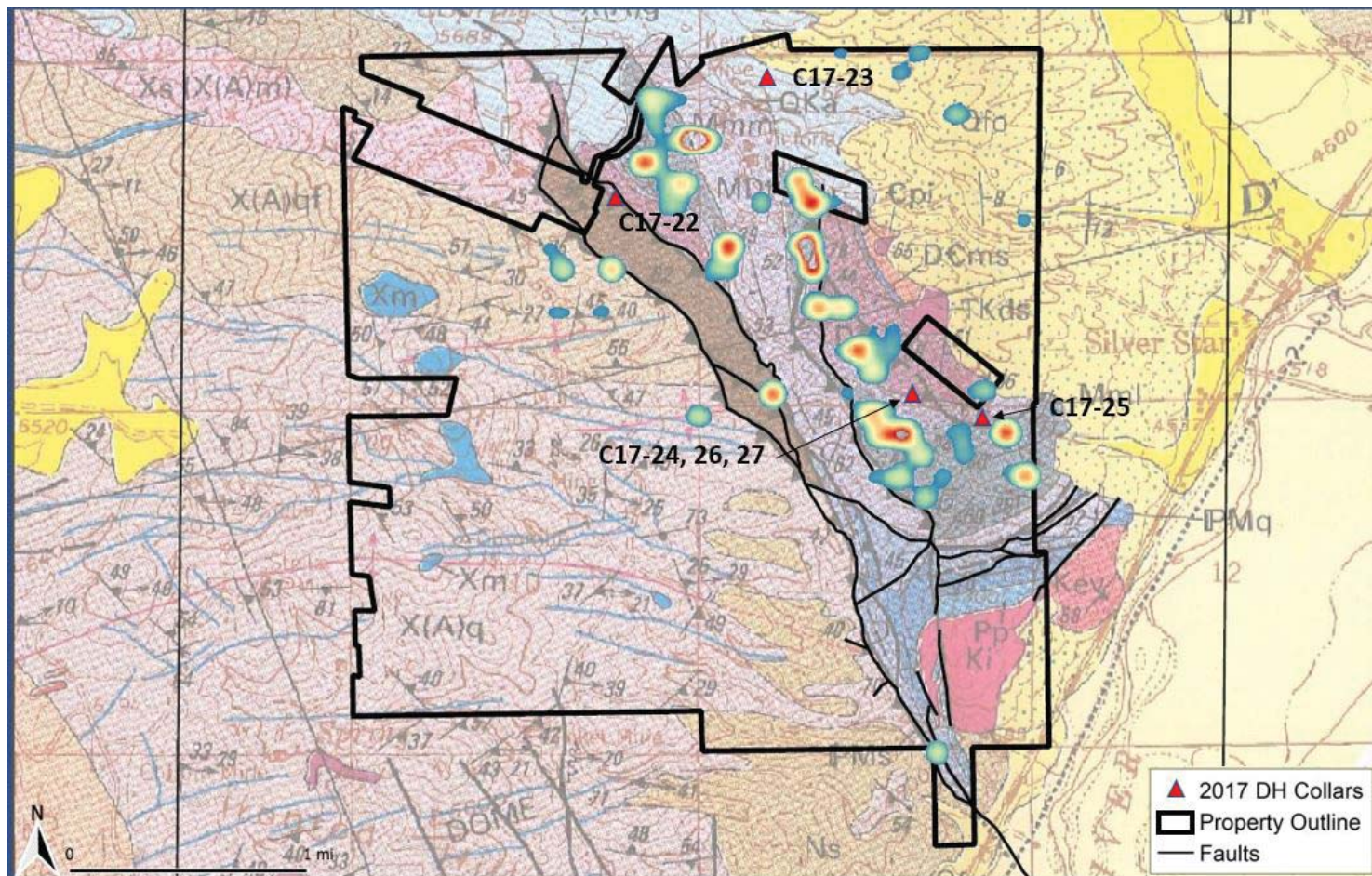


Figure 4. Map of Sr/Y ratio anomalies from soil samples and rock chips. Geology map taken from O'Neill and others (1996).

Prior to 2016, the Madison Project had 116 reverse circulation and core drill holes averaging 354 ft (108 m) per hole, for a total of 41,106 ft (12,529 m) completed by various companies since 1983. Starting in 2017, Broadway began surface drilling using AK Drilling, Inc. from Butte, Montana. There were three phases of drilling throughout the year, which totaled 26 core holes and 20,124 ft (6,134 m). Broadway also contracted Groundhog Mining out of Dillon, Montana to conduct an underground drilling program that included 7 drill holes for a total of 1,000 ft (305 m). Our drilling database now contains 150 drill holes for a total of 62,230 ft (18,968 m) of drilling at the mine site.

Phase I and Phase II of drilling intercepted favorable skarn alteration and mineralization, confirming results from past drill programs. Broadway also completed the Phase II underground core drilling program, consisting of seven drill holes, designed to test the down-dip extension of high-grade Au mineralization found in a massive sulfide skarn pod located at the lowest level of the mine (600 Level).

Phase III of surface drilling began in August 2017, and was aimed at testing several of the better coincident geophysical and geochemical targets (fig. 5) for signs of a Cu–Au porphyry system at depth.

Hole C17-24 was drilled to evaluate a chargeability anomaly identified within a highly prospective part of the property (fig. 5). It is the first hole drilled into an area of scattered historic prospect pits within a 2,300-ft-thick (700 m) section of carbonate rocks that display skarn and jasperoid alteration.

The contact between carbonate and latite porphyry was intercepted at 988 ft (301 m) depth, where it was characterized by phyllic, followed by pervasive propylitic alteration (fig. 6; table 3). A zone of phyllic alteration was encountered that measured 54 ft (16 m) and contained closely spaced quartz–pyrite veinlets and pyrite micro-veinlets. The core of the phyllic alteration zone contained numerous 2- to 3-mm quartz–pyrite veinlets and pyrite micro-veinlets that cut the latite porphyry and formed a sheeted fabric. Some of the veinlets are cross-cutting and offset other veinlets. Disseminated pyrite and pyrite blebs are rimmed by a fine-grained gray

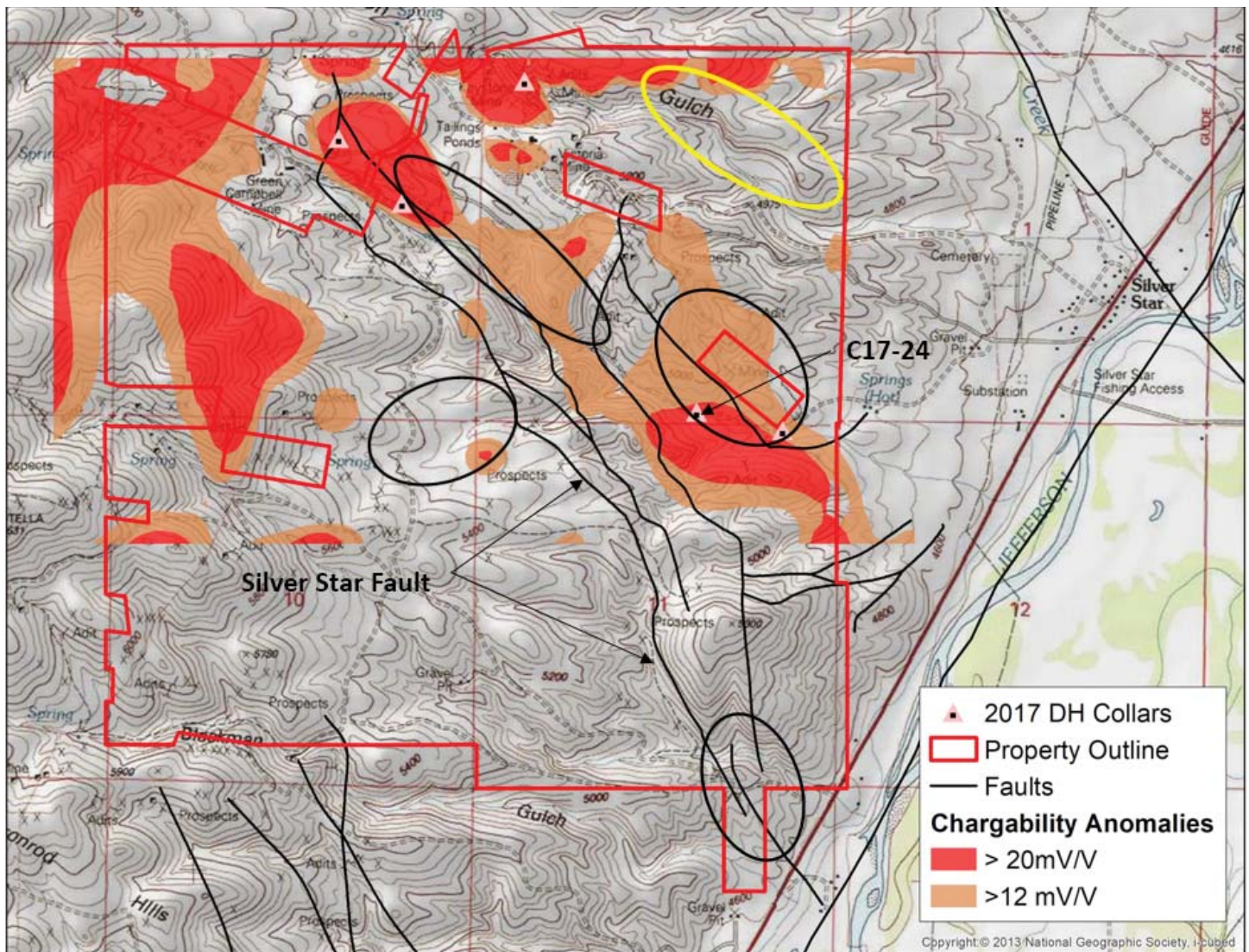


Figure 5. Map of geophysical chargeability anomalies and coincident geochemical anomalies (Au, Ag, Cu, Mo, Mn, Pb, Zn).



Figure 6. Lattite porphyry drill core that shows phyllic (A) and propylitic (B) alteration.

sulfide, that is likely either sphalerite or galena. In core characterized by phyllic alteration, narrow micro-breccia and hydrothermal streaming textures are conspicuous in places.

Current Work

Cu skarn mineralization is modeled in cross sections and 40-ft-level (12 m) plans constrained within common geologic formations. Hosted primarily by jasperoid and skarn, copper grades were determined by a weighted average of all drill samples found within the ore shell and are based on a total of 1,375 drill samples from 55 drill intersections (fig. 7). The modeling reveals three resource classifications that are reliant on key economic factors: mining costs, transportation and milling costs,

recoveries, and metal prices. These key factors will be defined by an economic assessment.

A preliminary evaluation of the skarn hosted resource is underway to develop a better understanding of the high-grade Cu–Au skarn mineralization. Cu-rich skarn–jasperoid mineralization is developed along the contact between the Late Cretaceous Radar Creek granodiorite and the Paleozoic Madison

limestone. In places, the skarn–jasperoid zones appear to be linear, or vein-like, but at other locations they blossom into zones that measure over 100 ft (30 m) wide. The main skarn–jasperoid zone strikes east–west and maintains a -33° rake towards the west. Scattered high-grade Au intercepts that occur within the Cu-rich skarn will require follow-up drilling to determine their continuity.

Table 3. Geochemical characteristics of alteration zones in drill core (see fig. 6).

Core Geochemistry in C17-27	363 to 511 m	272 to 363 m
Alteration Zones	Phyllic (fig. 6A)	Propylitic (fig. 6B)
Au (ppm)	0.019	<0.001
Ag (ppm)	1.0 (4.7 high)	<0.05
Cu (ppm)	54	46
Mn (ppm)	1,343	657
Pb (ppm)	129	20
Zn (ppm)	225	63

Madison Mine – Longsection, looking north

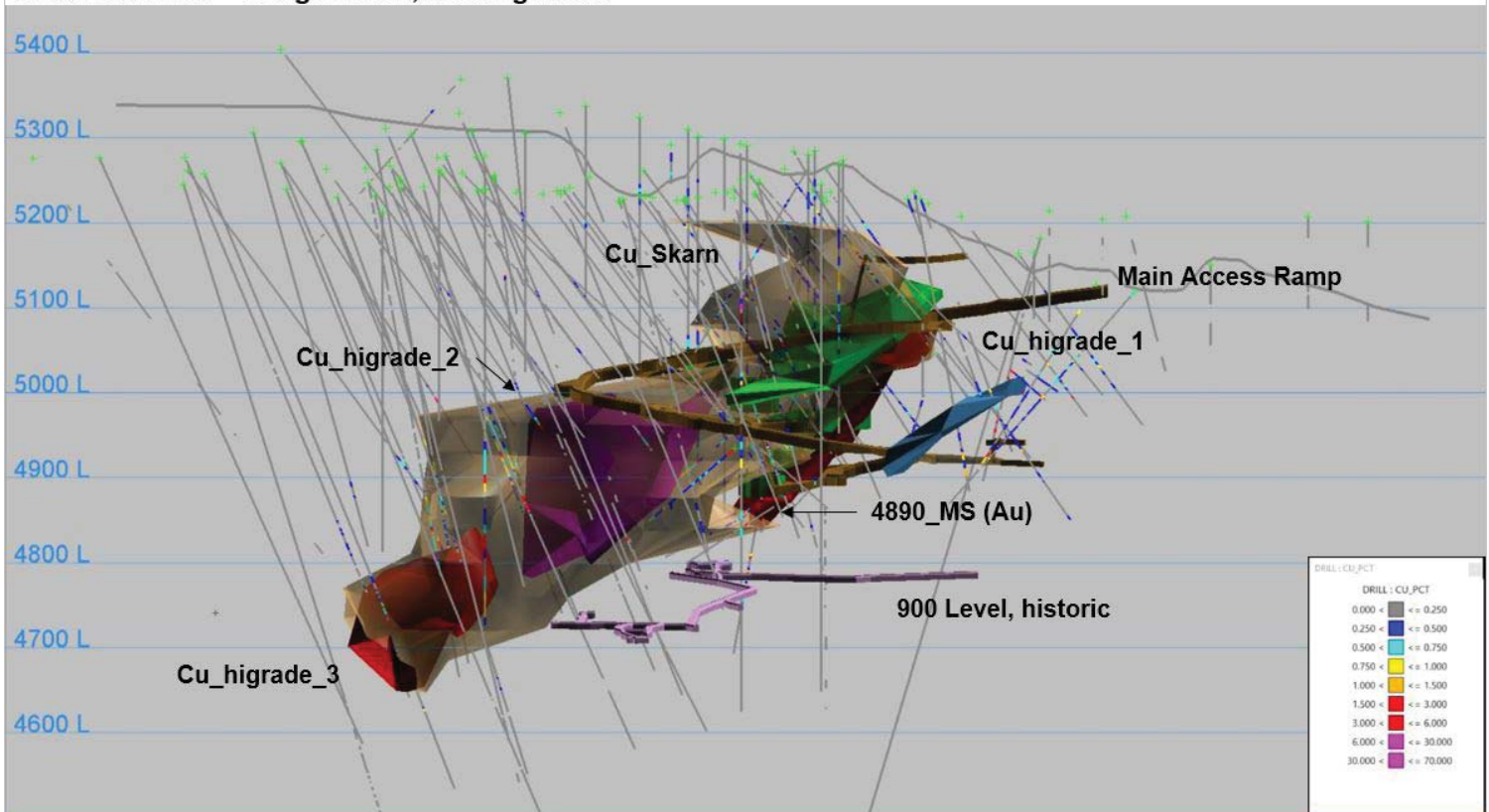


Figure 7. The Madison Mine Copper Skarn, Cu-Au Ore Shells, mine workings, and drilling.

A small high-grade massive sulfide-skarn pod (4890_MS, fig. 7) identified from 2017 underground drilling is particularly interesting. Drill intersections through the massive sulfide–skarn pod contain 0.788 oz per ton (OPT) Au that continues for over 100 ft (30 m), and 1.22 OPT Au over 36 ft (11 m), with copper grades that average around 1%. This pod is located at the bottom of the main access ramp and immediately below the deepest level of the Madison Mine. The potential to expand this sulfide–skarn pod is promising, as it rakes down to the historic 900 level of the Broadway Mine (fig. 7). Drilled to a maximum depth of 814 ft (248 m) and mined to a depth of 400 ft (122 m) over the past 150 years, the modelled Cu–Au mineral zones are open to the west, and down projection of the rake. Other Cu–skarn mineralization zones have been identified by this study, and additional drilling is required to confirm their grade, continuity, and tonnages.

References Cited

- Foote, M.W., 1987, Contact metamorphism and skarn development of the precious and base metal deposits at Silver Star, Madison County, Montana: Laramie, University of Wyoming, Ph.D. dissertation.
- Forster, D.B., and Downes, P.M., 2008, Skarns in the porphyry copper-gold environment: PACRIM Congress 2008, Researchgate.net publication 283618644.
- Kolb, M., Von Quadt, A., Peytcheva, I., Heinrich, C.A., Fowler, S.J., and Cvetkovic, V., 2013, Adakite-like and normal arc magmas: Distinct fractionation paths in the East Serbian segment of the Balkan-Carpathian Arc: *Journal of Petrology*, v. 3, p. 421–451.
- Loucks, R.R., 2014, Distinctive composition of copper-ore-forming arc magmas: *Australian Journal of Earth Sciences: An International Geoscience Journal of the Geological Society of Australia*, v. 61, no. 1, p. 5–16, doi: 10.1080/08120099.2013.865676.
- McDonald, C., Elliott, C.G., Vuke, S.M., Lonn, J.D., and Berg, R.B., 2012, Geologic map of the Butte South 30' x 60' quadrangle, southwest Montana: MBMG Open-File Report 622, 1 sheet, scale 1:100,000.
- O'Neill, J.M., Klepper, M.R., Smedes, H.W., Hanneman, D.L., Fraser, G.D., and Mehnert, H.H., 1996, Geologic map and cross-sections of of central and southern Highland Mountains, southwestern Montana: USGS Miscellaneous Investigations Series Map I-2525, 1 sheet, scale 1:50,000.
- Rohrlach, B.D., and Loucks, R.R., 2005, Multi-million-year cyclic ramp-up of volatiles in a lower-crustal magma reservoir trapped below the Tampakan copper–gold deposit by Mio–Pliocene crustal compression in the southern Philippines, *in* Porter, T.M., ed., *Super porphyry copper & gold deposits—A global perspective*: Adelaide, PCG Publishing, v. 2, p. 369–407.
- Sotendahl, J.M., 2012, Economic geology of the Madison gold Au-Cu skarn, Silver Star District, Montana: Butte, Montana Tech, M.S. thesis.
-



Rock hounding at the Cable Mine (photo: K. Scarberry).

Cathodoluminescent Quartz Textures Reveal Importance of Recrystallization in Veins Formed in the Butte Porphyry Cu-Mo Deposit

Marisa D. Acosta, Mark H. Reed, and James M. Watkins

Department of Earth Sciences, University of Oregon, Eugene, Oregon

Abstract

Cathodoluminescent (CL) variations within quartz veins can be used to understand how hydrothermal quartz veins formed in the Butte porphyry Cu-Mo deposit in Montana. CL intensity correlates positively with titanium concentration in quartz, and when combined with observations of recrystallization microstructures, reveals that the stress field within and around quartz veins is not the same as the deposit-scale stress field at the time of fracture opening. The coexistence of CL-euhedral crystals and CL-mottled crystals at the scale of a thin section presents the question of whether the mottled CL texture is primary or secondary. We compare CL patterns to the orientations of grains and find that CL-euhedral crystals share a common orientation with c-axes perpendicular to vein walls. We conclude that CL mottling arises by crystal plastic deformation of susceptible grains; i.e., those with glide planes oriented sub-parallel to the resolved shear stress. We use Ti in quartz concentrations, grain boundary configurations of recrystallized grains, and the distribution of CL-euhedral and CL-mottled crystals within the veins to construct a more detailed picture of hydrothermal quartz vein formation. The abundance of recrystallization textures in samples from a fossilized cupola emphasize the role that crystal plastic deformation plays in repeatedly isolating the cupola above a crystallizing magma body where mineralizing magmatic fluids collect before and after hydrofracturing events. That is, a quartz flow may dynamically heal brittle fractures in a cupola after it has been perforated by over-pressurized fluids.

Introduction

CL textures within quartz veins in the Butte porphyry Cu-Mo deposit in Montana are widely varied (Rusk and Reed, 2002). The phenomenon explained here is based on the observation that two seemingly antithetical textures, CL-euhedral and CL-mottled, coexist in adjacent crystals (fig. 1). To determine the origin of the mottled texture, we combined optical microscope observations, scanning electron microscope (SEM)-CL imaging, and electron probe microanalyses (EPMA), and conclude that the mottled texture is created by strain-induced recrystallization of some quartz grains, but not others, in a single specimen. By analyzing mottled crystals and a set of neighboring crystals with euhedral cores and mottled edges, we find that the average Ti concentrations in the mottled grains are slightly higher than those of the dark bands in euhe-

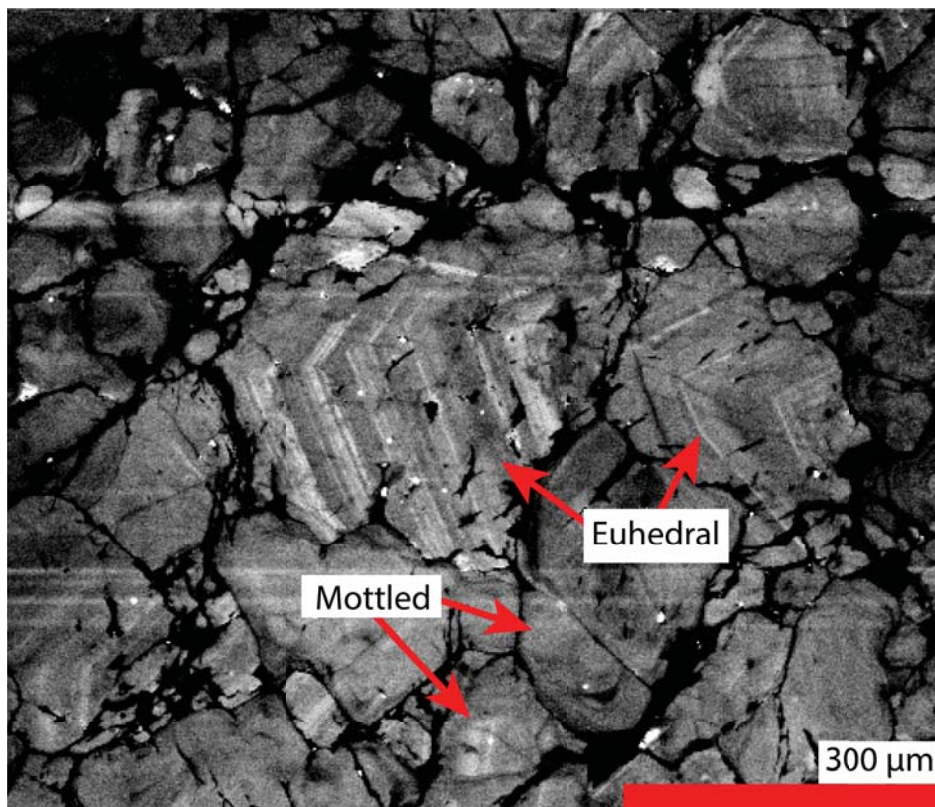


Figure 1. CL image of vein from the Butte porphyry Cu deposit (sample BMA-018-16fa_15), suggesting that both textures may be primary. Euhedral quartz crystals occur surrounded by mottled crystal in veins.

dral CL quartz; i.e., Ti concentration in mottled CL quartz is similar to that in the dark bands of nearby euhedral CL crystals and distinctly lower than Ti in the light bands. The intensity of cathodoluminescence in hydrothermal quartz is positively correlated with the amount of Ti in the quartz, which is fixed, in part, by the pressure and temperature of quartz formation/deformation (Thomas and others, 2010; Huang and Audetat, 2012; Nachlas and Hirth, 2015).

The 65 Ma Butte porphyry Cu-Mo deposit is hosted by the ~75 Ma Butte granite at the southern end of the Boulder Batholith in southwest Montana (Smedes and others, 1973). The porphyry Cu-Mo deposit contains chalcopyrite and molybdenite in narrow (1–20 mm) quartz-dominated veins surrounding a set of porphyritic dikes. These early veins, known as Pre-Main Stage veins, are commonly bordered by potassic alteration, containing biotite, plagioclase, K-feldspar, quartz, and sericite (Brimhall, 1977). A subset of Pre-Main stage veins, quartz–molybdenite veins that grade at depth into barren quartz veins, lack alteration envelopes. The close of the Pre-Main Stage mineralization is marked by lower temperature pyrite mineralization accompanied by intense gray sericitic alteration containing quartz, sericite, and pyrite (Reed and others, 2013). In the current study, we focus on a quartz–molybdenite vein taken from a paleodepth of ~7 km. Quartz–molybdenite veins form as a result of hydrofracturing, then fluid expulsion through an adiabatic pressure decrease. The veins lack alteration envelopes owing to their rapid opening and filling, which did not allow time for wall–rock reaction (Rusk and others, 2008a).

Mottled CL textures are common (e.g., Holness and Watt, 2001; Seyedolali and others, 1997; Tovey and Krinsley, 1980). In metamorphic rocks, mottled CL has been interpreted as resulting from annealing of original CL textures (e.g., Spear and Wark, 2009). However, in many Butte porphyry Cu-Mo deposit veins, grains with mottled CL textures are contiguous with euhedral CL grains, an observation that, to our knowledge, has not been documented at other localities.

Results

Locating crystals that are CL-mottled and CL-euhedral on the SEM and then locating those same crystals on an optical microscope enabled us to deduce that the CL-mottled crystals have recrystallized, as indicated by grain boundary geometries and patchy undulose extinction. On the scale of a thin section we find textural evidence for each of three quartz recrystallization processes, from low temperature to high: bulging recrystallization, subgrain rotation, and grain boundary migration. The latter two are the most common in Pre-Main Stage quartz. A key observation is that all CL-euhedral crystals are oriented with c-axes sub-parallel to one another and roughly perpendicular to the vein wall. Many of the CL-euhedral crystals have mottled edges and all are surrounded by separate grains of CL-mottled texture. There can be seen an apparently progressive “blurring” of euhedral textures to mottled (fig. 2). Furthermore, recrystallized grains are found in the centers of vein samples and CL-euhedral crystals occur near the edges of veins. Veins from deep drill holes are completely recrystallized.

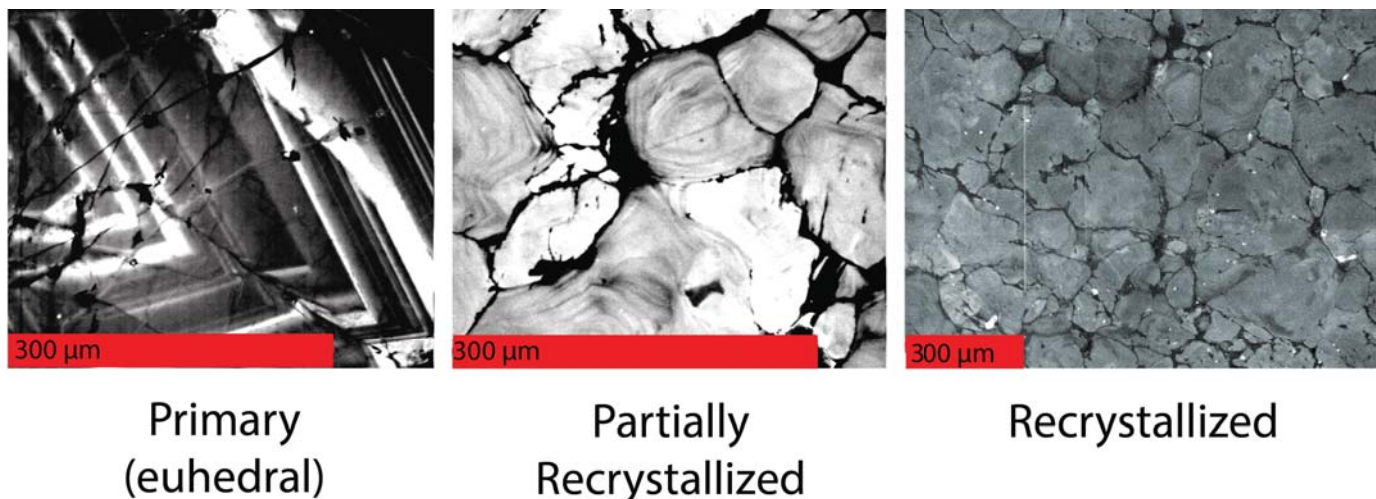


Figure 2. Within one vein there is a progression from primary euhedral-CL textures to an intermediate CL texture characterized by subgrain rotation recrystallization grain boundaries, to mottled CL with grain boundary migration recrystallization textures.

EPMA of CL-bright–dark oscillations in single CL-euhedral crystals yield average Ti concentrations of 100 ppm in the bright zones and 30 ppm in the dark zones. In a single crystal, Ti in the bright domains ranges from 332 to 16 ppm (fig. 3). Mottled edges of the same crystals yield an average of 30 ppm.

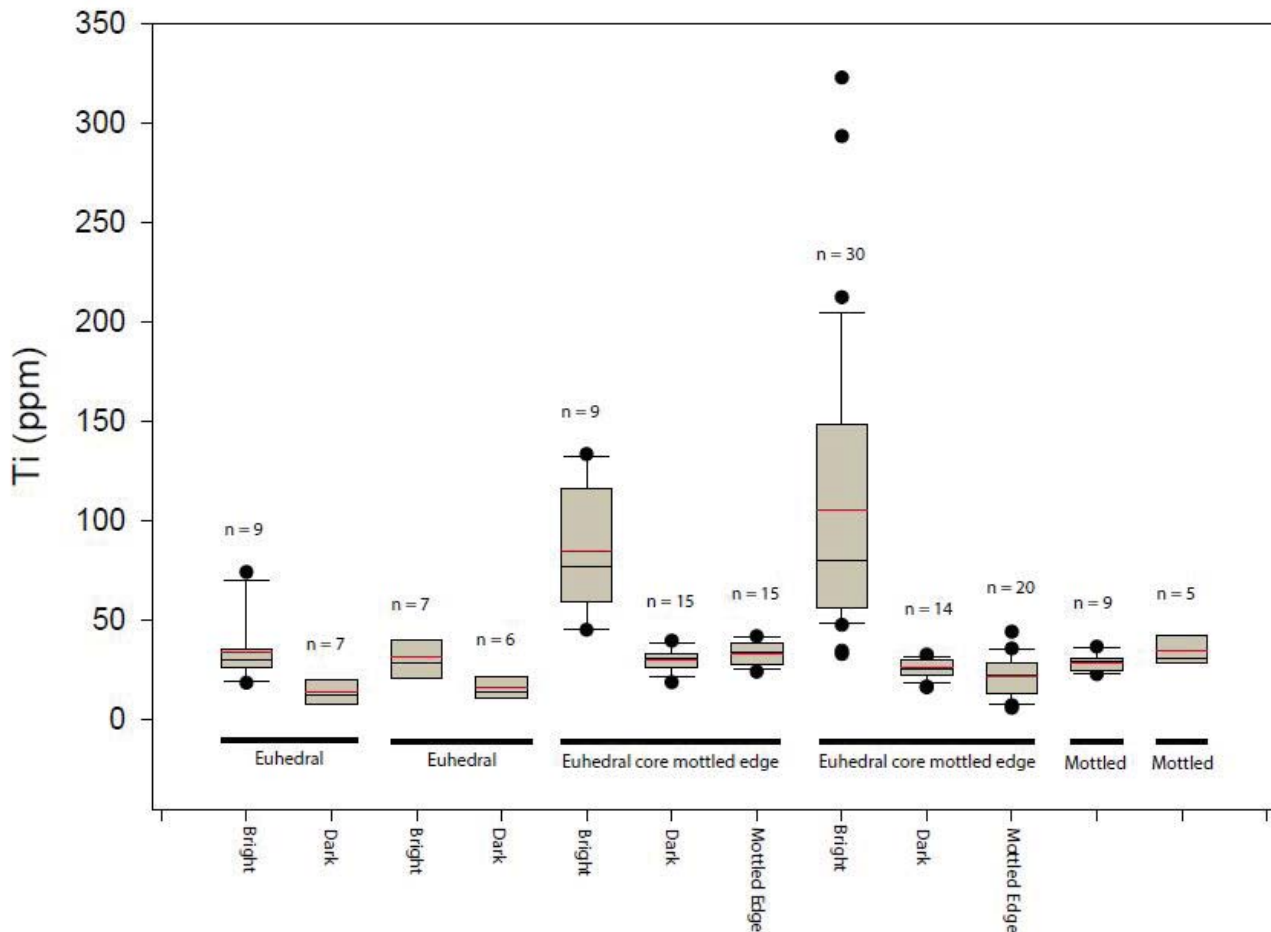


Figure 3. Box-and-whisker plot of the microprobe analyses on Butte quartz. Ti concentrations in the bright domains of various CL-euhedral crystals are highly variable (median shown as black line, average indicated in red), whilst the Ti concentrations in the dark domains of the same CL-euhedral grains are much more tightly clustered and similar from grain to grain. Crystals with euhedral cores and mottled edges show the mottled edge having approximately the same Ti values as the dark domains, a relationship reflected in the Ti concentrations of mottled crystal.

Interpretations

Where both recrystallized and un-recrystallized crystals occur in a single vein, the CL-euhedral crystals are along the edge of vein fracture surfaces and the CL-mottled crystals are in the center of the vein (fig. 4). The CL-euhedral remnants of what was once comb quartz, a term that refers to the comb-like appearance of vein quartz crystals all oriented sub-parallel to one another and growing into the center of a vein, with c-axes perpendicular to the vein wall, indicate that the resolved shear-stress on crystal glide planes was less than the critical resolved shear-stress necessary to activate movement along those planes. However, randomly oriented crystals in the centers of veins would have been susceptible to the small amounts of stress needed to activate wet quartz crystal plastic deformation.

In an isotropic stress field (e.g., lithostatic pressure), recrystallization is static. Static recrystallization, also called thermal annealing, results in uniform grain size distribution with straight, polygonized grain boundaries (granoblastic texture) and dominates when recrystallization continues after deformation. There are isolated pockets of granoblastic quartz textures in the Pre-Main Stage veins from Butte; however, they are less common than grain boundary outlines indicative of dynamic recrystallization. Dynamic recrystallization, in which deformation and recrystallization occur simultaneously, occurs in a deviatoric stress field, and is characterized by irregular grain boundaries.

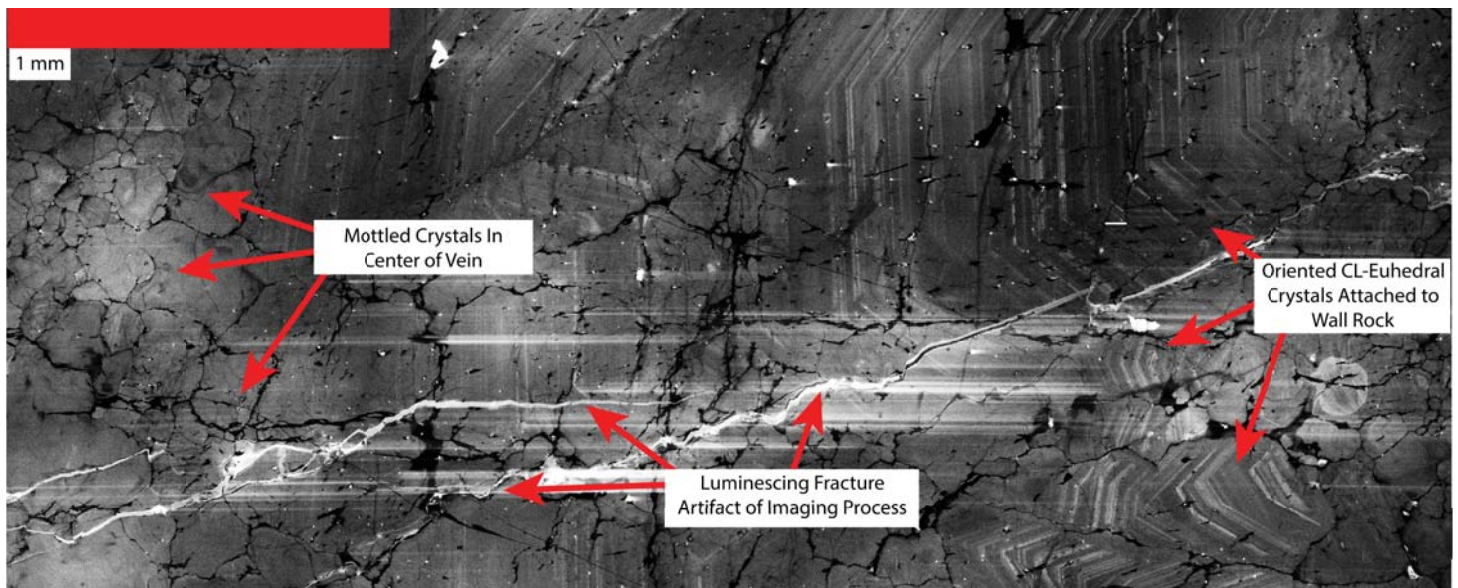


Figure 4. SEM-CL montage of sample BMA-09-16fa_15 showing the transition from oriented CL-euhedral grains sub-parallel to one another and recrystallized, CL-mottled grains in the center of the vein.

The observation that CL-euhedral grains share a common orientation suggests that the primary compressive stress (σ_1) was oriented sub-parallel to the c-axes of the crystals nucleated on the wall-rock and growing into the center of the vein. All other grains with different orientation were subject to dynamic recrystallization, resulting in CL-mottled texture.

The absence of CL-euhedral textures in very deep samples (>1.8 km down from the modern surface and at an approximate paleodepth of 7 km) coincides with the ubiquity of mottled CL and recrystallization textures. This is consistent with the idea that quartz creep is a fundamental control on the recurrent nature of fluid expulsion from a cupola (Fournier, 1999). It is the mechanism for the recurrent sequestration of magmatic fluids above a magma chamber between hydrofracturing events. The scarcity of oriented euhedral crystals in the deepest parts of the deposit is likely due to repeated brecciation and annealing.

Ti concentrations in the CL-dark bands and the neighboring mottled crystals range from 40 ppm to 16 ppm, and yield temperature estimates using the TitaniQ geothermobarometer (Huang and Audétat, 2012) between 619°C and 538°C, assuming lithostatic pressure of 1.8 kbar. At a hydrostatic pressure of 0.69 kbar, the temperature range becomes 538°C to 487°C. The bright bands yield erroneously high temperature estimates of 876°C and 802°C for 320 ppm Ti at lithostatic and hydrostatic pressure, respectively. The CL-dark and mottled temperature ranges likely represent near-equilibrium conditions, as they are similar to values obtained from fluid inclusion measurements by Rusk and others (2008b) on barren quartz/quartz-molybdenite veins from moderate depth, which indicate a formation temperature of 500°C at a hydrostatic pressure of 0.8 kbar. Thus, growth of comb quartz nucleated on the wall rock must have occurred at a temperature and pressure that were similar to the temperature and pressure of recrystallization of the quartz in the center of veins.

Conclusion

Quartz veins formed at moderate depth and in deep parts of the Butte system exhibit recrystallization textures seen on both the optical and scanning electron microscopes. These textures formed at or near the temperature of vein formation. At moderate depth, recrystallization in a given vein was inhibited in grains nucleating along the fracture surface and occurred preferentially in crystals randomly oriented in the center of veins. At greater depth, this relationship has been overprinted by strain caused by repeated fluid expulsion and thermal annealing.

References

- Brimhall, G.H., 1977, Early fracture-controlled disseminated mineralization at Butte, Montana: *Economic Geology*, v. 72, no. 1, p. 37–59.
- Fournier, R.O., 1999, Hydrothermal processes related to movement of fluid from plastic into brittle rock in the magmatic-epithermal environment: *Economic Geology*, v. 94, no. 8, p. 1193–1211.
- Holness, M.B., and Watt, G.R., 2001, Quartz recrystallization and fluid flow during contact metamorphism: A cathodoluminescence study: *Geofluids*, v. 1, no. 3, p. 215–228.
- Huang, R., and Audétat, A., 2012, The titanium-in-quartz (TitaniQ) thermobarometer: A critical examination and re-calibration: *Geochimica et Cosmochimica Acta*, v. 84, p. 75–89.
- Nachlas, W.O., and Hirth, G., 2015, Experimental constraints on the role of dynamic recrystallization on resetting the Ti-in-quartz thermobarometer: *Journal of Geophysical Research: Solid Earth*, v. 120, no. 12, p. 8120–8137.
- Reed, M., Rusk, B., and Palandri, J., 2013, The Butte magmatic-hydrothermal system: One fluid yields all alteration and veins: *Economic Geology*, v. 108, no. 6, p. 1379–1396.
- Rusk, B.G., Lowers, H.A., and Reed, M.H., 2008a, Trace elements in hydrothermal quartz: Relationships to cathodoluminescent textures and insights into vein formation: *Geology*, v. 36, no. 7, p. 547–550.
- Rusk, B.G., Reed, M.H., and Dilles, J.H., 2008b, Fluid inclusion evidence for magmatic-hydrothermal fluid evolution in the porphyry Cu-Mo deposit at Butte, Montana: *Economic Geology*, v. 103, no. 2, p. 307–334.
- Rusk, B., and Reed, M., 2002, Scanning electron microscope–cathodoluminescence analysis of quartz reveals complex growth histories in veins from the Butte porphyry copper deposit, Montana: *Geology*, v. 30, no. 8, p. 727–730.
- Seyedolali, A., Krinsley, D.H., Boggs Jr., S., O’Hara, P.F., Dypvik, H., and Goles, G.G., 1997, Provenance interpretation of quartz by scanning electron microscope–cathodoluminescence fabric analysis: *Geology*, v. 25, no. 9, p. 787–790.
- Smedes, H.W., Klepper, M.R., and Tilling, R.I., 1973, The Boulder Batholith, Montana (a summary), *in* Miller, R.N., *Guidebook for the Butte Field Meeting of Society of Economic Geologists*, Butte, Montana: Littleton, Colo., Society of Economic Geologists, p. E1–E18.
- Spear, F.S., and Wark, D.A., 2009, Cathodoluminescence imaging and titanium thermometry in metamorphic quartz: *Journal of Metamorphic Geology*, v. 27, no. 3, p. 187–205.
- Thomas, J.B., Watson, E.B., Spear, F.S., Shemella, P.T., Nayak, S.K., and Lanzirrotti, A., 2010, TitaniQ under pressure: The effect of pressure and temperature on the solubility of Ti in quartz: *Contributions to Mineralogy and Petrology*, v. 160, no. 5, p. 743–759.
- Tovey, N.K., and Krinsley, D.H., 1980, A cathodoluminescent study of quartz sand grains: *Journal of Microscopy*, v. 120, no. 3, p. 279–289.



I. Kallio (left) and E. Coppage (right) discuss ore deposits with Stan and Joyce Korzeb (center) during the Map Chat at the Butte Brewing Company (photo: A. Roth).



Mesozoic sediments and bentonite beds at Egg Mountain, northwestern Montana (photo: K. Scarberry).

An Overview of the Pogo Gold Mine (AK)

Ethan L. Coppage

M.S. Student, Geological Engineering
Montana Tech, Butte, Montana

Introduction

The Pogo gold mine is located within the Goodpaster Mining District of the Titina Gold Province in east central Alaska. Vein systems at Pogo formed in an extensional environment after the termination of Mesozoic metamorphic-related compressional deformation, and are temporally separated from these events by a set of post-metamorphic granitic intrusions. Host rocks consist of late Proterozoic to mid-Paleozoic high-grade gneisses of the Lake George subterrane within the Yukon–Tanana terrane (fig. 1). The granite intrusions are Cretaceous (107–94 Ma) I-type granitic bodies (Smith and others, 1999) and are a potential source of gold-bearing fluids.

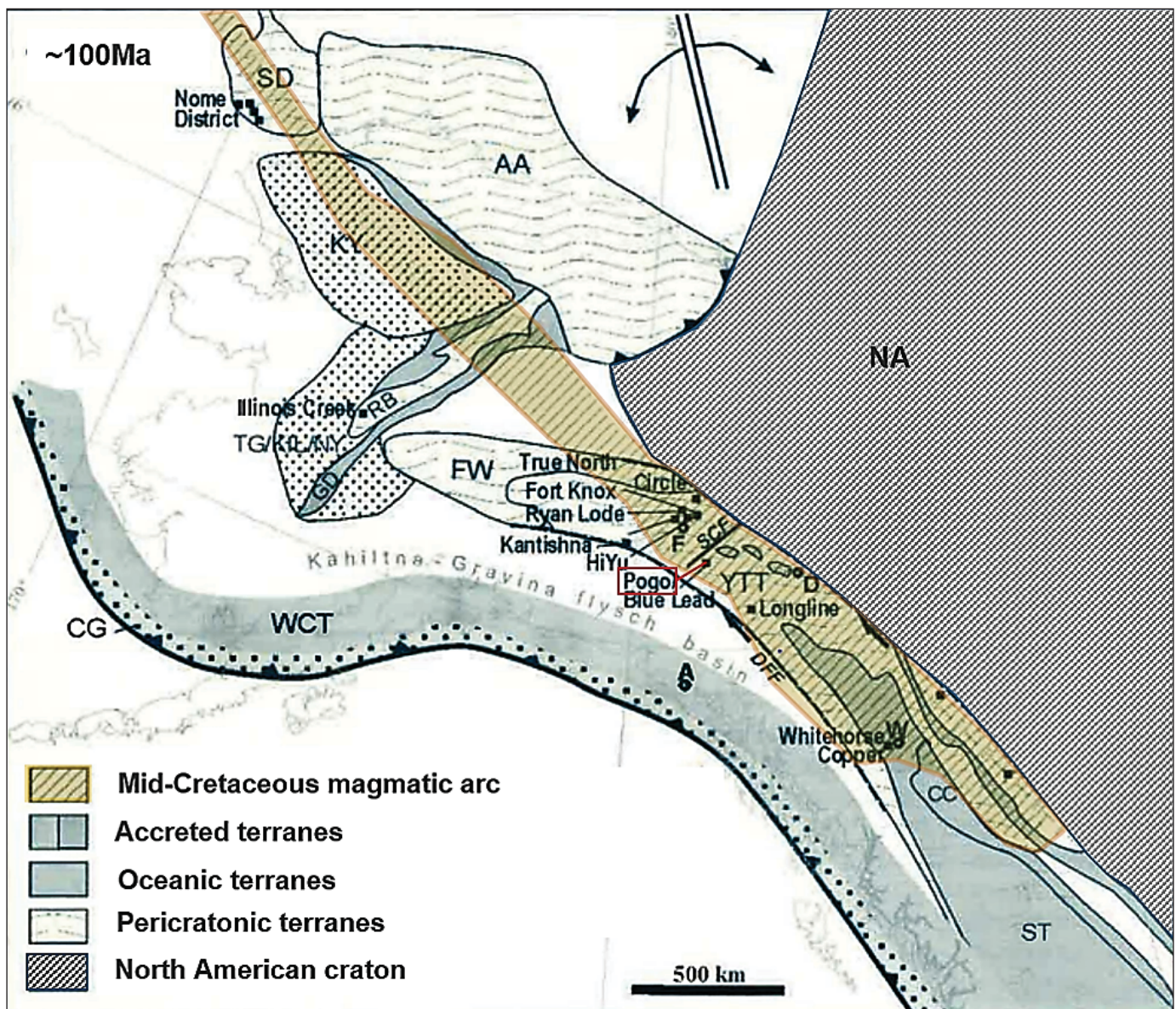


Figure 1. Distribution of mid-Cretaceous gold deposits within the eastern half of the Tintina Gold Province at ~105–90 Ma. Base-map reconstruction after Plafker and Berg (1994). Some of the terrane boundaries have been removed. Terranes: NA, North America craton; AA, Arctic Alaska; YTT, Yukon–Tanana; ST, Stikine; CC, Cache Creek; WCT, Wrangellia; RB, Ruby; CG, Chugach; FW, Farewell; SD, Seward; TG-KIL-NY, Togiak–Kilibuck–Nyack; GD, Goodnews; KY, Koyukuk. Faults: DFF, Denali–Farewell; TKF, Tintina–Kaltag; SCF, Shaw Creek. Towns: F, Fairbanks; A, Anchorage; D, Dawson; M, Mayo; W, Whitehorse. Modified from Goldfarb and others (1998).

Debating the Origin of the Deposit

The classification and origin of the Pogo gold deposit is contentious (i.e., Smith and others, 1999; Rhys and others, 2003; Goldfarb and others, 2005). The deposit exhibits characteristics of both mesothermal lode-gold deposits and of plutonic gold deposits related to reduced granitic I-type, mainly ilmenite-series, calc-alkaline, felsic to intermediate intrusions. The mineralization at Pogo is still disputed but has more recently been considered to be a mesothermal orogenic deposit that is proximal to, or hosted by, coeval intrusive rocks (Groves and others, 2003; Goldfarb and others, 2004).

Unlike typical mesothermal shear vein hosted gold systems, Pogo is temporally and tectonically separated from metamorphic deformation events (Groves and others, 2003). Additionally, Pogo shares many comparable kinematic and geometric attributes with other Cretaceous plutonic gold deposits in the region (Rhys and others, 2003). This interpretation of the deposit suggests formation occurring during a regional Mesozoic (Cretaceous) extensional event that allowed for a multi-stage exploitation of extensional fault planes by hydrothermal fluid from a cooling magmatic source at depth.

Geologic Setting

The country rock at Pogo includes biotite-quartz-feldspar orthogneiss and paragneiss of the Lake George subterrane within the Yukon–Tanana terrane (fig. 2). Few marker units occur in the Lake George subterrane, which poses difficulties when attempting to identify units in the Goodpaster district. However, bands of calc-silicate gneiss, amphibolite, and felsic K-feldspar augen orthogneiss are locally traceable between exploration drill holes in the mine area.

Signs of amphibolite-grade conditions affecting the metamorphic sequence are indicated by the presence of biotite, sillimanite, and garnet. Retrograde metamorphism is indicated by chlorite commonly replacing biotite. Within the Goodpaster district, metamorphic lithologies trend northwest with moderate to steep northeast dips. The Pogo gold deposit is located approximately 2 km southwest of the “main body” of the Goodpaster Batholith.

Although the geologic setting has been called “far back arc” (Thompson and others, 1999), the gold deposit and its potentially associated magmatism do not share many similarities with arc magmatism. Past investigations have shown that formation and mineralization of the stacked veins took place post-plutonism along the arc, several hundred to a thousand kilometers inland from the arc (Hart and Goldfarb, 2005). There are no extrusive volcanic rocks associated with the post-arc intrusions at Pogo, and all gold-related intrusions in the Titina Gold Province are undeformed (Hart and Goldfarb, 2005).

Regional Structure

Extension during the Jurassic transitioned to regional compression by the Mesozoic. The stress change was driven in large part by accretion of the Wrangellia terrane along the southern margin of Alaska. Initiation of oblique subduction at the North American plate boundary was accommodated along a strike-slip suture zone (Denali–Farewell Fault system) and long-lived strike-slip faulting further inland along the Tintina–Kaltag Fault system. Swarms of northeast-trending left-lateral faults formed within these master strike-slip fault systems (Denali–Farewell Fault and Tintina–Kaltag Fault). These northeast faults dominate the structural terrain of the Goodpaster and surrounding districts.

Magmatism

The mechanism of formation of granitic intrusive bodies at Pogo is disputed. One setting that has been applied to the intrusive bodies is a back arc setting. Emplacement of melts in this setting occurred during the final stages of regional uplift and compression (Richter and others, 1975; Smith and others, 1999). Melt characteristics are dominated by I-type, mainly ilmenite-series, calc-alkaline, felsic to intermediate magmas (Newberry and Burns, 1988; Newberry and others, 1995). Granitic intrusive bodies exploited the northeast-trending left-lateral faults between tectonically thinned Yukon–Tanana terrane and the Denali–Farewell Fault system. The granitic intrusions cooled at depths of about 2–4 km (Newberry and Burns, 1988; Newberry and others, 1995).

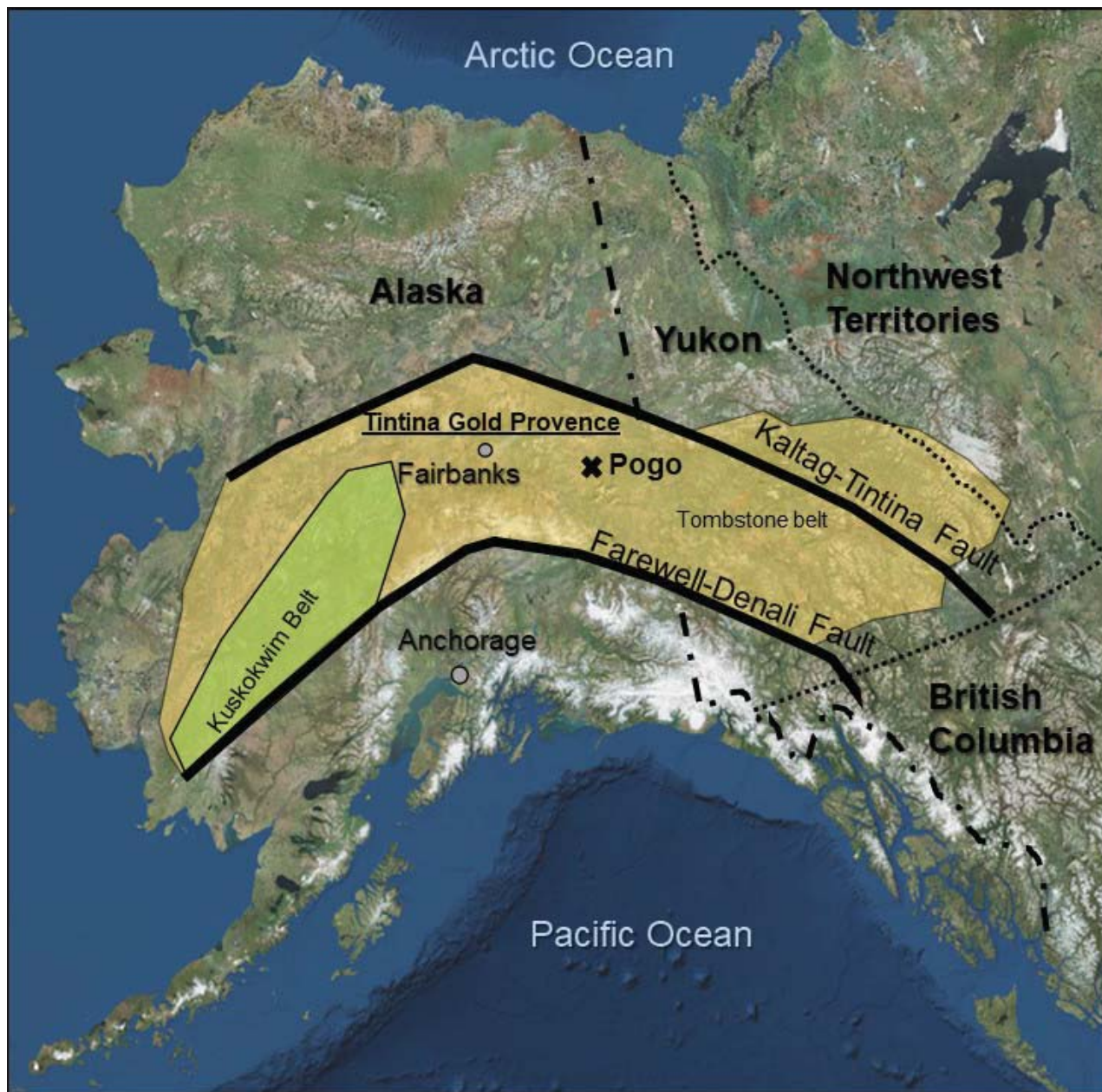


Figure 2. The Tintina Gold Province and associated mineral belts. The belts include the ~800-km-long Tombstone Belt (110–90 ma) that extends from the Yukon to Fairbanks area and the 550-km-long Kuskokwim Belt (75–95 Ma) that extends from Fairbanks to the western extent of Alaska. The Pogo Deposit is identified by the black “x”.

Ore at Pogo

The major ore bodies at Pogo occur as stacked shallow dipping (15–30°) tabular veins 0.5 to 15 m in width with varying gold grades. The veins overprint, are directly adjacent to, and are up to 2 km away from local granitic intrusions. The proximity and gentle contacts between quartz veins and intrusives are characteristic of ore veins at Pogo. Ore mineralogy consists primarily of arsenopyrite, chalcopyrite, löllingite, and free gold.

Three types of veins can be characterized at the Pogo Mine: (1) early, narrow, biotite-bearing shear veins; (2) bull quartz veins encased in sericite-Fe-Mg carbonate alteration and containing pyrite-arsenopyrite-löllingite bands (main stage quartz veins); and (3) extensional veins that form as steeper offshoots from the main stage veins.

Structures developed in the early biotite-bearing shear veins indicate “top-to-the-south” displacement under ductile to semi-brittle conditions at higher temperatures (Rhys and others, 2003). The orientation of the extension veins and local sigmoidal shapes indicate a component of “top-to-the-northwest” normal displacement on the main stage veins in their present orientation, and brittle to semi-brittle conditions of formation (Rhys and

others, 2003). Dolomite-sericite alteration surrounding main stage veins indicates utilization of vein margins by late to post-mineralization hydrothermal fluid during ongoing displacement of vein systems. All types of veining overprint 107–106 Ma, post-metamorphic granitic dikes.

The intrusion and cooling of these granitic dikes are thought to be coeval with mineralization in the Tombstone belt section of the Tintina Gold Province (fig. 2). Smith and others (1999) date ore mineralization in the Goodpaster District at 105–94 Ma (mid-Cretaceous).

References

- Goldfarb, R.J., Phillips, G.N., and Nokleberg, W.J., 1998, Tectonic setting of synorogenic gold deposits of the Pacific Rim: *Ore Geology Reviews*, v. 13, p. 185–218.
- Goldfarb, R.J., Ayuso, R., Miller, M.L., Ebert, S.W., Marsh, E.E., Petsel, S.A., Miller, L.D., Bradley, D., Johnson, C., and McClelland, W., 2004, The Late Cretaceous Donlin Creek deposit, southwestern Alaska—Controls on epizonal formation: *Economic Geology*, v. 99, p. 643–671.
- Goldfarb, R.J., Bake, T., Dubé, B., Groves, D.I., Hart, C.J.R., and Gosselin, P., 2005, Distribution, character, and genesis of gold deposits in metamorphic terranes: *Society of Economic Geologists, 100th Anniversary Volume*.
- Groves, D.I., Goldfarb, R.J., Robert, F., and Hart, C.J.R., 2003, Gold deposits in metamorphic belts: Overview of current understanding, outstanding problems, future research, and exploration significance: *Economic Geology*, v. 98, p. 1–29.
- Hart, C.J.R., and Goldfarb, R.J., 2005, Distinguishing intrusion-related from orogenic gold systems: *Proceedings of the 2005 New Zealand Minerals Conference, Auckland, November 13–16*, p. 125–133.
- Newberry, R.J., and Burns, L.E., 1988, North Star Gold Belt, Alaska: A briefing report to assist in making a rockval mineral resource analysis: *Alaska Division of Geological & Geophysical Surveys Public Data File 88-30*, p. 55.
- Newberry, R.J., McCoy, D.T., and Brew, D.A., 1995, Plutonic-hosted gold ores in Alaska: Igneous versus metamorphic origins: *Resource Geology Special Issue*, v. 18, p. 57–100.
- Plafker, George, and Berg, H.C., eds., 1994, *The geology of Alaska*: Geological Society of America, 1068 p.
- Rhys, D., DiMarchi, J., Smith, M., Friesen, R., and Rombach, C., 2003, Structural setting, style and timing of vein-hosted gold mineralization at the Pogo deposit, east central Alaska: *Mineralium Deposita*, v. 38, p. 863–875.
- Richter, D.H., Lanphere, M.A., and Matson, N.A., Jr., 1975, Granitic plutonism and metamorphism, eastern Alaska range, Alaska: *Geological Society of America Bulletin*, v. 86, p. 819–829.
- Smith, M.T., Thompson, J.F.H., Bressler, J., Layer, P., Mortensen, J.K., Abe, L., and Takaoka, H., 1999, Geology of the Liese Zone, Pogo property, east central Alaska: *Society of Economic Geologists Newsletter*, no. 38, p. 12–21.
- Thompson, J.F.H., Sillitoe, R.H., Baker, T., Lang, J.R., and Mortensen, J.K., 1999, Intrusion-related gold deposits associated with tungsten-tin provinces: *Mineralium Deposita*, v. 34, p. 197–217.

For further information, see: Patriot Gold, The Current State of Gold Production in the US, 1970, <http://www.patriotgoldcorp.com/investors/articles/?id=101> [Accessed October 2018].

Preliminary Structural Analysis and Geologic Relationships between Precambrian Belt Rocks and Oligocene Igneous Rocks in the Kofford Ridge 7.5' Quadrangle, Northwestern Montana

Christopher P. Smith and Kaleb C. Scarberry

Geologists, Montana Bureau of Mines and Geology, Butte, Montana

Introduction

Cenozoic extension and isolated volcanic activity overprints the Mesozoic Fold-Thrust belt in northwestern Montana (fig. 1). The Hog Heaven Volcanic Field formed in the hinge of a Mesozoic fold during Cenozoic extension between about 28 and 37 Ma (K-Ar ages in Lange and others, 1994), and is the only occurrence of Cenozoic igneous activity in the Polson 30' x 60' quadrangle (fig. 2). The volcanic field has the highest known Ag:Au (2,230:1) ratio of high-sulfidation-type mineral deposits (Lange and others, 1994). Total production at the mine includes 92.7 oz Au, 317,097 oz Ag, and 11,753 lbs Cu. Anaconda Copper Mining Company geologists estimated a remaining resource of about 200,000 tons of 12–16 oz/t Ag.

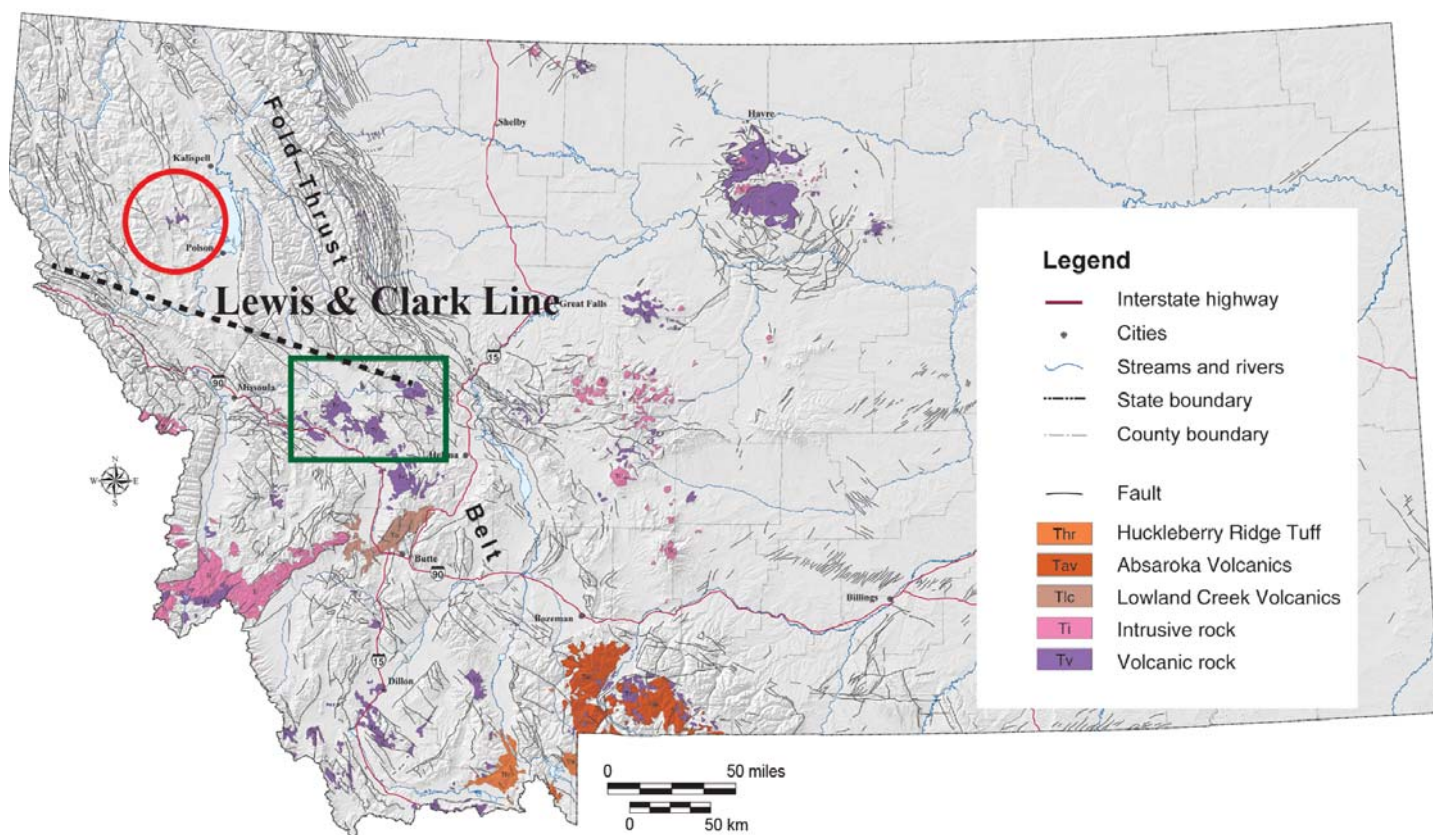


Figure 1. Cenozoic igneous rocks in Montana. Also shown is the location of the Hog Heaven volcanic field (red circle) and the Lewis and Clark Zone (green box).

The Hog Heaven Volcanic Field is the northwesternmost Cenozoic Volcanic Field in Montana (fig. 1) and may represent the northernmost site of Cenozoic Basin and Range volcanism in the conterminous United States (Lange and Zehner, 1992; Lange and others, 1994). Although the volcanic field is isolated with respect to other Cenozoic igneous systems in Montana, it formed concurrent with right-lateral shear (LaPoint, 1971) and in a tectonic setting similar to 49 Ma to 30 Ma volcanic fields described by Mosolf (2015) in the Lewis and Clark Zone between Missoula and Helena (fig. 1).

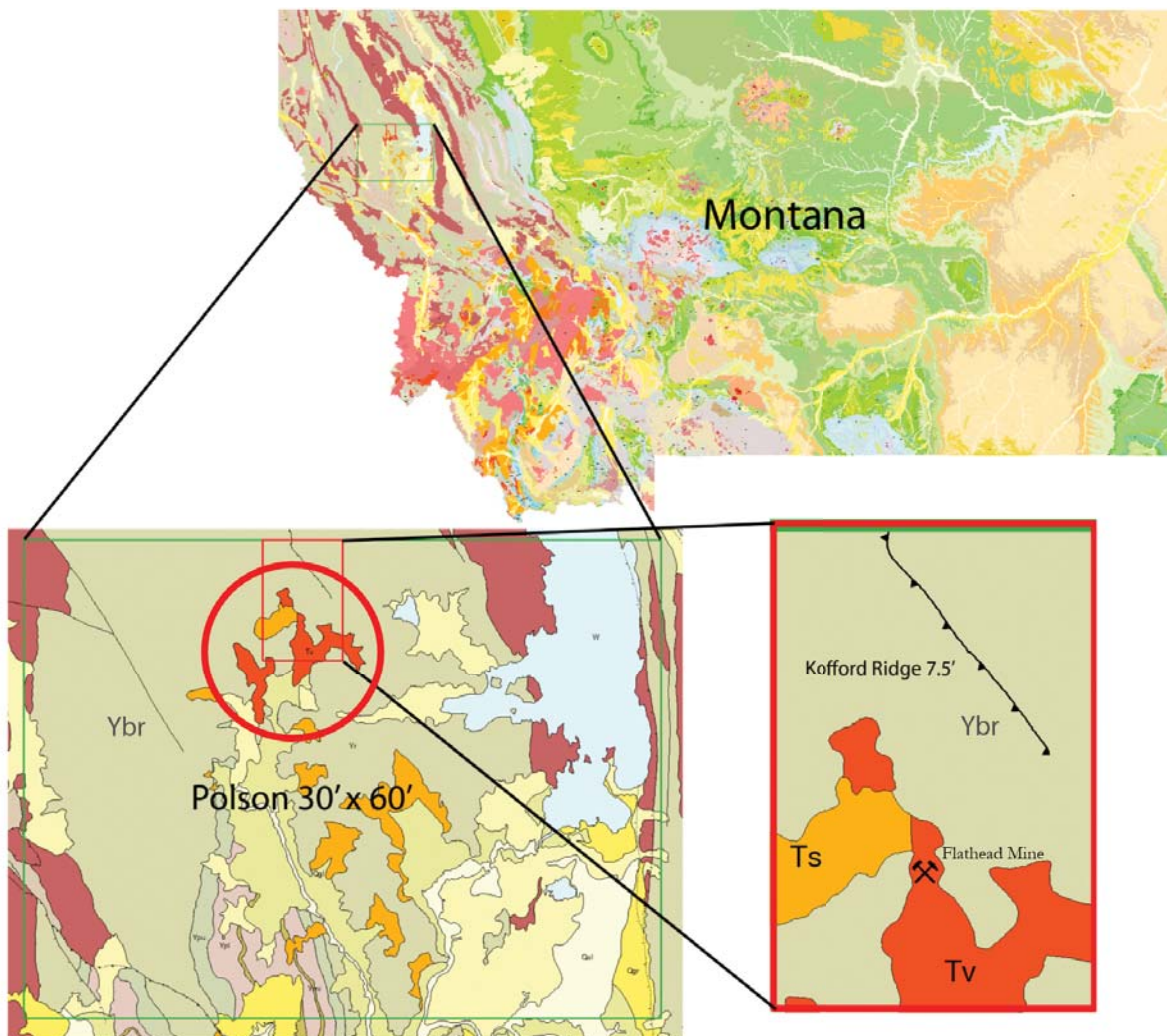


Figure 2. Location of the Kofford Ridge 7.5' quadrangle, the Polson 30' x 60' quadrangle, and the Flathead Mine in northwestern Montana. Ybr, Mesoproterozoic Belt Supergroup (Revett Formation); Tv, Tertiary volcanic rocks; Ts, Tertiary sediments.

Geologic Setting and Previous Work

Mesoproterozoic Belt Supergroup rocks are the dominant lithology in northwestern Montana (fig. 2). Belt sediments accumulated in a northwest-elongate intracontinental rift basin between 1,500 and 1,370 Ma (Evans and others, 2000; Lonn and others, 2016; Winston, 1986). Individual thrust sheets contain Belt rock sections that are over 18,000 m (60,000 ft) thick (summary in Harrison and others, 1974). Belt rocks in the Kofford Ridge 7.5' quadrangle (fig. 2) consist exclusively of bedded gray-tan siltite and quartzite (fig. 3A) interbedded with blue-purple argillite (fig. 3B), and represent the middle unit of the Revett Fm.

The Hog Heaven Volcanic Field (Page, 1963) consists mainly of dacitic porphyry lavas, domes, and tuffs (Lange and others, 1994) that rest with marked angular unconformity, commonly 50° or more, on deformed Belt rocks (Harrison and others, 1986).

Field Mapping

MBMG geologists Kaleb Scarberry and Catherine McDonald mapped in the Kofford Ridge 7.5' quadrangle during the summer of 2018, initiating new geologic mapping in the Polson 30' x 60' quadrangle, the first 30' x 60' tackled by MBMG geologists in northwestern Montana (fig. 2). The distribution of Belt rocks (fig. 3), precious-metal-related alteration (fig. 4A), vent brecciation (fig. 5A), and pyroclastic deposits (figs. 4B, 5B) were carefully mapped. Scarberry collected a suite of Hog Heaven rocks for future radiometric age determinations, and both MBMG geologists measured and compiled bedding, metamorphic cleavage, and pencil cleavage data

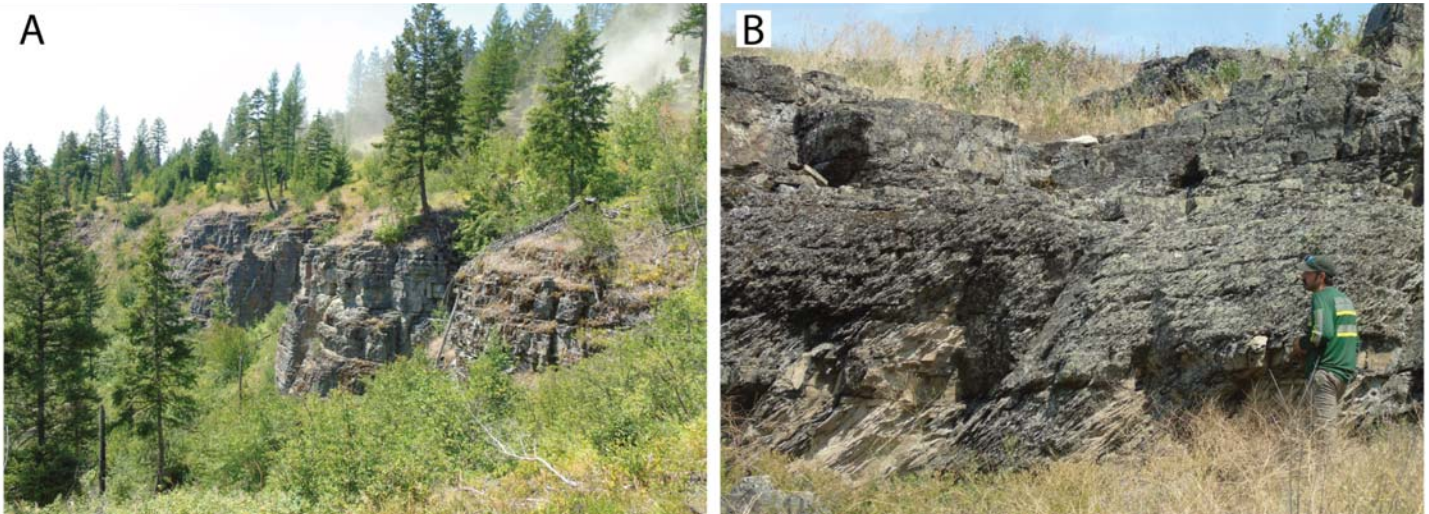


Figure 3. (A) Outcrops of Precambrian Belt Supergroup argillite. (B) Ethan Coppage examining interbedded Precambrian Belt Supergroup siltite and argillite. Note that metamorphic cleavage is prominent in the argillite but not in the siltite.

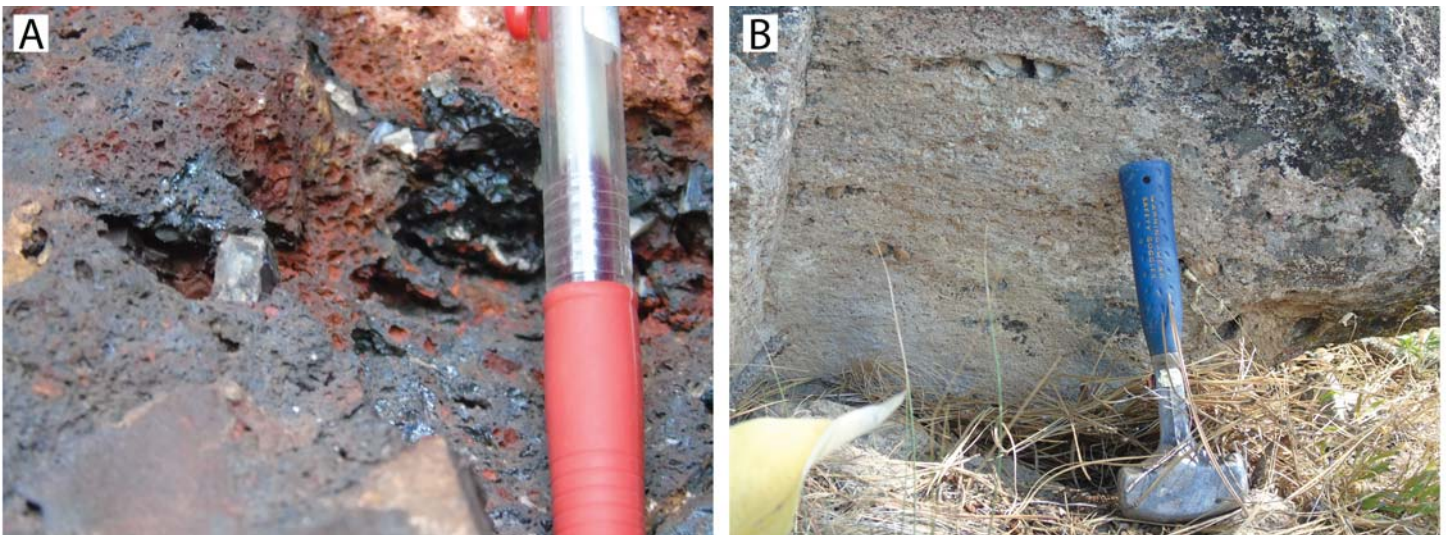


Figure 4. (A) Barite crystal in oxide gossan near the West Flathead Mine. (B) Lithophyseae in densely welded tuff south of the Flathead Mine.

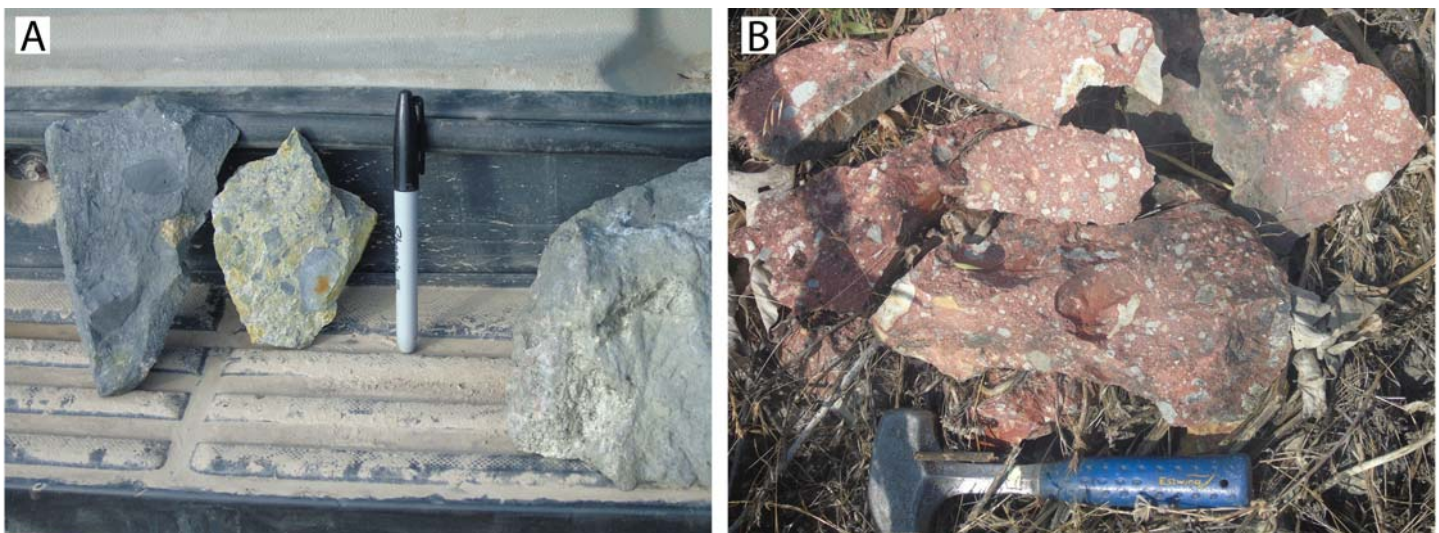


Figure 5. (A) Mineralized diatreme breccia from the Flathead Mine. Note angular clasts of Precambrian Belt Supergroup rocks in an igneous matrix. (B) Lithic tuff from the southeastern edge of the Hog Heaven Volcanic Field also contains angular Belt rock clasts.

from outcrops of Precambrian Belt Supergroup strata. Montana Tech professor Chris Gammons and two of his M.S. students, Ian Kallio and Ethan Coppage, assisted with the mapping efforts. The M.S. students also worked with project geologists from Brixton Metals to organize and sample drill core from the Flathead Mine for future analytical work.

Structural Analysis

Approximately 200 Precambrian bedding, metamorphic cleavage, and pencil cleavage measurements from Precambrian Belt Supergroup rocks are presented here (figs. 6, 7). These rocks are gently folded (beds dip 0° to 25°) and have axial planes that strike N–NW. Metamorphic cleavage is generally oriented N–NW and dips steeply (average of about 70°) to the SW (fig. 7). Pencil cleavage data show that folds plunge about 10° to 15° towards the north (figs. 6, 7). Intersections of these structures at any given location near the Flathead Mine (fig. 2) would make favorable “vector” exploration targets within and at the margins of the Hog Heaven diatreme (fig. 8).

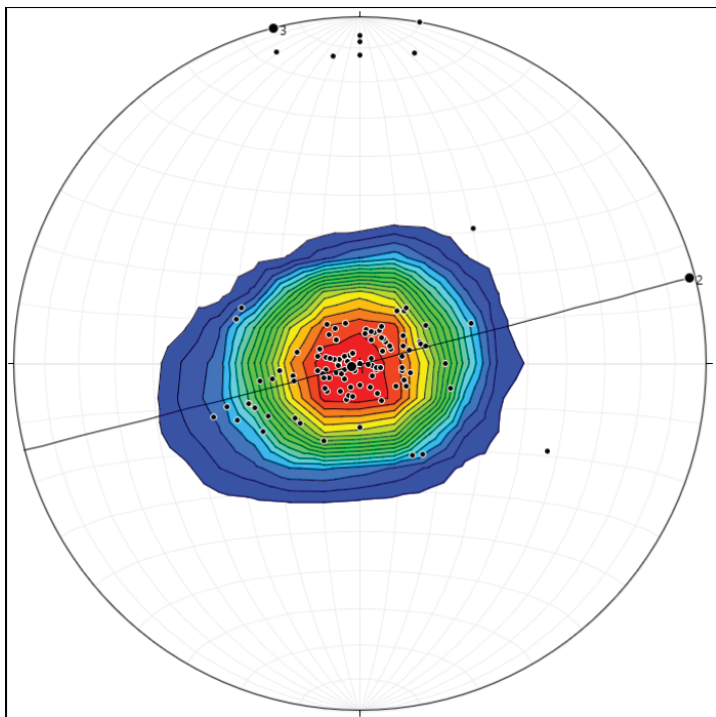


Figure 6. Bedding data from Lange and Zenner (1992) and 2018 mapping by K. Scarberry and C. McDonald in the Kofford Ridge 7.5 minute quadrangle. Stereonet program from Allmendinger and others (2012) and Cardozo and Allmendinger (2013) (also for fig. 7).

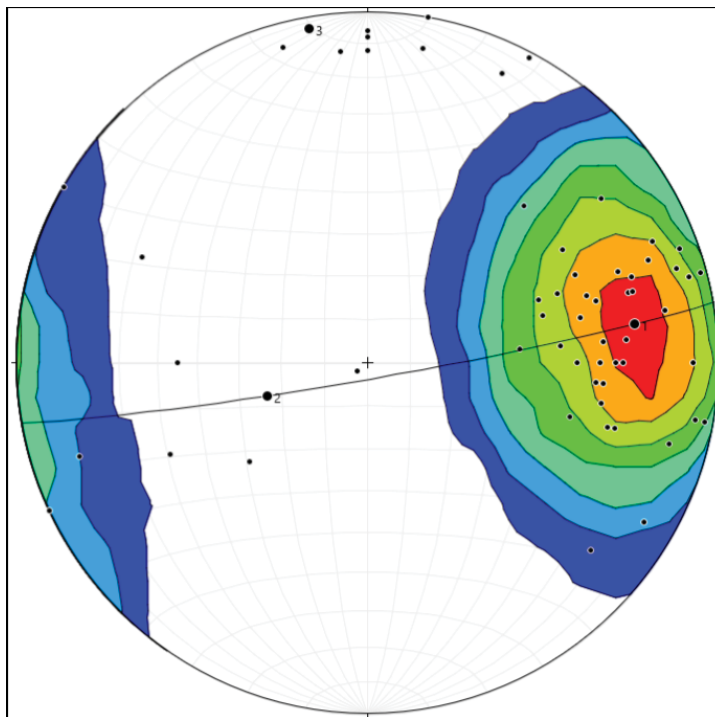


Figure 7. Cleavage data from Lange and Zenner (1992) and 2018 mapping by K. Scarberry and C. McDonald in the Kofford Ridge 7.5 minute quadrangle.

Discussion of Results

Gentle folding (fig. 6) and steeply inclined metamorphic cleavage in Precambrian Belt rocks (figs. 7, 3A) in the Kofford Ridge 7.5' quadrangle formed during Mesozoic Sevier Fold–Thrust belt deformation in western Montana. The NW–SE orientation of Mesozoic fold axes in the Belt rocks is a first-order control on Cenozoic mineral deposits in the Hog Heaven Volcanic Field (figs. 2, 4). Second-order structural controls on mineralization include bedding and cleavage planes. The vector that results from the intersection of these first- and second-order structures is defined by a pencil cleavage formed in Belt rock argillites.

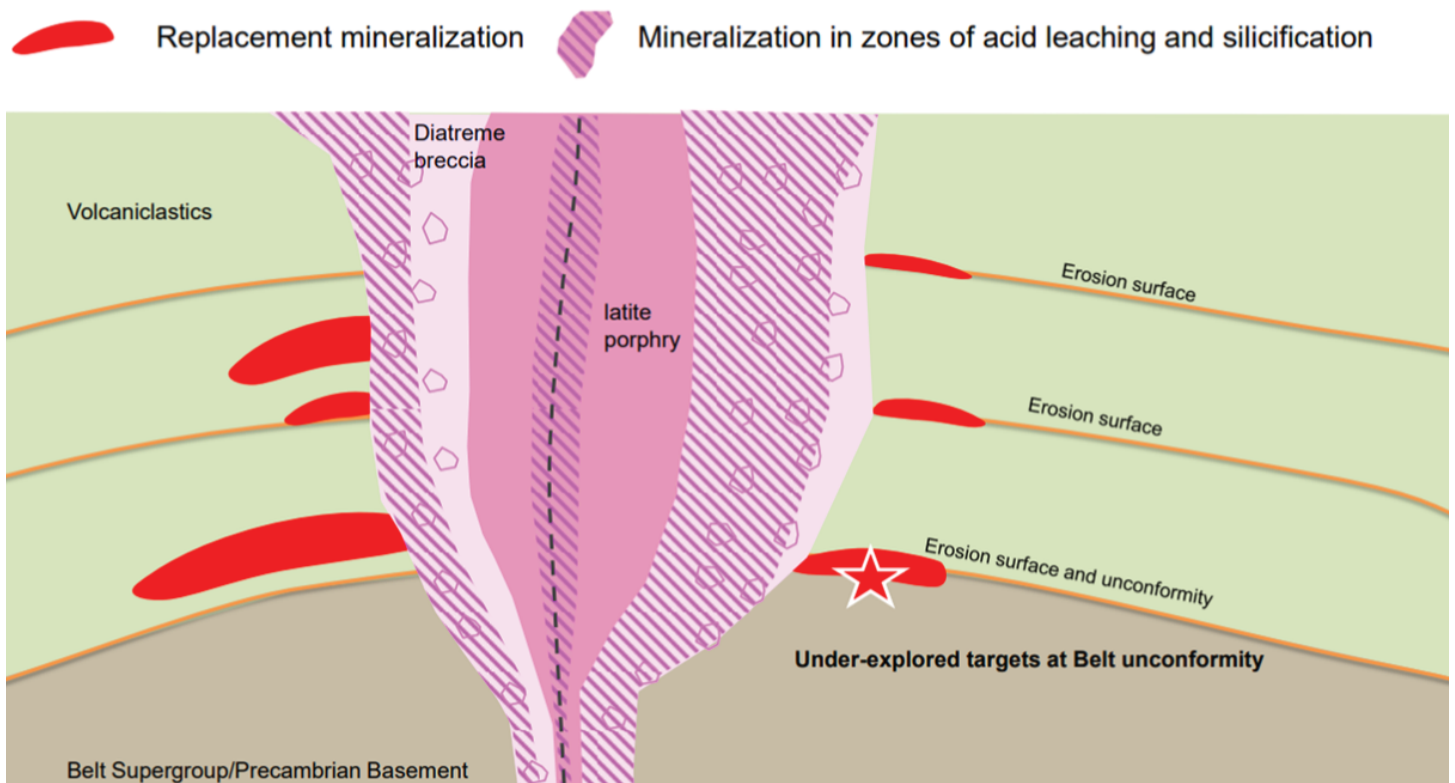


Figure 8. Schematic cross section through the mineralized zone of the Hog Heaven volcanic field. Image from Brixton Metals. Used here by permission.

References

- Allmendinger, R.W., Cardozo, N., and Fisher, D., 2012, *Structural geology algorithms: Vectors and tensors in structural geology*: Cambridge University Press.
- Cardozo, N., and Allmendinger, R.W., 2013, Spherical projections with OSXStereonet: *Computers & Geosciences*, v. 51, p. 193–205, doi:10.1016/j.cageo.2012.07.021.
- Evans, K.V., Aleinikorr, J.N., Obradovich, J.D., and Fanning, C.M., 2000, SHRIMP U-Pb geochronology of volcanic rocks, Belt Supergroup, western Montana: Evidence for rapid deposition of sedimentary strata: *Canadian Journal of Earth Sciences*, v. 37, p. 1287–1300.
- Harrison, J.E., Griggs, A.B., and Wells, J.D., 1974, Tectonic features of the Precambrian Belt Basin and their influence on post-Belt structures: U.S. Geological Survey Professional Paper 866, 19 p.
- Harrison, J.E., Griggs, A.B., and Wells, J.D., 1986, Geologic and structure maps of the Wallace 1° x 2° quadrangle, Montana and Idaho: U.S. Geological Survey Miscellaneous Investigations Series Map I-509-A.
- Lange, I.M., and Zehner, R.E., 1992, Geologic map of the Hog Heaven Volcanic Field, northwestern Montana: Montana Bureau of Mines and Geology Geologic Map 53.
- Lange, I.M., Zehner, R.E., and Hahn, G.A., 1994, Geology, geochemistry, and ore deposits of the Oligocene Hog Heaven volcanic field, northwestern Montana: *Economic Geology*, v. 89, p. 1939–1963.
- LaPoint, D.J., 1971, Geology and geophysics of the southwestern Flathead Lake region, Montana: Missoula, University of Montana, M.S. Thesis, 120 p.
- Lonn, J.D., Burmester, R.F., Lewis, R.S., and McFaddan, M.D., 2016, Giant folds and complex faults in Mesoproterozoic Lemhi strata of the Belt Supergroup, northern Beaverhead Mountains, Montana and Idaho, *in* MacLean, J.S., and Sears, J.W., eds., *Belt Basin: Window to Mesoproterozoic Earth*: Geological Society of America Special Paper 522, p. 139–162.

Mosolf, J.G., 2015, Geologic field guide to the Tertiary volcanic rocks in the Elliston 30' x 60' quadrangle, west-central Montana: Northwest Geology, v. 44, p. 213–232.

Page, W.D., 1963, Reconnaissance geology of the north quarter of the Horse Plains quadrangle, Montana: Boulder, University of Colorado, M.S. Thesis, 66 p.

Winston, D., 1986, Stratigraphic correlation and nomenclature of the Middle Proterozoic Belt Supergroup, Montana, Idaho and Washington, *in* Belt Supergroup, Roberts, S.M., ed.: Montana Bureau of Mines and Geology Special Publication 94, p. 69–84.



The Map Chat at the Butte Brewing Company (photo: A. Roth).

Carlin-Type Gold Deposits: Exploration Targets and Techniques at the Gold Bar District, Roberts Mountains, Nevada

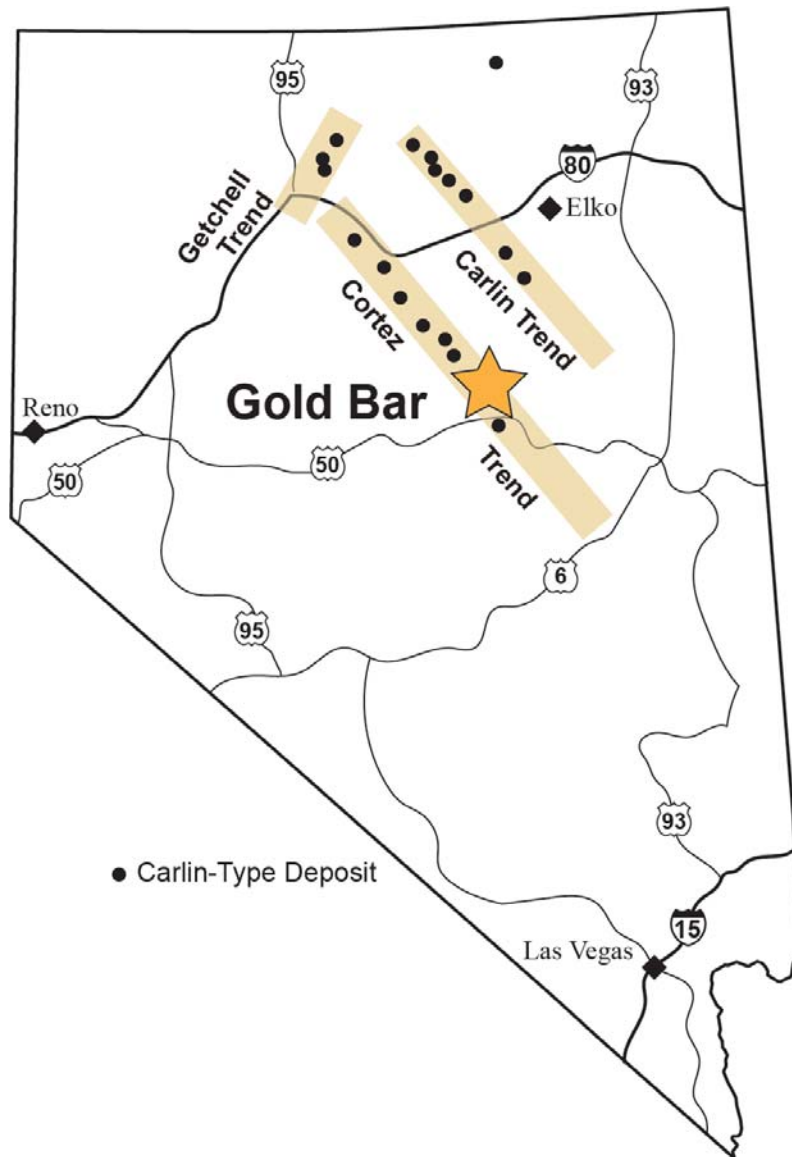
Ian Kallio

M.S. Student, Montana Tech, Butte, Montana

Introduction

Northeastern Nevada is one of the largest gold-producing regions in the world. Carlin-type Au deposits in Nevada have produced over 200 Moz. Approximately 0.5 Moz of gold has been recovered from the Gold Bar Mining District, located in the Roberts Mountains along the Cortez Trend in northeastern Nevada (fig. 1). Gold Bar has nearly all the characteristics of a large Carlin-type gold district; therefore there is a high level of confidence in the discovery potential of the Gold Bar District. Current exploration types and techniques include geologic mapping; shallow definition drilling; deep, large, high-grade target drilling; soil geochemistry; geophysics; and hyperspectral analysis.

New target area concepts can be divided into three subgroups: (i) down-dip extensions of known mineralization; (ii) surrounding shallow targets based on geology, geophysics, geochemistry, and spectral data; and (iii) deep conceptual targets based on geologic modeling using all available layers of data.



Carlin-type deposits formed during passive margin rifting in North America from the late Proterozoic (~600 Ma) to the Devonian (~360 Ma). A roughly 5,000-m-thick carbonate platform formed in northeastern Nevada as turbidites, debris flows, slides, and slumps were transported from shallow to deep waters. Pre-Eocene compression (Roberts Mtn thrust?) and Tertiary extension created favorable structures. For hydrothermal fluids that transported millions of ounces of gold into the carbonate sediments and volcanic flows during the Eocene (42–36 Ma). The host and surrounding rocks are strongly altered by hydrothermal fluids.

Carlin-Type Characteristics at Gold Bar

Gold Bar has many, if not all, of the characteristics of a large Carlin-type gold district. Gold Bar is near the continental margin and contains favorable carbonate host rocks (fig. 2) with Carlin-type alteration (decalcification, silicification), and gold in arsenian pyrite. Pre-Eocene ore structures include a WNW-trending anticline, west-dipping ramp structures, east-dipping rollovers, folded thrusts, and high-angle NW- and NE-striking normal faults (Wall, Roberts Creek Faults). Igneous rocks, lamprophyre dikes, and deep magnetic anomalies are present beneath the district. Open

Figure 1. Location of Gold Bar in relation to Carlin-type ore deposit trends.

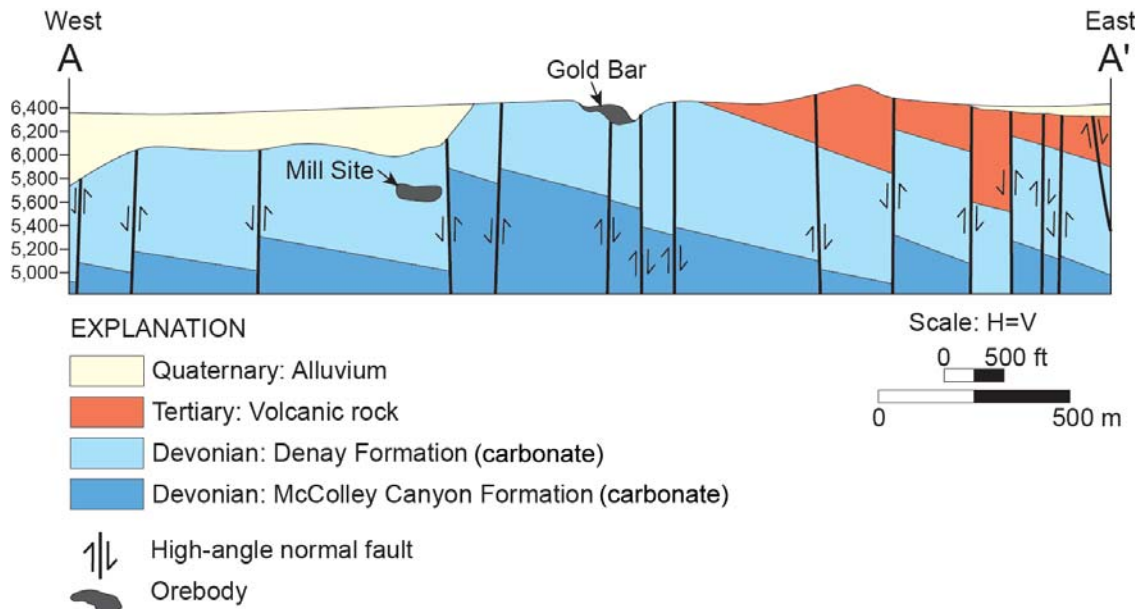


Figure 2. Cross section of the carbonate suite at Gold Bar (modified from Yigit and others, 2003).

sulfide mineralization is below down-dip oxidized zones with arsenic-rich trace elements. There are multiple stacked carbonate host rocks linked by steep feeder structures, with a style of mineralization similar to that of Cortez and Jerritt Canyon.

Exploration Targets

Priority target areas lie along the WNW-trending faults and anticline that contain most of the Gold Bar deposits. These deposits are associated with Fe-oxide, argillic, and silicic alteration. Although McEwen's exploration team uses multiple exploration techniques for targeting deposits, the geologists are currently focusing on two techniques.

All of the past resources discovered and recovered at Gold Bar are from shallow oxide deposits. Most of the high-priority shallow targets fall along the WNW anticlinal trend and structural intersections.

Deep, large, high-grade targets are the next step for large-scale discoveries. The >300-m-thick Lone Mountain dolomite acted as a trap for ore-forming fluids. Favorable carbonate host rocks lie beneath the Lone Mountain Formation. A potential difficulty with deep target exploration is the expense, with no guarantee of high grade ore at depth.

Current Exploration Techniques

Detailed mapping of existing pits and surrounding areas is underway to identify structures, such as faults and folds and intrusions, dikes and sills, alteration (Fe oxides, argillic, and silicification), and favorable host-rock lithologies near and below surface. Geophysics is applied by using resistivity and gravity anomalies as tools, and when interpreted correctly, can complement mapping and exploration. Integration of geophysics is useful for unidentified surface structures and deep subsurface lithology, alteration, structure, intrusions, etc.

Soil grids are useful for initially finding anomalous metal concentrations on the surface. Following structures down-dip or along faults from anomalous soil areas can help find deposits. Common alteration of clay minerals such as kaolinite and illite can also be identified via spectral anomalies. Ammonium illite can be associated with Au in silty rocks in the Carlin Trend, but target areas identified need field checking.

Summary: Carlin-Type Deposits and Gold Bar

Carlin-type gold systems are an important deposit type, as 45% of >3 Moz Carlin-type deposits have grown to be >10 Moz after deeper exploration. Multiple mines in Nevada, such as Cortez and Jerritt Canyon, which share similar geological attributes, host rocks, and styles of alteration and mineralization with Gold Bar, started with shallow pits that grew deeper into large, world-class deposits.

Current exploration techniques at Gold Bar help define priority areas that can lead to shallow and deep targets. Geology is a major exploration tool—alteration, structures, etc. can be identified and modeled with the help of exploration techniques. New targets lie along structural intersections such as the WNW anticlinal trend and large faults. Targets can be discovered and refined with additional detailed geologic mapping, geophysics, hyperspectral analysis, and soil geochemistry.

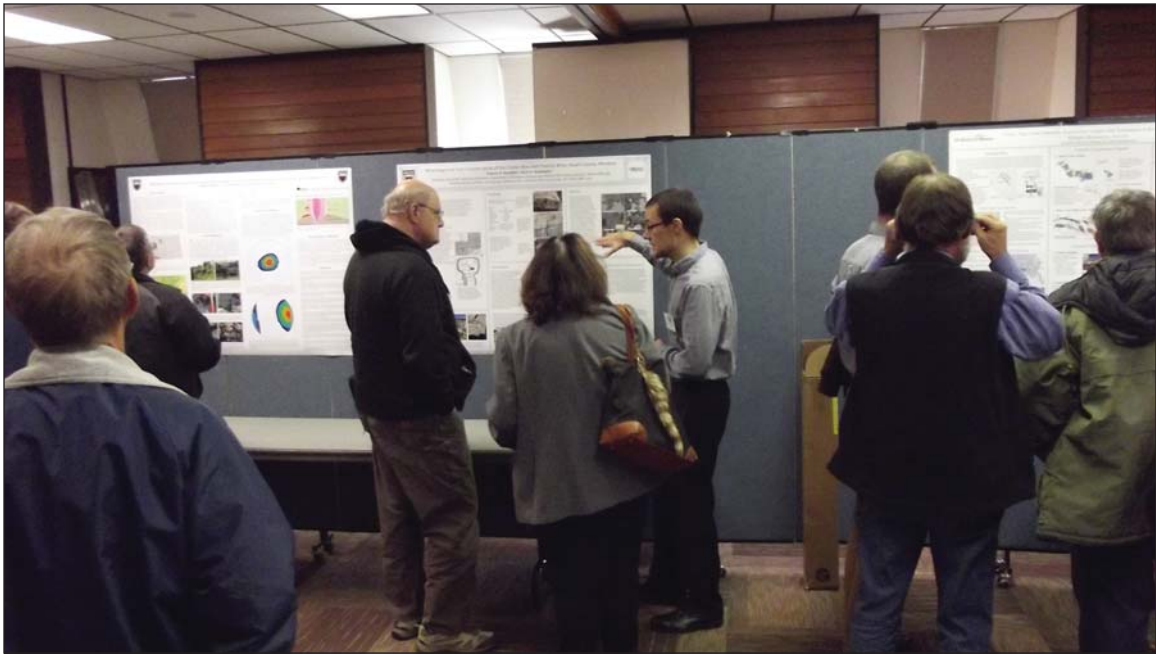
References

McEwen Mining Inc., 2018, Corporate Presentation. Retrieved from <http://www.mcewenmining.com/investor-relations/presentations-and-fact-sheet/default.aspx> [Accessed February 2018].

Yigit, O., Nelson, E., Hitzman, M., and Hofstra, A., 2003, Structural controls on Carlin-type mineralization in the Gold Bar district, Eureka County, Nevada: *Economic Geology*, v. 98, no. 6, p. 1173–1188.



Ian Kallio with a pyrite vein at the Golden Sunlight Mine (photo: K. Scarberry).



Francis Grondin explains his research results during the student poster session at Montana Tech (photo: A. Roth).



Interbedded siltite and argillite in the Revett Formation of the Mesoproterozoic Belt Supergroup, northwestern Montana (photo: K. Scarberry).

Mineralogy and Fluid Inclusion Study of the Crystal Mountain Fluorite Mine, Ravalli County, Montana

Francis Grondin¹ and Chris Gammons²

¹*M.S. Student, Department of Geological Engineering,*

²*Professor, Department of Geological Engineering,
Montana Tech, Butte, Montana*

The Crystal Mountain fluorite mine, known for its vast amounts of massively grown fluorite and rare accessory minerals including fergusonite (YNbO_4), allanite (a REE-bearing silicate), and thortveitite ($\text{Sc}_2\text{Si}_2\text{O}_7$; Foord and others, 1993), is located in the Sapphire Mountains District near the town of Darby, MT. This occurrence, in the southern Sapphire Mountains, is the only one reported for North America and one of fewer than a dozen areas in the world where thortveitite has been positively identified (Foord and others, 1993). This site was mined between 1954 and 1961. Prospecting of the area, followed by mining, has led to the accumulation of data in the form of core logs, hand samples, and thin sections. Specifically, the Taber collection of drill core, thin sections, mine maps, and miscellaneous reports on the Crystal Mountain Mine has been donated to the MBMG (Montana Bureau of Mines and Geology) Mining Archives Repository for future studies. The purpose of the current study has been to analyze the data and samples to better understand the complex geology of this district. We have made thin sections for SEM-EDS, micro-Raman spectroscopy, and fluid inclusion analysis from hand samples and core specimens. The fluorite varies from colorless to deep purple and is enriched in yttrium (Y). Fluid inclusions were classified as primary if they occurred randomly scattered throughout the fluorite, or secondary if they occurred as clusters along healed cracks. Primary inclusions average 10–15 μm in size and have homogenization temperatures from 350 to $>500^\circ\text{C}$. These inclusions contain many secondary daughter minerals including halite, sylvite, ankerite, siderite, and quartz. Most of the halite daughter minerals homogenize at $T > 400^\circ\text{C}$, whereas the carbonates and quartz do not dissolve completely, possibly because of slow kinetics. The secondary fluid inclusions, which have formed along the cracks and fractures of the fluorite, are bigger and average 30–50 μm , with no daughter minerals. These inclusions often contain a double bubble at room temperature, which indicates a high CO_2 content (fig. 1C).

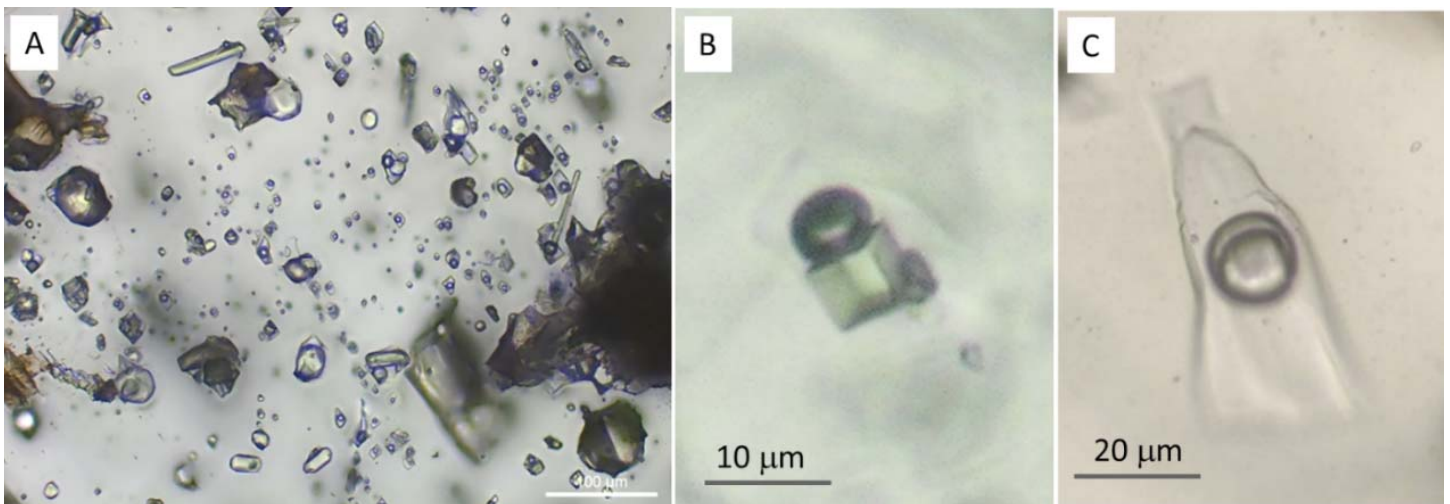


Figure 1. Fluid and solid inclusions in fluorite from Crystal Mountain. (A) General view of fluorite with numerous solid and fluid inclusions. Many of the solids are unidentified at this time. (B) Typical primary fluid inclusion with large halite daughter and several unidentified solids. (C) Typical secondary fluid inclusion with “double bubble” indicating the presence of liquid CO_2 .

Raman spectra for thortveitite obtained in this study (514 nm laser) look quite different from the reference spectra for natural and synthetic thortveitite in the U-Arizona RRUFF database (“Norway,” “synthetic”; fig. 2), especially at wavelengths $> 1,000$ nm. Powder X-ray diffraction of the material from Crystal Mountain confirms that it is thortveitite (fig. 3). The reason for the different Raman spectral signatures (fig. 2) could be related to

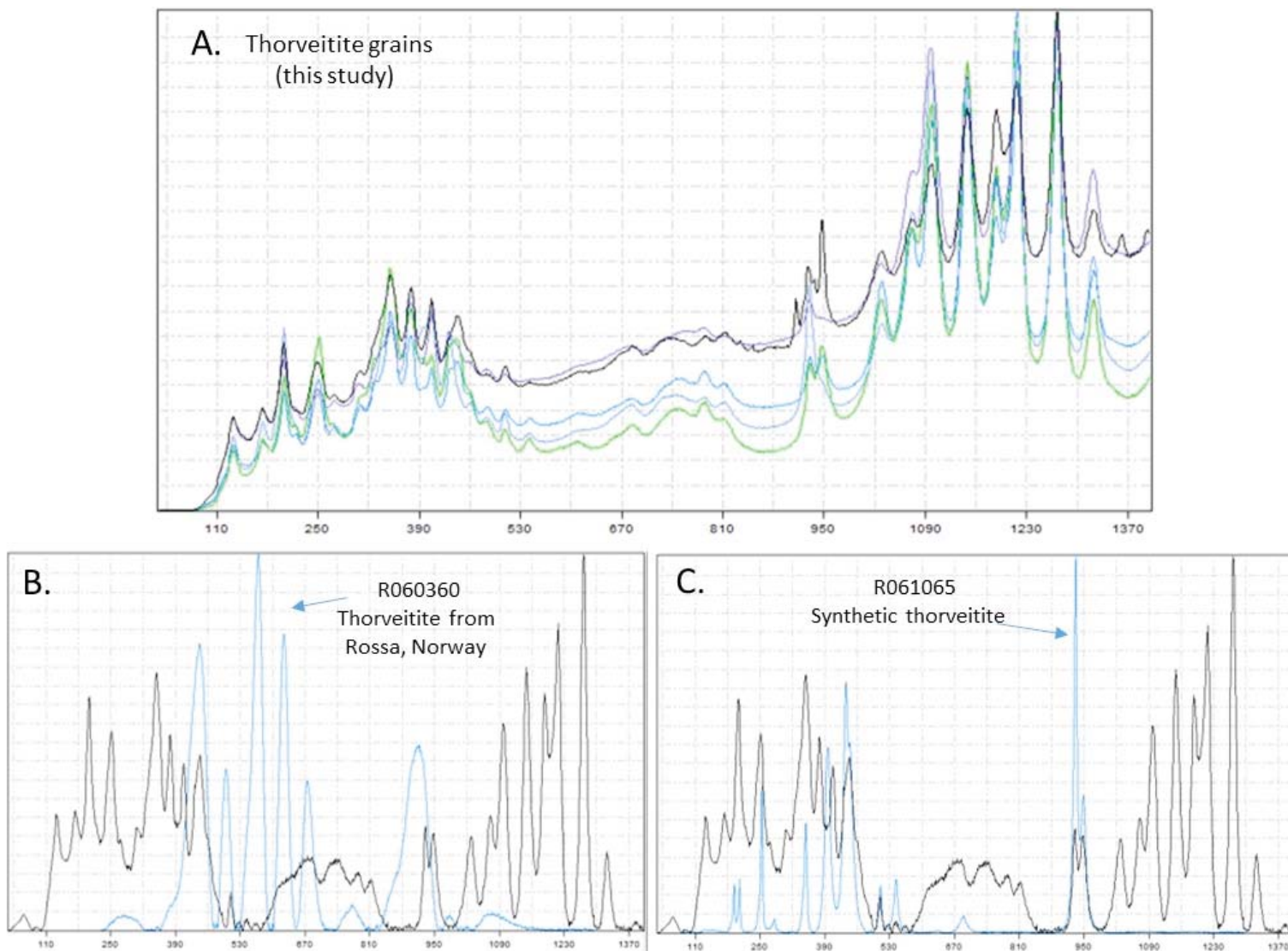


Figure 2. Raman spectra for thortveitite from Crystal Mountain. (A) 5 different grains, no background subtraction. (B) Background-corrected spectrum (this study, black) compared to thortveitite from Rossa, Norway. (C) Same, compared to synthetic thortveitite.

differences in the concentrations of trace impurities (e.g., yttrium) in the various thortveitite types (up to 4 wt. %).

SEM-EDS analysis was conducted on a sample of biotite-rich igneous rock containing disseminated purple fluorite (fig. 4) obtained from the Taber collection. In these electron backscatter images, minerals with higher atomic masses are brighter than those of lower mass. Overall, the textures show thortveitite, fluorite, and apatite occurring as disseminated grains surrounded by phlogopite and quartz.

The Crystal Mountain Mine hosts tabular bodies of massive fluorite up to 10 ft thick (Taber, 1952). The country rock of granodiorite and gneiss composition shows no evidence of hydrothermal alteration near contacts with the fluorite. These observations, coupled with the anomalous concentrations of apatite and minerals rich in high field strength elements (Sc, Nb, Ti, Y, REE, U, Th), suggest the possibility of the Crystal Mountain deposit being a magmatic fluorite deposit formed by crystallization of an immiscible F-silicate melt (Yang and van Hinsberg, 2018). Studies are in progress to compare fluid inclusions from Crystal Mountain with other fluorite occurrences in western Montana, including the Wilson Gulch and Spar (Bear Creek) fluorspar mines (Campbell, 1960), and the Snowbird fluorspar-parisite locality (Metz and others, 1985).

Acknowledgments

We thank Peggy Delaney of the MBMG for her help accessing information in the Mining Archives, and Gary Wyss for his help with the SEM-EDS.

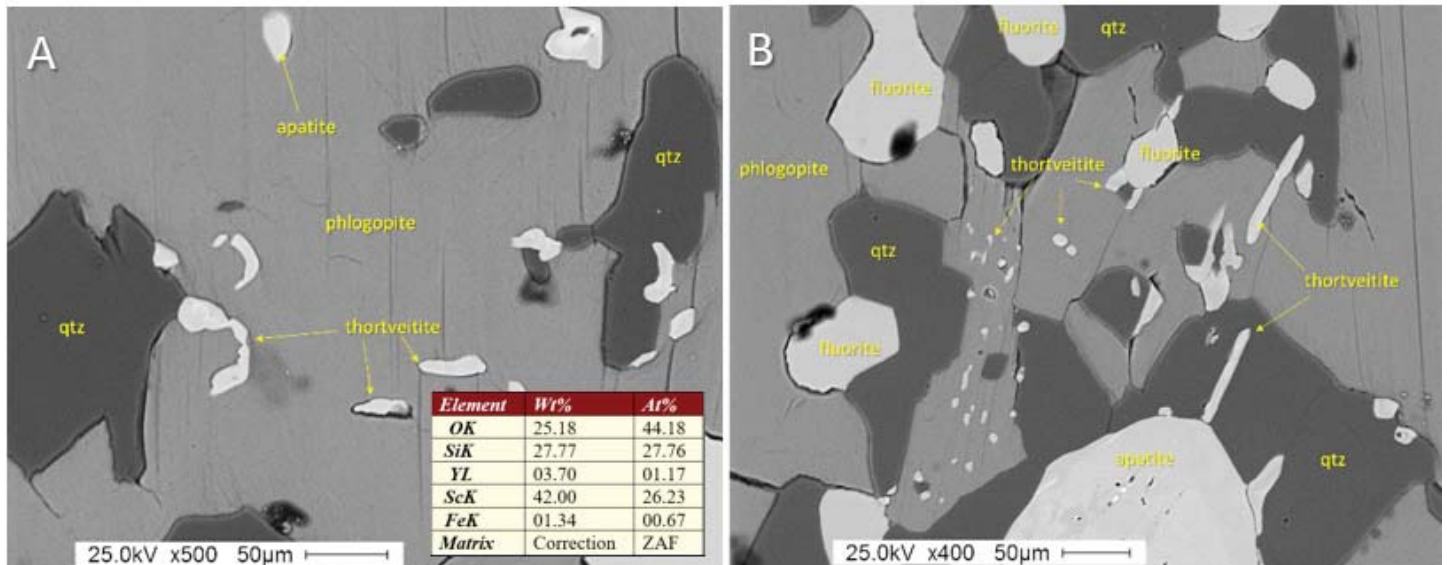


Figure 4. SEM-backscatter images of a fluorite-bearing igneous rock from Crystal Mountain showing intergrowths of thortveitite, fluorite, phlogopite, apatite, and quartz. The inset in A shows the SEM-EDS standardless chemical analysis for a thortveitite grain.

References

- Campbell, A.B., 1960, Geology and mineral deposits of the St. Regis-Superior area, Mineral County, Montana: U.S. Geological Survey Bulletin 1082-I, p. 542–612.
- Foord, E.E., Birmingham, S.D., Demartin, F., Pilati, T., Gramaccioli, C.M., and Lichte, F.E., 1993, Thortveitite and associated Sc-bearing minerals from Ravalli County, Montana: *Canadian Mineralogist*, v. 31, p. 337–346.
- Metz, M.C., Brookins, D.G., Rosenberg, D.G., and Zartman, R.E., 1985, Geology and geochemistry of the Snowbird deposit, Mineral County, Montana: *Economic Geology*, v. 80, p. 394–409.
- Taber, J.W., 1952, Crystal Mountain fluorite deposits, Ravalli County, Montana: U.S. Bureau of Mines Report of Investigation 4916.
- Yang, L., and van Hinsberg, V.J., 2018, Liquid immiscibility in the CaF₂-granite system: Boston, Mass., Proceedings of V. M. Goldschmidt Conference, August 2018.